THE UNIVERSITY OF CALGARY

Recovery of Hydrocarbon Contaminants at the Water-Table Capillary Fringe

by

Eden C. Koster

A THESIS

SUBMITTED TO THE FACULTY OF GRADUATE STUDIES

IN PARTIAL FULFILMENT OF THE REQUIREMENTS FOR THE

DEGREE OF MASTER OF SCIENCE IN CHEMICAL ENGINEERING

DEPARTMENT OF CHEMICAL AND PETROLEUM ENGINEERING

CALGARY, ALBERTA

FEBRUARY, 1998

ABSTRACT

The application of an evacuation process as a method to recover hydrocarbon spills in the capillary fringe was studied experimentally using a cylindrical glass bead column, water, and n-Heptane. Thirty-six experiments were executed with two different glass bead packs using a drainage capillary system, to address a series of parameters regarding contaminant recovery, including: the vacuum suction pressure applied, location of the production probe, volume of the spill, rainfall, and water table movement. The study concluded that the hydrology and capillarity of the subterranean strata play a major role in the recovery of the hydrocarbon. Further, there is an optimum location with regard to the point of drawdown and the water/hydrocarbon interface. According to the experimental setup used, the evacuation process is effective in containing the contaminant from spreading, but it is not efficient as an *in-situ* clean up method of a hydrocarbon spill.

ACKNOWLEDGEMENTS

I wish to express my gratitude to Dr. John Belgrave for providing me with the opportunity to work on this project, Dr. Apostolos Kantzas for taking on the supervisory role and his continuous encouragement to find engineering fundamentals in the experimental results, and to Neotechnology Consultants Ltd. (NEOTEC) of Calgary for providing funds for this project.

I would also like to thank: Fausto Nicola for his assistance in designing and his construction of the main pieces of the experimental apparatus; the members of the machine shops (main engineering shop and department shop) for their help with the little but important things that needed to be done; and Dr. Ayodeji Jeje and Matt Ursenbach for their great advice.

Further, I would like to thank Donald Eckford, Greg Krpan, and Rita Tobak for their friendship and interest.

Finally, a special thank-you to Ernst Kerkhoven for his support, encouragement, and enthusiasm.

Dedicated

to

My Parents

TABLE OF CONTENTS

LIST OF TABLES

LIST OF FIGURES

NOMENCLATURE

DD	Drawdown (inches of water)
F_{down}	Force of the weight of liquid pulling down (Equation 3)
F_{up}	Force of the weight of liquid pulling up (Equation 3)
g	Acceleration of gravity
h_1	Distance the production probe is above water/oil interface (cm)
h_2	Distance the production probe is below water/oil interface (cm)
h_3	Distance the production probe is above the free water table (cm)
h_c	Height of capillary rise
h_{cp}	Height of capillary rise in porous media (Table 5)
h_{cpt}	Height of capillary rise in a tube (Table 5)
$h_{c(o/a)}$	Capillary height of oil/air interface (Figure 21, cm)
$h_{c(w/a)}$	Capillary height of water/air interface (Figure 21, cm)
$h_{c(w/o)}$	Capillary height of water/oil interface (Figure 21, cm)
h_o	Height of oil in column (Equation 24)
h_w	Height of water in column (Equation 24)
P_A	Pressure on wetting side (or A side) of oil bubble (Equation 27)
P_{atm}	Atmospheric pressure
P_B	Pressure on wetting side (or B side) of oil bubble (Equation 28)
P_c	Capillary pressure
$P_{c\text{-}A}$	Capillary pressure exerted on A side of bubble (Equation 27)

$P_{c\text{-}B}$ Capillary pressure exerted on B side of bubble (Equation 28)

$P_{c(o/a)}$ Capillary pressure at the glass bead/oil/air interface

$P_{c(w/a)}$ Capillary pressure at the glass bead/water/air interface

$P_{c(w/o)}$ Capillary pressure at the glass bead/water/oil interface

P_f Pressure of the fluid

P_{nw} Pressure in the non-wetting phase

P_o Pressure of the oil

P_{probe} Pressure at the probe inlet (inches of water)

P_{st} Static pressure

P_w Pressure in the wetting phase

P_{wf} Wellbore flowing pressure

PH Production probe height (cm)

PI Productivity index

PPH Production pressure head (inches of water)

ΔP Pressure differential

q Flow rate

r Radius

r_1, r_2 Radii of curvature of liquid - fluid interface

r_b Radius of oil bubble

r_s Radius of sphere

r_t Inside radius of capillary tube

R_1, R_2 Nominal radii of curvature of liquid - fluid interfacial surface

R_m Mean radius of curvature

RF Recovery factor

RS Residual saturation capacity (Equation 1)

R_s Radius of the solid spheres (Equation 37)

S_g Specific gravity

T_b Boiling temperature

V_{hc} Volume of discharge of hydrocarbon (barrels, Equation 1)

VP Vacuum suction pressure (inches of water)

V_s Volume of soil required to attain residual saturation (cubic yards, Equation 1)

W/S Water supply valve

Greek

γ Interfacial Tension (Table 5)

θ Contact angle

θ_A Contact angle on A side (Equation 34)

θ_B Contact angle on B side (Equation 34)

θ_{oil} Contact angle for oil

θ_{water} Contact angle for water

ρ Density

ρ_o Density of oil

ρ_{oil} Density of oil

ρ_w Density of water

ρ_{water} Density of water

σ Interfacial tension

σ_A Interfacial tension on A side (Equation 35)

σ_B Interfacial tension on B side (Equation 35)

Φ Soil porosity

CHAPTER 1

INTRODUCTION

Ground water constitutes a very small fraction of the total world's available water, but it is the major source of fresh water available on land. In most countries, ground water is the only source of fresh water for human consumption and agriculture. Other uses are for orchards, plantations, and industries; as well, the whole well being and ecology of nature depend on it.

All ground water is accumulated in near-surface subterranean strata. All fresh water that enters this system is part of the hydrological cycle, which is a dynamic system. Consequently, any contamination of this system can have disastrous effects on the ecological system over large areas.

The behaviour of a contaminant can be predicted by observing its physical properties. Our senses can detect a chemical as solid, liquid, or gas; clear or coloured; and odourless or odorous (pleasant (aromatics) or pungent (mercaptans)). In general however, physical properties of contaminants are obtained using simple instruments such as a thermometer and an electric heat source to measure the melting point; litmus paper to measure pH; a vacuum pump and glass apparatus to measure vapour pressure; and a capillary tube to measure surface tension and wettability (Scaffidi, 1994).

By volume, petroleum products play a major role in today's society. Consequently, the risk of spills of crude oil and petroleum products is a reality that cannot be ignored during the production, processing, transportation and storage stages, as well as the utilization of

hydrocarbons. The potential of large hydrocarbon spills occur during transportation (whether by marine transport or underground pipeline) and storage, mainly due to the burst of a pipeline or the storage tank wall. Land spills invariably result in relatively large subsurface contamination, where the movement of ground water can play a major role in the spreading of the contaminant.

Much of the pollution in industrial countries is buried in the subsurface, ranging from abandoned hazardous waste disposal sites to uncontrolled releases at locations of manufacturing, transport, and storage; where cleanup methods such as excavation or vertical wells have been applied to extract contaminants from soil and ground water aquifer systems (Karlsson, 1993). The on-site treatment of petroleum contaminated soils and near surface sand formations is increasingly gaining attention by remediation companies as a viable cleanup method. Contamination of subsurface soils and ground water formations however, remain a pervasive environmental problem.

Public concerns and demands for cleaner air, soil, and water has led to increased governmental and industry actions, such as federal and private-sector spending on remediation, the progressively increasing level of environmental control guidelines, industry's commitments to waste management engineering, and the study of ecology emerging as a science taught at universities. Given this increasing level of government and public environmental awareness, environmental management has emerged as a key component in the overall management of hydrocarbon exploration, development, and production (Kosasih and Shobirin, 1995) in the petroleum industry.

Recently, *in-situ* subsurface remediation processes have been the focus of significant

attention by the scientific community involved with the cleanup of environmental contaminants. These efforts have shown that significant modelling and experimental research is needed to further understand the interaction of immiscible liquids in the capillary zone with unsaturated zone infiltration and saturated zone transport (Hoag *et al.* 1991).

The current technology for the extraction of liquid contaminants, contaminated ground water from aquifers, or vapour-phase contaminants from vadose soil zones is based on the same engineering principles as the production of oil and gas from reservoirs by means of wells. Because of similarities with petroleum reservoirs, the effective extraction of liquid hydrocarbon contaminants from ground water bearing formations is strongly influenced by the capillarity of the subterranean strata.

The research for this thesis was to experimentally investigate the subsurface hydrodynamics of contaminant recovery at the capillary fringe. For this purpose, the experiments focused on the recovery of hydrocarbon contaminants at the water table capillary fringe, by applying the evacuation process using two porous media, consisting of vertical, cylindrical glass bead packs.

CHAPTER 2

BACKGROUND

Ground water is accumulated in near surface subterranean strata, with all water entering and leaving the water bearing strata being a part of the hydrological cycle, which is a dynamic system. Consequently, any contamination of the ground water system can have disastrous effects on the ecological system over large areas. Contamination can occur by leakage from hazardous waste disposal sites to uncontrolled releases on locations of manufacturing, transport and storage. The potential of large hydrocarbon land spills occur during transportation and storage, mainly due to the burst of a pipeline or the storage tank wall. These spills invariably result in relatively big subsurface contamination, where the movement of ground water can play a major role in the spreading of the contaminant.

2.1 The Hydrological Cycle

The hydrological cycle, as seen in Figures 1 (diagram) and 2 (schematic), includes all movement of water in solid, liquid, and vapour form; throughout the atmosphere, on the earth's surface, and in the subterranean ground water bearing strata. Hence, it is necessary to study the entire cycle in order to understand subsurface-water motions.

The two causes for the movement of water in the hydrological cycle are heat from the sun and gravity. The hydrological cycle may be long or short, and it may be summarized, beginning with the short cyclic movement and ending with the longer and more complicated cycle, as follows (Tolman, 1937):

1. Water vapour condenses to rain, snow, or fog and vaporizes again before the water reaches the earth's surface.
2. Vapour condenses in the atmosphere into rain or snow which reaches the surface of the earth and is then evaporated before the water seeps underground. This evaporation may be directly from the rain water before it forms a runoff, or from streams, lakes, or the oceans.
3. Vapour condenses in the atmosphere and falls as snow or rain on the ground and seeps below the surface. The water which enters the soil may return to the atmosphere by the following methods:
    a) It may be held as soil moisture and returned directly by transpiration (from plants) and evaporation.
    b) It may become gravity (vadose) water and seep down to the saturated zone. After water reaches the saturated zone, it may percolate as free-moving water through pervious material, the openings of which are inter-connected, or it may move as confined water in and through ground water conduits.

The principal fresh water reservoirs of the hydrological cycle are (Tolman, 1937):

1. The atmosphere, a reservoir of atmospheric moisture which replenishes all the other reservoirs.
2. The ground surface which supports surface water in streams, lakes, ponds, and solid water in the form of snow and ice.
3. The soil zone, acting as a reservoir of soil moisture which is held against the pull of

gravity and is thus made available for plant consumption.

4. The ground-water reservoir.

Freeze and Cherry (1979) present an estimate of the spread, volume, and residence time of water molecules in the different water bodies of the hydrological cycle (Table 1).

2.2 Ground Water

About 94 percent of the worlds available water is in the oceans, which cover about 71 percent of the earth's surface. Oceanic water is unsuitable for drinking or for agricultural use due to its high salt content, mainly NaCl. The remaining 6 percent is fresh water and is mainly accumulated on land. Of all water on land, more than 33 percent is frozen in ice sheets and glaciers. Most of the rest, about 66 percent, is water collected below the earth's surface and is called ground water. Ground water constitutes only a very small fraction of the total water available and is therefore a precious, if not a strategic commodity, protected by stringent ecological and environmental controls in many countries.

Ground water is never chemically pure. Even rain water contains materials dissolved from the air as well as suspended dust. For instance, "red snow" or "blood rain" is coloured by intermixed organisms of microscopic size. The most common substances dissolved in ground water are the salts of the common basic radicals (e.g. sodium, potassium, calcium, magnesium, iron, and aluminum) and acid radicals (e.g. Cl^-, SO_4^{2-}, and CO_3^{2-}) derived from rock disintegration, from the gases of the air, volcanic gases, and from organic sources. Thus, the chemical make-up of ground water determines its suitability for agricultural and

industrial purposes, and as drinking water (Tolman, 1937).

Ground water enters the earth's surface into the near surface permeable strata which is called the zone of aeration (also called the zone of intermittent saturation, zone of suspended water, or unsaturated zone). Beneath this zone lies the formation where the pores and crevices are fully filled with water (saturated zone). This water bearing zone extends downwards until it reaches an impermeable zone, rock, or barrier lying below the fresh water holding layer or aquifer. This barrier is also called a ground water dam or aquiclude.

Underground water occurs in the two great zones of aeration and saturation, which are separated by the water table. The movement and occurrence in these two zones are markedly different. The following are four distinct types of movements of the subsurface water, whereby two occur exclusively above the water table, one can occur above or below the water table, and the last occurs only in the zone of saturation. Minor movements of soil moisture are due to subsurface evaporation and molecular attraction of soil particles for moisture by roots. (Tolman, 1937):

1. Seepage - takes place chiefly in a downward vertical direction. It is at first a slow, diffuse movement by which the surfaces of all openings are wetted; and second, a downward movement of water by gravity on the films coating the openings. The movement is complicated by the presence of ground air which is displaced in part by the downward seeping water, or completely displaced by a rising water table.
2. Capillary rise - is confined to water movement in the capillary fringe.
3. Ground water turbulent flow - may occur above or at the water table if large openings exist, or below the water table if large openings and free exit and entrance of water

exists, such as in caverns. However, natural ground water gradients are usually too small to develop turbulent flow except in large conduits above or at the water table, in conduits below the water table where free escape permits rapid movement, or in the vicinity of the intake of a pumping well.

4. Percolation - (or laminar flow) occurs only in the saturated zone in interconnected openings under ordinary hydraulic gradients existing underground.

The water table exists only in water bearing formations which contain openings of sufficient size to permit hydraulic movement of water. In literature, there are several definitions of the water table. It may be defined as the contact plane between free ground water and the capillary fringe zone (Tolman, 1937), or the surface separating the capillary fringe from the "zone of saturation" (Davis and DeWiest, 1966). The more accurate definition is that the water table is the surface on which the fluid pressure in the pores of a porous medium is exactly atmospheric, as is revealed by the level at which water stands in a well which taps an unconfined water saturated strata (Davis and DeWiest, 1966; Freeze and Cherry, 1979).

2.2.1 Zone of aeration

The zone of aeration extends from the earth's surface to the ground water table, and includes the capillary fringe zone. It is in this zone where destructive chemical action and disintegration of rocks occur. In this zone the oxygen of the atmosphere assisted by moisture, carbonic acid, organic acids, and where present sulphuric acid, acts on the rocks

and manufactures the manifold detrital products of weathering.

From the top of the soil surface, the water in the zone of aeration can be classified as follows (Todd, 1980; Tollman, 1937):

Soil Water - constitutes the upper portion of the zone of aeration and is limited to the surface layer penetrated by roots. Active root development occurs chiefly within 10 feet of the surface. Soil water is the reservoir of available soil moisture upon which plant life depends.

Vadose Water - includes:

1. Pellicular water - which adheres to rock surfaces throughout the zone of aeration. It is held in place by capillary forces and does not move by gravity, but may be abstracted by evaporation and transpiration. This water remains fixed and is only depleted very slowly by subsurface evaporation and chemical reaction of the water with rock particles, known as weathering.
2. Gravity (or vadose) water - which moves freely under the control of gravity only after the grains or rock surfaces have been coated with pellicular water.
3. Perched water - which occurs locally in the zone above an impervious barrier.

Capillary Water - also called capillary fringe water, lies above the water table and is in contact with it. The capillary fringe water is held above the water table by capillarity, and has a thickness ranging from a fraction of an inch to possibly 10 feet or more depending on the porosity, the size of the detritus, and the texture of the material above the water table (Table 2). If the depth to the water table is equal or less than the height of capillary lift, the capillary fringe will discharge ground water

by evaporation, or if the capillary fringe extends up to the zone of root penetration, ground water will be discharged by transpiration through plant foliage. It has been shown that if the depth to the water table is equal or less than the height of capillary lift, then the water table response to precipitation is greater than would be expected based on the specific yield of the geologic material and the amount of rainfall (Abdul and Gillham, 1984; Gillham, 1984).

2.2.2 Zone of saturation

The zone of saturation extends down from the ground water table to the aquiclude. As all openings in the zone of saturation are fully filled with water, the unbalanced film forces, which develop only at air-water surfaces and are important in the zone of aeration, are ineffective. The controlling factors in this zone are the geological structure, hydrological characteristics of water-bearing materials, and hydraulic gradient (i.e. gravity), whereby the following bodies of water can be identified (Todd, 1980; Tolman, 1937):

Free ground water - when water moves through an interconnected body of permeable material, unhampered by impervious confining material, it may be denominated as free ground water moving under the control of the slope of the water table (gravity effects).

Confined water - that moves in strata, conduits, or arteries under the control of the difference in head between the intake and discharge areas of the confined water body. If water is confined in compressible alluvial material (chiefly sand and gravel), and if high artesian pressure in the confined aquifer is reduced by pumping, the aquifer may be

compressed by weight of overlying material supported in part by artesian pressure; or if the confining strata are uncompacted, the reduction of pressure in the aquifer may allow water to be pressed out of confining material into the aquifer by the weight of overlying material (overburden pressure).

Fixed ground water - is held in small openings (chiefly subcapillary in size) that resist water movement under the usual hydraulic gradients existing underground. It is distinguished from pellicular water which exists only in undersaturated material.

Connate ground water - is saline water entrapped in the pores of consolidated sedimentary rock when originally deposited. The openings and interstices of all sedimentary rocks deposited beneath the ocean were originally filled with salt water. After the rocks have been lifted above the sea, fresh water slowly drives out and replaces the salt water. Exploration of oil fields has shown that bodies of sea water are preserved in anticlines and under barriers which prevent access of fresh water descending from the ground surface. These occurances indicate that under unfavourable structural conditions ground-water movement may be restricted even in porous sedimentary beds.

2.3 Petroleum Hydrocarbon Spills

The hydrodynamics of the subsurface formation is the primary factor governing the severity of ground water contamination. Important physical characteristics of the formation are the depth to the water table, the net recharge, the aquifer media (consolidated or unconsolidated strata), the soil media, the topography, the impact of the vadose zone, and the

hydraulic conductivity of the aquifer.

Aquifers that are at greater risk from contamination include (Duston *et al.*, 1992):

1. Shallow aquifers and those with high net recharge.
2. Formations with high hydraulic conductivities including aquifer media such as unconsolidated sand and gravel, karst limestone, tubular basalt, massive permeable limestone, thin-bedded sandstone, limestone, and shale sequences.
3. When the overlying soil is thin, absent, or consists of sand.
4. When the slope of the land is gradual (because there is less runoff, and therefore, more infiltration).

Less permeable soil media, such as clays and clay-rich materials, prevent or retard movement of the contaminants into the ground water due to capillarity effects. The less permeable the vadose zone media (e.g. shale, silt, and unconsolidated clay), the lower the risk of ground water contamination.

Hydrocarbon contaminants can reach the ground water zone either dissolved in water or as liquid phases that may be immiscible in water. There are many mechanical, chemical, and biological processes by which contaminants can be transported throughout the subsurface. Table 3 summarizes some of the natural processes that affect contaminant transport, while Table 4 summarizes the various effects that the subsurface processes have on the fate of contaminants. The subsurface transport of immiscible hydrocarbon liquids is governed by a set of factors different from those for dissolved contaminants.

2.3.1 Dissolved hydrocarbons

The migration of dissolved hydrocarbon solutes, Figure 4, are governed by (Mackay *et al.*, 1985):

1. Advection - which is the dominant factor of migration in sand and gravel aquifers. It is the process whereby solutes are transported by the main motion of flowing ground water.
2. Dispersion - whereby contaminants are spread as they move with the ground water. It results from two basic processes: molecular diffusion and mechanical mixing. The most important effect of dispersion is the spreading of a contaminant mass beyond the region it would occupy without dispersion.
3. Sorption and retardation - a process whereby some dissolved contaminants may interact with the aquifer solids encountered along the flow path through adsorption, ion exchange, and other processes. These interactions result in the contaminants distribution between the aqueous phase and the aquifer solids, a decrease of contaminant concentration in the aqueous phase, and retardation of the movement of the contaminant relative to ground water flow. The higher the fraction of the contaminant sorbed, the more retarded is its transport.
4. Chemical and biological transformation - a process whereby contaminants can be transformed into other compounds by an extraordinarily complex set of chemical and biological interactions. The effects, relative importance, and interactions of these processes in the ground water zones are not well understood, but are increasingly the subject of research.

2.3.2 Immiscible hydrocarbons

Many hydrocarbon liquids released into the subsurface may migrate as discrete non-aqueous phases, generally immiscible with water, and with some components possibly dissolving (in part) into the surrounding ground water. The migration of an immiscible phase in the subsurface is governed largely by its density, viscosity, and capillarity (i.e. residual saturation, which in principle is a form of liquid hold-up). The experiments of this thesis deal with immiscible hydrocarbon spills.

When a significant quantity of a light liquid petroleum hydrocarbon (i.e. lighter than water) is released into the subsurface (e.g. due to leaks in underground storage tanks or pipelines), several migration pathways exist. These migrations of liquid petroleum into the subsurface can be divided into three stages as follows (Testa and Winegardner, 1991):

1. Seepage through the unsaturated zone.
2. Stability within the water capillary zone.
3. Spreading over the water table.

Once a significant volume of a light liquid hydrocarbon is released, it generally migrates downward under the influence of gravity, its viscosity, and subordinate capillary forces until it reaches the capillary fringe above the water table, Figure 5, where it starts to spread out. Primary factors affecting the amount of lateral spreading include the rate of release, the volume of the release, and the presence of significant permeability contrasts. For example, a large instantaneous release into the unsaturated zone will have a higher degree of spreading in comparison to a continuous small release.

When vertically migrating hydrocarbon nears the water table, the capillary fringe is initially encountered. This capillary zone rises above the water table to a certain height dependent upon the grain size distribution in the formation, and the rate of aeration that takes place in the zone. Essentially, finer grained soils such as silt or clay attain a thicker capillary zone (higher water saturation) than coarser grained soil, such as sand or gravel (due to capillarity differences).

As the light hydrocarbon enters the water capillary zone, it begins to fill the non - capillary pore spaces (drainage process). Little mixing occurs since the two fluids are immiscible (interfacial tension effects). Additional light hydrocarbon accumulation then begins to spread laterally above the water table to form what is referred to as a pancake.

The initial stage of lateral spreading is dominated by gravity forces and may locally depress the water table. But as the gravitational potential diminishes, capillary forces (residual saturation) tend to control the rate of lateral spreading, with its shape determined by the movements of ground water. In addition, subsequent water infiltration from the surface (e.g. due to rainfall) influences the subsurface migration of hydrocarbon contaminants.

The basic principles governing the downward migration of light hydrocarbons are applicable to dense hydrocarbons (heavier than water) as well. The difference is, that once ground water is encountered, dense hydrocarbons continue to migrate downward, reflecting a specific gravity or density greater than that of water, Figure 6. Although a pancake may initially form at the free water table because the spill encounters a denser medium (i.e. water) than air and due to interfacial tension effects, downward migration occurs once significant

mass is attained.

The depth of the dense hydrocarbon liquid penetration into the ground water bearing formation depends on the amount spilled and the capillary characteristics of the strata. Consequently, it may not be equal to the permeability barrier of the aquiclude because of capillary pressure; that is, the spill may pancake out on top of a less permeable porous zone within the ground water bearing strata.

2.3.3 Hydrocarbon residual saturation

Once a hydrocarbon liquid has passed through an alluvial material bed, or a porous sedimentary rock, a certain amount of the liquid is held up in the porous medium, called a residual saturation, constituting an immobile contaminate volume. It is a form of liquid hold-up, or liquid entrapment due to capillary effects. This residual saturation is referred to as the residual oil saturation in petroleum reservoir engineering terms. The residual saturation capacity of a soil or sand is generally about one third that of its water-holding capacity (Testa and Winegardner, 1991). Immobilization of a certain volume of hydrocarbon is dependent upon the soil make up (e.g. the relevant content of sand, clay, and organic material), the soil porosity, the capillary characteristics of the sedimentary bed, and the physical characteristics of the hydrocarbon product. The volume of soil required to immobilize a volume of liquid hydrocarbon can be estimated using basic petroleum reservoir engineering principles (e.g. Craft and Hawkins, 1959) as presented by Testa and Winegardner (1991) as follows:

$$V_s = \frac{0.2 V_{hc}}{\Phi(RS)} \qquad (1)$$

where: V_s = cubic yards of soil required to attain residual saturation

V_{hc} = volume of discharge of hydrocarbon, in barrels

Φ = soil porosity

RS = residual saturation capacity (is the irreducible saturation in petroleum engineering terms, and is primarily dependant on capillary forces)

0.2 = conversion factor (1 barrel = 0.2 cubic yard)

The porosity of an alluvial detritus is in the order of 30 to 40 percent. The residual saturation capacity of a detrital material depends on many factors with capillarity (wetting) as a major one. On average, this saturation is in the order of 30 to 35 percent for a sand, but it can be significantly higher for true soil, that is, with a high content of organic detritus due to adhesion and adsorption effects upon contact with organic material.

Assuming an alluvial sedimentary bed, with average porosity of 35 percent, and a residual saturation of 33 percent, the residual saturation capacity of one cubic yard of soil is:

$$V_{hc} = \frac{\Phi(RS)}{0.2 V_s} = \frac{0.35 * 0.33}{0.2} \qquad (2)$$
$$= 0.58 \textit{ Barrels of contaminant}$$

This example shows that with the spreading and migration of the hydrocarbon contaminant in the ground water system, a significant volume fraction of the progressing

spill is continuously made immobile (trapped) by the residual saturation (e.g. a form of liquid hold up), and thus acts as a form of slowing down of the frontal spreading of the spill. Also, the total volume that was spilt determines the maximum areal and volumetric spreading of the contaminant zone. This identifies that as soon as a liquid hydrocarbon spill has occurred, the first rule for clean-up is the immediate stoppage of the spreading by pumping, the evacuation of the mobile portion of the spill in the zone of aeration, and over the area of the pancake to stop further migration by the ground water system.

When a petroleum spill occurs at the capillary fringe, the contaminant enters a very complex environment. The pre-existing conditions include air filled pores, partially water saturated pores that are under strong capillary pressure (pellicular water), and a degree of permeability that is variable depending on whether the soil has been recently in a wetting or draining phase (capillary hysteresis effects). In addition, the contaminant has its own properties of density, viscosity, surface tension, and any chemical transformation due to weathering, all of which influence its ability to flow.

Table 1: Occurance of Water Worldwide (Freeze and Cherry, 1979)

Parameter	Surface Area (km^2)X10^6	Volume (km^3)X10^6	Volume (%)	Residence Time
Oceans and Seas	361	1370	94	4000 years
Lakes and Reservoirs	1.55	0.13	< 0.01	10 years
Swamps	< 0.01	< 0.01	< 0.01	1 - 10 years
River Channels	< 0.01	< 0.01	< 0.01	2 weeks
Soil Moisture	130	0.07	< 0.01	2 weeks - 1 year
Ground Water	130	60	4	2 weeks - 10,000 years
Icecaps and Glaciers	17.8	30	2	10 - 1000 years
Atmospheric Water	504	0.01	< 0.01	10 days
Biospheric Water	< 0.1	< 0.1	< 0.01	1 week

Table 2: Capillary Rise in Unconsolidated Materials (Todd, 1980)

Material	Grain Size (mm)	Capillary Rise (cm)
Fine Gravel	5 - 2	2.5
Very Coarse Sand	2 - 1	6.5
Coarse Sand	1 - 0.5	13.5
Medium Sand	0.5 - 0.2	24.6
Fine Sand	0.2 - 0.1	42.8
Silt	0.1 - 0.05	105.5
Silt	0.05 - 0.02	200 (still rising after 72 days)

Table 3: Some Natural Processes Affecting Contaminants During Transport (LaGrega *et al.*, 1994)

Process Type	Process
Mechanical (Physical) Processes	Advection Dispersion Diffusion Density stratification Non-aqueous phase fluid flow Fractured media flow
Chemical Processes	Oxidation-reduction reactions Ion exchange Complexation Precipitation Immiscible phase partitioning Sorption
Biological Processes	Aerobic degradation Anaerobic degradation Cometabolism Biological uptake

Table 4: Summary of Natural Processes Affecting the Fate of Hazardous Constituents in the Subsurface (LaGrega *et al.*, 1994)

Process	Class of Chemical	Effect
Sorption	Organic	Retardation
Precipitation	Inorganic	Retardation
Ion exchange	Inorganic	Retardation
Filtration	Organic/Inorganic	Retardation
Chemical oxidation-reduction	Organic/Inorganic	Transformation/Retardation
Biological uptake	Organic/Inorganic	Retardation
Biodegradation	Organic	Transformation
Hydrolysis	Organic	Transformation
Volatilization	Organic	Elimination by intermedia transfer
Dissolution	Organic/Inorganic	Mobility enhancement
Co-solvation	Organic	Mobility enhancement
Ionization	Organic	Mobility enhancement
Complexation	Inorganic	Mobility enhancement
Immiscible phase	Organic	Various partitioning

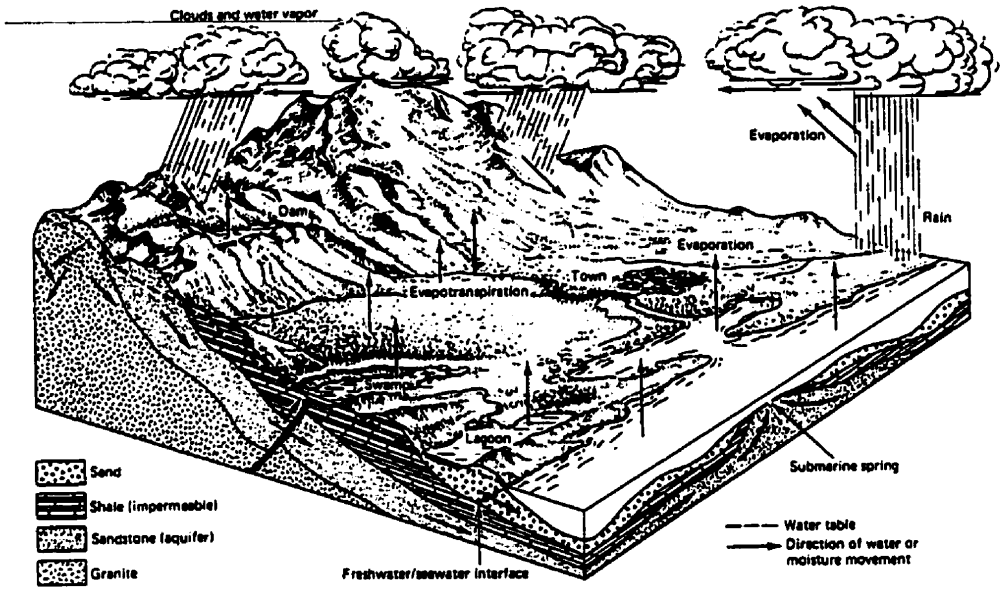

Figure 1: Diagram of the Hydrological Cycle (Todd, 1980)

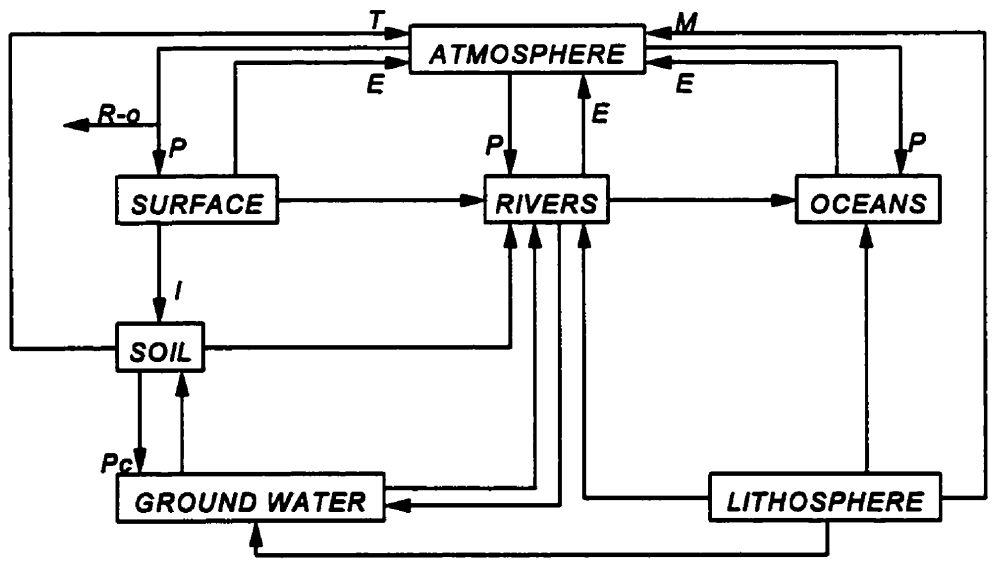

R-o - runoff
T - transpiration
P - precipitation
E - evaporation
I - infiltration
Pc - percolation
M - volcanic or magmatic water

Figure 2: Schematic of the Hydrological Cycle (Bowen, 1980)

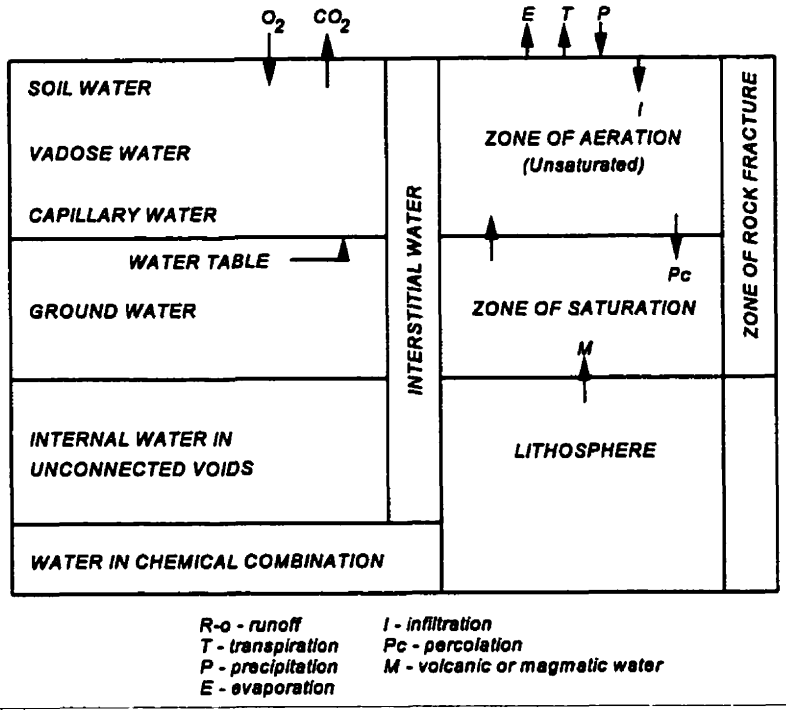

Figure 3: Ground Water in Relation to the Subsurface (Bowen, 1980)

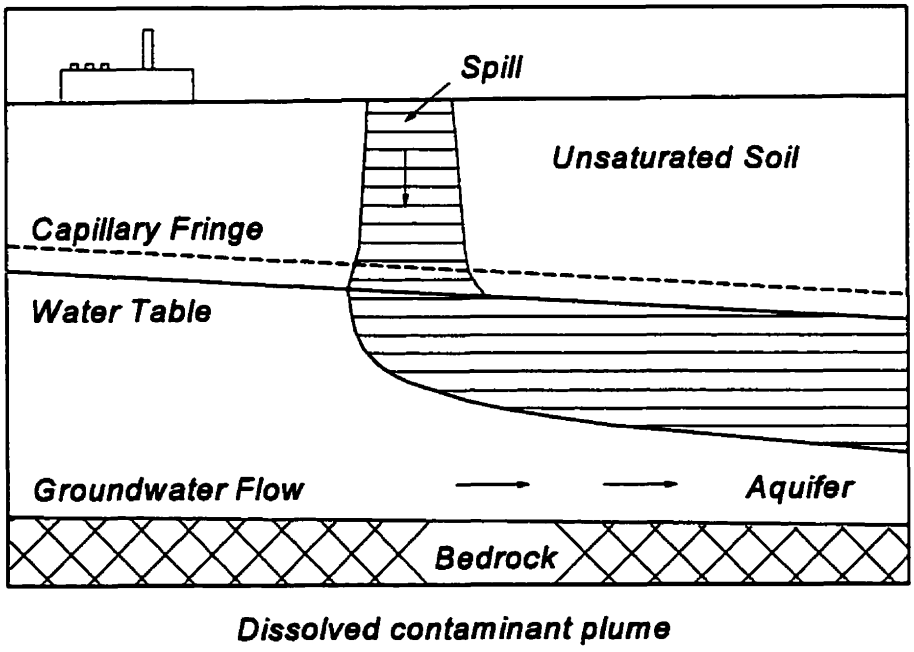

Figure 4: Movement of Dissolved Contaminant Plume (Davis and Cornwell, 1991)

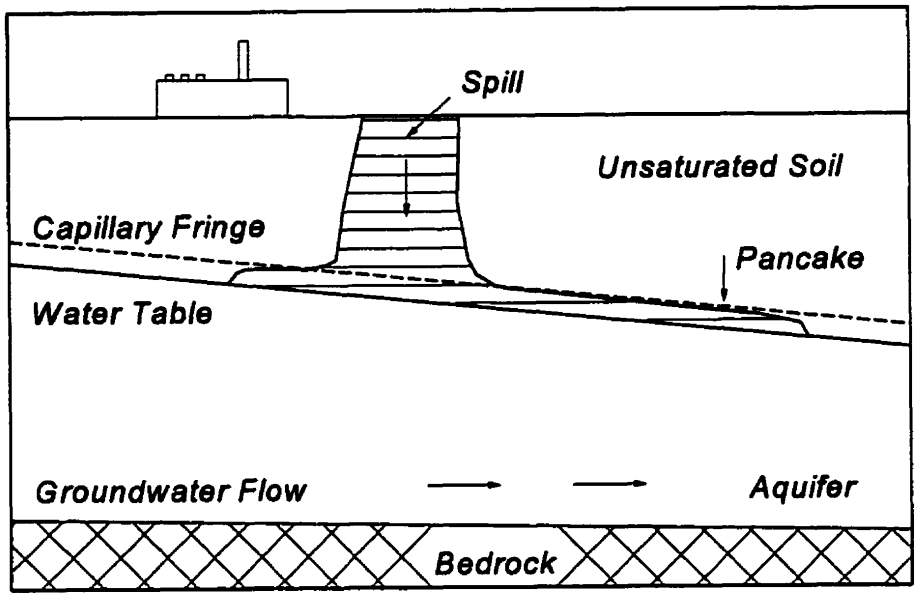

Figure 5: Movement of an Immiscible Contaminant Plume less Dense than Water (Davis and Cornwell, 1991)

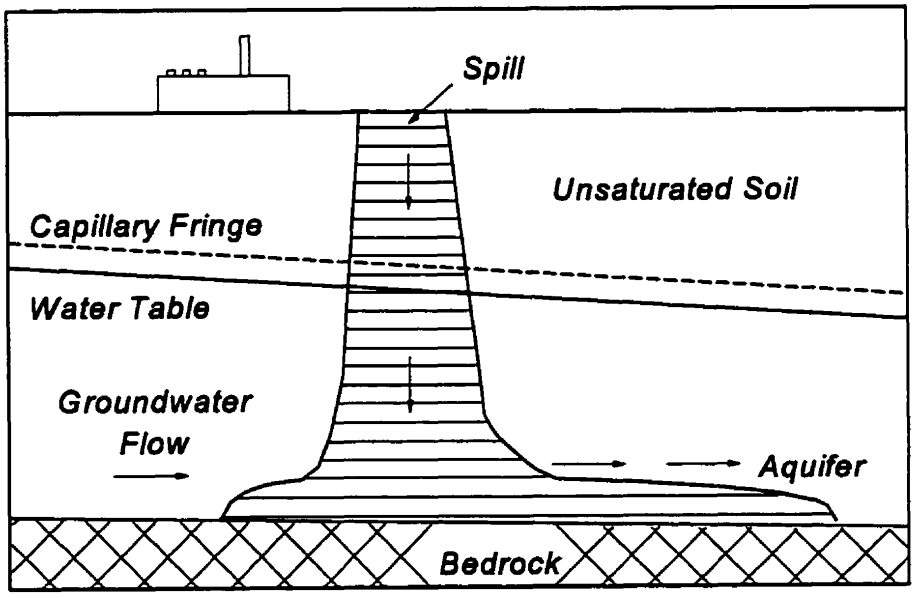

Figure 6: Movement of an Immiscible Contaminant Plume Denser than Water (Davis and Cornwell, 1991)

CHAPTER 3

CAPILLARITY

Capillary pressure and capillary action play a central role in the description of multiphase flow in porous media (Hassanizadeh and Gray, 1993). In addition, viscous and capillary forces significantly influence the effective removal of hydrocarbons from subsurface strata, and for the residual saturations left behind. Therefore, the understanding of the capillarity of the ground water bearing strata is essential for the effective recovery of hydrocarbon contaminant spills.

Capillarity, which is defined as the property or state of being capillary, initially referred to the action of liquids in very small diameter bore tubes, known as capillary tubes (Richards, 1931). In soil science, hydrology, petroleum reservoir engineering, and other fields, the term capillarity is used in connection with a variety of similar fluid phenomena within the confines of the capillary of pore spaces, these being: the thin wedge-shaped (sometimes disc like) open spaces; the sharp corners, very fine or hairlike crevices and interstices; and irregularities at the edges of pore openings of soils, alluvial beds, and sedimentary rock formations (Morrow and Harris, 1965; Richards, 1931). As well, if the whole pore opening is small enough, as in clays, then the whole pore opening is a capillary. Capillarity is the action by which the surface of a liquid-fluid interface, when in contact with a solid, is curved; and this curved interface is called meniscus.

Meniscus means crescent or crescent shaped body. It is the curved upper surface of a liquid in a (partially filled) container where it contacts the solid due to capillarity (Figure

7). The curvature of the interphase surface (meniscus) is the result of cohesion forces minimizing the contact liquid interfacial surface area, and is determined by the geometry of the pore space, the wettability of the solid (rock) surface, and the relative quantity (i.e. saturation) of the wetting phase present (Perkins, 1957).

The classical example of capillarity is the action whereby the liquid-fluid interface in a capillary tube (air-liquid-glass system), is elevated or depressed, Figure 7.

The molecular forces acting in the boundary surfaces of liquids are directly responsible for all capillary phenomena and have their origin in the cohesive and adhesive attractions which are exerted between molecules of fluids in capillary spaces (Richards, 1931). Cohesion is the attraction of the molecules of a pure substance for each other, and by which the molecules of a body are united throughout the substance mass. Adhesion is the molecular attraction exerted between the surface molecules of two different substances (mediums) in contact with each other.

The cohesion and adhesion force (F) is inversely proportional to the distance (r) between the molecules, in the order of : $F = f(r^{-6}$ to $r^{-7})$. Consequently, F diminishes rapidly with distance and approximates zero for a distance in the order of : $r = 10^{-6}$ to 10^{-9} m (Kronig, 1966). Therefore, for the cohesion and adhesion force to work, the distance between molecules must be small enough. For a liquid-liquid and liquid-solid system, the distance between different molecules can be small enough (in the order of the diameter of a molecule) for the adhesion forces to be a real entity. However, for a solid-gas and liquid-gas system, the distance of the solid or liquid surface molecule to the nearest gas molecule is too great to have any effect. Consequently, for solid-gas and liquid-gas systems, the only force

working is the cohesion force of the solid or liquid molecules.

In the center of a pure liquid medium, each molecule is attracted (cohesion) by all those surrounding it, and the net effect is zero. However, at the surface where the molecules are in contact with the molecules of a second pure medium, the molecules in the surface are not only subject to the cohesion forces inwards, but are also countered by the adhesion forces of the molecules across the interface, and vice versa. The net result is that:

a) For a liquid-liquid system, the surface molecules of the liquid with the greater cohesion force tend to be pulled (sucked) into its own body, the number of molecules at the surface becomes the smallest possible when in static equilibrium, and the surface behaves as if it were in tension and had a skin on it. The cohesion and adhesion force acting in the skin is called interfacial tension. It causes a drop of liquid in air, or in an other immiscible liquid body to have the form of a sphere (Calhoun, 1982). This is the smallest surface for a volume of liquid (Experiment of Plateau, Figure 8a (Kronig, 1966)). Richards (1931) identifies this as the most common case of capillary action.

b) For the interface of a liquid-fluid-solid system (e.g. Figure 8b and 8c), when the adhesion force is greater than the cohesion force for a liquid molecule at the solid surface (as in for a water-air-glass system), the liquid molecules tend to spread over the solid surface. Consequently, the liquid is called the wetting phase, the meniscus is concave (hollow shaped), and the fluid tends to rise in a capillary tube dipped in the fluid. On the other hand, when the adhesion force is less than the cohesion force for the liquid molecule at the solid surface (as in for a mercury-air-glass system), the

liquid molecules tend to withdraw from the solid surface. Consequently, the liquid is called the non-wetting phase, the meniscus is convex (ball shaped), and the fluid surface will be depressed when a capillary tube is dipped in the fluid.

c) For a gas-solid or gas-liquid system, the distance between the molecules at the solid or liquid surface to the nearest gas molecule is too great for the adhesion forces to have any effect, and consequently is zero for the molecules on either side of the interface.

Interfacial tension (IFT) is the net result of the molecular cohesion and adhesion forces associated with the boundary layer of a liquid in contact with another medium. It is an expression of the net attractive forces between two adjacent molecules at the boundary surface of a medium. It works in the interfacial surface of two mediums, and tangent to the interfacial surface.

The interfacial tension of a liquid-liquid system is determined by the liquid with the larger surface tension, and the interfacial tension is then approximately equal to the difference of the surface tensions of the two liquids. For instance, the surface tension of water is 72 dynes/cm, and for n-Hexane is 18 dynes/cm. The water - n-Hexane interfacial tension is 51 dynes/cm. Interfacial tension is influenced by a variety of factors like: temperature, pressure, the presence of impurities or dissolved gasses, the composition for petroleum liquids (e.g. the presence of dissolved gasses reduces surface tension, or bitumen like compounds increases surface tension), and the presence of surface active agents (surfactants) in the liquid phase(s) (Lyons, 1996).

In published literature the terms "surface tension" and "interfacial tension" are used interchangeably. The proper term is "interfacial tension", with the term "surface tension" correctly used for a system of a liquid with its own vapour (or air) (Lyons, 1996).

Surface tension is the more commonly used term for surface energy. Surface energy is defined as the amount of work in ergs which must be done to create 1 cm^2 of a liquid surface, while surface tension is defined as the force per unit length (dyn/cm) required to create a unit of liquid surface area. Numerically, surface energy and surface tension are the same value.

Measured at equilibrium conditions, the surface tension of a pure substance and the interfacial tension between two pure substances are definite and constant characteristics of substances (Calhoun, 1982). Surface tension (σ) can be measured in a number of ways; Mungan (1994) lists the following methods: Maximum Bubble Pressure, Drop Volume, Du Nouy Tensiometer, Vertical Plate, Capillary Height, Pendant Drop, Sessile Drop, Furguson's Horizontal Capillary, and Spinning Drop.

The forces which express the molecular actions between the various solid, liquid, and gas phases in a porous medium are called capillary forces (Calhoun, 1982). They result from the combined effects of pore geometry, interfacial tension, and wettability (i.e. contact angle). Interfacial tension alone is insufficient to define capillary forces because it does not describe the manner in which two immiscible fluids behave when together in contact with a solid surface; that is, where their interfacial surface contacts a solid (a third medium). The extra variable necessary to describe this behaviour is the "contact angle" that the fluids interfacial surface (meniscus) makes at the solid surface (Calhoun, 1982).

The contact angle is a measure of the relative adhesional attraction of two fluids with respect to a solid surface, as schematically shown in Figure 9; and is evidence of a general property called "wettability" (Calhoun, 1982). It is a measure of the relative wetting or spreading characteristic by a liquid in the presence of another fluid on a solid surface. In general, for a liquid-liquid-solid system, the liquid with the lowest IFT with the solid surface has the smaller contact angle, and is consequently the wetting phase. The liquid having a contact angle of less than 90° is defined as the "wetting" phase, and the fluid having a contact angle of greater than 90° is defined as the "non-wetting" phase. A liquid having a contact angle of 90° is called a neutral wetting phase.

The distribution of a liquid in a porous system is dependent upon its wetting characteristics (Frick and Taylor, 1962). Because of their effect on the contact angle, adhesive forces are directly involved in an initial wetting process such as the spreading of a liquid on the pore surface of a dry porous (solid) medium (Richards, 1931). Because of the action of interfacial tension, the wetting liquid tends to collect first in the capillary of the porous medium. This is also referred to as the capillary liquid. Depending on the amount of liquid present in the pore medium (also referred as liquid saturation) and by increasing the liquid volume (i.e. saturation), the wetting liquid will then spread in thin films over the surface of the open pores connecting the capillary liquid bodies. But after the solid medium is completely wetted with a thin film (funicular distribution), adhesive forces are no longer effective in producing a motion of the liquid and influence capillary action only to the extend that they hold a thin liquid film firmly in contact with the solid pore wall surface (Richards, 1931). Only when the liquid saturation is greater than the minimum funicular saturation, is

liquid motion by hydraulic forces possible. The "minimum funicular saturation" is here assumed to be as that liquid saturation whereby all liquid is held by capillarity alone for a funicular distribution.

In petroleum engineering, by convention, the contact angle is the angle the "water-oil (or water-gas)" interfacial surface makes with the solid surface, and with respect to the water body, here referred to as θ_{water} (Anderson, 1987). (If the contact angle with respect to the oil body is θ_{oil} , then: $\theta_{water} + \theta_{oil} = 180°$). Then, for those "water-oil-rock" systems whereby $\theta_{water} < 90°$, the rock is defined as water wet, and for those systems whereby $\theta_{water} > 90°$, the rock is defined as oil wet. In a "hydrocarbon liquid-air-rock" system and in a "water-air-rock" system, both liquids are wetting the solid. However, for an "oil-water-rock" system either liquid can be the wetting phase (Lyons, 1996). Individual researchers have identified that petroleum reservoirs range from water wet to oil wet (Frick and Taylor, 1962; Lyons, 1996).

Based on wettability studies (Lyons, 1996) on cores, a qualitative indication of wettability was established consisting of the three regions of wettability: water-wet, intermediate wet, and oil wet. However a quantitative definition of the separation of the three regions is still arbitrary, although there is some consensus for the interval brackets. Generally, the definition of the "water-wet and intermediate-wet" separation is for a contact angle of: $\theta_{water} = 62°$ to $80°$, and for the "intermediate-wet and oil-wet" separation is for a contact angle of: $\theta_{water} = 105°$ to $133°$. With very few exceptions, all hydrocarbon bearing formations are considered intermediate wet.

The measurement of the contact angle for a porous solid medium in petroleum

engineering is a very onerous task seldom yielding conclusive results for a variety of reasons (Calhoun, 1982; Frick and Taylor, 1962; Lyons, 1996; Mungan, 1981), including: the petrology of the detritus strata, the purity of the solid medium in which the pores are located, the geometric aspects of the pores, the mineralization inside the pores, the impact of chemicals used when drilling the core, core preserving technique used, the method of contact angle measurement, and contact angle hysteresis (i.e. "advancing" and "receding" contact angles). Generally, there exists no such thing as an "unaltered core" (Mungan, 1981). Therefore, the contact angle measurement is very difficult and is fraught with uncertainty (Dullien, 1992). Consequently, as Mungan (1981) acknowledges: "The measurement and use of the contact angle in reservoir wettability work is complex, far from routine, and should be done by an expert".

The advancing contact angle is when water is brought into contact with oil on a solid surface previously in contact with oil. The receding contact angle is the contact angle formed when oil comes into equilibrium with water on a surface previously covered with water (Mungan, 1981). Unless otherwise qualified, the term contact angle always refers to "advancing contact angle" as measured in the water phase.

The contentious nature of reservoir rock wettability determination is further evidenced by the work of researchers who arrived at a variety of additional wettability definitions (Lyons, 1996) like: uniform wettability vs fractional wettability; preferential wettability, "squatters rights" concept for intermediate wettability; neutral wettability; heterogeneous wettability, also called spotted or dalmatian wettability; mixed wettability; speckled wettability; advancing and receding contact angles (i.e. wettabilities).

Regardless of the nature of the wettability of a reservoir rock, the general consensus is that the wettability of the hydrocarbon bearing strata plays a role in the recovery of hydrocarbons (e.g. impact on relative permeability curves (Figure 10), residual saturations, mobility ratio, and imbibition (Mungan, 1981; Lyons, 1996)).

3.1 Capillary Tube

A capillary tube is defined as a tube with a diameter that is small enough to cause, when dipped into a strongly wetting liquid (contact angle, $\theta = 0.0°$), the whole air-liquid interfacial surface (meniscus) inside the tube to be completely curved. In general, for a liquid-fluid system in capillarity, the meniscus separates the two fluid phases. The surface of water in an "air-water-glass" system is concave (hollow shape), Figure 7a, as water is the wetting phase. In an "air-mercury-glass" system the mercury surface is convex (ball shape), Figure 7b, as mercury is the non-wetting phase. There where the liquid-fluid interfacial surface (meniscus) contacts the solid is called: "contact line", "common line", "three phase line of contact" (Dullien, 1992), or "meniscus rim".

Consider the rise of a liquid (e.g. water) in a capillary glass tube, Figure 9, (liquid-air-glass system). This figure illustrates the static condition of a liquid held in capillarity. The contact angle (θ) is the angle at which the liquid-fluid interfacial surface contacts a solid surface at the meniscus rim, measured tangent to the interfacial surface, at and perpendicular to the rim. Since surface tension acts in the liquid surface, it acts at the angle "θ" to the solid surface and at the meniscus rim.

For the tube capillarity system shown in Figure 9, the total force in the liquid surface

at the meniscus rim which holds the liquid column up (capillary suction (Mungan, 1981)) is:

$$F_{up} = 2\pi r_t \sigma \cos(\theta) \quad (3)$$

The total force of the weight of the liquid column above the free water table, pulling down at the liquid meniscus in the tube (gravity pull due to the capillary rise (Mungan, 1981)) is:

$$F_{down} = \pi r_t^2 h_c \rho g \quad (4)$$

Under static conditions, these two forces keep each other in equilibrium, and yield the value for the surface tension as follows:

$$F_{up} = F_{down} \quad (5)$$

or:

$$2\pi r_t \sigma \cos(\theta) = \pi r_t^2 h_c \rho g \quad (6)$$

Therefore:

$$\sigma = \frac{r_t h_c \rho g}{2\cos(\theta)} \quad (7)$$

where: r_t = inside radius of the capillary tube

h_c = height of the capillary rise (capillary height)

ρ = density of the liquid

g = acceleration due to gravity

θ = contact angle of the liquid surface with the solid at the meniscus rim

σ = interfacial tension

Researchers have used equation 7 to measure the radii of capillary tubes, surface tension, contact angles, and the height the rise of liquids in capillary tubes (Calhoun, 1982).

The surface tension equation (equation 7) can be rearranged to yield:

$$h_c \rho g = \frac{2\sigma\cos(\theta)}{r_t} \quad \textbf{(8)}$$

From Figure 9 and the equations 7 and 8, the following observations can be made:

1. The meniscus in the capillary tube acts like a piston, and there is a pressure differential (ΔP) between the pressure of the fluid (air) on the convex side of the meniscus and the pressure of the liquid (water) on the concave side of the meniscus. The quantitative value of this pressure differential is related to the capillary height as follows:

$$\Delta P = \frac{F_{down}}{\pi r_t^2} = \frac{\pi r_t^2 h_c \rho g}{\pi r_t^2} = h_c \rho g \quad \textbf{(9)}$$

The pressure of the air (the non-wetting phase) just above the meniscus is higher than the pressure of the liquid (the wetting phase) just below the meniscus by ΔP. Here ΔP is also referred to as capillary pressure, P_c.

2. Equations 7 and 8 for σ and ΔP respectively are for an "air-water-glass" system, whereby the density for air was neglected, because it is many times smaller than the density for water. For an "oil-water-glass" system (with the oil lighter than water and the non-wetting phase) these equations can be derived similarly to yield (Calhoun, 1982; Mungan, 1994):

$$\sigma_{H_2O\text{-}oil} = \frac{r_t h_c (\rho_{H_2O} - \rho_{oil}) g}{2\cos(\theta_{H_2O\text{-}oil})} \tag{10}$$

$$\Delta P = h_c (\rho_{H_2O} - \rho_{oil}) g \tag{11}$$

3. The capillary tube presents a relationship between interfacial tension, contact angle, capillary height, and the inside radius of the tube, as per equation 7. From this relationship the capillary height can be determined as follows:

$$h_c = \frac{2\sigma\cos(\theta)}{r_t \rho g} \tag{12}$$

From this relationship one concludes (Calhoun, 1982) for a capillary tube:

a) The parameter which determines whether a fluid will rise or fall in the capillary tube (Figure 7) is the contact angle.

b) A high surface tension alone will not permit a liquid to rise (or fall) to a great height in capillary.

c) The capillary height is inversely proportional to the tube diameter, consequently, the parameter which has the greatest influence on the capillary height is the inside diameter of the tube.

Correspondingly, for an alluvial strata, the smaller the pores the higher the capillary fringe zone above the water table; and, discontinuities in the pore size in the layers of the alluvial strata may cause limits to the rise of the capillary fringe zone above the ground water table.

3.2 Capillary Pressure

When a discontinuity of phases exists at equilibrium conditions, there will be a pressure differential across the liquid-fluid interphase boundary (Calhoun, 1982). This pressure differential, called capillary pressure (P_c), is related to the curvature of the interfacial surface by the Laplace equation (Lyons, 1996; Mungan, 1981). The Laplace [1839] capillary pressure equation identifies an abrupt pressure difference across the liquid-fluid interfacial (or boundary) surface in capillarity; that is, between the pressure of the non-wetting phase and the pressure of the wetting phase, opposite the interfacial surface (meniscus) under static equilibrium conditions (Morrow and Harris, 1965):

$$\Delta P = P_c = P_{nw} - P_w = \sigma\left(\frac{1}{R_1} + \frac{1}{R_2}\right) \qquad (13)$$

where: ΔP = pressure differential across the interfacial surface boundary

P_c = capillary pressure

P_{nw} = pressure in the non-wetting phase

P_w = pressure in the wetting phase

σ = the interfacial tension in the liquid-fluid interfacial surface (the term fluid meaning either liquid or gas)

R_1, R_2 = two nominal (principal) radii of curvature of the liquid-fluid interfacial surface contained by two mutually perpendicular planes, usually taken as positive if the centre of the curvature lies on the same side of the interface as the non-wetting phase (Morrow and Harris, 1965).

It is customary to introduce the term "mean curvature" (R_m), defined by Dullien (1992) as the harmonic mean:

$$\frac{1}{R_m} = \frac{1}{2}\left(\frac{1}{R_1} + \frac{1}{R_2}\right) \qquad (14)$$

Consequently, the Laplace capillary pressure equation (equation 13) is then written as:

$$P_c = \frac{2\sigma}{R_m} \qquad (15)$$

The Laplace capillary pressure equation assumes a complete liquid wetting of the

solid surface (funicular distribution, $\theta = 0.0°$). To account for a non-zero contact angle, the Laplace equation is written (Calhoun, 1982; Mungan, 1981; and Muskat, 1949) as:

$$P_c = \sigma(\frac{1}{R_1} + \frac{1}{R_2})\cos(\theta) = \frac{2\sigma}{R_m}\cos(\theta) \qquad \textbf{(16)}$$

The capillary pressure is the effect of the exertion of the interfacial tension forces in capillarity, resulting in the advancement (or withdrawal) of the meniscus rim, that is the wetting (or non-wetting) of the solid (porous rock). The radii of curvature of the interphase surface, and hence the capillary pressure, are determined by local pore geometry, wettability, saturation, and saturation history (Anderson, 1987). For porous media of alluvial strata and sedimentary rock formation, the equations for the interfacial curvature are much too complicated, if not impossible, to be solved analytically, and hence, capillary pressure can only be determined experimentally. In these cases, a simple relationship between contact angle and capillary pressure can not be derived (Anderson, 1987). However, the intrinsic nature of capillarity in porous media can be deduced from capillarity for simple pore geometry as shown in the following examples.

3.2.1 A bubble of liquid suspended in a fluid

Because of interfacial tension, a bubble (or drop) of liquid suspended in a fluid will assume the shape of a sphere, the smallest energy level for the system, e.g. the Experiment of Plateau, Figure 8a. Because the liquid - fluid interfacial surface is spherical, the two principle radii of curvature (R_1, R_2) of the interfacial surface are, due to symmetry, equal to

each other, and equal to the radius of the bubble (r_b). For a drop of oil suspended in a fluid, the pressure of the oil (P_o) inside the bubble is greater than the pressure of the all surrounding fluid (P_f) at the same level as the centre of the bubble, and this pressure difference is the capillary pressure for the bubble.

The capillary pressure for a spherical liquid bubble is as follows:

$$P_c = P_o - P_f = \sigma\left(\frac{1}{R_1} + \frac{1}{R_2}\right) = \frac{2\sigma}{r_b} \qquad (17)$$

The capillary pressure for the bubble of liquid is inversely proportional to the radius of the bubble, and therefore, the bigger the bubble the smaller the capillary pressure. Consequently, it is easier to break up a big bubble (into smaller ones) than a small bubble, and therefore:

a) Emulsions are very difficult to alleviate in oil field production operations.

b) For a water flood, small bubbles of oil (or gas for that matter) inside the pore openings of a porous rock, which is completely water wet, cause blocking of water movement through the porous media, in the event that the pore throat vs pore size ratio is sufficiently small enough (Jamin effect).

3.2.2 A horizontal liquid table

For a liquid - air interfacial surface in a wide container in equilibrium, the interfacial surface is flat, a horizontal "free liquid surface". This flat surface can be considered as a portion of a sphere with a radius of infinite (∞) proportion. Two perpendicular planes with

a common line perpendicular to the flat liquid surface, will intersect the sphere according to two circles, both with a radius of infinite (∞) length. Due to symmetry therefore, the two principle radii of curvature of the liquid surface are equal to each other ($R_1 = R_2$), and equal to the radius of the sphere (r_s). Consequently, the capillary pressure for a flat liquid surface (e.g. a water table) is:

$$P_c = P_o - P_f = \sigma(\frac{1}{R_1} + \frac{1}{R_2}) = \frac{2\sigma}{r_s} = \frac{2\sigma}{\infty} = 0 \qquad (18)$$

3.2.3 A vertical capillary tube

The Laplace capillary pressure equation can be used to solve for the capillary pressure as function of IFT, contact angle, and the radius of the tube (r_t), Figure 9. For the capillary tube the meniscus (i.e. liquid-fluid interphase surface) can be approximated as a portion of a sphere (with radius r_s) at the meniscus rim. Because the liquid surface is spherical, the two principle radii of curvature are, due to symmetry, also equal to each other ($R_1 = R_2$), being the two circular intersections of two perpendicular planes through the sphere with a common line through the centre of the tube. The radius of the interfacial sphere can then be expressed in the radius of the tube as follows:

$$r_t = r_s\cos(\theta) \qquad (19)$$

The Laplace capillary pressure can then be written as:

$$P_c = \sigma\left(\frac{1}{R_1} + \frac{1}{R_2}\right) = \frac{2\sigma}{r_s} = \frac{2\sigma\cos(\theta)}{r_t} \qquad (20)$$

This equation is equal to the previously established capillary pressure equation for a vertical tube (combination of equations 8 and 9).

3.2.4 A horizontal capillary tube (Case 1)

Consider a horizontal cylindrical capillary tube, half filled with water, the wetting phase, and the other half filled with oil, the non-wetting phase; with the two phases separated by a meniscus (interfacial surface) approximately in the middle of the tube, as shown in Figure 11.

Assuming static equilibrium conditions, that is the meniscus stays in place, then:

a) The pressure in the water phase in the centre of the capillary tube is:

$$P_w = h_w \rho_w g \qquad (21)$$

the pressure in the oil phase in the centre of the capillary tube is:

$$P_o = h_o \rho_o g \qquad (22)$$

The pressure in the oil phase (P_o) and the water phase (P_w) is in equilibrium with the capillary pressure (P_c), as follows:

$$P_w + P_c = P_o \qquad (23)$$

or:

$$P_c = P_o - P_w = (h_o\rho_o - h_w\rho_w)g \qquad (24)$$

This identifies (EPRCo, 1968) that:

i. An "entry pressure" equal to the capillary pressure is required to force the oil (or gas for that matter) into a water filled capillary.

ii. A "suction pressure" equal to the capillary pressure is required to cause water to spontaneously imbibe into an oil filled capillary.

b) As for the vertical capillary tube, the curvature of the interfacial surface at the meniscus rim can be expressed in the radius of the tube as follows:

$$r_t = r_s\cos(\theta) \qquad (25)$$

And, along similar lines as for the vertical capillary tube, the Laplace capillary pressure equation can be written as follows:

$$P_c = \sigma\left(\frac{1}{R_1} + \frac{1}{R_2}\right) = \frac{2\sigma}{r_s} = \frac{2\sigma\cos(\theta)}{r_t} \qquad (26)$$

This equation is equal to the previously established capillary pressure equation for a vertical capillary tube, equation 20.

c) The capillary phenomena in the vertical and horizontal capillary tubes can be extended to a porous media in that the capillary pressure is a measure of the tendency (or force) of the wetting phase to wedge out (drive out) the non-wetting phase from

the capillary pore space, also referred to as imbibition. The strength of this tendency (or force) depends on the contact angle (the wedge) for the wetting fluid and the (average) pore size (or radius of the channel) of the alluvial strata or the sedimentary rock formation. That is, the smaller the contact angle and/or the smaller the capillary pore space, the stronger the tendency (i.e. the capillary pressure). Or, the capillary pressure is the incremental pressure that the wetting phase meniscus imposes on the non-wetting phase in the capillary of a porous medium, due to interfacial tension forces (i.e. molecular cohesion and adhesion forces) alone.

Imbibition, sometimes also referred to as spontaneous imbibition, is a process in which a wetting fluid will enter and replace a non-wetting fluid from a porous medium by the action of capillary forces alone, i.e. without a driving pressure force (Mungan, 1981).

Richardson [1961] has found that the rate of imbibition depends on such factors as permeability of the porous medium, wettability (θ), pore structure and pore size distribution, pore throat versus pore size ratio, viscosity of the fluid and the interfacial tension between the two fluid involved (Mungan, 1981).

3.2.5 A horizontal capillary tube (Case 2)

When more than one interface (meniscus) is present in a given channel, conditions may be such that the resistance to flow is markedly increased or may become great enough to prohibit flow. This is named after its discoverer, Jamin (Calhoun, 1982).

Consider a discrete bubble of oil inside a horizontal cylindrical capillary tube (porous

channel) filled with water, as shown in Figure 12a. The oil is immiscible with water, with water as the wetting phase and oil as the non-wetting phase. In this scenario there are two interfaces, with the capillary pressure drop across each interphase the same but in opposite direction to each other.

The pressure exerted by the water on the oil bubble via the "A" side meniscus is:

$$P_A + P_{c-A} \tag{27}$$

The pressure exerted by the water on the oil bubble via the "B" side meniscus is:

$$P_B + P_{c-B} \tag{28}$$

where: P_A = the pressure in the wetting phase on the left or "A" side of the oil bubble in the tube

P_B = the pressure in the wetting phase on the right or "B" side of the oil bubble in the tube

P_{c-A} = the capillary pressure exerted on the oil bubble by the meniscus on the "A" side

P_{c-B} = the capillary pressure exerted on the oil bubble by the meniscus on the "B" side

Assuming static equilibrium conditions (i.e. the bubble does not move), the pressures exerted by the water on either side of the oil bubble are in equilibrium (but in opposite direction), therefore:

$$P_A + P_{c-A} = P_B + P_{c-B} \tag{29}$$

Consequently, for equilibrium conditions:

$$P_B - P_A = P_{c-A} - P_{c-B} = 0 \tag{30}$$

or:

$$P_B - P_A = \left(\frac{2\sigma\cos(\theta)}{r}\right)_A - \left(\frac{2\sigma\cos(\theta)}{r}\right)_B = 0 \tag{31}$$

Now, if either capillary pressure term of the right hand side of the equation were modified, the net pressure drop between points "A" and "B" would not be zero. This condition gives the Jamin effect, i.e. a resistance to flow. The difference may not be zero due to a change in any of the three parameters: r, σ, or θ, for side "B" as compared to side "A" as shown in the following three examples.

3.2.5.1 Variation in channel radius

Consider a variation in radius as shown in Figure 12b. The capillary is no longer considered to have a uniform radius. The difference in pressure between points "A" and "B" is now:

$$P_B - P_A = \left(\frac{2\sigma\cos(\theta)}{r_A}\right) - \left(\frac{2\sigma\cos(\theta)}{r_B}\right) \tag{32}$$

or,

$$P_B - P_A = 2\sigma\cos(\theta)\left(\frac{1}{r_A} - \frac{1}{r_B}\right) \quad (33)$$

Inasmuch as r_B is less than r_A, a positive pressure is required at point "A" to retain the bubble in the position shown in the figure. If the water flow were to the right (i.e. deeper into narrowing capillary), a bubble of oil (or gas for that matter) in the water stream could block such a channel until the pressure drop between points "A" and "B" was sufficiently great to push the bubble past the smallest constriction (the pore throat) at the point where the channel again widened.

3.2.5.2 Variation in contact angle

Consider a variation in contact angle as shown in Figure 12c. This situation generally occurs when there is a difference in advancing and receding contact angles. The contact angle at "A" is defined as an "advancing contact angle", and that at "B" the "receding contact angle" (for the case that water flows from left to right). The former is always larger that the latter (Calhoun, 1982). Such a deformation of a bubble takes place when it is on the verge of movement, toward the right as shown in Figure 12c. The resulting pressure between points "A" and "B" then is:

$$P_B - P_A = \frac{2\sigma}{r}(\cos(\theta_A) - \cos(\theta_B)) \quad (34)$$

Inasmuch as θ_A is larger than θ_B, P_A will be larger than P_B, i.e. a positive pressure drop between "A" and "B" is necessary to initiate flow to the right. A total of "n" such

bubbles within a tube would require a pressure drop of: $n(P_B - P_A)$ to move them.

3.2.5.3 Variation in interfacial tension

Consider a variation in interfacial tension. This situation occurs, for example, if a bubble of gas is straddled by water and oil, as shown in Figure 12d; in which it is assumed that the contact angle for either gas-liquid interface with the solid is the same (this is generally not the case). The net effect is a pressure difference between points "A" and "B":

$$P_B - P_A = \frac{2}{r}(\sigma_A \cos(\theta_A) - \sigma_B \cos(\theta_B)) \qquad (35)$$

Again, if "$\sigma_B \cos(\theta_B)$" is greater than "$\sigma_A \cos(\theta_A)$", a positive pressure drop from "A" to "B" would be necessary to initiate flow to the right.

In the above three parameter (r, σ, and θ) examples, the absolute pressures of P_A and P_B are not considered (which is the operating reservoir pressure, and could be in the order of thousands of pounds per square inch). The magnitude of the pressure drop between points "A" and "B" (e.g. for a particular reservoir flow channel) is related to the number of flow channels that would be blocked by the Jamin effect, and it is in direct proportion to the total number of oil (or gas) bubbles that exist in a given flow channel (Calhoun, 1982).

3.3 Capillarity in Porous Media

3.3.1 Pore geometry of perfect spheres

Capillary action and pressure both play a central role in the description of multiphase flow in porous media (Hassanizadeh and Gray, 1993). The porous medium of hydrocarbon

or water bearing subterranean strata varies in complexity of pore structure and associated tortuosity of flow channels. To explain the basic concepts of capillary behaviour for such a medium, an ideal pore structure is required. The ideal pore configuration usually chosen is one made up of spherically uniform particles of a definite size (e.g. a glass bead of a specific mesh size).

Consider two spherical grains (or glass beads) in contact as shown in Figure 13, with a wetting liquid in capillarity at the point of contact, for a pendular liquid distribution system. The capillary pressure for this system is given by:

$$P_c = \sigma\left(\frac{1}{r_1} + \frac{1}{r_2}\right)\cos(\theta) \qquad \textbf{(36)}$$

where r_1 and r_2 are the principle radii defining the curved liquid-fluid interfacial surface as shown. The centre of the meniscus curvature for r_1 is in the non-wetting phase, and therefore is taken positive. The centre of the interfacial curvature r_2 is in the wetting phase, and therefore is taken negative, whereby $r_2 > r_1$. The values of r_1 and r_2 reflect the amount of liquid that is contained at the contact, and therefore reflect the saturation of that liquid present in the porous media if a number of such contacts are considered. Since r_1 and r_2 are proportional to the liquid saturation (i.e. the fractional pore volume occupied by the wetting phase), the capillary pressure increases with the reduction of the liquid saturation; and therefore, capillary pressures are commonly displayed as a function of liquid (e.g. water) saturation (Hagoort, 1988).

Nerpin [1970] (Lu *et al.*, 1995) calculated the height of capillary rise, h_c, into an

idealized porous medium of spheres to be:

$$h_c = \frac{4\sigma}{\rho g R_s} \tag{37}$$

where: R_s = the radius of the solid spheres

Nerpin developed this equation from an analysis of the liquid meniscoid necks (i.e. pendular rings) between the spheres and the contact angle, which he assumed to be zero. Nerpin's equation suggests that the capillary rise in a dry glass bead pack is twice the capillary rise for a capillary tube, assuming $R_s = r_t$, and a contact angle of zero.

When describing capillary rise into porous media, it is common in the literature to use a system of capillary tubes with different diameters to describe capillary rise into porous media (Anderson, 1987; Lu *et al.*, 1994). Qualitatively the comparison has merit but quantitatively, although directionally correct, it has discrepancies (Richards, 1931).

Lu *et al.* (1995) studied the capillary rise into initially dry glass bead porous media, and compared this with the capillary rise in a capillary tube. They studied four packing arrangements of uniform spheres: cubic, orthorhombic (hexagonal), tetragonal sphenoid, and rhombohedral, for which they determined the porosity and the capillary height, Table 5. They concluded that:

1. The capillary rise into a porous medium is different from that into a capillary tube. The capillary rise into an initially dry glass bead porous medium is not stable, with any slight disturbance being able to slow down or even stop the process.
2. The maximum possible height of the capillary rise into an initially dry glass bead

porous medium with radius R_s is 1.65 - 3.00 times higher than that into a cylinder of the same internal radius (r_t), when the contact angle is zero. This comparison goes limp in that R_s is the radius of the solid sphere, whereas r_t is the inside diameter of the hollow space inside the tube; although admittedly, the smaller the radius of the sphere, the smaller the pore space between the spheres.

Lu *et al.* (1994) further comment that the capillary rise into porous media is a two-dimensional movement with sequential jumps and water film thickening associated with water film flow. The contact angle between liquid, gas, and solid plays an important role in this process inasmuch as it can change the initiation point of the jump. It also causes differences for capillary rise into initially dry and initially wet profiles, as its value along the water films relates to a receding contact angle produced by a previous drying process as compared to the capillary rise into an initially dry profile, when it relates to an advancing contact angle at the wetting front. The length of contact lines associated with the gas-liquid interface is much longer in an initially dry profile.

3.3.2 Non-uniform pores of ground water bearing strata

The fluid distribution and capillary character of a non-ideal porous medium is influenced by several factors, which can be categorized as follows (Hassanizadeh and Gray, 1993; Rose and Bruce, 1949):

a) Geometry of the porous medium - this includes the consideration of the packing of the particles in the porous medium, grain size distribution, and microscale and

macroscale heterogeneties. The packing of the medium itself is subject to solid matrix deformation, and secondary processes of mineralization, which introduces factors of cementation, and of solution action which causes alteration of pore structure.

b) Physical and chemical nature of the interstitial spaces - this includes the consideration of the wettability of the solid surfaces, the existence of non-uniform wetting surfaces, and the presence of microscopic scale fluid-fluid interfaces.

c) Physical and chemical properties of the fluid phases - this includes surface, interfacial, and adhesion tensions, contact angles, viscosity, density difference between immiscible phases, and other fluid properties.

It is generally considered that all ground water bearing alluvial formations and soils are water wet. However, because hydrocarbon liquids also wet dry alluvial strata, the preferential wettability of the strata plays a role in the recovery of hydrocarbon contaminants from the zone of aeration and therefore from the capillary fringe zone (extrapolation from petroleum engineering concepts).

In the zone of aeration, the liquid films on the pore walls (pellicular water) connecting the liquid bodies in the capillary spaces tend to dry up first, because it has the larger surface area. This results in the break up of the hydrological continuity; it causes the water bodies in the capillary spaces to become isolated from each other and to retract within the confines of the capillary (pendular distribution). Further aeration will then dry up the water bodies in the capillary spaces, but at a much reduced rate due to the limited surface

exposed to aeration, and subject to the capillary rise from the water table (capillary suction).

The movement of water in the capillary fringe zone is only possible for the pellicular water (funicular) distribution.

3.4 Capillary Hysteresis

Capillary hysteresis is the retardation or discrepancy of the capillary effect due to the difference in capillarity for the drainage process as compared with that of the imbibition process.

Imbibition is the capillary process in which a wetting fluid will enter and displace a non-wetting fluid from a porous medium by the action of capillary forces, starting with the smaller pore spaces and pore throats, or capillary spaces. Drainage is the capillary process in which a non-wetting fluid will (i.e. is forced to) enter and displace a wetting fluid from a porous medium, starting with the larger pore openings or non-capillary spaces, by applying an external force and against the action of capillary forces.

For the drainage and imbibition capillary process the irreducible saturation is reached when the hydraulic continuity is lost (Anderson, 1987). The irreducible wetting phase saturation constitute capillary liquid while the irreducible non-wetting phase saturation is caused by liquid entrapment, due to capillary effect in the pores.

Capillary hysteresis implies that the capillary effect in a porous medium is subject to the liquid saturation history of the medium. The saturation history causes a hysteresis in the contact angle (advancing and receding contact angles), Figure 14, and consequently results in a hysteresis in relative permeability and capillary pressure curves, Figure 15.

Capillary hysteresis is conceptually illustrated in Figure 16 (Mungan, 1981). Consider three water-wet capillaries, two of uniform radius (r_1 and r_2), and a third of radius r_1 with a bulb (with a radius r_2) located in the middle of the tube. If all three tubes are initially full of water (due to the water table level being high), and are then subject to a lowering of the water table level (drainage process), the final equilibrium position would then be as shown in the figure. Tubes 1 and 3 will drain to a height dictated by the Laplace equation, while Tube 2 will drain to the same height as Tube 1, as the radius at that position is the same. On the other hand, in an imbibition process situation all the tubes are empty, and then are subject to a rise in water level in the tube. The rise in the two uniform tubes will be the same as before. However, for Tube 2, the water will rise to an elevation inside the bulb where the radius of the bulb equals r_2. Thus, the non-uniform tube gives different saturations depending on whether the saturation is approached by the drainage process (the non-wetting phase displacing the wetting phase) or by the imbibition process (the wetting phase displacing the non-wetting phase).

Literature suggests that contact angle hysteresis is caused by a variety of factors, including roughness of the solid surface, adsorption effects, solid surface impurities, and elastic forces developed within the solid-fluid interfacial surface that act upon the contact line and resist its movement. Hassanizadeh and Gray (1993) concluded that the primary cause of the hysteresis is the fact that the stresses in the solid-fluid interface will develop such that they will oppose the movement of the contact line, and these stresses are different for the drainage as compared to the imbibition capillary process. Others attribute hysteresis to contact angle effects and non-wetting fluid entrapment (Lu *et al.*, 1994). Morrow and

Harris (1965) identify that "Except where there is no hysteresis of contact angle and the solid is of simple geometry (such as a capillary tube of uniform cross section), there is hysteresis in the relationship between capillary pressure and saturation".

Table 5: Comparison of Parameters (Lu *et al.*, 1995)

Packing or Model	Porosity	Capillary Rise (h_{cp})	h_{cp}/h_{cpt} ($\theta = 0$)
Cubic Packing	0.4764	$3.2973(\gamma \cos^2(\theta/2))/(\rho g R_s)$	1.65
Hexagonal Packing	0.3954	$4.5872(\gamma \cos^2(\theta/2))/(\rho g R_s)$	2.29
Tetragonal Packing	0.3019	$5.2036(\gamma \cos^2(\theta/2))/(\rho g R_s)$	2.60
Rhombohedral	0.2595	$6.0527(\gamma \cos^2(\theta/2))/(\rho g R_s)$	3.03
Capillary Tube		$2\gamma \cos(\theta)/(\rho g r_t)$ $(= h_{cpt})$	1.0
Nerpin's Model		$4\gamma/\rho g R_s$, $(\theta = 0)$	2.0

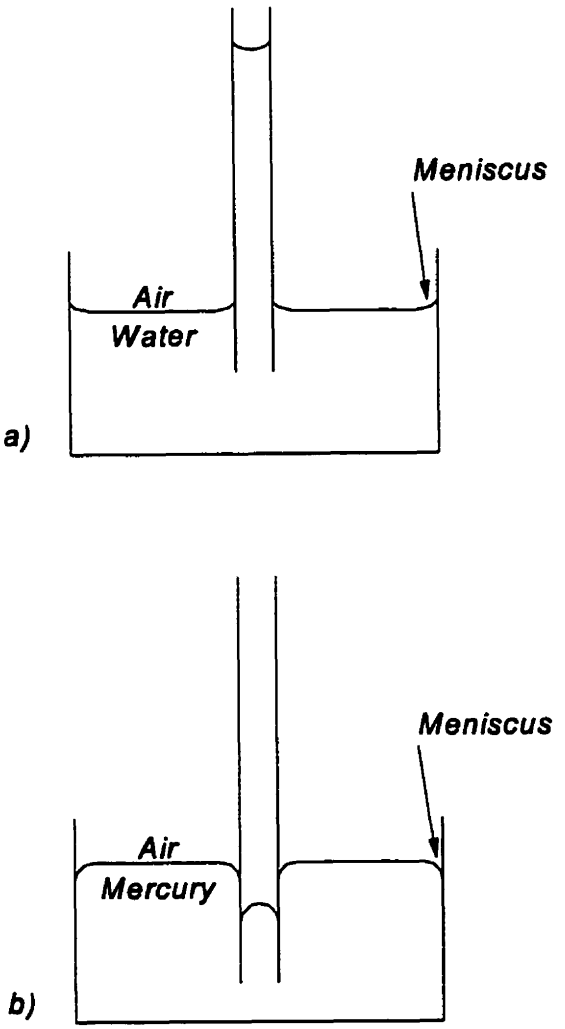

Figure 7: Capillary Phenomena in a Glass Capillary Tube (Calhoun, 1982)

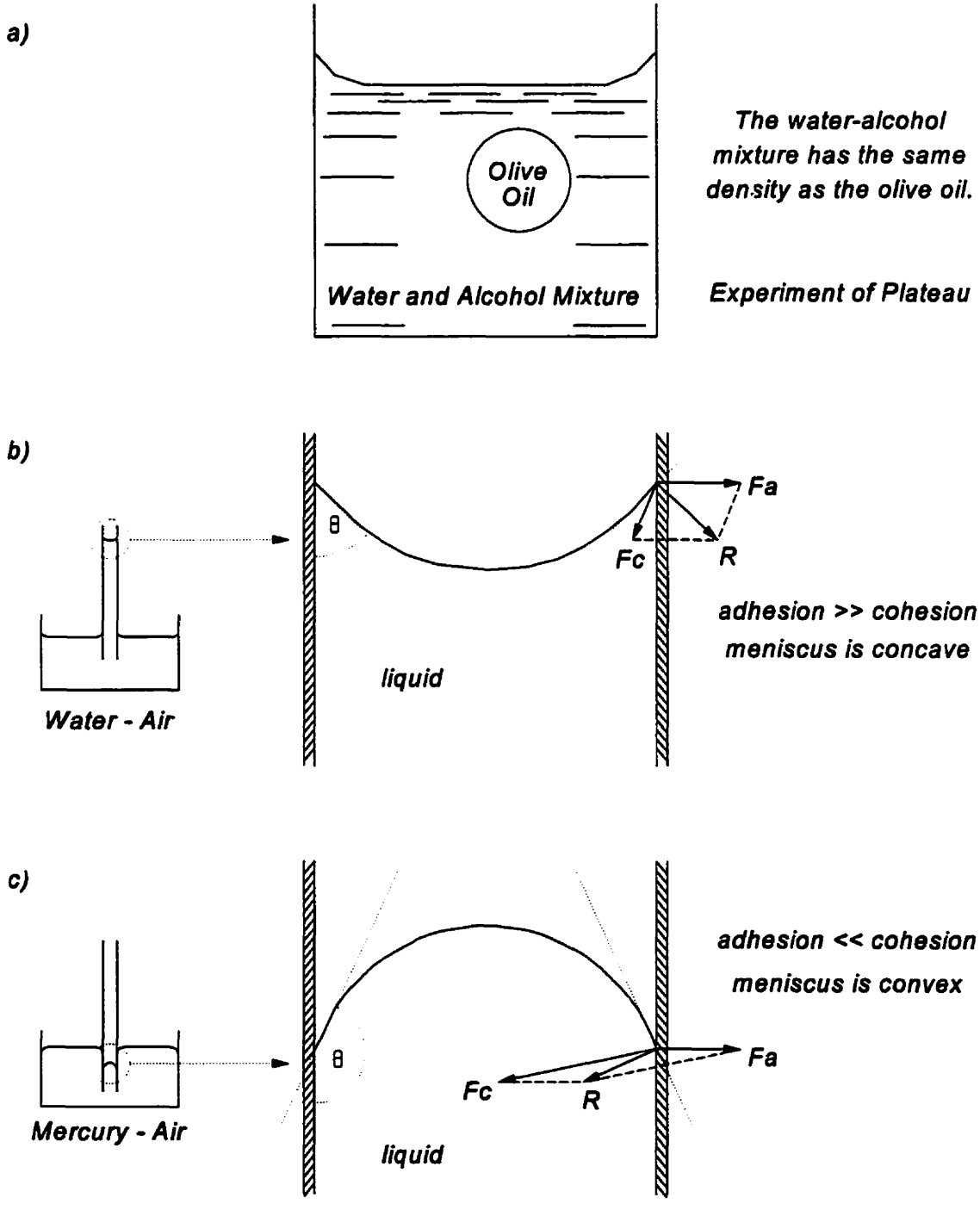

Figure 8: Capillary Phenomena (Kronig, 1966)

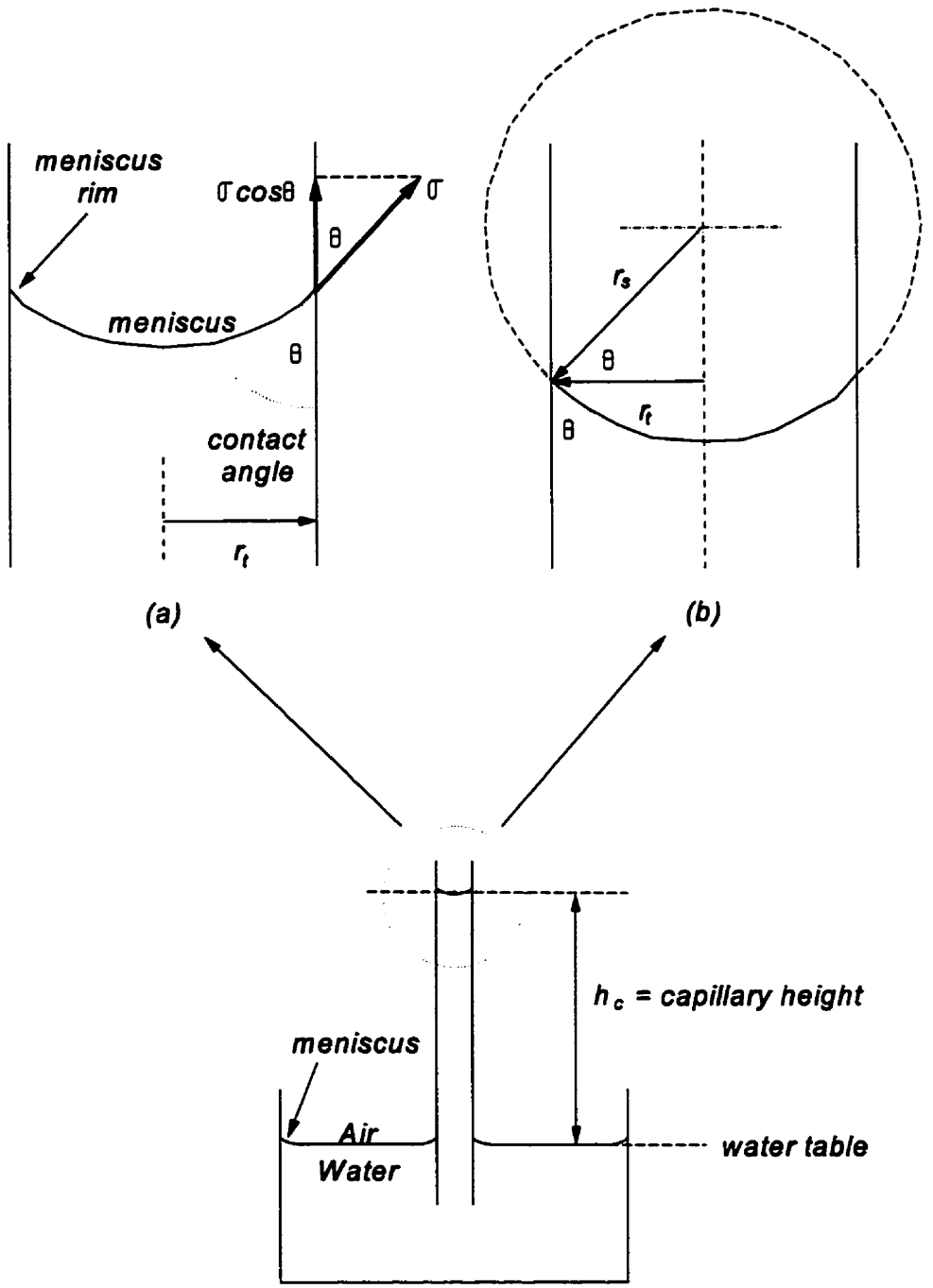

Figure 9: Vertical Capillary Tube (Bouman and Westerdijk, 1956)

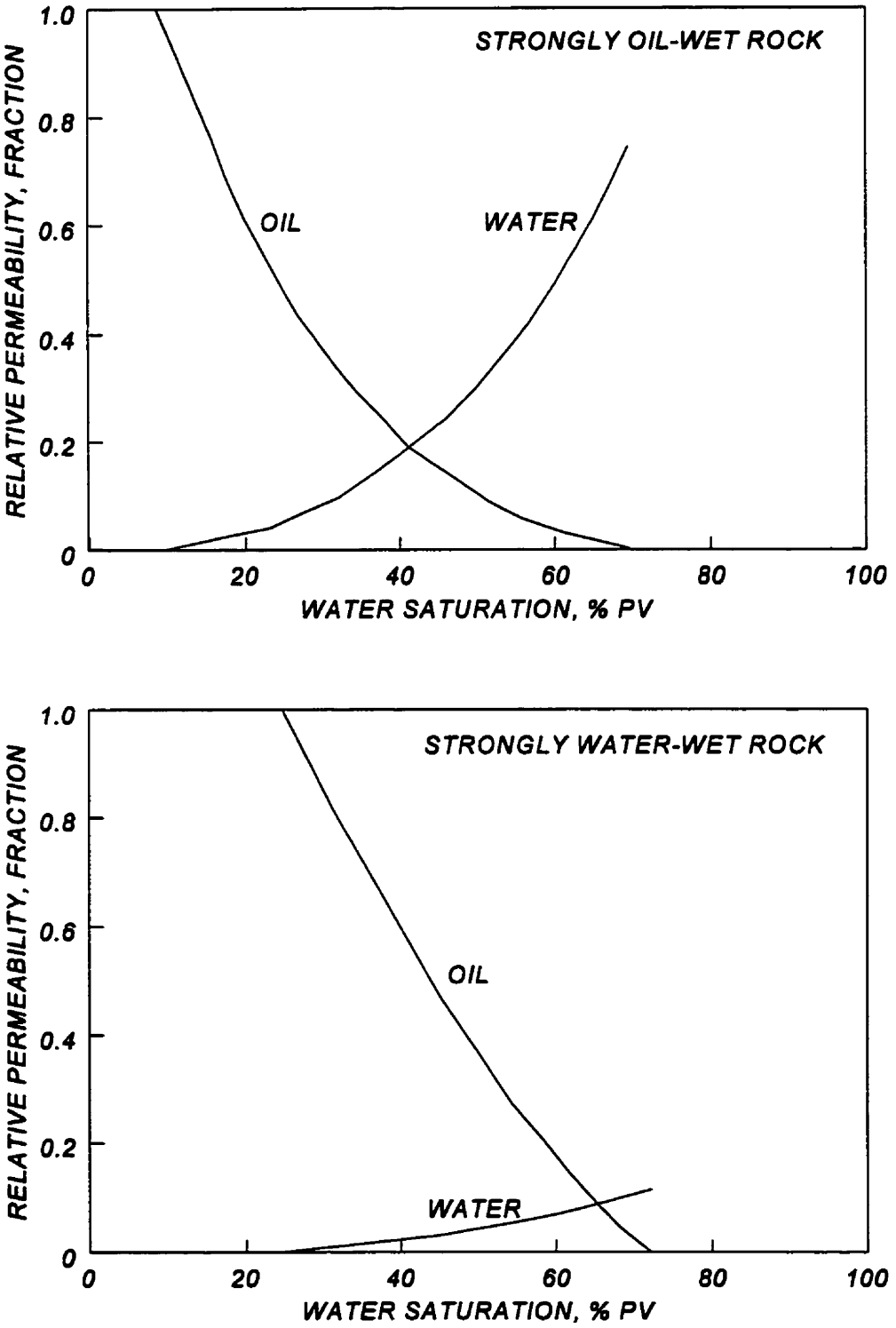

Figure 10: Relative Permeability Curves for Strongly Oil-Wet and Water-Wet Reservoir Rock (Craig, Jr., 1993)

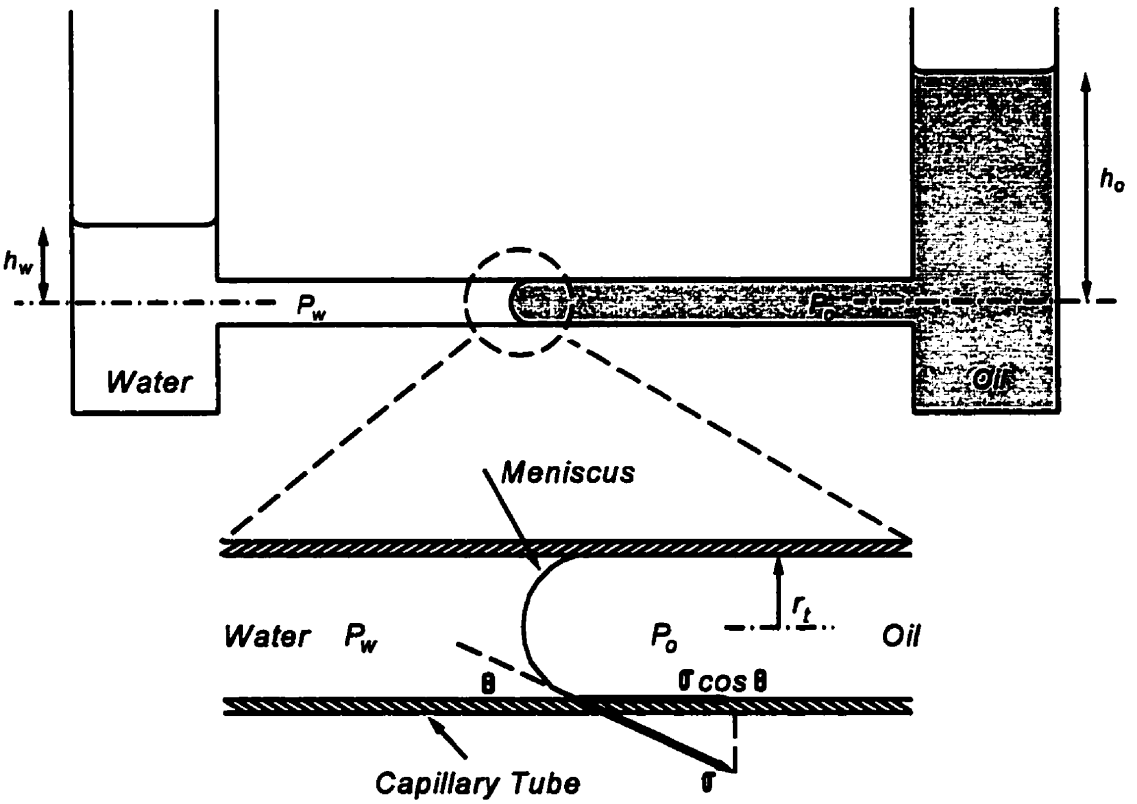

Figure 11: Horizontal Capillary Tube, Case 1 (Calhoun, 1982; EPRCo, 1968)

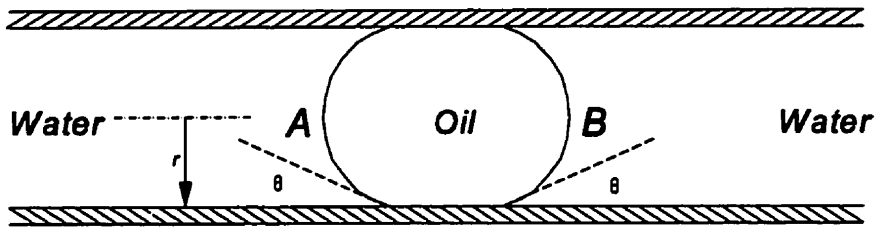

a) Two Fluid Phases

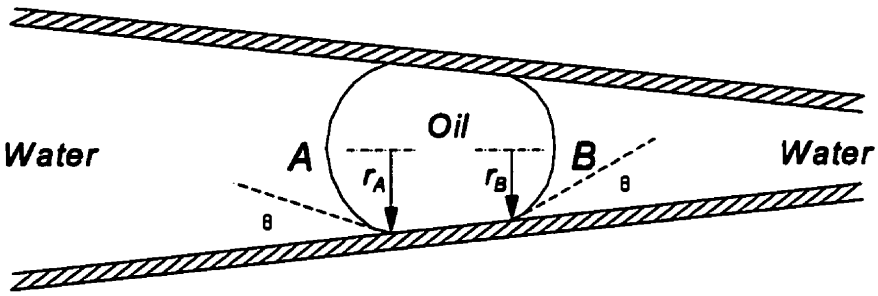

b) Two Fluid Phases: Variation in Channel Radius

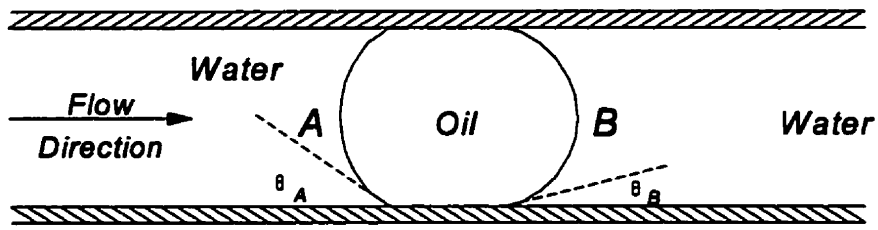

c) Two Fluid Phases: Variation in Contact Angle

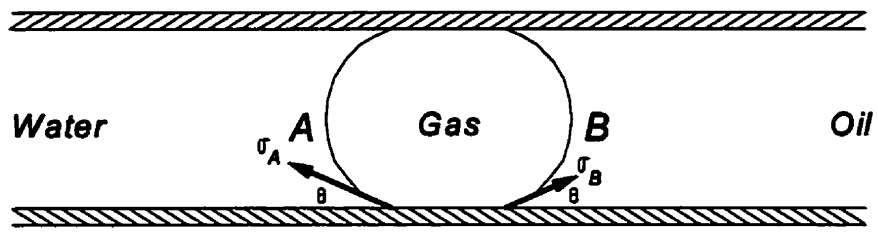

d) Three Fluid Phases: Variation in Interfacial Tension

Figure 12: Horizontal Capillary Tube, Case 2 (Calhoun, 1982)

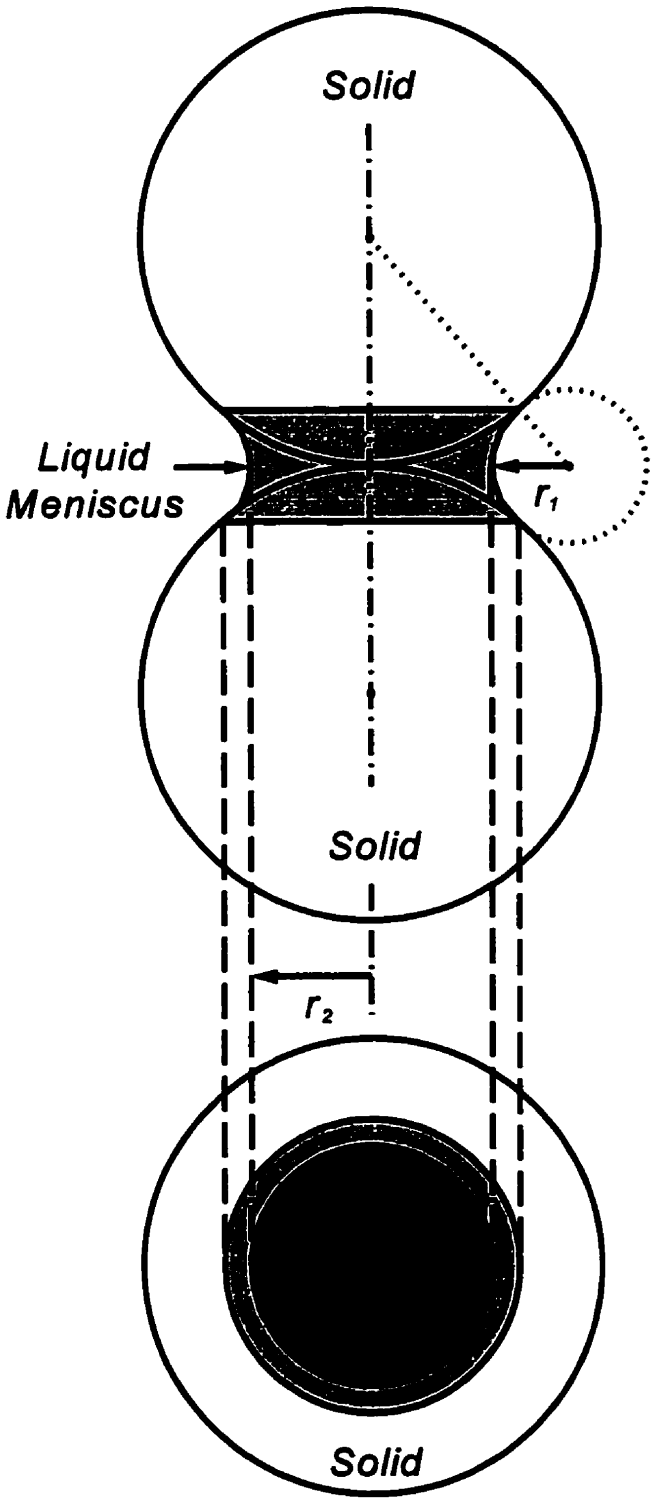

Figure 13: Capillary Phenomena in Porous Media of Perfect Spheres for a Pendular Liquid Distribution, (Amyx *et al.*, 1960; Leverett, 1941)

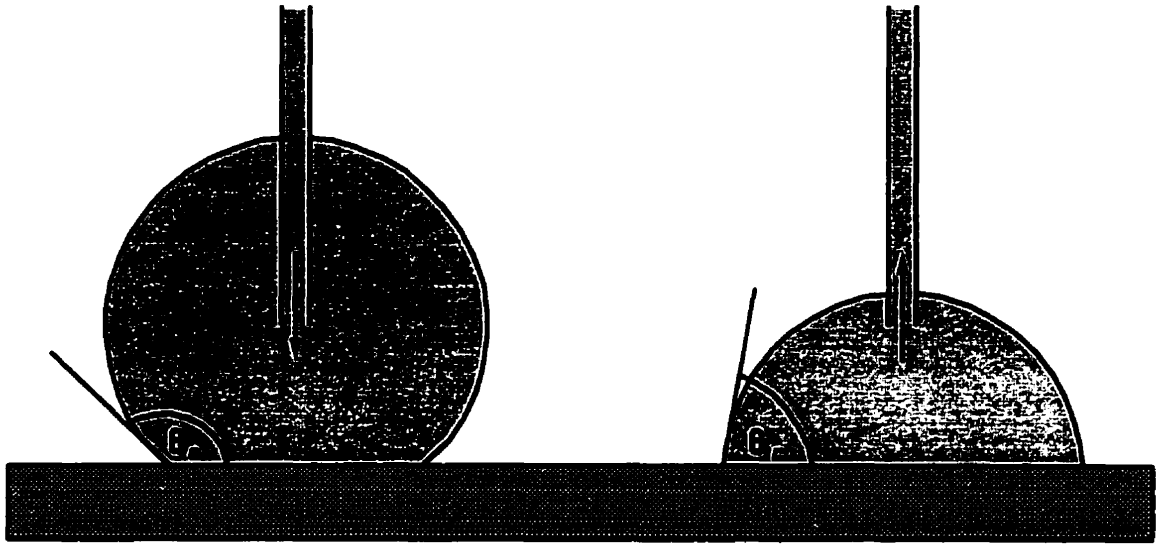

Figure 14: Schematic of Hysteresis in Contact Angle

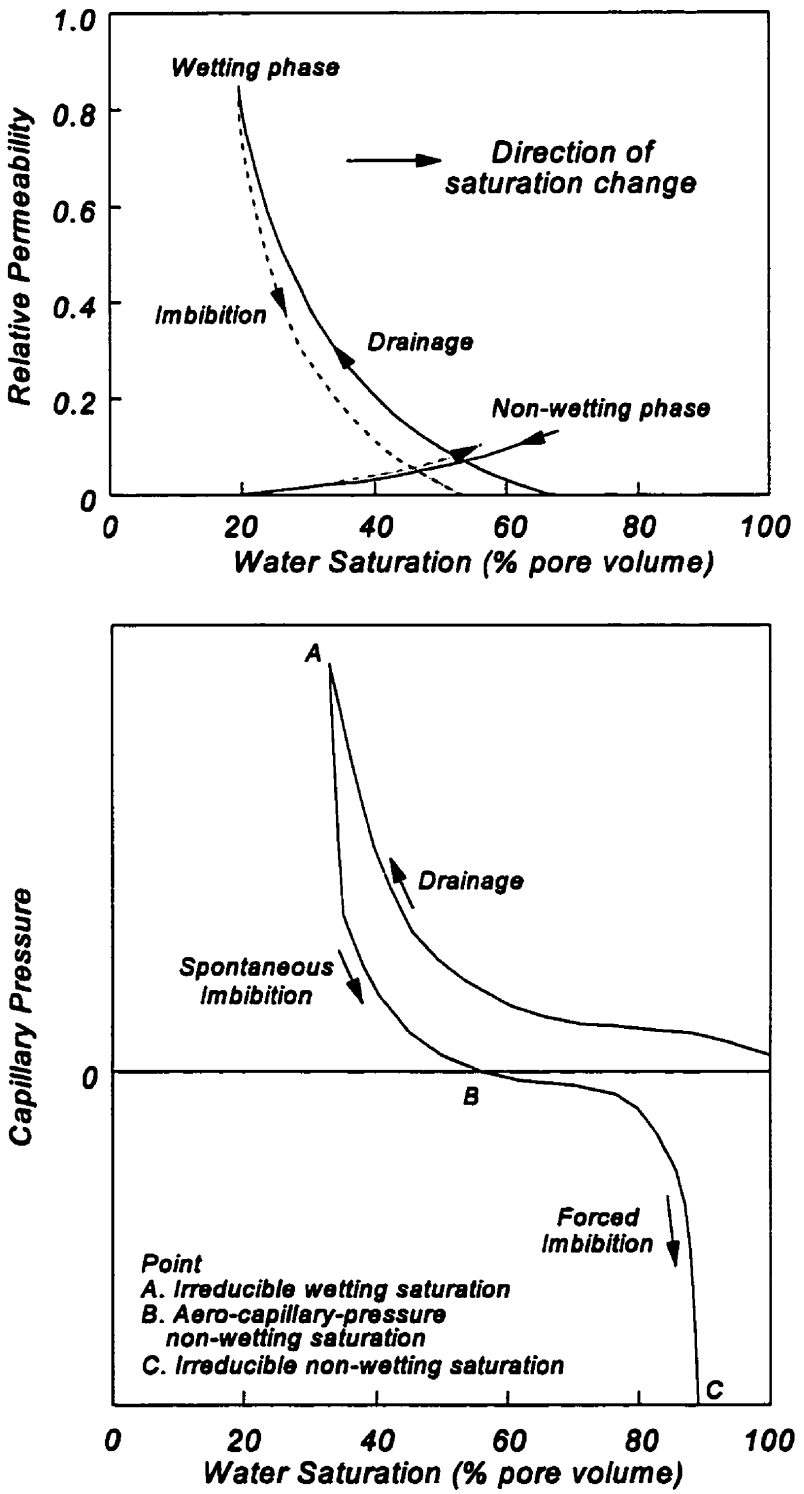

Figure 15: Schematic of Drainage and Imbibition Relative Permeability (Mungan, 1981) and Capillary Pressure (Anderson, 1987) Curves

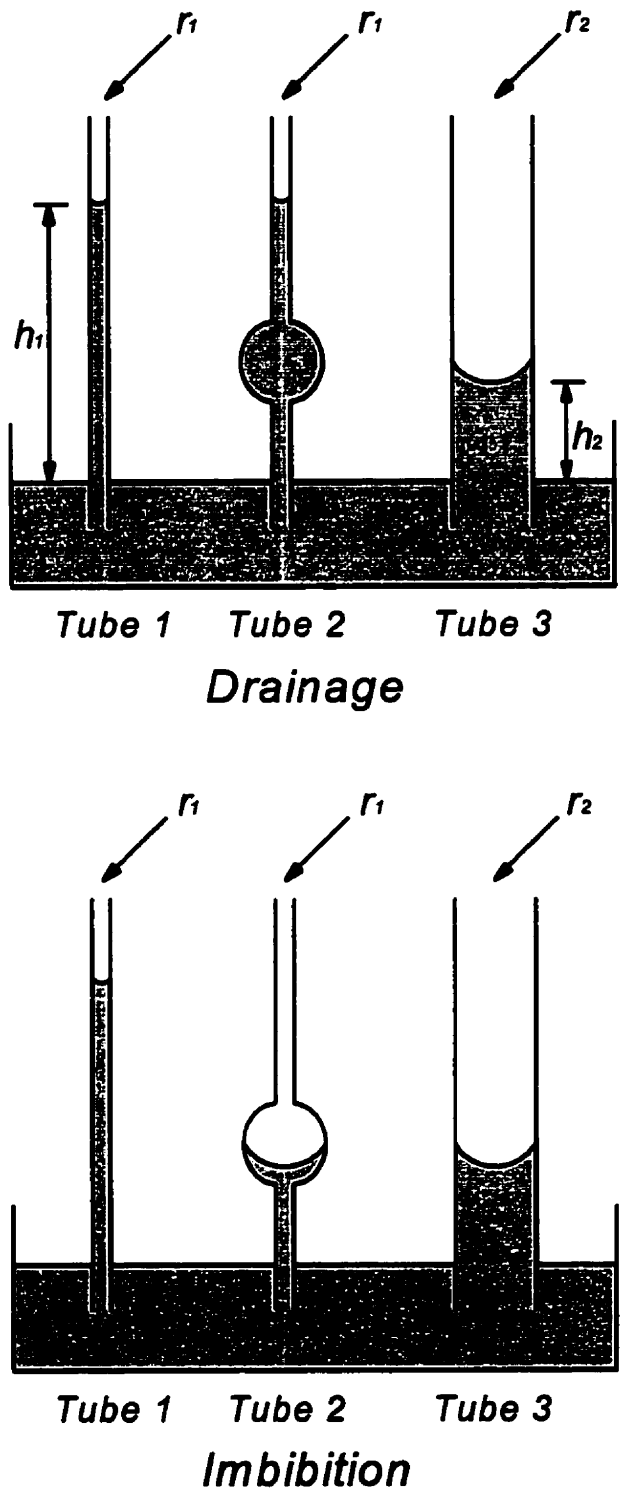

Figure 16: Capillary Pressure Hysteresis (Mungan, 1981)

CHAPTER 4

LITERATURE REVIEW

Since the mid 1980's, *in-situ* subsurface remediation processes have been the focus of significant attention by the scientific community involved with the cleanup of environmental contaminants (Hoag *et al.*, 1991). Such technologies generally use one of three methods to either remove the contaminates from the subsurface ground water, or to contain them within a fixed area in the subsurface. They are: 1) the physical methods such as ground water pump and treat, subsurface drains, and low permeability sub-surface barriers, 2) the biological method of bioremediation with the use of engineered enzymes emerging as a way to enhance this process (Trombly, 1995), and 3) the chemical method of permeable subsurface barriers. Currently, there are two methods of subsurface barriers being developed, one is the use of treated zeolites (Newman, 1995) and the second is the use of iron filings (Strauss, 1995).

The applicability of these technologies depends on the contaminant mass exchange between the water saturated and unsaturated zones of the ground water bearing strata. Because many contaminant sources occur on the land surface or within the unsaturated zone, mass transport from the unsaturated zone to the saturated zone is a common mechanism of ground water contamination. Some of the pollution processes involved include: aqueous and gas phase molecular diffusion, mechanical dispersion, aqueous and gas phase advection, and partitioning among the aqueous, gas, and solid phases. The extent to which each of these processes contributes to mass transfer between the saturated and unsaturated zones depends

on both the properties of the contaminant compound and the petrophysical conditions within the ground water bearing subsurface (McCarthy and Johnson, 1993).

Of the physical processes, research has focused mainly on two areas of study: the movement of liquid contaminants in the porous water bearing zones, and the evacuation processes of light volatile hydrocarbons. To the first area of research belongs the works by Schwille (1988), Hoag *et al.* (1991), and McCarthy and Johnson (1993), and to the second area belongs the work of Hoag and Cliff (1988).

Schwille (1988) performed several experiments, using a variety of porous media models including glass frits, sand packed glass columns (of different sizes), a 560 x 160 x 28 cm trough, as well as a glass bead packed frame cell for macroscopic examination. Experiments were conducted to determine the behaviour of several heavier than water contaminants (dichloromethane; tetrachloroethylene; 1,1,1,-trichloroethane; and trichloroethylene) in the water saturated and unsaturated zones. In several experiments, it was observed that the hydrocarbons, when falling down from the unsaturated to the saturated zone, spread laterally when in contact with the capillary fringe (before "fingering" into the saturated zone). Also observed was that, when compared to the infiltration of water, tetrachloroethylene penetrated the unsaturated region easier than water, but it slowed at the capillary fringe, while the water passed through the fringe more easily.

Hoag *et al.* (1991) performed theoretical hypothetical examinations of possible relationships near the capillary fringe, and the importance of contaminant mass transfer from the capillary zone into the saturated flow regime for a contaminant that is immiscible and lighter than water. They concluded that the rate of contaminant transport into the saturated

zone was dependant on the circumstances present. In one case, if ground water flow was relatively steady, a zone of floating contaminant may exist on the capillary fringe. Infiltrating water, under draining conditions, would reach an equilibrium with the immiscible liquid resulting in a saturated contaminant condition. Assuming that only vertical ground water flow exists in the capillary zone, the rate of contaminant input to the saturated zone will be limited by the rate of infiltration. Assuming that a horizontal flow boundary exists at the ground water table, then mass transfer of contaminant from the capillary zone into the saturated zone will have only limited effects on contaminant input into the saturated zone. The result is a relatively ineffective transfer of contaminant from the capillary fringe zone to the saturated zone.

In a second case, if there was an impingement of the saturated zone by penetration of the capillary zone (resulting from the depression of the capillary zone where considerable quantities of an immiscible contaminant are spilled), the potential for contaminant transfer from the unsaturated zone to the saturated zone is greatly increased. In another case, fluctuating ground water tables may result from a rise in the ground water table through wetting (imbibition) of the capillary zone. Since immiscible contaminants become immobilized at residual saturation, the net result is that saturated contaminant concentrations exist at the top of the horizontal flow zone of the saturated zone. This boundary condition enables a substantially greater mass transfer of contaminant into the saturated zone, principally resulting from the upper flow boundary being the immiscible contaminant itself.

McCarthy and Johnson (1993) conducted physical experiments using a heavier than water volatile organic compound (tri-chloroethylene, TCE) to examine and quantify the

transport mechanisms of dissolved TCE from shallow ground water to the unsaturated zone. The aquifer model used in their experiments was 0.75 m wide, 1.0 m long, and 1.0 m deep; and using a two dimensional sampling net work installed along the longitudinal axis of the model. The aquifer model was filled with type 8 flint shot Ottawa sand. Three experiments were performed. The first experiment investigated the movement of dissolved TCE from the ground water to the unsaturated zone under drainage conditions. The second experiment investigated the transport of TCE from ground water during a water table drop. The third experiment examined the movement of TCE from ground water under imbibition conditions.

They concluded that at moderate ground water velocities, molecular diffusion was the dominant vertical transport mechanism, while vertical dispersion was negligible.

The authors then developed a two dimensional advection-diffusion model, and a one dimensional diffusion-dispersion model, and compared the results of the models with the experimental data. They determined that there was agreement between both models and the data, and suggested that in cases in which the ground water velocities are low, flow is predominantly horizontal, and horizontal concentration gradients are small; a simple, one-dimensional approximation of vertical transport across the capillary fringe can be useful in the qualitative sense.

Hoag and Cliff (1988) reported on an *in-situ* vapour extraction (soil venting) system that was effective in removing 1,330 ℓ of gasoline from residually saturated soils and from the top of the capillary zone. The entire remediation process took less than 100 days, with the majority of the recovery achieved within one month.

Of the physical *in-situ* processes researched to date, vapour extraction holds perhaps

the most widespread application to the remediation of volatile and semi-volatile organic chemicals frequently found in the subsurface. *In-situ* vapour extraction has been applied at many sites by means of significantly different approaches (Hoag *et al.*, 1991). However, for this process, it is essential that all components will vaporize at the *in-situ* operating evacuation pressures, otherwise heavy residues will be left behind.

An understanding of the air-immiscible liquid-water three-phase conduction and distribution in the porous media is important, including the capillary phenomena in the capillary fringe zone (unsaturated zone). Additionally, the site history of ground water fluctuation (hysteresis), capillarity, and immiscible contaminant behaviour in the capillary fringe and saturated zones is essential information (Hoag *et al.*, 1991). In general, it is observed that because of the current limited insight into the subsurface transport mechanisms, it is not known to what extent technologies such as soil venting are applicable in removing contaminants from the capillary fringe.

CHAPTER 5

EXPERIMENTAL APPARATUS

5.1 Experimental Apparatus

The apparatus used for the experiments was constructed of several components. It consists of a vertical cylindrical column packed with glass beads (the cylindrical core cell), and is equipped with two rows of equally spaced side ports (or probes) along the length of the cylinder. The permeability and porosity of the core was then measured. A water reservoir connected to the bottom of the cell serves as the water table, and an air flow meter connected to the top of the cell measures the air flow into the cell. In order to produce the fluids from the core (i.e. glass bead pack), a liquid collection system is hooked up to the desired side port (also called production probe). This collection system is connected to a manometer (to monitor the vacuum pressure that the core was exposed to), as well as to a vacuum cylinder (reservoir), which is connected to a vacuum pump. A schematic diagram of the apparatus is shown in Figure 17.

The original experimental program prescribed one lighter than water hydrocarbon and one heavier than water hydrocarbon to act as the contaminant for the experiments, as well a cleaning fluid was needed to clean the core after each experiment was completed, therefore, a group of chemicals were tested for their suitability and use in the experiments.

5.1.1 The cylindrical core cell

A one-dimensional cylindrical cell, filled with glass beads and stationed vertically, was used in order to investigate the recoverability of a hydrocarbon contaminant from the capillary fringe. The two foot cylindrical cell was fabricated from a clear acrylic tube with a 7 cm (2¾ inch) outside diameter (O.D.) and a 5.1 cm (2 inch) inside diameter (I.D.). Stainless steel probes (side ports) 10.2 cm (4 inches) long and 0.3 cm (⅛ of an inch) in O.D. were positioned at 2.5 cm (1 inch) intervals along the cylindrical cell length, radially extending to the centre. The glass bead pack (the core) inside the acrylic tube is 5.1 cm (2 inches) in diameter and 61 cm (2 feet) in height. On the top and bottom of the tube are end caps that were constructed from 7 cm (2¾ inch) O.D. clear solid acrylic. These end caps, screwed into the tube ends, have a wire screen mesh on the inside surface that is in contact with the glass beads. Each cap was machined such that, the flow of liquid (bottom cap) or air (top cap) was transitioned from the 0.6 cm (¼ inch) O.D. stainless steel line fitted into the center of the cap to the 5.1 cm (2 inch) I.D. core of the acrylic cylinder. This transition was done by machining a conical path into the cap that starts at 0.6 cm (¼ inch) in diameter from about midway in the cap, and ending at the inside cap surface where the wire mesh is located.

5.1.2 Packing of the cylindrical core cell

The cylindrical cell was cleaned by washing it with hot tap water and dish-washing soap. This was necessary in order to remove the oils that were used during the machining of the cylinder. The end caps were also cleaned using the same method. Any excess grease was removed by using a grease-dissolver, and then washing the pieces with soap and rinsing

with tap water. Everything was then re-rinsed using distilled water, and allowed to air dry.

The glass beads were cleaned by washing them with hot tap water and dish washing soap. The beads were rinsed repeatedly, first with tap water and then with distilled water. They were then poured into a metal tray and placed into an oven of 105°C and allowed to dry for 12 hours. The oven was then turned off allowing the glass beads to cool before being poured into a clean glass jar for storage until use.

The cell was then filled by pouring the glass beads into the cell in approximately 2.5 cm (1 inch) layers at a time. Then the side of the cell was tapped to achieve the densest packing of the glass beads. Each mass of glass beads added to the cell was measured, so that the total mass of beads in the cell was a known quantity. When the cell was filled to the top (space was reserved for the top end cap), a thread scraper was used to ensure that the threads for the top cap were relatively free of any glass beads. The top cap was then screwed into place.

Two identical clear acrylic cylindrical cells were constructed and filled with glass beads (Core 1 and Core 2) to speed up the experimental testing procedures because of the significant time it took to establish an equilibrium fringe. The clear acrylic cylinder allowed only the outer layer of glass beads to be visible. For Core 1, the end caps had a layer of grease as lubrication put on the threads (V - thread, 12 thread per inch), and the end caps were screwed into the core. For Core 2, a layer of Teflon tape was wrapped around the threads, and the end caps was screwed into place. Core 2 was built after Core 1. It was observed form Core 1, that the glass beads had the tendency to become embedded in the threads of the top cap, causing the top cap to seize before it could be fully closed on the core.

For the second core, the threads were made looser and Teflon tape was used so that if some of the glass bead were embedded in the threads, the cap could still be screwed into place.

Experiments were performed with homogeneous glass bead packs of two different mesh sizes. Core 1 has glass beads of 16 - 20 mesh, and Core 2 has glass beads of 30 - 40 mesh. Figure 18 shows the results of a sieve analysis performed on the glass beads. The sieve sequence was Mesh size 18, 25, 35, 60, and 80. Table 6 shows the mesh sizes in metric units (mm). According to Todd (1980), both glass bead packs belong to the category of coarse sand, Table 2.

5.1.3 Core porosity, permeability, and connate water saturation

The porosities of the cores were measured by first completely filling the empty cell with a measured mass of water. This water was then drained out, and the core allowed to dry. The empty cell was completely filled with the glass beads. The cores were then filled with water from the bottom up until completely saturated with a measured mass of water. By dividing the mass of water after the cell was packed with glass beads by the mass of water before the cell was packed, the porosity of the core was determined, Table 7. Theoretical porosity calculations for perfect spheres have computed the porosity to be 47.6 % for cubical packing (the least dense packing) and 25.96 % for rhombohedral packing (the most dense packing), regardless of the size of the spheres (Frick and Taylor, 1962). The measured values, Table 7, are somewhat in between, because the core is filled with a mesh size range, and most likely the densest packing was not achieved.

To determine the permeability of the core, the fully (water) saturated core was laid

horizontal on its side, with the "bottom" end of the core connected to the water table apparatus and the "top" end over the sink. Water was allowed to flow through the core with the water table level being at a fixed height above the center line of the core, and water produced from the "top" end was collected in a cylinder. The mass of water collected over each given time interval was measured. For each core, 6 experiments were performed using 3 different water table heights. A cross plot was then made in order to determine the permeabilities of the cores, as is shown in Figure 19. It should be noted that the viscosity of water was assumed to be 1.0 cP.

To determine the connate water saturation, each core was filled from the bottom up until completely saturated with a measured mass of water. The bottom valve of the core was then opened, and the water that poured out of the cores was collected and weighed. The residual mass of water in each core was calculated by subtracting the mass of water collected from the core from the mass of water originally imbibed into the core. By dividing the mass of water remaining in the core by total mass of water that was imbibed into the core, the connate water saturation for Cores 1 and 2 was calculated (Table 7).

5.1.4 The water table

Since the experiments involved the need for a water table, a water table reservoir was made using an upside down graduated cylinder and a rubber stopper with two stainless steel tubes going through it. One tube was slightly longer than the other. The stopper was inserted into the top of the cylinder such that the uneven ends of the stainless steel tubes were outside (not inside) the cylinder. To control the water table level, the cylinder (filled with

water) was placed upside down over a funnel on a wooden sled that could travel up and down and parallel to the core. The bottom ends of the stainless steel tubes were suspended over the funnel with the shorter tube monitoring the level of the water table, and the longer tube releasing the water into the funnel. The funnel was connected to a plastic tube that was connected to the bottom of the core. The free water table level was established inside the funnel. The water table height in the funnel was maintained within an accuracy of +/- 1 mm for Core 1 and +/- 1.75 mm for Core 2 from the average. This difference was due to the fact, that when the water table touched the shorter tube, interfacial tension, i.e. the meniscus, prevented the air from entering the cylinder, and hence, prevented water from leaving the cylinder to become part of the water table. Only when the water table had dropped sufficiently (about 2 to 3.5 mm) would the film (the meniscus) break and water pour through the longer tube submersed in the water table, while air flowed up the shorter tube into the cylinder. When 8 - 15 ml of water from the cylinder was released, the water level reached the shorter tube and the flow of air and water stopped due to the re-establishment of the meniscus.

5.1.5 Air flow meter

Since for all experiments, the rate of air entering the core was to be measured, a Lab-Crest Mark III Flowmeter was provided. This meter can measure the flow rates of single phase liquids or gases (e.g. air). The flowmeter kit came with four tubes, and each tube had two corresponding meter floats. For purposes of the experiments, it was decided that the glass tube numbered 448-035 would provide the best readings for air flow rates (the other

tubes were for increasingly higher flow rates). For this tube, two floats could be used: one, a sapphire float for an air flow rate range of 0.4 - 43.5 cm^3/min and second, a stainless steel float for an air flow rate range of 0.4 - 83.5 cm^3/min.

Initially, it was decided that the sapphire float would be the best choice given the anticipation that the air flow rates would be low. However, during the preliminary testing with the experimental apparatus, it was discovered that the sapphire float in the air flow meter would not respond appropriately to the flow of air into the core. For example, the float regularly either remained at the bottom of the air flow meter, or the float would jump up due to a surge in the flow of air, and then remain stuck in the middle of the tube regardless of whether or not there was any air flow. This was tested by disconnecting the air flow meter from the core leaving both end of the meter open to atmosphere. It was therefore decided that the float should be changed from sapphire to stainless steel. This meant that the readings for air flow rate would be coarser than with the sapphire float, but the readings would then be accurate.

Also, as part of the kit, a chart was provided that would correlate the readings of the meter with the air rate at standard temperature and pressure. A reproduction of this graph is shown in Figure 20.

5.1.6 Liquid collection system

The liquid production collection (measurement) system consists of a glass graduated cylinder capped with a rubber stopper. The stopper has two holes in it to allow for two tubes: one, a 0.6 cm (¼ inch) O.D. copper tube to be connected to the production probe in

the glass bead core, and the second, a 0.6 cm (¼ inch) O.D. copper tube connected (via a splitter) to the vacuum cylinder and the water manometer. The line to the vacuum cylinder is a 0.6 cm (¼ inch) O.D. plastic tube, while the line to the manometer is a 0.3 cm (⅛ inch) O.D. plastic tube. The vacuum cylinder connects to the vacuum pump via a valve and a line. For the duration of each experiment, the pump was always left running. When the vacuum pressure (according to the manometer) started to drop, e.g. due to the production of air, the valve from the vacuum cylinder to the pump was (carefully) opened manually to allow control over the vacuum pressure. The steel vacuum cylinder (a T size Helium cylinder with a volume of about 49 ℓ) acted mainly as a vacuum reservoir, and buffered the action of the vacuum pump.

The production probe inside the collection cylinder was curved to the wall of the cylinder so that production liquids could flow down the glass wall (of the cylinder) instead of dropping down onto the liquid surface. This prevented any bubble/emulsion forming on top of the liquid surface in the cylinder which made volume readings problematic.

5.1.7 Selection of chemicals

A number of chemicals were initially tested for the purpose and suitability of using them for the experiments. Two liquids were tested for cleaning the core. Refer to the list in Table 8 for the initial chemicals tested.

The original plan was to conduct two series of experiments, one with a hydrocarbon lighter than water, and the other with a hydrocarbon heavier than water. The constraints on the hydrocarbons were:

1. The hydrocarbon could not cause damage to the acrylic material that the core was made of. This was tested by immersing a rectangular piece of acrylic in the test fluid for several days. If the liquid caused hairlike surface fractures, here called "scratches", or dissolved the acrylic test piece, the fluid was rejected.
2. The hydrocarbon needed a vapour pressure that was low enough (i.e. low volatility), such that exposure to a vacuum would not cause a measurable loss of hydrocarbon recovered.

Three conditions were set for the cleaning fluid. The first condition was the same as the first constraint for the hydrocarbon selection. The second condition was that the fluid had to clean the core, i.e. both the hydrocarbon and water are to be soluble in the cleaning fluid. The third condition was that the cleaning fluid should vaporize easily.

After the testing of the chemicals listed in Table 8 was completed, the following were selected for the experiments: n-Heptane and di-Ethyl-Phthalate for the lighter and heavier than water hydrocarbons respectively. Isopropyl alcohol was selected as the cleaning fluid.

During the necessary testing it was observed, that any chlorinated hydrocarbon would cause damage to the acrylic and hence, none of these were suitable as test fluids. In the case of methylene chloride, the fluid began to dissolve the acrylic on contact with most of the other fluids causing severe scratch marks on the surface of the acrylic piece. On completion of the suitability tests, it was decided that di-Ethyl-Phthalate was the best choice as a heavier than water hydrocarbon. However, later after the first experiment using di-Ethyl-Phthalate (experiment 57), it was discovered that this liquid did in fact damage the acrylic cylinder,

causing severe scratching on the inside surface of the acrylic wall. It was assumed however, that the damage caused by the di-Ethyl-Phthalate was due to the fact that the wall of the core was already scratched from a previous use of isopropyl alcohol. This alcohol was originally tested and deemed to be not damaging to the acrylic, hence it was selected to clean the core. Over time it was observed that this alcohol did indeed cause minor scratching of the acrylic wall, making it difficult to see through the cylinder wall to monitor capillary fringe development. Therefore, the continued use of this fluid to clean the core was stopped and hot water used instead. The effect of hot water was two fold: one, the hot water would anneal the surface of the acrylic, and second, the n-Heptane used would vaporize and exit at the top of the core. Further, from consultation with the machinist who constructed the two cells, it was learned that the stresses in a piece of circular acrylic are different than those in a rectangular piece and this may have had an influence on the effect that the different liquids can have on acrylic.

5.2 Experimental Procedure

The procedure for conducting the experiments consisted of the following stages: cleaning of the core, preparation of the core for the next experiment, and the experiment itself. Before proceeding with the prescribed experiments, 20 initial tests on the cores were performed to evaluate the experimental apparatus, the experimental system set-up, the testing procedures for both the capillary drainage and imbibition processes, and the monitoring/recording of the data.

5.2.1 Cleaning of the core

Once an experiment was terminated, the vacuum pump was stopped, the vacuum production - collection system was disconnected from the production probe, the probe's stop cap put back on, and the air flow meter was disconnected. The valve connecting the core to the water reservoir was subsequently closed, and the water line and reservoir system disconnected from the core. The bottom valve was then opened to allow all remaining liquids to pour from the core. After the liquids had drained by gravity, an air hose was attached to the top of the core, and air was blown from top to bottom of the core until completely dry. Once the core had dried, the air hose was removed and one end of a 1.8 m (6 ft) long plastic tube was attached to the bottom of the core. The other end of the plastic tube had a funnel attached to it, and was positioned vertically above the top of the core. Distilled hot water (80 - 90 °C) was poured into the funnel, and then flushed from bottom to top through the core. Approximately 7 *l* (about 14 pore volumes) of hot water was flushed through the core in order to clean it. Once the core was cleaned the water was drained and the air hose was re-attached to the top. The caps on the probes ends were removed, and air was blown through the core so that the glass bead pack and the probes could dry out. As the core dried, the caps for the probes were put back onto the probes. Air was allowed to flow through the core (top to bottom) overnight (approximately 12 hours) to insure that the glass bead pack was fully dry. The air was laboratory provided pressured air, and was put though a stainless steel tube that was filled with "Indicating Drierite" (8 mesh) to remove water and oils that may have existed in the lines and air. Once the core was dry, it was ready for the next experiment.

5.2.2 Preparation of the core for the next experiment

The experimental study involved the establishment of a water table in the cylindrical core cell, the establishment of the capillary fringe, and the subsequent introduction of a hydrocarbon contaminant above the capillary fringe. All experiments were performed at ambient (20 - 24°C) conditions. The preparation of the core for the next capillary drainage experiment consisted of the following steps:

a) The core was fully saturated with water to a height of 25 - 30 cm for Core 1 and 30 - 35 cm for Core 2 above the bottom of the glass bead pack. The system was allowed to equilibrate at that saturation for about 30 minutes.

b) The water table was then dropped about 15 to 20 cm for Core 1 and 25 to 30 cm for Core 2 (relative to the bottom of the glass bead pack) to establish the drainage capillary fringe zone. As the water flowed from the core back into the water table reservoir, it was removed from the funnel using an eye-dropper so that the water table level remained constant. Once water had stopped flowing back from the core into the funnel, the system was allowed to equilibrate for 24 hours for Core 1, and 72 hours for Core 2, to establish the drainage capillary fringe. It was visually observed from the 16-20 mesh core (Core 1) that it took about 24 hours for the drainage capillary fringe to reach equilibrium, and about 72 hours for the 30-40 mesh core (Core 2).

c) After the capillary fringe had equilibrated, the desired amount of hydrocarbon (the contaminant) was injected into the core at about 5.1 cm (2 inches) above the top of the capillary fringe, using a small funnel hooked up to a probe (side port). The

hydrocarbon was poured into the funnel, and allowed to filter into the core at its own pace. It was observed from both cores, that, as the hydrocarbon entered the core, water was immediately displaced from the core into the water table reservoir, i.e. a drainage process. In addition, for Core 2 it was observed that, the hydrocarbon level in the core rose above the level of the injection probe before falling back down to below the level of the probe. After the required volume of hydrocarbon was injected, the system was left standing 24 hours for Core 1, and 72 hours for Core 2, to allow the system to equilibrate. This 24 and 72 hours was an arbitrary decision, because the hydrocarbon-water meniscus was not readily visible. However, for some Core 2 experiments, 48 hours was used.

d) After the liquid system had stabilized, an air flow meter was connected to the top of the core. The vacuum production - collection system was hooked up to the core at the desired production probe (relative in height to the free water table), and the desired vacuum pressure was established in the vacuum production - collection system using the vacuum cylinder and the vacuum pump. With the opening of the production valve, connecting the collection system to the production probe of the core and exposing the core to the vacuum pressure, the measurement of the flow and recovery of n-Heptane (the contaminant), water, and air commenced.

All of the experiments conducted were done using the drainage capillary fringe because the imbibition capillary fringe was either too small (1.4 - 1.6 cm for Core 1, and developed almost immediately) or took an extensive period of time to develop (17 - 18 cm

for Core 2 over 18 days (Figure 21)).

It was visually observed that for all drainage tests, the distribution of the liquids in the capillary fringe was not completely the same at the start of each experimental test. The top of the capillary fringe itself was never the same height, and showed a variance in the range in height. The drainage capillary fringe showed a "jagged" top, with peaks and valleys. These peaks and valleys for Core 1 would range in height from 8 to 9.15 cm for the peaks, and 6.8 to 8.2 cm for the valleys; while for Core 2 they would range in height from 16.2 to 18.2 cm for the peaks, and 14.4 to 17.1 cm for the valleys (all measured from the free water table), Tables 9 and 10. This would suggest that the formation of the drainage capillary fringe, like the imbibition capillary fringe, is not stable, and is subject to fluctuations in the system that can disrupt its formation (as was found by Lu *et al.*, 1994). Consequently, when the hydrocarbon is added to the top of the capillary fringe, the hydrocarbon will not exactly distribute (equilibrate) itself in the same manner from test to test.

5.2.3 The experiment: monitoring and data collection

The actual experiment started when the valve linking the production - collection system to the core was opened, exposing the production probe to the desired vacuum pressure (in the Helium cylinder), as shown on the water manometer. At that moment, a stop watch was started, and the production of fluids (hydrocarbon, water, and air) was monitored over time. Measurements were taken each time when the total liquid produced reached a whole ml (not at specific time intervals), at which time the total water produced was also

recorded. The hydrocarbon/air and water/hydrocarbon menisci in the glass cylinder could be read accurately. If no liquids were produced, the connecting valve was closed, the vacuum pressure was increased, and the valve linking the production probe to the vacuum production - collection system was reopened. The cumulative volumes of water and contaminant withdrawal at the fringe, as well as the air flow rate, were measured. For all experiments, the valve in the water line connecting the water table to the core was left open. For a couple of experiments, the valve connecting the core to the water table was closed from the beginning of the experiment, to see the effect of no water supply. The valve was also closed when water became the only fluid that was being produced. When this was the case, water production tended to be very rapid. The experiment was terminated when there was no further hydrocarbon recovery from the core. There could be air flow, or, only the remaining mobile water was being produced.

A listing of the experiments performed with the initial conditions of the test are presented in Tables 9 - 10.

All tests were performed manually, data monitoring was done by visual observation, and recording was done manually. Although due diligence was exercised for each test, differences between experimental results will occur due to measurement accuracies and tolerances, and variances in capillary fringe equilibration. In addition, it was observed that when the valve between the production probe and the collection cylinder was closed at the end of the experimental test, at times a drop or two of liquid would fall from the line into the collection cylinder. For some tests, this manifests itself in the recovery increasing at the end of the test (the last data point), rather than the recovery being held at a constant value.

5.2.4 Initial testing of the core

The original experimental plan proposed was to perform a set of tests using glass beads of a specific mesh size, for six different mesh sizes of glass beads: 10-14, 16-20, 20-30, 30-40, 60-80, 120-170, and 230-325 mesh.

The experimental test (for all tests) prescribed the following test procedures for a given glass bead pack:

a) Establish a constant water table level.

b) Introduce water into the glass bead pack (to a predetermined height).

c) Allow the water-air transition zone (capillary fringe zone) to equilibrate.

d) Introduce a pre-determined volume of a lighter than water hydrocarbon through a side port, above the top of the capillary fringe, and allow it to equilibrate (such that one of the other side ports lies in the center of the transition zone).

e) Turn on the vacuum pump and set the flow meter to a low air extraction rate.

f) Record the volume of hydrocarbon and water produced as a function of time.

g) Record the extraction (vacuum) pressure below atmospheric (as a function of time).

Each test was to be repeated up to five times, using different air extraction rates, to determine the effect of rate (i.e. lack of equilibrium) on the relative withdrawal rate of hydrocarbon and water. In addition, an arbitrarily small number of tests were to be duplicated in order to determine the quality of the reproducibility of tests.

The above test procedures were to be repeated to evaluate different parameter settings like:

a) Using a heavier than water hydrocarbon, and address capillary pressure (see Chapter 3).

b) Introduce water above the (lighter than water) hydrocarbon to simulate the effect of "rainfall".

c) The use of a laminated glass bead pack, consisting of 10-14 mesh and 60-80 mesh glass beads in alternating one inch layers.

Twenty experiments were performed to evaluate the experimental apparatus, the equipment system set up, and the proposed prescribed test procedures. During these experiments, deficiencies and problems were encountered with the experimental apparatus, system set up, and test procedures.

In review consultations, this resulted in the elimination of tests, changes to the experimental set up, modifications to the testing of parameters (see Chapter 6), and the procedures (as per this thesis). For example:

a) It was discovered that the vacuum collection system needed to be improved. The original system used the smaller 0.3 cm (⅛ inch) lines whereby the produced fluids became stuck on the inside of the line. This was corrected with the use of 0.6 cm (¼ inch) lines wherever possible. Further, the produced liquids tended to form bubbles (emulsion) as it dropped into the collection cylinder due to the high speed at which the fluids flowed through the line. This emulsion made the determination of the volume of liquids produced very difficult, and required a visual estimation of the interface between water and hydrocarbon and the total volume of liquids in the

cylinder. It was reasoned, that if the portion of the copper production tube inside the cylinder was bent so that the produced liquids could flow along the wall of the cylinder, no emulsion would form. This modification to the tube corrected the problem.

b) During the initial capillary fringe development tests, it became apparent that for glass bead packs of different mesh sizes, tests would only be practical with the 16-20 mesh (for Core 1) and the 30-40 mesh (for Core 2). The larger glass bead (10-14 mesh) pack would not provide a workable capillary fringe zone; and the smaller glass bead packs (less than 30-40 mesh) would take too long to establish a capillary fringe zone.

c) The capillary fringe can be established by either the capillary drainage or the capillary imbibition process. During the initial tests for an imbibition capillary system, it became immediately apparent that the capillary fringe for Core 1 appeared to develop almost immediately to a height of 1.4 to 1.6 cm, and developed over an extensive period of time for Core 2 (Figure 21). On the other hand, the drainage capillary fringe could be established within a reasonable time frame, namely 24 hours for Core 1 and 72 hours for Core 2. Based on these findings, it was decided not to pursue any further testing for the imbibition capillary system.

d) Another problem observed was that the capillary fringe would not develop to the same height for the same mesh glass bead packs, and it would not be a straight (level) line around the cylinder wall. Similar findings are observed in the literature (Lu *et al.*, 1994), and therefore this was accepted as a matter of fact (see Section 5.2.2).

e) The experimental set up and equipment used did not allow for the control of the air

flow to a low extraction rate. On the other hand, the utilization of a large (49 ℓ) helium cylinder would allow for the control of the vacuum pressure with a good degree of accuracy. Therefore, the testing procedures were modified such that the vacuum pressure was held constant and the air flow meter reading was recorded as a function of time.

f) The experimental tests could only be performed using low vacuum pressures, namely 0.6 to 4.0 inches of water. To perform the experiments at higher vacuum pressures caused severe water coning, and made monitoring/recording of the progression of the tests not practical/possible.

In addition to the above, during the actual experiments performed, problems did develop with respect to the cleaning fluid and the heavier than water hydrocarbon. These matters are discussed in Section 5.7.1. For the heavier than water hydrocarbon, it was decided not to perform any experiments (see Chapter 6).

Table 6: Mesh Sizes for Glass Beads and Sieves

Mesh Size	Size in mm
16	1.18
18	1.0
20	0.85
25	0.707
30	0.6
35	0.5
40	0.425
60	0.25
80	0.18

Table 7: Porosity and Connate Water Saturation of Core 1 and Core 2

Core	Porosity	Connate Water Saturation
Core 1	36.3 %	6.2 %
Core 2	35.0 %	13.2 %

Table 8: Physical Properties of Chemicals Tested[1]

Name	Formula	S_g	T_b (°C)	Solubility (g/100g H_2O)	Vapour Pressure at 20°C (mm Hg)	Surface Tension at 20°C (dyn/cm)
Acetone	C_3H_6O	0.792	56.5	∞	176.5	24.02
Benzene	C_6H_6	0.879	80.1	0.07 at 22°C	74.6	28.88
Cyclohexane	C_6H_{12}	0.779	80-81	insoluble	77.1	25.24
Cyclopentane	C_2H_{10}	0.745	49-50	insoluble	256.6	22.61
di-Ethyl Phthalate	$C_{12}H_{14}O_4$	1.121	298-299	insoluble	N/A	N/A
Isopropyl Alcohol	C_8H_8O	0.789	82.5	∞	31.3	21.32
Methyl Alcohol	CH_4O	0.792	64.7	∞	93.5	22.5
Methylene Chloride	CH_2Cl_2	1.336	40-41	2.0 at 20°C	335.1	N/A
n - Heptane	C_7H_{16}	0.684	98.4	0.005 at 15°C	35.4	20.14
n - Hexane	C_6H_{14}	0.659	69.0	0.014 at 15°C	119.7	18.4
n - Pentane	C_5H_{12}	0.630	36.3	0.036 at 16°C	424.7	16.05
Tetrachloro-ethylene	C_2Cl_4	1.624	120.8	0.02 at 20°C	14.0	N/A
Toluene	C_7H_8	0.866	110.8	0.05 at 16°C	21.9	28.52
1,1,1- Tri-chloroethane	$C_2H_3Cl_3$	1.325	74.1	insoluble	100.0	25.8
Trichloro-ethylene	C_2HCl_3	1.466	87.2	0.1 at 25°C	60.0	N/A

[1] All data except for surface tension is from Perry's Chemical Engineers Handbook 6th Edition. Surface tension is from Jasper (1972).

Table 9: Drainage Experiments for Core 1

Exp.	Water/Air Capillary Fringe Height (from Free Water Table) (cm)	Additions	Production Height (from Free Water Table) (cm)	Initial Vacuum Pressure (in H_2O)	Comments
21	6.8 - 8	36.1 ml C_7	6.3	0.6	Allowed 48 hours for C.F. growth, and between HC injection and production
22	6.9 - 8	36.1 ml C_7	6.3	0.6	
23	7.4 - 8.1	36.3 ml C_7	3.8	0.6	Had HC leakage when connecting collection system to probe
24	7.05 - 8.3	35.7 ml C_7	1.2	0.6	
25	7.3 - 8.05	36.4 ml C_7	6.3	0.6	Closed off water supply before introducing C_7, re-opened during C_7 injection
26	7.3 - 8	36.0 ml C_7	5.1	0.6	
27	7.25 - 8.25	36.3 ml C_7	2.5	0.6	
28	7.55 - 8.45	36.1 ml C_7	2.5	1.0	
30	7.25 - 8.5	36.3 ml C_7	2.5	1.0	
31	7.45 - 8.45	36.1 ml C_7	5.1	0.6	
32	7.95 - 8.75	36.0 ml C_7	5.1	1.0	
33	7.75 - 8.65	36.1 ml C_7	5.1	1.0	
34	7.55 - 8.45	36.3 ml C_7	5.1	1.4	
35	7.4 - 8.45	36.3 ml C_7	2.5	1.0	

Table 9: Drainage Experiments for Core 1, Continued

Exp.	Water/Air Capillary Fringe Height (from Free Water Table) (cm)	Additions	Production Height (from Free Water Table) (cm)	Initial Vacuum Pressure (in H_2O)	Comments
36	7.55 - 8.7	36.0 ml C_7	2.5	0.6	
37	7.8 - 8.9	36.1 ml C_7	2.5	1.4	
38	7.95 - 8.85	36.1 ml C_7	2.5	0.8	Unable to shut off water supply (water production only)
39	7.95 - 8.7	36.1 ml C_7	2.5	1.8	
41	7.6 - 8.85	36.1 ml C_7	3.8	1.0	
42	7.75 - 8.8	28.9 ml C_7	3.8	1.0	
43	8.15 - 9	43.9 ml C_7	3.8	1.0	
44	8.05 - 8.9	35.8 ml C_7 9.9 ml H_2O	3.8	0.6	
46	8.2 - 9.15	36.4 ml C_7 19.9 ml H_2O	6.3	0.6	
48	7.95 - 8.95	36.0 ml C_7 19.9 ml H_2O	5.1	0.6	
56	8.1 - 8.95[2]	36.5 ml C_7	5.1[3]	1.0	Dropped water table level by: 2.25 cm

[2] Measured from original water table

[3] Measured from final water table

Table 10: Drainage Experiments for Core 2

Exp.	Water/Air Capillary Fringe Height (from Free Water Table) (cm)	Additions	Production Height (from Free Water Table) (cm)	Initial Vacuum Pressure (in H_2O)	Comments
29	14.4 - 16.2	36.5 ml C_7	10.2	2.0	Allowed 552 hours for growth, and 264 hours between HC injection and production
40	16.65 - 17.9	36.5 ml C_7	5.2	1.6	Allowed 216 hours between HC injection and production
45	16.6 - 17.8	36.3 ml C_7	10.2	1.0	
47	16.05 - 17.5	36.5 ml C_7	7.7	1.0	
49	16.15 - 17.8	36.4 ml C_7	7.7	2.0	
50	17.1 - 17.85	36.5 ml C_7	7.7	3.0	
51	16.8 - 17.7	36.3 ml C_7	7.7	4.0	
52	16.4 - 17.65	36.4 ml C_7	7.7	4.0	Water supply cut off from start of experiment
53	16.3 - 17.75	36.3 ml C_7	7.7	3.0	Water supply cut off from start of experiment
54	17.05 - 17.75	36.4 ml C_7 24.9 ml H_2O	10.2	1.0	Allowed 48 hours for CF growth, between injection of HC and water, and HC production

Table 10: Drainage Experiments for Core 2, Continued

Exp.	Water/Air Capillary Fringe Height (from Free Water Table) (cm)	Additions	Production Height (from Free Water Table) (cm)	Initial Vacuum Pressure (in H_2O)	Comments
55	16.9 - 18.2	36.5 ml C_7 34.9 ml H_2O	10.2	1.0	Allowed 48 hours for CF growth, between injection of HC and water, and HC production
58	16.75 - 17.75[4]	36.4 ml C_7	6.2[5]	1.0	Raised water table level by: 4.0 cm

[4] Measured from original water table

[5] Measured from final water table

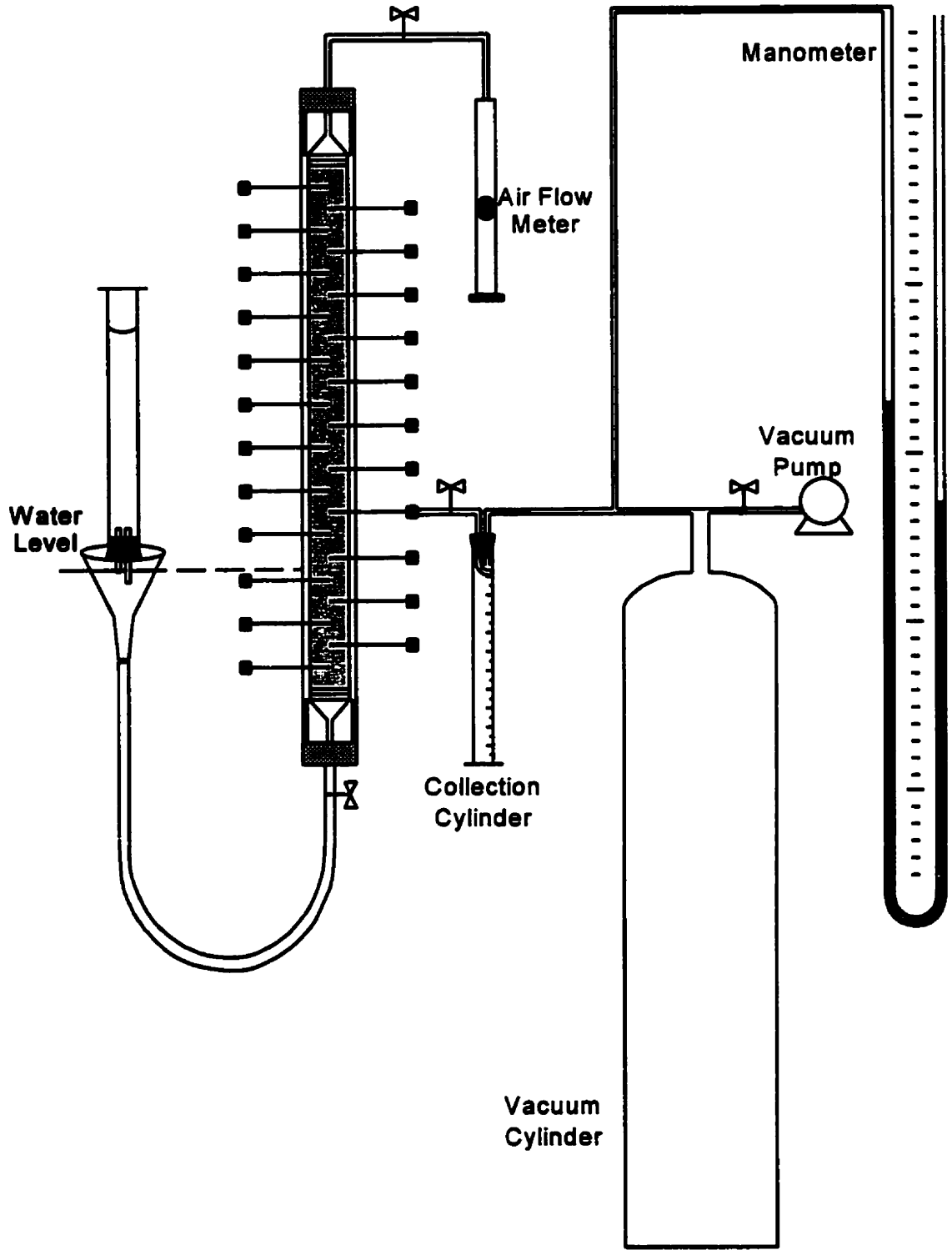

Figure 17: Experimental Apparatus

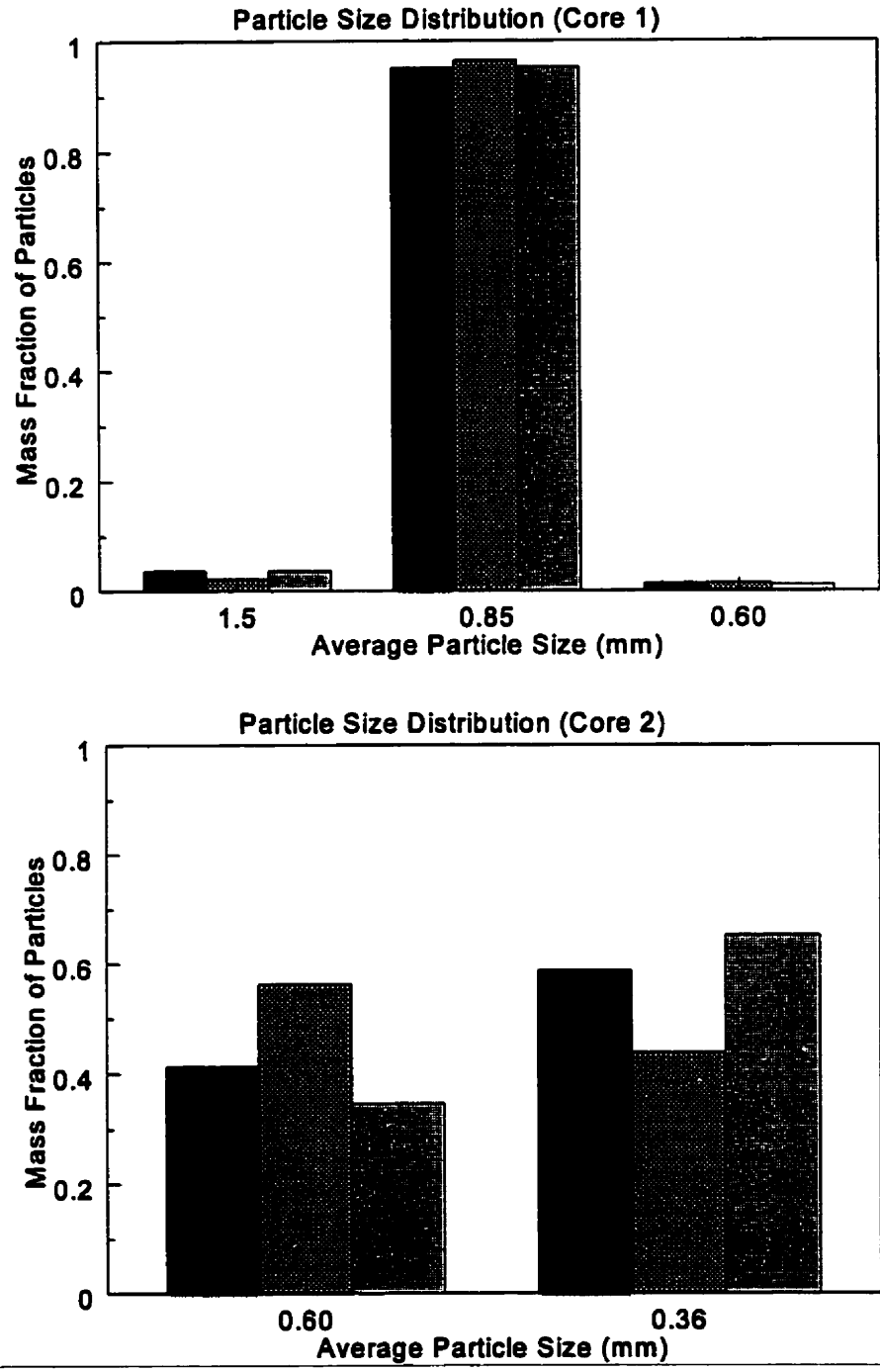

Figure 18: Particle Size Distribution for Glass Bead Packs

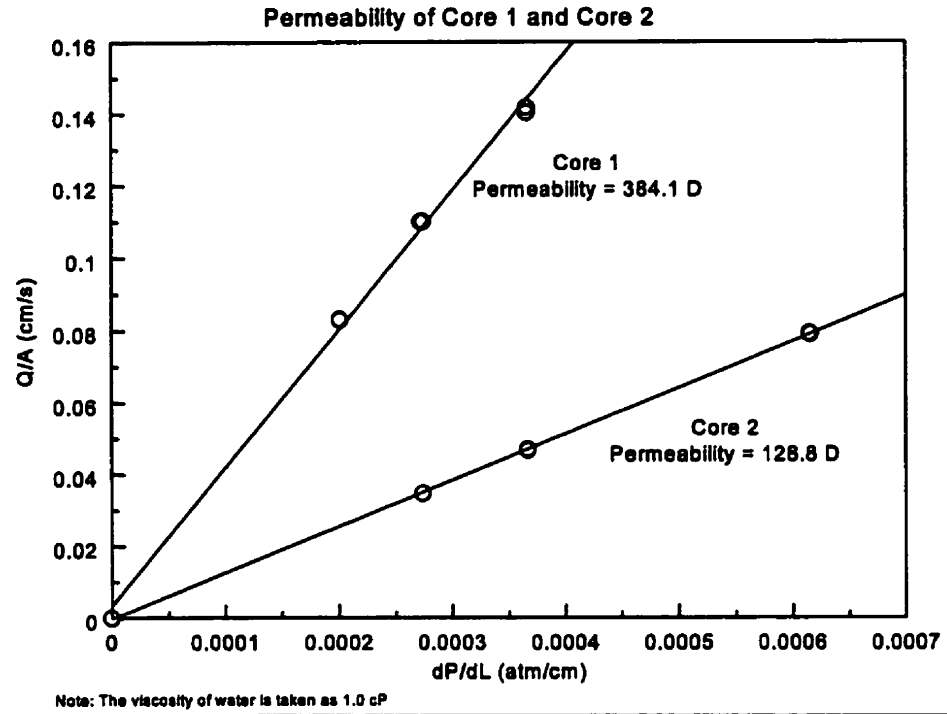

Figure 19: Permeability Plots for Core 1 and Core 2

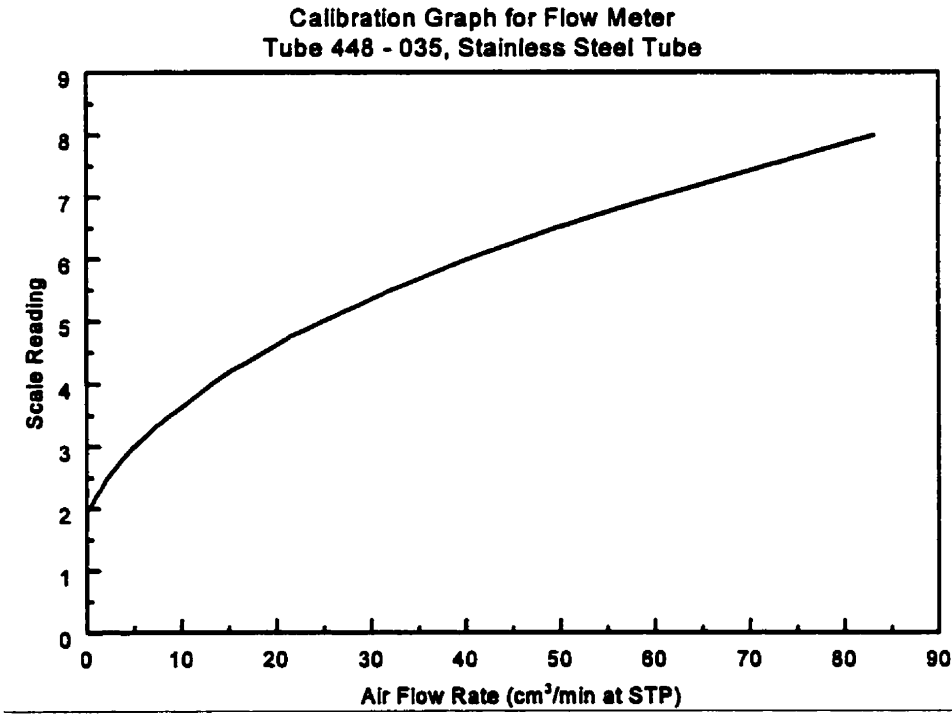

Figure 20: Calibration Graph for Air Flow Meter (Fisher Scientific Company)

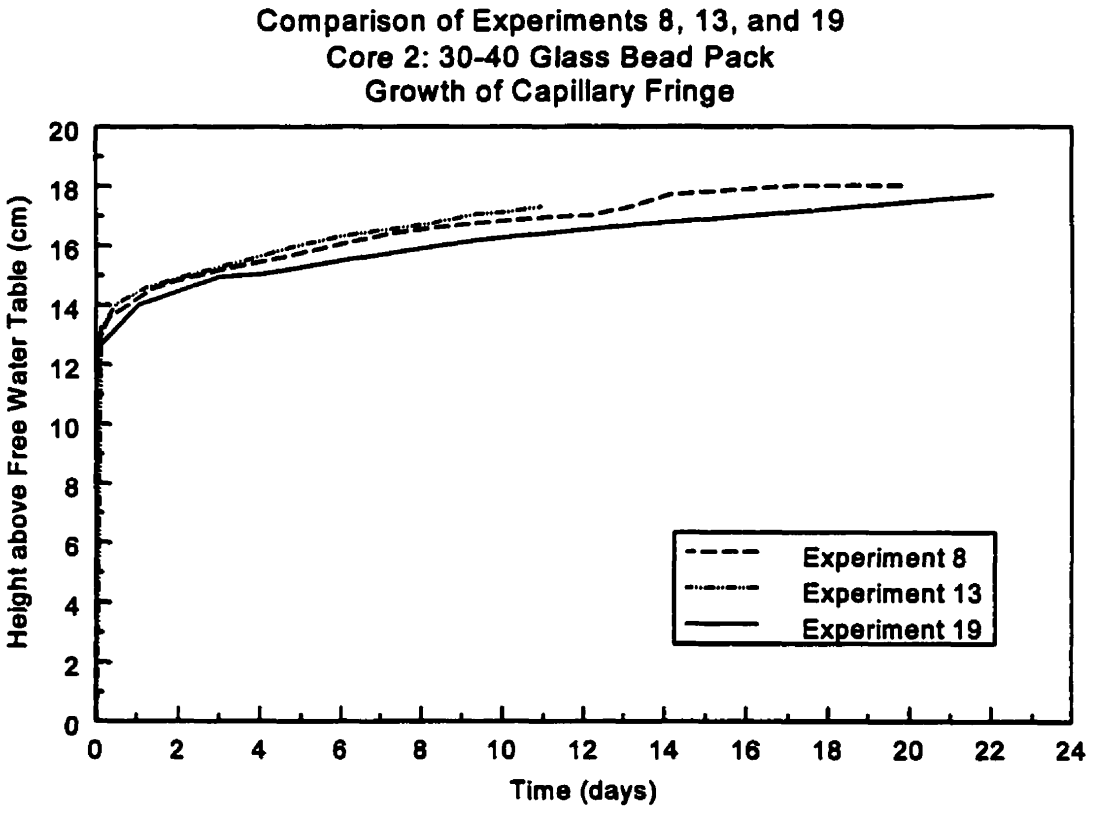

Figure 21: Growth of Capillary Fringe for Core 2

CHAPTER 6

APPLICATION OF CAPILLARY THEORY

The concept and theory of capillarity in Chapter 3, identifies that the presence of mobile water in a porous medium causes the development of the capillary fringe zone. The rise of the capillary fringe above the free water table depends on a number of conditions, such as: the available water supply below the free water table, the pore size and pore size distribution of the porous medium, the wettability of the porous system, and whether there is an imbibition or drainage process.

For the subjected experiments, two cores with different mesh size glass beads were used and identified as Core 1 and Core 2. For Core 1, the large mesh size glass bead pack, the imbibition capillary height was about 1.5 cm and the drainage capillary height was about 8.1 cm, identifying a scenario as depicted in Figure 16, for tube 2, i.e. a non-uniform mix of glass beads. For Core 2, the smaller mesh size glass bead pack, the imbibition capillary height was about 18.0 cm and the drainage capillary height was about 17.0 cm, which is about equal, suggesting a rather uniform mix of glass beads.

The workings of the molecular cohesion and adhesion forces, being on a very small scale, caused the drainage fringe to be developed much faster than the imbibition fringe. The difference in time for the capillary fringe development, i.e. imbibition versus drainage, is thought to be due to porosity size and distribution, wettability, and the fact that the interfacial tensions or the molecular adhesion forces are working against the gravity forces for imbibition, and are aided by the gravity forces for the drainage fringe. This difference in the

working of the adhesion forces was observed with the preliminary experiments and led to the decision to use the drainage fringe for all experiments.

All experiments were started first with the development of the glass bead/water/air drainage capillary fringe zone, Figure 22. As shown in this figure by the axial liquid pressure distribution curve, the water/air meniscus interface caused the water phase pressure in the core above the free water table, but below the meniscus, to be reduced from atmospheric pressure, here called "under-pressure" as annotated in the figure. That is, the pressure differential or under-pressure is related to the height above the free water table with the water/air capillary fringe height "$h_{c(w/a)}$" as maximum, this being the capillary pressure ($P_{c(w/a)}$) for the glass bead/water/air system.

The visible water/air capillary fringe consisted of a rather jagged interface line of one or only a few glass beads against the inside acrylic cylindrical wall; the fringe surface inside the core, and not visible, may not be at the same height for each experiment and, most likely, was also not a smooth surface.

After the drainage capillary fringe was developed, a measured mass of oil was introduced into the connate water saturated region just above the capillary fringe zone. This oil influx volume was then allowed to equilibrate, and is presented schematically in Figure 23. The presence of the oil layer above the water/oil meniscus fringe caused the water/oil fringe height to be reduced due to interfacial tension and gravity effects, whereby the water/oil interface appears to act as a piston for an immiscible water/oil system. The thickness of the oil zone was generally very difficult to be determined visually, because the meniscus interfaces between the water and oil, and the oil and air, were generally not

conclusively discernable. Therefore, the oil height (h_o) was calculated as follows:

$$h_o = \frac{Oil\ Volume}{(A)(\phi)(1.0 - S_{cw})} \tag{38}$$

It was experimentally determined that the connate water saturation (S_{cw}, pendular ring water) for Core 1 was 6.2% and for Core 2 was 13.2%. In general, the average computed oil height (h_o) was 5.2 cm for Core 1 and 5.9 cm for Core 2.

The measured oil volume was introduced generally about 5.1 cm (2 inches) above the water-air capillary interface. The oil then, rather immediately for Core 1 but somewhat slower for Core 2, gravitated to the water/air interface, spread over it replacing the air, and thus immiscibly displacing the water, lowering the water/oil interface by the weight of the oil column. In this process, oil may have been left behind as residual oil (S_{ro}) above the capillary fringe, and air may have been trapped as residual gas saturation (S_{rg}) in the oil column. Because both the S_{ro} and S_{rg} could not be measured with the experimental set-up, it is here assumed that both parameters are 0 % and therefore left out of equation 38.

Since the interfaces between the air and the oil, and the oil and the water in the core were very difficult to observe, the water/oil capillary fringe height, $h_{c(w/o)}$ in Figure 23, was calculated using the water/air capillary fringe height in Figure 22 (which was easily visually measured) and the calculated oil height as per equation 38, as follows:

$$h_{c(w/a)}\ \rho_w = h_o\ \rho_o + h_{c(w/o)}\ \rho_w$$

$$h_{c(w/o)} = \frac{h_{c(w/a)}\ \rho_w - h_o\ \rho_o}{\rho_w} \tag{39}$$

If the calculated water/oil capillary fringe height ($h_{c(w/o)}$) and the calculated oil height (h_o) were added, the sum, i.e. total liquid height, would add up to a value that was within ±1.5 cm of the observed total liquid height in the core, which was not accurately discernable.

It is noted that for all experiments, $h_{c(w/o)}$ was kept above the free water table, limiting the mass of oil used in the experiments, and consequently h_o. In addition, in light of the fact that the water/oil and oil/air interfaces were difficult to discern, the production probe height was measured from the free water table. The production probe distance, h_1 or h_2 in Figure 23, was then computed using the calculated water/oil capillary height, $h_{c(w/o)}$ Figure 23, as determined for the subject experiment, which was slightly different from experiment to experiment; as the water/oil capillary height was calculated from the measured water/air capillary height, which had a variance range of about 0.5 to 1.0 cm for Core 1, and 0.75 to 1.5 cm for Core 2.

6.1 Drawdown

In the petroleum technology, the concept of drawdown (DD) (Lyons, 1996; Craft and Hawkins, 1959) is used, which relates to the well's ability to produce (q), as expressed in the productivity index (PI), as follows:

$$PI = \frac{q}{DD} \tag{40}$$

Where DD (also called pressure drawdown) is the pressure differential between the static reservoir pressure, P_{st}, and the bottom downhole wellbore flowing pressure, P_{wf}, as follows:

$$DD = P_{st} - P_{wf} \tag{41}$$

The drawdown concept can be applied to the subject experimental core, whereby the wellbore sandface is the production probe inlet inside the core, as follows:

$$DD = P_{st} - P_{probe} \tag{42}$$

For the production probe located in the oil column, h_1 above the water/oil interface, Figure 23, is:

$$P_{st} = P_{atm} + (h_o - h_1)\rho_o g \tag{43}$$

$$P_{probe} = P_{atm} - VP \tag{44}$$

where P_{atm} is the atmospheric pressure, and VP is the vacuum suction pressure exposed to the production probe.

In Figure 23 it is assumed that all glass beads in the oil column are covered with a film of water, and consequently the glass bead/oil/air capillary pressure is assumed to be: $P_{c(o/a)} = 0$, as annotated in Figure 23, and this term is left out of equation 43.

By applying equations 43 and 44 to the DD equation 42, it will yield:

$$\begin{aligned} DD &= (P_{atm} + (h_o - h_1)\rho_o g) - (P_{atm} - VP) \\ &= (h_o - h_1)\rho_o g + VP \end{aligned} \tag{45}$$

Because VP is measured in inches of water, the oil column term is to be expressed in inches

of water, as follows:

$$DD = \frac{(h_o - h_1)\rho_o g}{(2.54 cm/inch)(\rho_w)} + VP \qquad (46)$$

where h_o and h_1 were measured in centimeters.

For the production probe located at a depth h_2 below the water/oil interface, Figure 23, the DD concept yields:

$$P_{st} = P_{atm} - h_3\rho_w g \qquad (47)$$

$$P_{probe} = P_{atm} - VP \qquad (48)$$

therefore:

$$\begin{aligned} DD &= (P_{atm} - h_3\rho_w g) - (P_{atm} - VP) \\ &= -h_3\rho_w g + VP \end{aligned} \qquad (49)$$

Because VP is measured in inches of water, and h_3 is measured in centimeters, the equation is written in terms of inches of water as follows:

$$\begin{aligned} DD &= \frac{-h_3\rho_w g}{(2.54\ cm/inch)(\rho_w)} + VP \\ &= \frac{-h_3 g}{2.54\ cm/inch} + VP \end{aligned} \qquad (50)$$

It is observed that in equation 50, the capillarity of the glass bead/water/oil system is

incorporated in h_3.

6.2 Production Pressure Head

For water wells, the term production pressure head (PPH) is used, which is defined as the pressure differential between the weight of the liquid (water) column, and the suction pressure of the water pump. When this concept is applied to the subject experimental core, this would yield for the production probe in the oil column, expressed in inches of water,

$$PPH = \frac{(h_o - h_1)\rho_o g}{(2.54\ cm/inch)\rho_w} + VP \qquad (51)$$

where VP was measured in inches of water and h_o and h_1 measured in centimeters. One would observe that the PPH equation 51 and the DD equation 46 are identical for the production probe being in the oil column, assuming $P_{c(o/a)} = 0$, Figure 23.

For the production probe being h_2 below the water/oil interface, Figure 23, the PPH would interpret, expressed in inches of water, as follows:

$$\begin{aligned} PPH &= \frac{h_o\rho_o g}{(2.54\ cm/inch)\rho_w} + \frac{h_2\rho_w g}{(2.54\ cm/inch)\rho_w} + VP \\ &= \frac{h_o\rho_o g}{(2.54\ cm/inch)\rho_w} + \frac{h_2 g}{2.54\ cm/inch} + VP \end{aligned} \qquad (52)$$

Here though, it was immediately concluded that for the production probe being below the water/oil interface, the DD equation 49 and the PPH equation 52 are incompatible, because the PPH does not take into account the capillary pressure at the water/oil interface and the

oil/air interface.

It is observed that for most experiments the VP, in inches of water, is less than the water capillary height, $h_{c(w/a)}$, in Figure 22, and consequently the capillarity of the cores cannot be ignored in the results of the tests, as illustrated in the following section.

6.3 Comparison of the Experimental Core with a Capillary Tube

Literature (e.g. Lu *et al.*, 1995) identified that the capillary effect in a glass bead pack can be illustrated with a capillary tube with a normalized inside tube radius (r), as follows:

$$P_c = \rho g h_c = \frac{2\sigma\cos(\theta)}{r} \tag{53}$$

When this tube is vertically dipped into water, Figure 24(a), the water capillary pressure is expressed as:

$$P_{c(w/a)} = h_{c(w/a)}\rho_w g \tag{54}$$

Similarly, for this tube dipped into oil, Figure 24(b), the oil capillary pressure is expressed as:

$$P_{c(o/a)} = h_{c(o/a)}\rho_o g \tag{55}$$

Whether $h_{c(w/a)}$ will be larger or smaller than $h_{c(o/a)}$ depends on the relevant value of the interfacial tensions, contact angles, and densities. In Figure 24 it is assumed that $h_{c(w/a)} > h_{c(o/a)}$, or $\theta_{w/a} < \theta_{(o/a)}$ with $\theta_{(o/a)} < 90°$, and $\rho_w > \rho_o$.

When this capillary tube is dipped into a liquid, which consist of a small oil layer on

top of water in a container, whereby, when the tube is in the water, the oil layer in the container is removed, the capillary effects are as illustrated in Figure 25. For Figure 25 the same concepts can be applied as equations 3 and 4 yielding equation 9, resulting in:

$$P_{c(w/o)} + P_{c(o/a)} = h_w \rho_w g + h_o \rho_o g \qquad (56)$$

Whether the oil/air capillary pressure will contribute to raising the water column, h_w, depends on the relevant heights of h_o, Figure 25, and $h_{c(o/a)}$ in Figure 24. Thus, for $h_o < h_{c(o/a)}$, the $P_{c(o/a)}$ will contribute to increase the water column, h_w; and for $h_o > h_{c(o/a)}$, the oil column difference $h_o - h_{c(o/a)}$ will depress the water column h_w.

For purposes of the subject experiments, the oil column h_o (equation 38) was chosen such that an adequate water column was available above the free water table, h_w, to conduct the required experiments; however the glass bead/oil/air capillary height, $h_{c(o/a)}$, was not experimentally determined with the cores.

Analogous to Calhoun's (1982, Section 43) elucidation, the liquid pressure at Point A, Figure 25, is:

$$P_A = P_{atm} - P_{c(o/a)} + (h_o - h_1)\rho_o g \qquad (57)$$

the pressure in a production probe at point A is:

$$P_{probe} = P_{atm} - VP \qquad (58)$$

Consequently, the drawdown for point A is:

$$\begin{aligned} DD &= P_A - P_{probe} \\ &= (P_{atm} - P_{c(o/a)} + (h_o - h_1)\rho_o g) - (P_{atm} - VP) \\ &= (h_o - h_1)\rho_o g + VP - P_{c(o/a)} \end{aligned} \tag{59}$$

wherein:

$$\begin{aligned} P_{c(o/a)} &= \frac{2\pi r\sigma\cos(\theta_{o/a})}{\pi r^2} \\ &= \frac{2\sigma}{r}\cos(\theta_{o/a}) \end{aligned} \tag{60}$$

This identifies that $P_{c(o/a)}$ has an effect on the drawdown.

For the cores it was assumed that the glass beads in the oil zone are completely wetted with a film of water (Section 6.1) and consequently there is no glass bead/water/oil interface line (meniscus). This is analogous to the $\theta_{o/a}$ being 90° which renders $P_{c(o/a)} = 0$ in equation 60 and consequently this DD equation is reduced to:

$$DD = (h_o - h_1)\rho_o g + VP \tag{61}$$

which is identical to equations 45 and 51.

Calhoun's elucidation for the liquid pressure in Point B below the oil column, Figure 25, is:

$$P_B = P_{atm} - P_{c(o/a)} + h_o\rho_o g - P_{c(w/o)} + h_2\rho_w g \tag{62}$$

or:

$$P_B = P_{atm} - h_3\rho_w g \tag{63}$$

with the drawdown for the production probe located at point B being:

$$\begin{aligned} DD &= P_B - P_{probe} \\ &= (P_{atm} - h_3\rho_w g) - (P_{atm} - VP) \\ &= -h_3\rho_w g + VP \end{aligned} \tag{64}$$

Since equations 62 and 63 are equal, h_3 can be expressed as follows:

$$h_3\rho_o g = -h_2\rho_w g - h_o\rho_o g + P_{c(o/a)} + P_{c(w/o)} \tag{65}$$

or:

$$h_3 = -h_2 - \frac{h_o\rho_o}{\rho_w} + P_{c(o/a)} + P_{c(w/o)} \tag{66}$$

The assumption that all glass beads in the oil zone are covered with a film of water makes the glass bead/water/oil interface non-existent, and consequently it is assumed that $P_{c(o/a)} = 0$, and therefore:

$$h_3 = -h_2 - \frac{h_o\rho_o}{\rho_w} + P_{c(w/o)} \tag{67}$$

One concludes, that for h_3 to be positive, as was the case for all experiments, i.e. above the free water table, the following condition applies:

$$P_{c(w/o)} > h_2 + \frac{h_o \rho_o}{\rho_w} \qquad \textbf{(68)}$$

identifying that the capillarity, $P_{c(w/o)}$, in the porous medium has a direct impact on the DD for all experiments performed, as identified in the comment for DD equation 50. In principle, equation 68 is a condition for PPH equation 52 in that h_o and h_2 are dependant on $P_{c(w/o)}$.

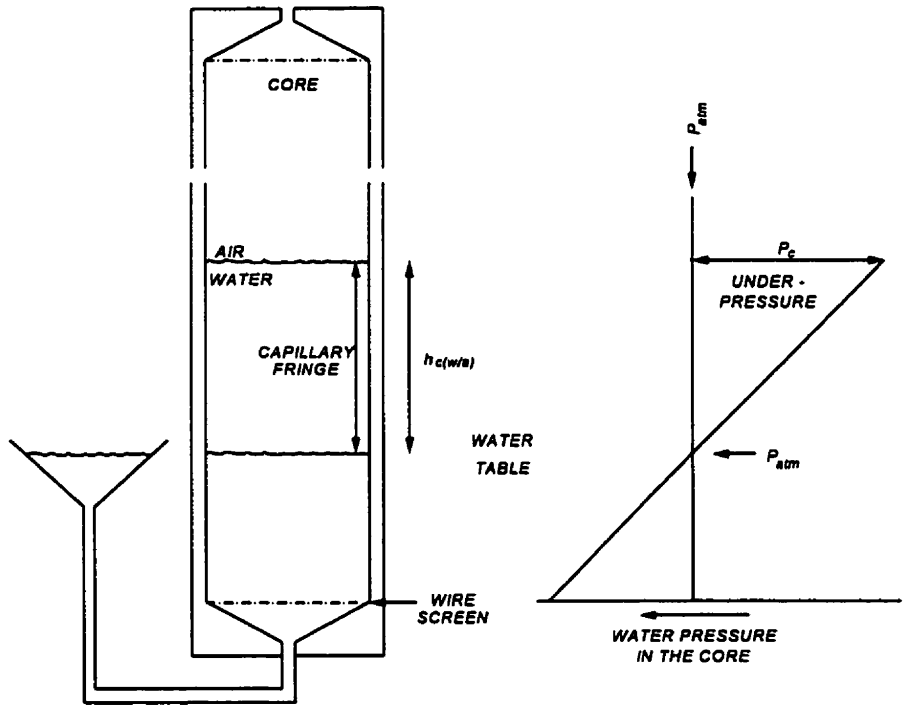

Figure 22: Schematic Diagram of Core with Water/Air Capillary Fringe and the Axial Water Pressure Profile

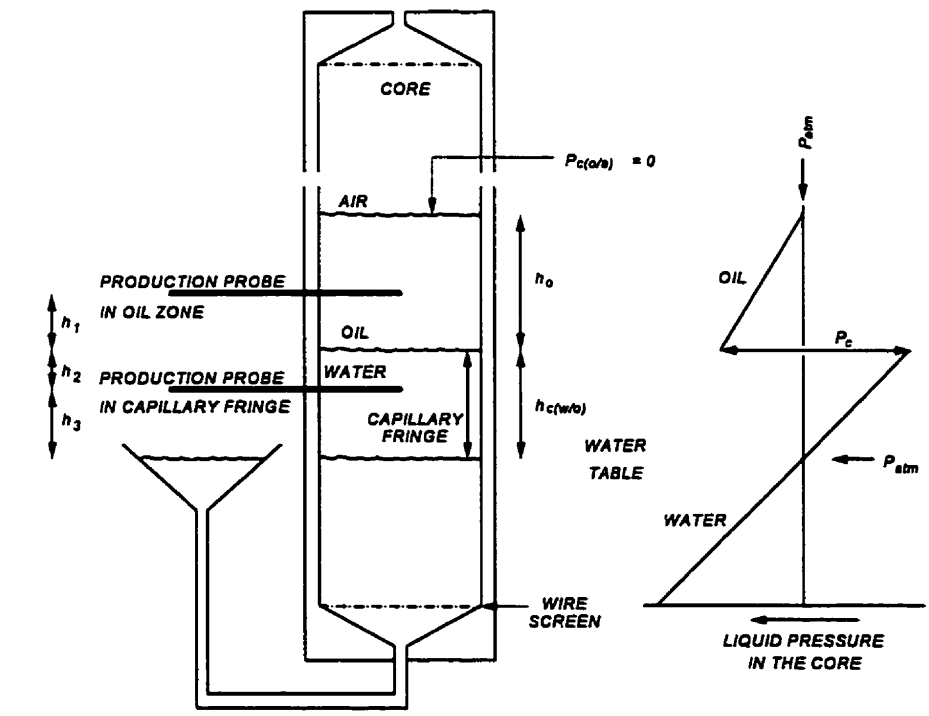

Figure 23: Schematic of Fluid Levels when Oil has been Introduced into the Core, and the Axial Liquid Pressure Profile

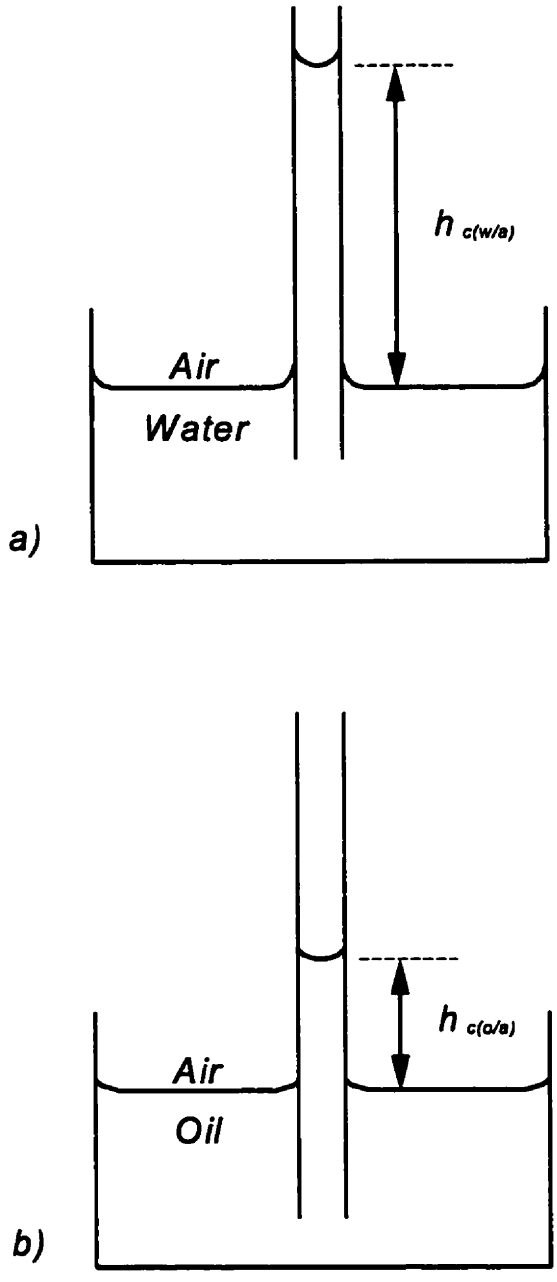

Figure 24: Liquids in Capillary Tubes

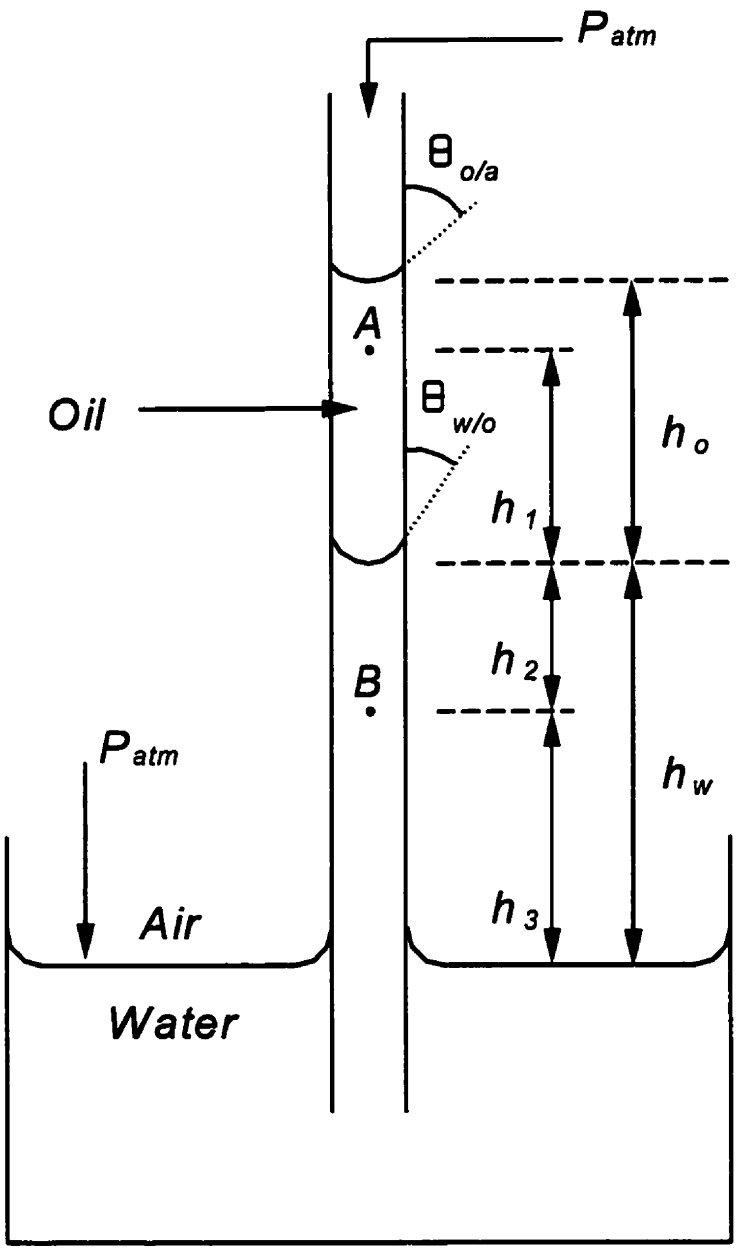

Figure 25: Oil and Water in same Capillary Tube

CHAPTER 7

RESULTS AND DISCUSSION

A series of experiments were performed to investigate the recovery performance of a hydrocarbon spill from the capillary fringe. In total, 24 experiments with Core 1 and 12 experiments with Core 2 were performed using the drainage capillary fringe system. The raw data collected from all experiments were plotted and these plots are presented in Appendix A. An example of an original raw data set is presented in Appendix B.

The plots show the cumulative water and hydrocarbon production, as well as the gas flow rate as a function of time. For some of the experiments the gas meter bobbed between a minimum and a maximum and hence, for these experiments the minimum and maximum readings were taken and plotted. For other experiments the gas flow rate was either more steady and only one reading was taken (annotated as the maximum) or, there was no gas flow observed in the core (it is noted that the threshold air flow rate for the meter is 0.4 cc/min).

There are no plots for experiments 38 or 57 with Core 1. In the case of experiment 38, there was an inability to completely shut off the water valve (it was stuck) and only water was produced straight from the water reservoir. Therefore, this experiment was considered a failure. In the case of experiment 57, the chemical di-Ethyl-Phthalate was used, which is heavier than water. Although the collection system was hooked up to a probe located below the water table level, it was quickly discovered that the chemical had completely sunk to the bottom of the core before the experiment was started and thus producing only water. Upon opening the bottom valve of the core (for cleaning) the di-Ethyl-Phthalate poured out. The

only chemical remaining in the core was most likely at residual saturation. This did demonstrate for Core 1, that although the hydrocarbon and water are immiscible, the capillarity did not prevent easy hydrocarbon liquid movement through the glass bead porous medium, caused by a small gravity difference. In consultation, it was concluded that the experiments with the heavier than water hydrocarbon were not doable with the apparatus. In addition, with experiment 57, it was discovered that di-Ethyl-Phthalate had a detrimental effect on the acrylic wall of the core (see Section 5.1.7). Based on the above, it was also concluded that all further planned experiments with this chemical could not be carried out for either core.

Two experiments, numbered 29 and 40, did not produce meaningful interpretations and are therefore not discussed. They are stand alone tests and could be considered exploratory tests, and their results are shown in Appendix A.

In addition to all experimental tests being performed according to an initial set of test conditions regarding the location of the production probe and vacuum pressure; all tests were extended to evaluate the incremental hydrocarbon recovery with respect to raising the vacuum pressure and for shutting off the water supply to the core.

For all experiments under the initial test conditions, whenever there was no water production, there was also no water released from the water reservoir into the water table in the funnel, regardless of the volume of hydrocarbon produced.

All sets of experiments were performed in sequence and/or randomly, with the assumption that the core cleaning process resulted in the exact same standard of cleanliness of the core for every experimental procedure (Section 5.2).

For several experiments it was observed that with the closing of the production probe valve at the end of the experiment, a notable drop of hydrocarbon was released from the production flow line into the production collection cylinder. This resulted in a small increase in the recovery of hydrocarbon, which appears as a blip at the end of the rate versus cumulative production curve.

All tests performed were done to address the following parameters with regard to the recovery performance of hydrocarbon spills in the vicinity of the capillary fringe zone:

1. The reproducibility of experiments,
2. The effect of vacuum suction pressure,
3. The effect of production probe height above the free water table,
4. The effect of the volume of hydrocarbon spill,
5. The effect of "rainfall",
6. The effect of time allowed for equilibration,
7. The effect of dropping the water table,
8. The effect of raising the water table,
9. Method of entering the hydrocarbon into the core, and
10. The effect of production probe drawdown and its distance to the water/hydrocarbon interface on the recovery factor.

7.1 Reproducibility of Experiments

The reproducibility of an experiment implies that for identical experiments, all fluids will settle in the same or similar manner in the pore spaces during the experimental set up,

i.e. during the development of the air/water capillary fringe, during the placement of the hydrocarbon spill in the core, and during equilibration time; and in the way that the fluids are produced during the experimental test itself, within acceptable measurement accuracies and tolerances (see Sections 5.2.2 and 5.2.3). Four randomly chosen sets of experimental tests for Core 1 were subject to reproducibility: experiments 32 and 33; experiments 28, 30 and 35; experiments 27 and 36; and experiments 26 and 31.

7.1.1 Set 1: Experiments 32 and 33 (Core 1)

This set of experiments was performed under the initial conditions of the production probe being in the hydrocarbon column 5.1 cm above the free water table, and a vacuum pressure (VP) of 1.0 inches of water, Table 11. Figure 26 shows that the production profiles are very similar in shape and deflections with comparable recovery factors (RF). These two experiments are therefore considered to show good reproducibility.

7.1.2 Set 2: Experiments 28, 30, and 35 (Core 1)

This set of experiments was performed under the initial conditions of the production probe being in the water capillary fringe below the hydrocarbon column, and 2.5 cm above the free water table using a VP of 1.0 inches of water, Table 12 (there is no figure). This set of experiments shows a good reproducibility in that none of these tests produced any fluid for the initial conditions. The cause is thought to be that the drawdown (DD), being 0.2 inches of water, was insufficient to initiate production. The under-pressure in the capillary fringe balanced the VP.

In order to evaluate the DD, all three experiments were then subjected to a VP of 2 inches of water yielding varying responses of simultaneous hydrocarbon and water production, Appendix A. In the extended part of the experiment, all three were eventually exposed to a maximum VP of 5.0 inches of water, and the water supply was shut off, whereby the ultimate end recovery was about 47.4 %.

7.1.3 Set 3: Experiments 27 and 36 (Core 1)

This set of experiments was performed under the initial conditions of the production probe being in the water capillary fringe below the hydrocarbon column, 2.5 cm above the free water table using a VP of 0.6 inches of water, Table 13. This set of experiments was similar to Set 2 with the exception, that the VP of Set 3 was 0.6 inches of water, i.e. a lesser VP.

The comparison of these two experiments, Figure 27, shows that the experiments were not reproducible in that experiment 27 went to a RF of 63.4 % while experiment 36 stopped producing hydrocarbon at a RF of 27.8 %. For both experiments, the DD was negative identifying that the VP was less than the under-pressure in the fringe. Surprisingly, a negative DD for these two experiments produced hydrocarbon, while for Set 2, which was identical except for the VP, did not produce any fluids with a DD of 0.2 inches of water. Although the causes could be various, it is speculated that opening the production probe to a negative DD caused some air to enter the core, resulting in the capillary fringe to be broken up. In addition for experiment 36, it is perceived that when production stopped at 10 cc, a Jamin effect may have occurred. On the other hand, for experiments 36, $h_{c(w/a)}$ was higher

than for experiment 27, causing the production probe to be further below the water/hydrocarbon interface, yielding a lesser recovery performance. Further, for experiment 36, it was necessary to increase the VP to 2.0 inches of water to re-induce flow, i.e. water production only. As with Set 2, it was necessary to close the water supply valve and increase the VP to see more incremental hydrocarbon production. Experiment 27 achieved a RF of 63.4 %, while experiment 36 achieved a RF of 59 %, both greater than for the previous set under similar final conditions of the extended experiment.

7.1.4 Set 4: Experiments 26 and 31 (Core 1)

This set of experiments was performed under the initial conditions of the production probe being in the hydrocarbon column 5.1 cm above the free water table, and using a VP of 0.6 inches of water, Table 14. This set of experiments was similar to Set 1 with the exception that the VP was 0.6 inches of water, i.e. a lesser VP; and, the water/air capillary fringe was lower, resulting in h_1 to be greater, i.e. the production probe was higher up in the hydrocarbon zone. A comparison of these two tests show that they were not reproducible, Figure 28. The performance of test 31 followed a similar pattern as the two experiments of Set 1, while experiment 26, after a cumulative production of 2.5 ml, completely stopped producing. Raising the VP to 1.4 inches of water did not result in any additional flow, but with a VP of 2.0 inches of water the production of hydrocarbon achieved a RF of 55.6 %.

The test results suggest that the RF is related to "$h_o - h_1$", which is the length of the hydrocarbon column above the probe, and that there may be an under-pressure under the hydrocarbon/air capillary interface, i.e. there is a $P_{c(o/a)}$ for experiment 26 or a Jamin effect.

In review of the above four sets of tests, it can be concluded that the reproducibility of these experiments cannot be guaranteed because of the variances in capillary behaviour as the most likely cause; e.g. under-pressure in the capillary fringe, the Jamin effect, and the variable nature of the jagged liquid-fluid interfaces.

7.2 Effect of Vacuum Suction Pressure

Two sets of experiments were performed with Core 1 and with Core 2 to evaluate the effect of vacuum suction pressure (VP) on the recovery of hydrocarbons from the capillary region.

7.2.1 Set 1: Experiments 31, 32, 33, and 34 (Core 1)

The results of the first set of experiments with Core 1 are shown in Table 15 and Figure 27. For these experiments the production probe height (PH) was 5.1 cm above the free water table and located in the hydrocarbon column. Figure 29 shows that the VP does not strongly influence the ultimate recovery of hydrocarbons from the capillary fringe. It can also be observed that the rate of hydrocarbon production is not in proportion to Darcy's Law. The production rate is disproportionately higher for a VP of 1.4 inches of water as compared to a VP of 0.6 inches and 1.0 inch of water, suggesting that the fluids may not have equilibrated to comparable saturations, i.e. effective permeability for hydrocarbon effects. Table 15 would also suggest that the RF is related to DD and "h_o - h_l" at the start of the experiment.

7.2.2 Set 2: Experiments 27, 28, 30, 35, 36, 37, and 39 (Core 1)

The results from the second set of experiments with Core 1 are shown in Table 16 and Figure 30. For these experiments the PH was 2.5 cm above the free water table located below the water/hydrocarbon interface. Experiments 27 and 36 are identical experiments, as well as experiments 28, 30, and 35. Surprisingly, experiment 36, with a VP of 0.6 inches of water and a DD of -0.38 inches of water performed similar to experiment 37 with a VP of 1.4 inches of water and a DD of 0.42 inches of water. From this set of experiments it can be concluded, that there is no relationship between VP and RF. Notable is, that a small negative DD will produce hydrocarbon (see also Section 7.1.3), with a RF ranging from 28 - 63 %.

7.2.3 Set 3: Experiments 47, 49, 50 and 51 (Core 2)

The results from the third set of experiments with Core 2 are shown in Table 17 and Figure 31. For the third set, the PH was 7.7 cm above the free water table and located below the water/hydrocarbon interface, i.e. in the water column. For experiment 51, after being exposed to a VP of 4.0 inches of water for 30 minutes, rapid water production started bringing along 3.25 cc of hydrocarbon at the very start of water production and reverting to sole water production thereafter. Considering the production performances of Set 3 it can be argued that only experiments 49 and 50 share similarities in trend and deflections. However, there is no trend with respect to the production performance in relation to VP as for Set 2. It was also observed that all experiments with a negative DD produced hydrocarbon with the RF ranging from 45 - 57 %, while for experiment 51 the DD is 0.97

and yielded only a RF of 9 %.

7.2.4 Set 4: Experiments 52 and 53 (Core 2)

The results from the fourth set of experiments with Core 2 are shown in Table 18 and Figure 32. For the fourth set, the PH was 7.7 cm above the free water table and located in the water column below the water/hydrocarbon interface. The water supply was shut off from the very start of both experiments (after the time for equilibration). The results of these two experiments are not conducive for a meaningful conclusion, other than that the higher the VP the higher the rate of recovery and RF.

7.3 Effect of Production Probe Height Above the Free Water Table

Two sets of experiments with Core 1 and Core 2 were performed to evaluate the effect of production probe height above the free water table (PH) in the recovery of hydrocarbons from the capillary fringe.

7.3.1 Set 1: Experiments 22, 23, 24, 27, and 31 (Core 1)

The results of the first set of tests with Core 1 are shown in Table 19 and Figure 33. For this set, the VP was 0.6 inches of water. Experiments 22 and 23 had the production probe in the hydrocarbon column, while the three other tests had the production probe in the water column, i.e. in the water capillary fringe. When looking at the production performance curves, no relationship can be correlated between production performance and the PH. Also, it is noted that for the experiments with the production probe in the water column, a negative

DD for experiment 23 and 27 produced a large volume of hydrocarbon (RF is 63 to 67 %) while experiment 24 with DD = 0.13 inches of water produced no hydrocarbon. For experiment 22 the hydrocarbon recovery appears to be related to $(h_o - h_l)$, i.e. the higher the hydrocarbon column above the probe the higher the RF, as found in Section 7.1.4.

7.3.2 Set 2: Experiments 45 and 47 (Core 2)

The results of the second set of experiments with Core 2 are shown in Table 20 and Figure 34. For this set, experiments 45 and 47, the production probe was in the water column and the VP was 1.0 inch of water for both experiments. The results show that both experiments have a similar end recovery. However, the production performance curves suggest that the higher the production probe is in the water capillary fringe, the higher the rate of recovery of hydrocarbons without water production, i.e. it is related to distance travelled in the water column. For both experiments, a negative DD, i.e. the VP is less than the under-pressure in the capillary fringe, resulted in hydrocarbon recovery, as in Sections 7.1.3 and 7.2.2.

7.4 Effect of the Volume of Hydrocarbon Spill

Three experiments were performed with Core 1, Table 21 and Figure 35, to evaluate what the effect the volume of hydrocarbon added to the core had in the recovery of hydrocarbons from the capillary fringe. For this set, experiments 41 (36.1 ml hydrocarbon added), 42 (28.9 ml hydrocarbon added), and 43 (43.9 ml hydrocarbon added), the PH was 3.8 cm above the free water table, in the water capillary fringe, and the VP was 1.0 inch of

water. The DD for this set of experiments was -0.5 inches of water, noting that the VP was somewhat less than the under-pressure in the water capillary fringe below the hydrocarbon column. As was identified in the previous section for Core 1, there appears to be a relationship of the distance between the water/hydrocarbon interface and the production probe (h_2), the DD and the recovery of hydrocarbons. For experiment 42, no fluid production was recorded for the prescribed conditions of the experiment, suggesting that capillary under-pressure prevented fluid movements. On the other hand, the same negative DD yielded a RF of 61 and 73 % for experiments 41 and 43 respectively. It can therefore be observed, that the more hydrocarbon that was added above the capillary fringe, i.e. the smaller h_2, the higher the RF. As well, the performance trends for experiments 41 and 43 have similarities in the decline rate (rate vs cumulative production). It is noted that, with the closing of the production probe valve a drop of hydrocarbon was released from the flow line, presenting a blip at the end of the rate curve for experiment 41.

7.5 Effect of "Rainfall"

"Rainfall" was simulated by adding an amount of water above the hydrocarbon zone using a higher probe than the one that was used to inject the hydrocarbon. For these experiments, once the water was added, the unfortunate aspect was that the water/hydrocarbon interfaces were not discernable at all and hence fluid movements were open to speculation. When water was added above the lighter than water hydrocarbon, two effects took place. First, the density of the hydrocarbon was lighter than that of the water by 0.3, prompting the hydrocarbon to rise above the water. Second, the weight of the added

water column on top of the hydrocarbon caused an imbibition process on the top of the hydrocarbon zone and a drainage process on the bottom.

It was observed, that the liquid movements of the lighter than water hydrocarbon with a gravity difference of 0.3, were not comparable to the liquid movement of the heavier than water hydrocarbon with a gravity difference of 0.1, experiment 57 (page 115); and therefore, it is speculated that the glass bead/water/hydrocarbon contact angles are not comparable.

For these experiments, the equilibration time provided after the addition of water on top of the hydrocarbon zone was 24 hours for Core 1 and 48 hours for Core 2. It was observed that there was no water release from the water reservoir, and a minimal water table movement in the funnel from the start of water injection to the end of the equilibration time. This suggests that all fluids where held in capillarity. For these experiments, the position of the production probe was chosen arbitrarily and relative to the free water table and its position with respect to the water/hydrocarbon interface, i.e. whether or not the probe was in the hydrocarbon column after the equilibration time, is unknown. Hence, the concept of drawdown cannot be expressed.

Four sets of experiments were performed to evaluate the effect of "rainfall" on the recovery of hydrocarbons from the capillary fringe, three sets with Core 1 and one set with Core 2. Each set of experiments was, in principle, identical for the initial set up of the experiment including the PH, whereby, for the first experiment, no water was added.

7.5.1 Set 1: Experiments 22 and 46 (Core 1)

The results of the first set of experiments with Core 1 are shown in Table 22 and Figure 36. For this set, the PH was 6.3 cm which was in the hydrocarbon zone, $h_1 = 2.43$ cm, and the VP was 0.6 inches of water, which gave a DD = 1.35 inches of water for experiment 22. For experiment 46, before the "rainfall", $h_1 = 1.23$ cm, i.e. the production probe was lower in the hydrocarbon column than for experiment 22, due to the difference in $h_{c(w/a)}$. Figure 36 suggests that the hydrocarbon did not migrate to the top of the "rainfall" water and that "rainfall" is conducive for increased hydrocarbon production performance and recovery. However, it could also be speculated that for experiment 46 the production probe before the "rainfall" was lower in the hydrocarbon column, and consequently was able to produce more hydrocarbon, assuming that all liquids were held in place in capillarity after the "rainfall".

7.5.2 Set 2: Experiments 23 and 44 (Core 1)

The results of the second set of experiments with Core 1 are shown in Table 23 and Figure 37. For this set, the PH was 3.8 cm, which was in the water zone for experiment 23, with $h_2 = 0.35$ cm, and the VP was 0.6 inches of water, which gave experiment 23 a DD = -0.9 inches of water yielding a RF of 66.8%. The results of the second set were the opposite of the previous set in that "rainfall" (adding of 10 cc of water) resulted in no fluids being produced for experiment 44. Even raising the VP to 3.0 inches of water and closing off the water valve did not result in hydrocarbon production. From this experiment, it may be speculated that the hydrocarbon migrated due to gravity effects.

7.5.3 Set 3: Experiments 26, 31, and 48 (Core 1)

The results of the third set of experiments with Core 1 are shown in Table 24 and Figure 38. For this set, with experiments 26 and 31 being identical, the PH was 5.1 cm, which was in the hydrocarbon zone for experiments 26 and 31 with $h_1 = 0.73$ and 1.02 cm respectively, and the VP was 0.6 inches of water, which gave experiments 26 and 31 a DD of 1.73 and 1.81 inches of water respectively. The results from this set suggest that "rainfall" is detrimental to the recovery of hydrocarbons, although, increasing the VP and shutting off the water supply for the extended part of the experiments does result in comparable recoveries.

7.5.4 Set 4: Experiments 45, 54, and 55 (Core 2)

The results of the fourth set of experiments with Core 2 are shown in Table 25 and Figure 39. For this set, the PH was 10.2 cm and the VP was 1.0 inch of water. For experiment 45, the production probe was in the water zone with $h_2 = 2.97$ cm, and the DD was -3.02 inches of water, yielding a RF of 52.3 %. The results of the fourth set of experiments suggest that the greater the volume of the rainfall, the lesser the amount of hydrocarbons can be recovered. It appeared that all fluid movements were blocked, or held in capillarity, or hydrocarbon migration may have taken place.

In review of the above, these experiments suggests that "rainfall" may be conducive for the effective stabilization of a hydrocarbon contaminant spill, i.e. it prevents further spreading of the spill due to liquid blocking or phase trapping; however, it does not promote

a more effective recovery of a spill.

7.6 Effect of Time Allowed for Equilibration

Two experiments, numbers 21 and 22, with Core 1, Table 26 and Figure 40, were performed to evaluate the effect that the time allowed had for water/air and water/hydrocarbon capillary equilibration in the recovery of hydrocarbons from the capillary fringe zone. For these experiments, the PH was 6.3 cm which was in the hydrocarbon column, and the VP was 0.6 inches of water for a DD of 1.34 and 1.35 inches of water respectively. The time allowed for equilibration was 48 hours for experiment 21, and 24 hours for experiment 22. For both experiments, the hydrocarbon was the only fluid produced. The recovery performance curves show, that the end (ultimate) recovery is the same for both experiments. However, the production performance curves also show, that the longer the time given for equilibration, the better the production performance i.e. a higher rate. This is perceived to be due to the effect that the liquids achieved a better equilibrium state with regard to the fluid saturations. Because liquids are more segregated for a longer equilibrium time in favour of the hydrocarbon (the non-wetting phase) in the hydrocarbon zone, the result is a more uniform water/hydrocarbon interface due to gravity difference effects. This may also have affected the effective permeability for the hydrocarbon phase at different water saturations (a lower water saturation for experiment 21) above the water/hydrocarbon interface.

7.7 Effect of Dropping the Water Table

One set of experiments with Core 1, Table 27 and Figure 41, being experiments 32, 33, and 56, were performed to evaluate the effect of dropping the water table in the recovery of hydrocarbons from the capillary fringe zone. For experiments 32 and 33, which are identical experiments, the water table height was 10.25 cm. For experiment 56, the water table height was originally 10.25 cm (equilibration time was 24 hours), after which hydrocarbon was added (equilibration time was 24 hours), and subsequently the water table was dropped to 8.0 cm (relative to the bottom of the glass bead pack, equilibration time was 24 hours) for a water table fall of 2.5 cm. After that, the water/hydrocarbon and the hydrocarbon/air interfaces were not conclusively discernable. For all three experiments, the PH was 5.1 cm above the free water table at the time of production start, which gave a h_l of 0.32 and 0.48 for experiments 32 and 33 respectively, and the VP was 1.0 inch of water.

After the hydrocarbon column above the capillary fringe was equilibrated for experiment 56, the lowering of the water table caused the drainage process to take place at the hydrocarbon/water interface. This may have caused residual hydrocarbon to be left behind (non-wetting fluid entrapment) above the hydrocarbon column since the volume of the non-wetting fluid stays the same, but it spreads out over more porous medium in the core. One the other hand, lowering the water table caused the production probe to be higher up in the hydrocarbon column and consequently, as found in previous experiments, the RF being dependant on $h_o - h_l$, was 48.6 % for experiment 56 as compared to 67.4 % and 64.4 % for experiments 32 and 33 respectively.

7.8 Effect of Raising the Water Table

Two experiments, 45 and 58, with Core 2, Table 28 and Figure 42, were performed to evaluate the effect of raising the water table in the recovery of hydrocarbons from the capillary fringe zone. For experiment 45, the water table was 5.0 cm from the bottom of the glass bead pack. For experiment 58, the water table was originally 5.0 cm from the bottom of the glass bead pack, and after the introduction and subsequent equilibration of the hydrocarbon column, the water table was raised to 9.0 cm above the bottom of the glass bead pack. After raising the water table, the fluids were given 48 hours to equilibrate. The PH was 10.2 cm for experiment 45, and 6.2 cm for experiment 58, i.e. the production probe was not moved after the raising of the water table. The VP was 1.0 inch of water for both experiments.

The RF for experiment 45 was 52.3 % while the RF for experiment 58 was 0 %. Consistent with previous experiments, experiment 45 with h_2 = 2.97 cm and where the DD was -3.02 inches of water, produced hydrocarbon. However, although experiment 58 had a less negative DD, there was no hydrocarbon production. This may be attributed to the fact that the production probe for experiment 58 was further from the water/hydrocarbon interface than for experiment 45. It is noted that for experiment 58, in order to induce liquids production, it was necessary to increase the VP to 4.0 inches of water and to shut off the water supply.

7.9 Method of Entering the Hydrocarbon into the Core

Two experiments, 22 and 25, were performed with Core 1, Table 29 and Figure 43, to evaluate the effect of closing the water valve during hydrocarbon injection into the core. Experiment 22 followed the standard procedure, i.e. using an open water valve; while for experiment 25 the water valve was closed during injection, and after the hydrocarbon was injected the water valve was opened again to allow the fluids to equilibrate. For both experiments, the production probe was in the hydrocarbon column and the DD was 1.35 inches of water for experiment 22 and 1.42 inches of water for experiment 25.

Although the RF's are similar, i.e. 41.6 % for experiment 22 and 46.7 % for experiment 25, the production performance curves show a dramatic difference. For experiment 25, $h_o - h_l$ is 2.23 cm while for experiment 22 it is less, i.e., consistent with the trend of the RF. The cause for this difference may be attributed to the differences in capillarity after the equilibration times.

7.10 Effect of Production Probe Drawdown and its Distance to the Water/Hydrocarbon Interface on the Recovery Factor

It became apparent in the previous sections that there is a relationship between the location of the production probe above the free water table and the recovery factor, even though Section 7.3 alone did not completely bear this out. The production probe location is important in that it relates the position of the probe with respect to the hydrocarbon column.

If the production probe is relatively high in the hydrocarbon column, i.e. the distance between the hydrocarbon/air interface and the production probe is small, there will be air

coning from the top of the hydrocarbon column, and consequently very little hydrocarbon is produced. Further, a production probe located high in the hydrocarbon zone cannot produce the hydrocarbon that is below the production probe, because it was observed from the experiments that there was no movement of water from the reservoir into the water table regardless of the amount of hydrocarbon produced over the experimental time period. This indicates that the water/hydrocarbon interface did not rise during the experiment.

As the location of the production probe was moved further down the hydrocarbon column, the vacuum pressure was assisted by the "weight" of the hydrocarbon column that was above the production probe, as expressed by the drawdown, equation 46. On the other hand, if the production probe was far below the hydrocarbon column, i.e. near the free water table, there was water production only, provided that the vacuum pressure was sufficient to overcome the under-pressure in the water capillary fringe (equation 50).

There are two ways to look at the above aspects of the recovery phenomena: one, is to look at the recovery factor as a function of the production probe height (PH) above the free water table, and second, is to look at the recovery factor as a function of the distance between the water/hydrocarbon interface and the production probe.

With respect to the first way, Figure 44 shows the recovery factor as a function of production probe location relative to the free water table for a couple of different vacuum suction pressures used for Core 1. This figure suggests two things: first, there exists a minimum distance between the production probe and the free water table required in order to materialize the production of hydrocarbon, and this minimum distance increases with increased vacuum pressure. Second, there is an optimum location that would maximize the

recovery of hydrocarbon, and this location is higher up above the free water table for a higher vacuum pressure. However, Figure 44 does not take into consideration the location of the water/hydrocarbon interface with respect to the location of the production probe for each experiment. A similar correlation could not be established for Core 2, because of insufficient data points.

With respect to the second way, Figure 45 shows the recovery factor as a function of the distance between the water/hydrocarbon interface and the position of the production probe for Core 1. Looking at the recovery factor relationship in this manner, it allows for the differences in the heights of the water/hydrocarbon capillary fringe for each experiment to be taken into account. Figure 45 suggests several things: first, there is a maximum distance limit between the water/hydrocarbon interface and the production probe in order to have hydrocarbon production from below the hydrocarbon column. As the probe is located farther away from the interface and closer to the water table, water production would occur more readily than the recovery of hydrocarbon. Second, the maximum distance limit is closer to the water/hydrocarbon interface for a higher vacuum pressure. Third, when comparing the recovery factors for a vacuum pressure of 0.6 inches of water with those for 1.0 inch of water, the higher the vacuum pressure the higher the hydrocarbon recovery at the optimum location. It is noted that there are an insufficient number of data points to render a conclusion from a vacuum pressure of 1.4 inches of water. Finally, the optimum location for a production probe is in the proximity of the water/hydrocarbon interface, and this can be either in the bottom of the hydrocarbon column or just below the water/hydrocarbon interface.

A production probe located just above the water/hydrocarbon interface has the benefit of the "weight" of the hydrocarbon column along with the vacuum pressure, i.e. a drawdown that is larger than the vacuum pressure for the hydrocarbon production.

If the probe is located just underneath the water/hydrocarbon interface, the vacuum suction would have to be stronger than the under-pressure of the water/hydrocarbon capillary fringe as related to the available height, h_3, which in turn is determined by the "weight" of the hydrocarbon column., equation 67. However, this was not observed for more than several experiments, but rather the opposite was seen, i.e. a negative drawdown produced hydrocarbon (e.g. Sections 7.1.3, 7.2.2, 7.2.3, and 7.3.1). It is possible that a production probe located just below the interface could benefit from hydrocarbon coning into the capillary fringe, as the water/hydrocarbon capillary fringe is a "jagged" interface inasmuch as the water/air interface was jagged. Or, the jagged nature of the water/hydrocarbon interface caused the probe to be just in the hydrocarbon column, i.e. in a valley of the jagged interface, although the computed h_o, and consequently the $h_{c(w/o)}$ did not indicate this.

Inasmuch as that there is a relationship between the recovery factor and the location of the production probe relative to the water/hydrocarbon interface and the vacuum pressure, recovery factor distribution plots were made to analyse the combined effect of production probe location and drawdown on the recovery factor.

Figures 46 - 48 show the recovery factor distributions for Core 1, while Figures 49 - 50 show the recovery factor distributions for Core 2. For Figures 46 and 49, only the initial production data points were considered. In both figures, the water supply was open. For the other figures, the plots include the data points that are from the extended part of the

experiments. The recovery factors for all data points were calculated from the "hydrocarbon-in-place" at the time when each step of an experiment started.

Figure 46 suggests that a positive drawdown combined with a positive distance between the water/hydrocarbon interface, i.e. the production probe is above the water/hydrocarbon interface, yields the best recovery. Further, it suggests that a near zero drawdown results in no hydrocarbon recovery.

Since Figure 47 includes the data points from the extended parts of the experiments, it is noted that the extended part of the test had less hydrocarbon in place, and also had the greater possibility of air and water production, especially as the drawdown increases.

For Core 2, no experiments were done with the production probe above the water/hydrocarbon interface. The results for Core 2 are shown in Figures 49 and 50. Remarkably, as seen in Figure 49, a negative drawdown can yield the best recovery. It is possible that when the vacuum suction was applied to the probe, some air flowed into the core breaking up the capillary fringe forming a hydrocarbon migration pathway towards the probe, resulting in hydrocarbon production. On the other hand, there could have been a similar scenario as postulated for Core 1, in that the jagged nature of the water/hydrocarbon interface caused the probe to be just in a valley of the interface, although the computed h_o, and consequently $h_{c(w/o)}$ did not indicate this. For Figure 50, the water supply valve was closed only for the extended part of the experiments, except for two experiments, 52 and 53 for Core 2, where the water supply valve was closed from the start of the experiment.

Generally, it can also be noted that Core 1 yielded a better overall recovery than Core 2, which could be a consequence of Core 1 having a larger pore opening than Core 2,

meaning that the hydrocarbon can be easier trapped in Core 2 than in Core 1.

Table 11: Reproducibility Set 1: Experiments 32 and 33 (Core 1)

Exp.	W/S valve	$h_{c(w/a)}$ (cm)	h_o (cm)	h_1 (cm)	h_2 (cm)	PH (cm)	VP (in H_2O)	DD (in H_2O)	RF (%)
32	open	8.35	5.22	0.32		5.10	1.0	2.32	67.36
	closed						5.0	5.32	67.36
33	open	8.2	5.23	0.48		5.10	1.0	2.28	64.4
	closed						5.0	5.32	65.1

Note: W/S = water supply

Table 12: Reproducibility Set 2: Experiments 28, 30, and 35 (Core 1)

Exp.	W/S valve	$h_{c(w/a)}$ (cm)	h_o (cm)	h_1 (cm)	h_2 (cm)	PH (cm)	VP (in H_2O)	DD (in H_2O)	RF (%)
28	open	8.0	5.23		1.92	2.5	1.0	0.2	0
	open						2.0	1.02	5.31
	closed						2.0	1.02	36.7
	closed						5.0	4.02	45.71
30	open	7.88	5.26		1.78	2.5	1.0	0.2	0
	open						2.0	1.02	5.51
	closed						2.0	1.02	36.5
	closed						5.0	4.02	48.9
35	open	7.93	5.26		1.83	2.5	1.0	0.2	0
	closed						1.0	0.2	0
	closed						2.0	1.02	38.57
	closed						5.0	4.02	47.52

Table 13: Reproducibility Set 3: Experiments 27 and 36 (Core 1)

Exp.	W/S valve	$h_{c(w/a)}$ (cm)	h_o (cm)	h_1 (cm)	h_2 (cm)	PH (cm)	VP (in H_2O)	DD (in H_2O)	RF (%)
27	open	7.75	5.26		1.65	2.5	0.6	-0.38	63.36
	open						4.0	3.02	63.36
36	open	8.13	5.22		2.06	2.5	0.6	-0.38	27.78
	open						1.0	0.02	27.78
	open						2.0	1.02	27.78
	closed						2.0	1.02	47.92
	closed						5.0	4.02	59.03

Table 14: Reproducibility Set 4: Experiments 26 and 31 (Core 1)

Exp.	W/S valve	$h_{c(w/a)}$ (cm)	h_o (cm)	h_1 (cm)	h_2 (cm)	PH (cm)	VP (in H_2O)	DD (in H_2O)	RF (%)
26	open	7.65	5.22	0.73		5.1	0.6	1.73	6.94
	open						1.4	2.43	6.94
	open						2.0	3.03	55.56
	open						5.0	5.31	56.94
	closed						5.0	5.29	56.94
31	open	7.95	5.23	1.02		5.1	0.6	1.81	49.86
	open						2.0	2.47	49.86
	closed						5.0	5.47	59.97

Table 15: Effect of Vacuum Suction Pressure Set 1: Experiments 31, 32, 33, and 34 (Core 1)

Exp.	W/S valve	$h_{c(w/a)}$ (cm)	h_o (cm)	h_1 (cm)	h_2 (cm)	PH (cm)	VP (in H_2O)	DD (in H_2O)	RF (%)
31	open	7.95	5.23	0.73		5.1	0.6	1.81	49.86
	open						2.0	2.47	49.86
	closed						5.0	5.47	59.97
32	open	8.35	5.22	0.32		5.1	1.0	2.32	67.36
	closed						5.0	5.32	67.36
33	open	8.2	5.23	0.48		5.1	1.0	2.28	64.4
	closed						5.0	5.32	65.1
34	open	8.0	5.26	0.7		5.1	1.4	2.63	61.98
	closed						4.0	4.3	63.36

Note: Experiments 32 and 33 are identical

Table 16: Effect of Vacuum Suction Pressure Set 2: Experiments 27, 28, 30, 35, 36, 37, and 39 (Core 1)

Exp.	W/S valve	$h_{c(w/a)}$ (cm)	h_o (cm)	h_1 (cm)	h_2 (cm)	PH (cm)	VP (in H_2O)	DD (in H_2O)	RF (%)
27	open	7.75	5.26		1.65	2.5	0.6	-0.38	63.36
	open						4.0	3.02	63.36
28	open	8.0	5.23		1.92	2.5	1.0	0.02	0.0
	open						2.0	1.02	8.31
	closed						2.0	1.02	36.7
	closed						5.0	4.02	45.71
30	open	7.88	5.26		1.78	2.5	1.0	0.02	0.0
	open						2.0	1.02	5.51
	closed						2.0	1.02	36.5
	closed						5.0	4.02	48.9
35	open	7.93	5.26		1.83	2.5	1.0	0.02	0.0
	closed						1.0	0.02	0.0
	closed						2.0	1.02	38.57
	closed						5.0	4.02	47.52
36	open	8.13	5.22		2.06	2.5	0.6	-0.38	27.78
	open						1.0	0.02	27.78
	open						2.0	1.02	27.78
	closed						2.0	1.02	47.92
	closed						5.0	4.02	59.03

Table 16: Effect of Vacuum Suction Pressure Set 2: Experiments 27, 28, 30, 35, 36, 37, and 39 (Core 1) Continued

Exp.	W/S valve	$h_{c(w/a)}$ (cm)	h_o (cm)	h_1 (cm)	h_2 (cm)	PH (cm)	VP (in H_2O)	DD (in H_2O)	RF (%)
37	open	8.35	5.23		2.27	2.5	1.4	0.42	33.93
	open						2.0	1.02	33.93
	open						3.0	2.02	33.93
	closed						5.0	4.02	49.86
	closed						8.0	7.02	56.79
39	open	8.3	5.23		2.22	2.5	1.8	0.82	0.0
	closed						1.8	0.82	27.0
	closed						5.0	4.02	46.4
	closed						7.0	6.02	52.63

Note: Experiments 27 and 36 are identical, as well as 28, 30, and 35

Table 17: Effect of Vacuum Suction Pressure Set 3: Experiments 47, 49, 50, and 51 (Core 2)

Exp.	W/S valve	$h_{c(w/a)}$ (cm)	h_o (cm)	h_1 (cm)	h_2 (cm)	PH (cm)	VP (in H_2O)	DD (in H_2O)	RF (%)
47	open	16.78	5.93		5.03	7.7	1.0	-2.03	55.48
	closed						10.0	6.97	55.48
49	open	16.98	5.91		5.24	7.7	2.0	-1.03	45.33
	closed						6.0	2.97	46.7
50	open	17.48	5.93		5.73	7.7	3.0	-0.03	57.53
	closed						8.0	4.97	57.53
51	open	17.25	5.9		5.52	7.7	4.0	0.97	8.95
	closed						4.0	0.97	31.68

Table 18: Effect of Vacuum Suction Pressure Set 4: Experiments 52 and 53 (Core 2)

Exp.	W/S valve	$h_{c(w/a)}$ (cm)	h_o (cm)	h_1 (cm)	h_2 (cm)	PH (cm)	VP (in H_2O)	DD (in H_2O)	RF (%)
52	closed	17.03	5.91		5.29	7.7	4.0	0.97	32.28
	closed						8.0	4.97	41.9
53	closed	17.03	5.9		5.3	7.7	3.0	-0.03	13.77
	closed						4.0	0.97	13.77
	closed						5.0	1.97	19.28
	closed						10.0	6.97	26.86

Table 19: Effect of Production Probe Height Above the Free Water Table Set 1: Experiments 22, 23, 24, 27, and 31 (Core 1)

Exp.	W/S valve	$h_{c(w/a)}$ (cm)	h_o (cm)	h_1 (cm)	h_2 (cm)	PH (cm)	VP (in H_2O)	DD (in H_2O)	RF (%)
22	open	7.45	5.23	2.43		6.3	0.6	1.35	41.55
	open						2.0	2.0	50.55
	open						5.0	5.0	70.64
23	open	7.75	5.26		0.35	3.8	0.6	-0.9	66.8
	open						2.0	0.5	66.8
	open						5.0	3.5	66.8
	closed						5.0	3.5	66.8
24	open	7.68	5.17		2.94	1.2	0.6	0.13	0.0
	open						1.0	0.53	0.0
	closed						0.8	0.33	7.0
	closed						5.0	4.53	44.82
	closed						7.0	6.53	50.42
27	open	7.75	5.26		1.65	2.5	0.6	-0.38	63.36
	open						4.0	3.02	63.36
31	open	7.95	5.23	0.73		5.1	0.6	1.81	49.86
	open						2.0	2.47	49.86
	closed						5.0	5.47	59.97

Table 20: Effect of Production Probe Height Above Free Water Table Set 2: Experiments 45 and 47 (Core 2)

Exp.	W/S valve	$h_{c(w/a)}$ (cm)	h_o (cm)	h_1 (cm)	h_2 (cm)	PH (cm)	VP (in H_2O)	DD (in H_2O)	RF (%)
45	open	17.2	5.9		2.97	10.2	1.0	-3.02	52.34
	closed						6.0	1.98	53.03
	closed						10.0	5.98	59.23
47	open	16.78	5.93		5.03	7.7	1.0	-2.03	55.48
	closed						10.0	6.97	55.48

Table 21: Effect of the Volume of Hydrocarbon Spill: Experiments 41, 42, and 43 (Core 1)

Exp.	W/S valve	$h_{c(w/a)}$ (cm)	h_o (cm)	h_1 (cm)	h_2 (cm)	PH (cm)	VP (in H_2O)	DD (in H_2O)	RF (%)
41	open	8.23	5.23		0.85	3.8	1.0	-0.5	60.94
	closed						5.0	3.5	66.48
42	open	8.28	4.19		1.62	3.8	1.0	-0.5	0.0
	open						1.6	0.1	0.0
	open						2.4	0.9	13.84
	closed						2.4	0.9	42.39
	closed						6.0	4.5	55.36
43	open	8.59	6.36		0.43	3.8	1.0	-0.5	72.89
	closed						6.0	4.5	72.89

Table 22: Effect of "Rainfall" Set 1: Experiments 22 and 46 (Core 1)

Exp.	W/S valve	$h_{c(w/a)}$ (cm)	h_o (cm)	Water added (ml)	PH (cm)	VP (in H_2O)	RF (%)
22	open	7.45	5.23	0.0	6.3	0.6	41.55
	open					2.0	50.55
	open					5.0	70.64
46	open	8.68	5.27	19.9	6.3	0.6	54.95
	closed					2.0	56.32

Table 23: Effect of "Rainfall" Set 2: Experiments 23 and 44 (Core 1)

Exp.	W/S valve	$h_{c(w/a)}$ (cm)	h_o (cm)	Water added (ml)	PH (cm)	VP (in H_2O)	RF (%)
23	open	7.75	5.26	0.0	3.8	0.6	66.8
	open					2.0	66.8
	open					5.0	66.8
	closed					5.0	66.8
44	open	8.48	5.19	9.9	3.8	0.6	0.0
	closed					1.4	0.0
	closed					3.0	0.0
	closed					5.0	19.55
	closed					8.0	25.14

Table 24: Effect of "Rainfall" Set 3: Experiments 26, 31, and 48 (Core 1)

Exp.	W/S valve	$h_{c(w/a)}$ (cm)	h_o (cm)	Water added (ml)	PH (cm)	VP (in H_2O)	RF (%)
26	open	7.65	5.22	0.0	5.1	0.6	6.94
	open					1.4	6.94
	open					2.0	55.56
	open					5.0	56.94
	closed					5.0	56.94
31	open	7.95	5.23	0.0	5.1	0.6	49.86
	open					2.0	49.86
	closed					5.0	59.97
48	open	8.45	5.22	19.9	5.1	0.6	4.86
	open					1.4	7.64
	closed					3.0	53.47
	closed					6.0	56.94

Note: Experiments 26 and 31 are identical

Table 25: Effect of "Rainfall" Set 4: Experiments 45, 54, and 55 (Core 2)

Exp.	W/S valve	$h_{c(w/a)}$ (cm)	h_o (cm)	Water added (ml)	PH (cm)	VP (in H_2O)	RF (%)
45	open	17.2	5.9	0.0	10.2	1.0	52.34
	closed					6.0	53.03
	closed					10.0	59.23
54	open	17.4	5.91	24.9	10.2	1.0	49.45
	closed					8.0	49.45
55	open	17.55	5.93	34.9	10.2	1.0	0.0
	closed					2.0	0.0
	closed					3.0	0.0
	closed					4.0	0.0
	closed					6.0	28.77
	closed					10.0	34.25

Table 26: Effect of Time Allowed for Equilibration: Experiments 21 and 22 (Core 1)

Exp.	W/S valve	$h_{c(w/a)}$ (cm)	h_o (cm)	h_1 (cm)	h_2 (cm)	PH (cm)	VP (in H_2O)	DD (in H_2O)	RF (%)
21	open	7.4	5.23	2.48		6.3	0.6	1.34	41.55
	open						1.0	1.0	47.09
	open						2.0	2.0	47.78
	open						5.0	5.0	73.41
22	open	7.45	5.23	2.43		6.3	0.6	1.35	41.55
	open						2.0	2.0	50.55
	open						5.0	5.0	70.64

Table 27: Effect of Dropping the Water Table: Experiments 32, 33, and 56 (Core 1)

Exp.	W/S valve	$h_{c(w/a)}$ (cm)	h_o (cm)	PH (cm)	VP (in H_2O)	RF (%)
32	open	7.95	5.23	5.1	1.0	67.36
	closed				5.0	67.36
33	open	8.2	5.22	5.1	1.0	64.4
	closed				5.0	65.1
56	open	8.53		5.1	1.0	48.63
	closed				5.0	49.32

Note: Experiments 32 and 33 are identical

Table 28: Effect of Raising the Water Table: Experiments 45 and 58 (Core 2)

Exp.	W/S valve	$h_{c(w/a)}$ (cm)	h_o (cm)	PH (cm)	VP (in H_2O)	RF (%)
45	open	17.2	5.9	10.2	1.0	52.34
	closed				6.0	53.03
	closed				10.0	59.23
58	open	17.25		6.2	1.0	0.0
	open				2.0	0.0
	closed				4.0	21.29
	closed				10.0	27.47

Table 29: Effect of Method of Entering the Hydrocarbon into the Core: Experiments 22 and 25 (Core 1)

Exp.	W/S valve	$h_{c(w/a)}$ (cm)	h_o (cm)	h_1 (cm)	h_2 (cm)	PH (cm)	VP (in H_2O)	DD (in H_2O)	RF (%)
22	open	7.45	5.23	2.43		6.3	0.6	1.35	41.55
	open						2.0	2.0	50.55
	open						5.0	5.0	70.64
25	open	7.68	5.27	2.23		6.3	0.6	1.42	46.7
	open						1.0	1.0	49.45
	open						2.0	2.0	57.69
	open						5.0	5.0	63.19

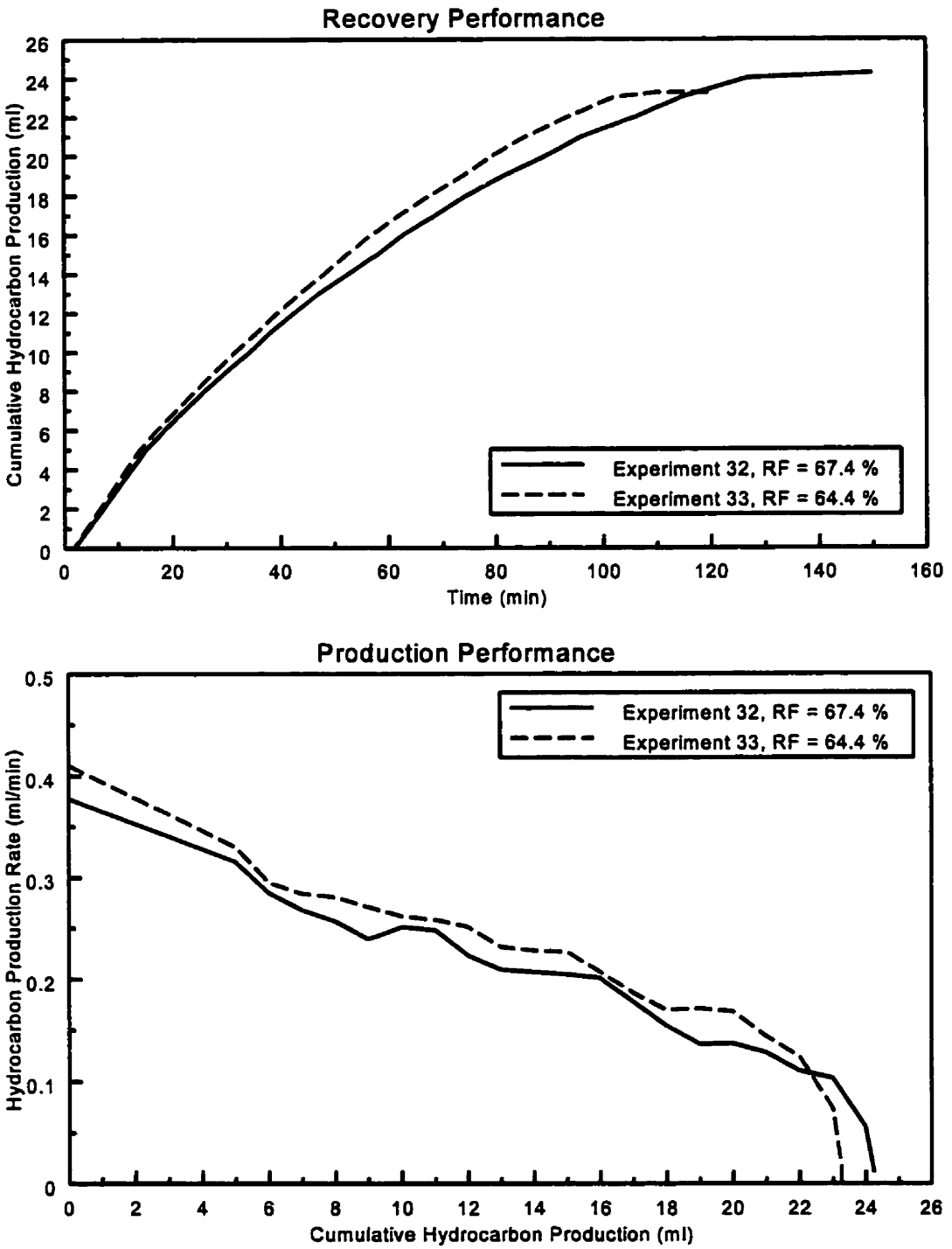

Figure 26: Reproducibility Set 1: Experiments 32 and 33 (Core 1)

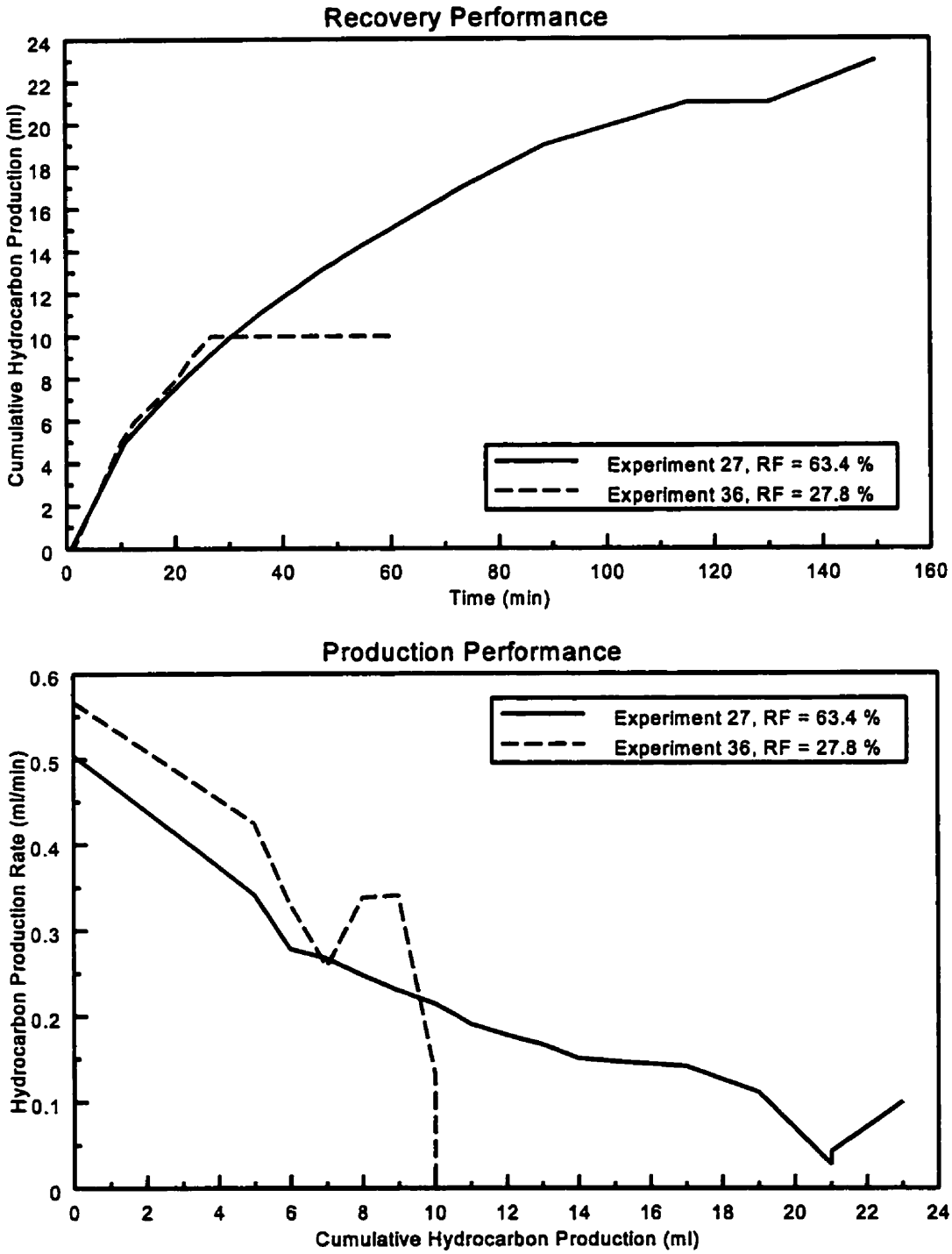

Production Height Above Free Water Table = 2.5 cm
Vacuum Pressure = 0.6 inches of water

Figure 27: Reproducibility Set 3: Experiments 27 and 36 (Core 1)

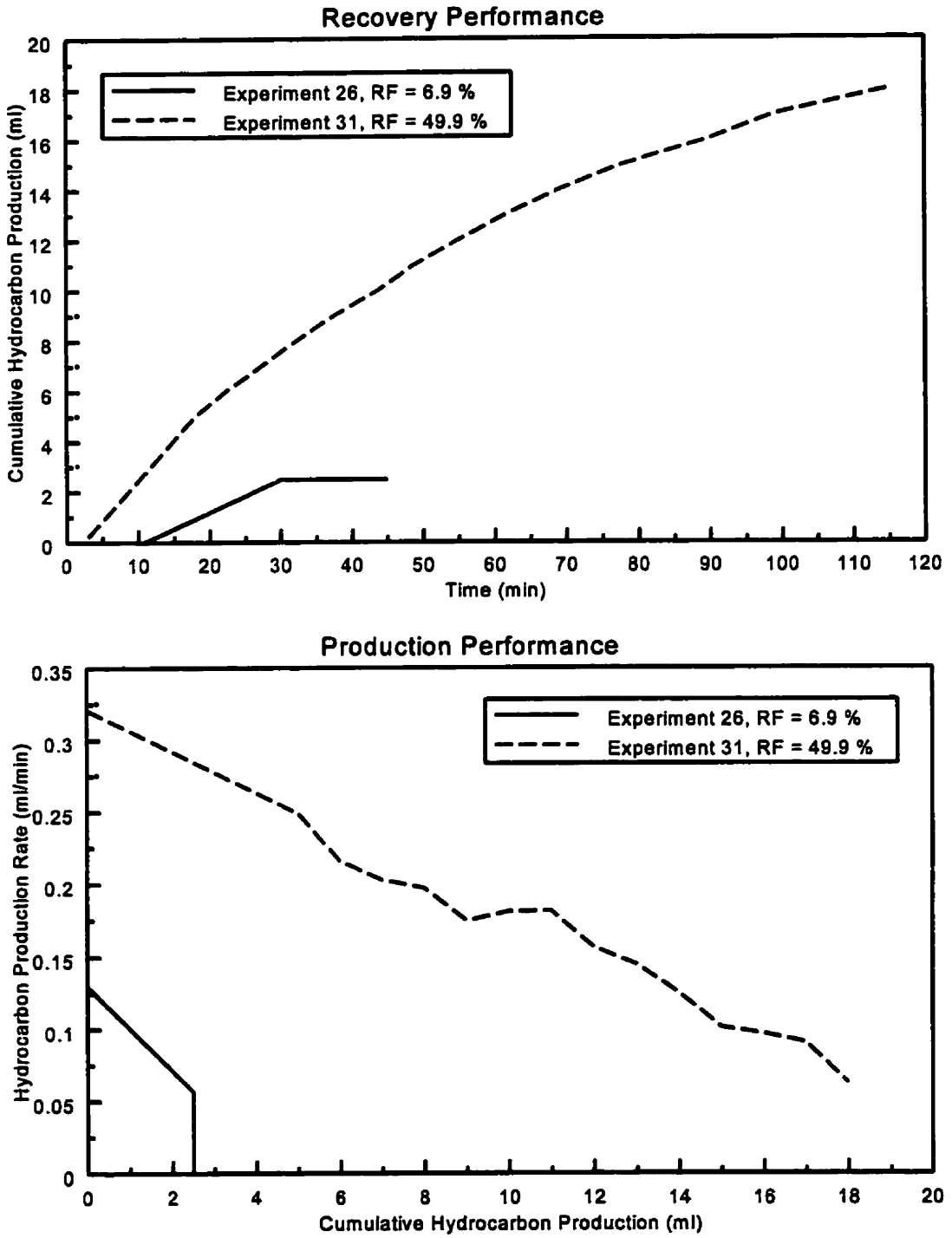

Figure 28: Reproducibility Set 4: Experiments 26 and 31 (Core 1)

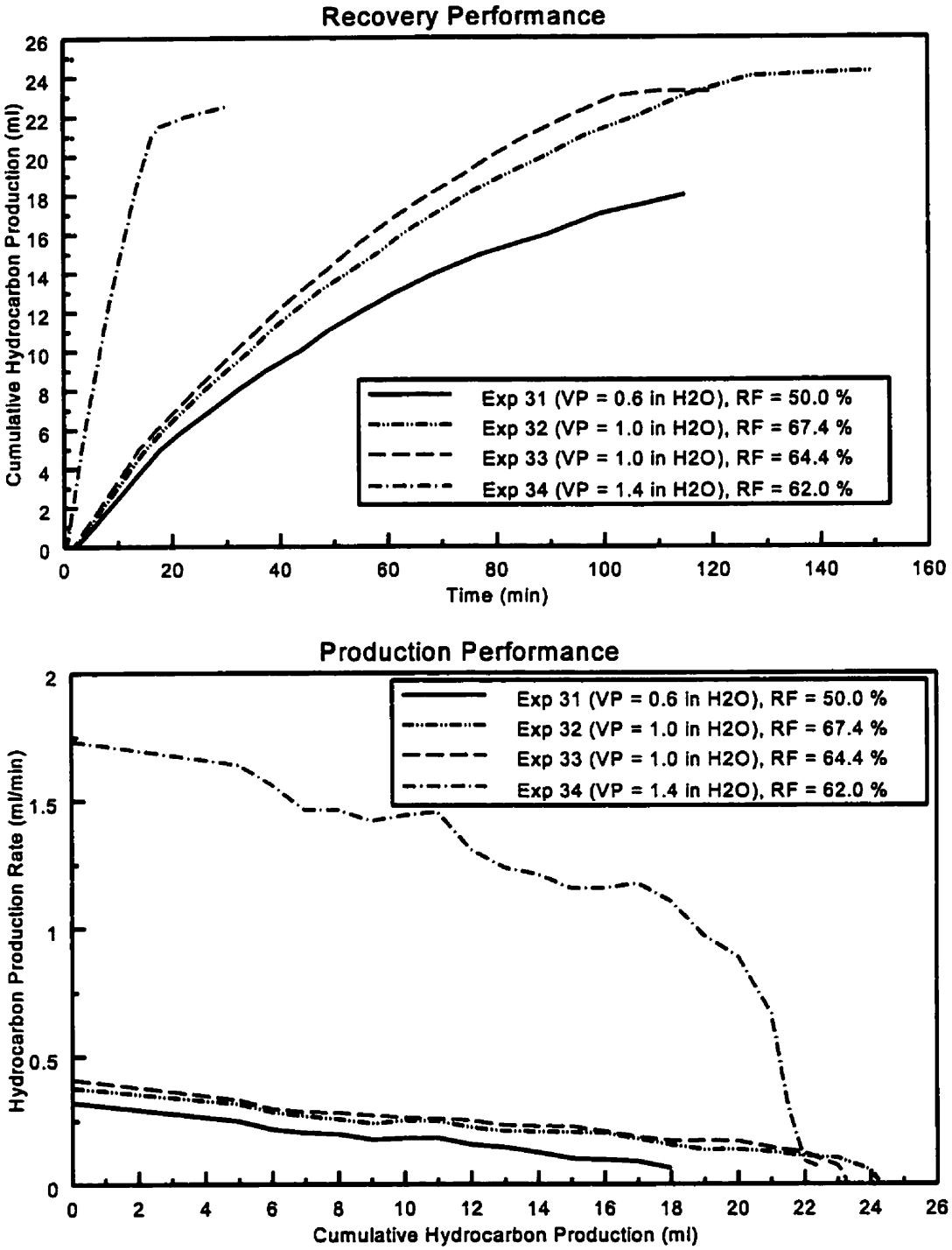

Figure 29: Effect of Vacuum Suction Pressure Set 1: Experiments 31, 32, 33, and 34 (Core 1)

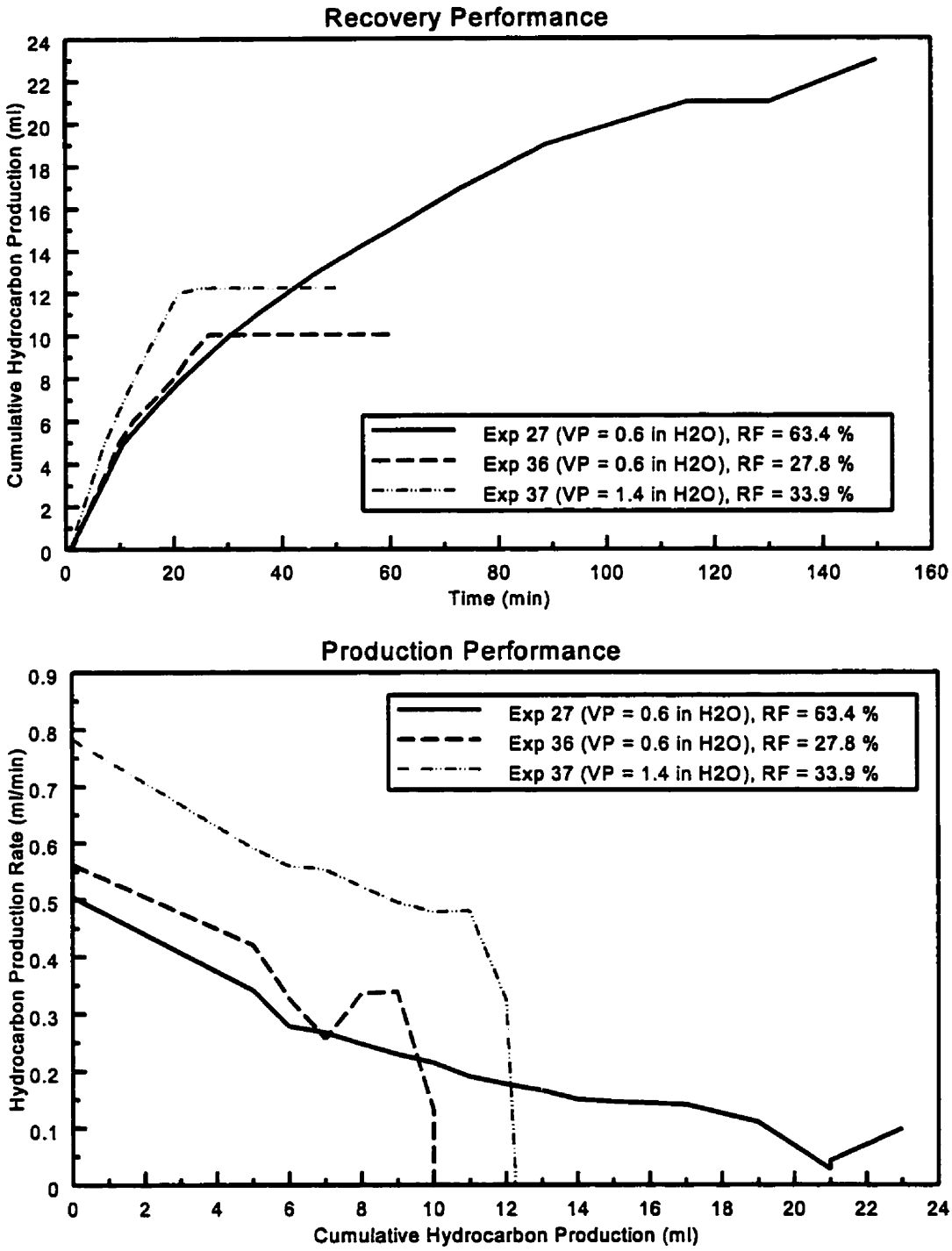

Figure 30: Effect of Vacuum Suction Pressure Set 2: Experiments 27, 28, 30, 35, 36, 37 and 39 (Core 1)

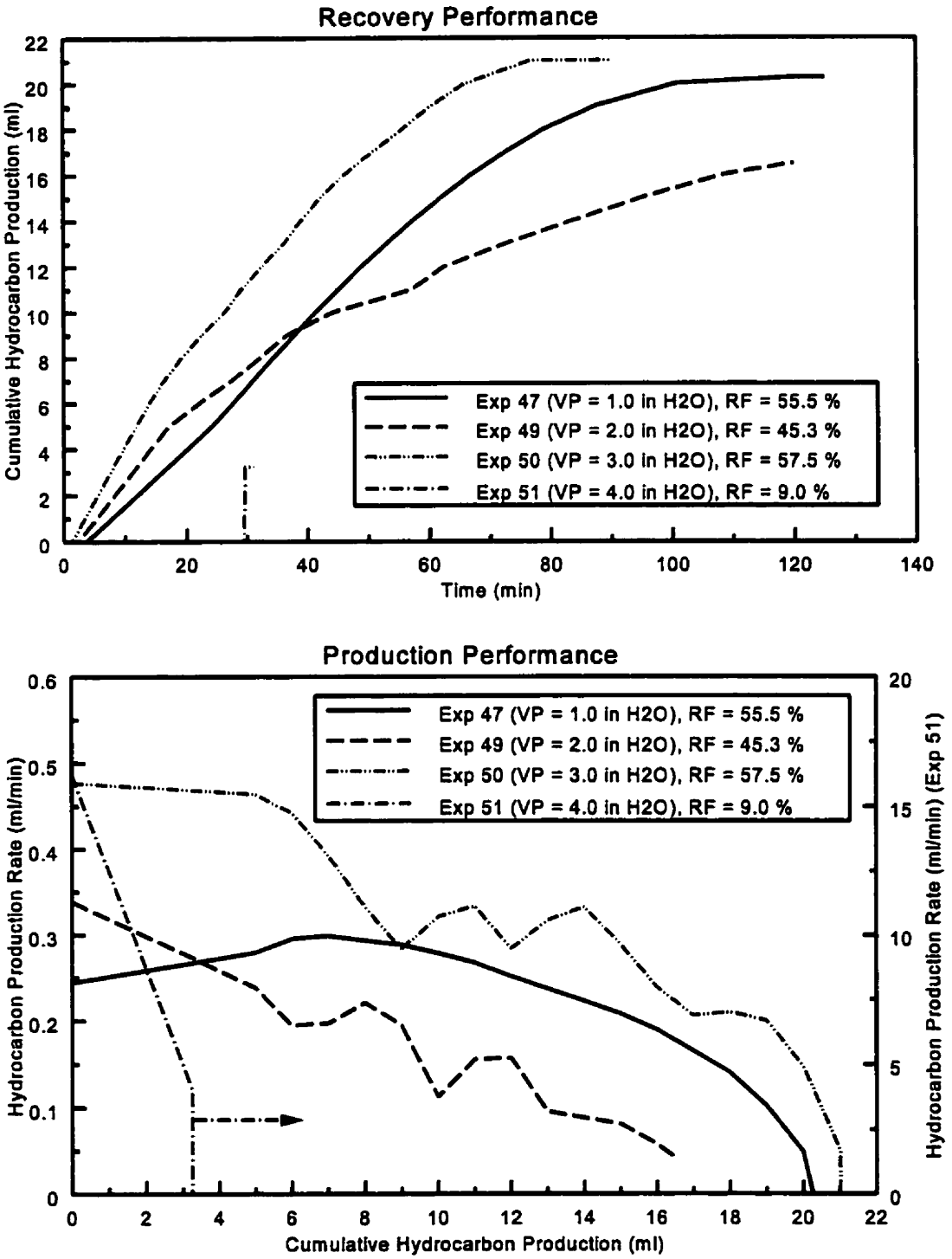

Figure 31: Effect of Vacuum Suction Pressure Set 3: Experiments 47, 49, 50, and 51 (Core 2)

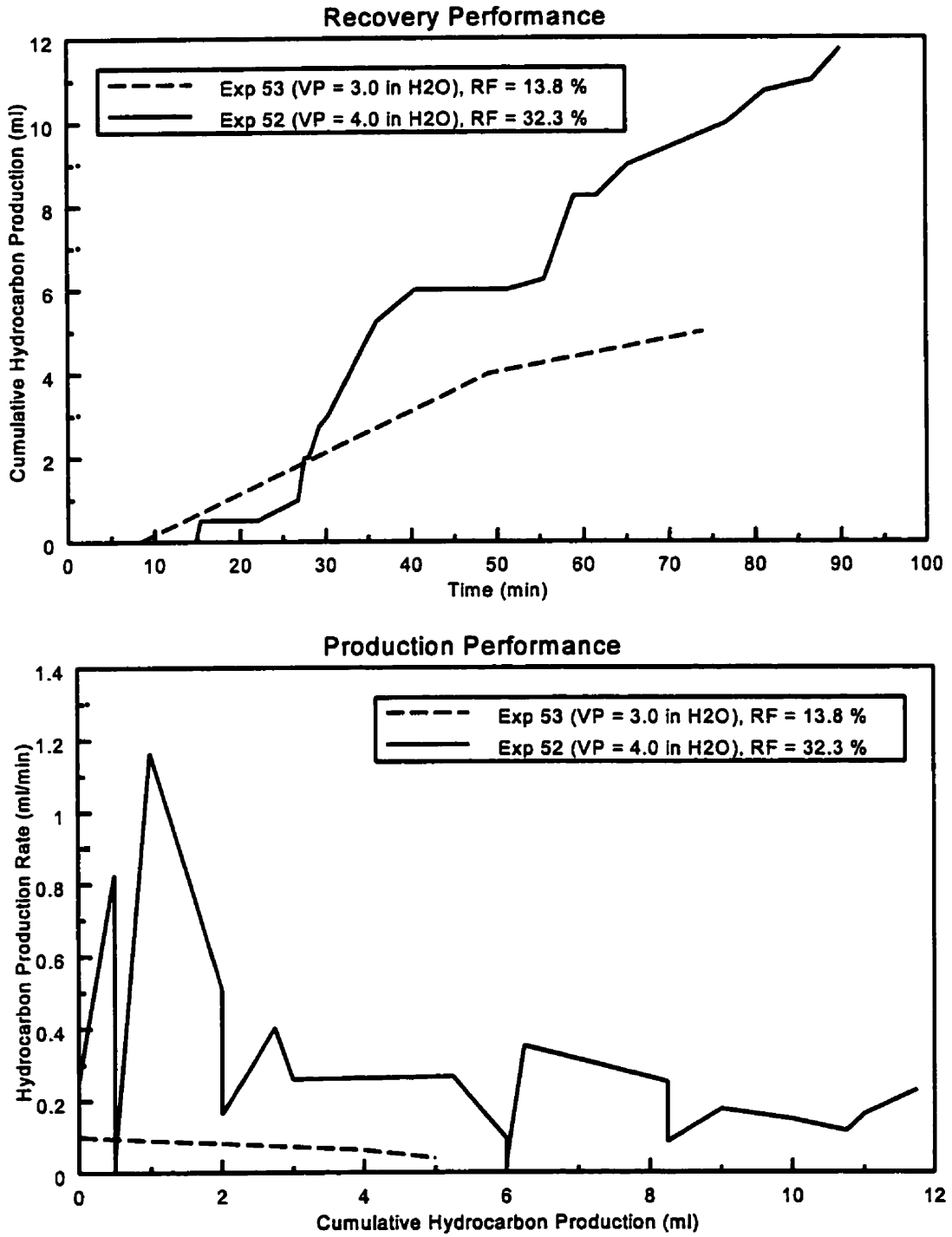

Figure 32: Effect of Vacuum Suction Pressure Set 4: Experiments 52 and 53 (Core 2)

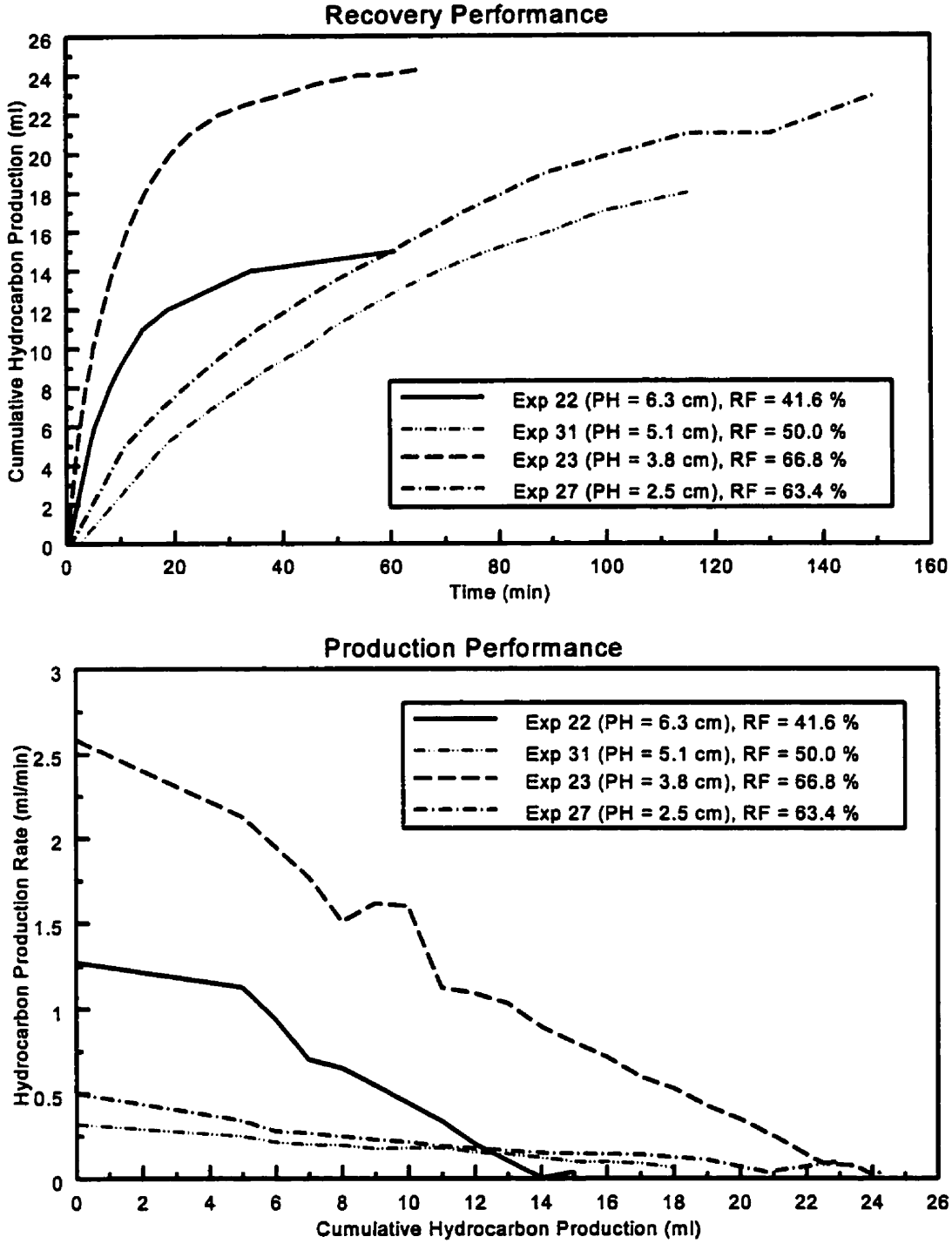

Figure 33: Effect of Production Probe Height Above the Free Water Table Set 1: Experiments 22, 23, 24, 27, and 31 (Core 1)

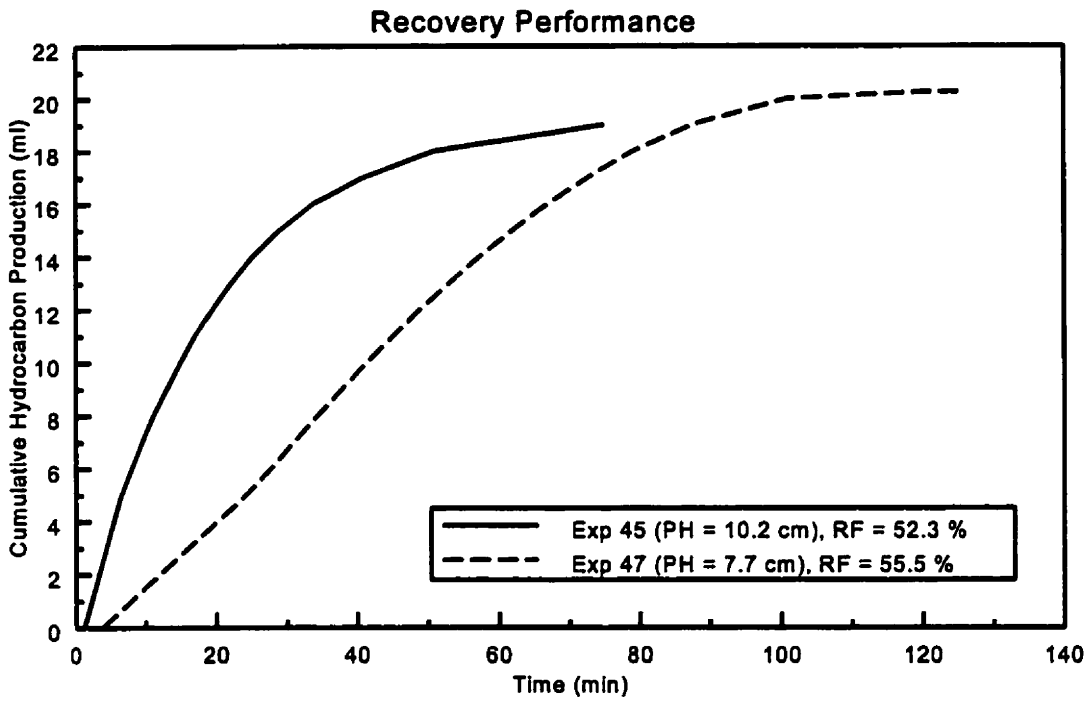

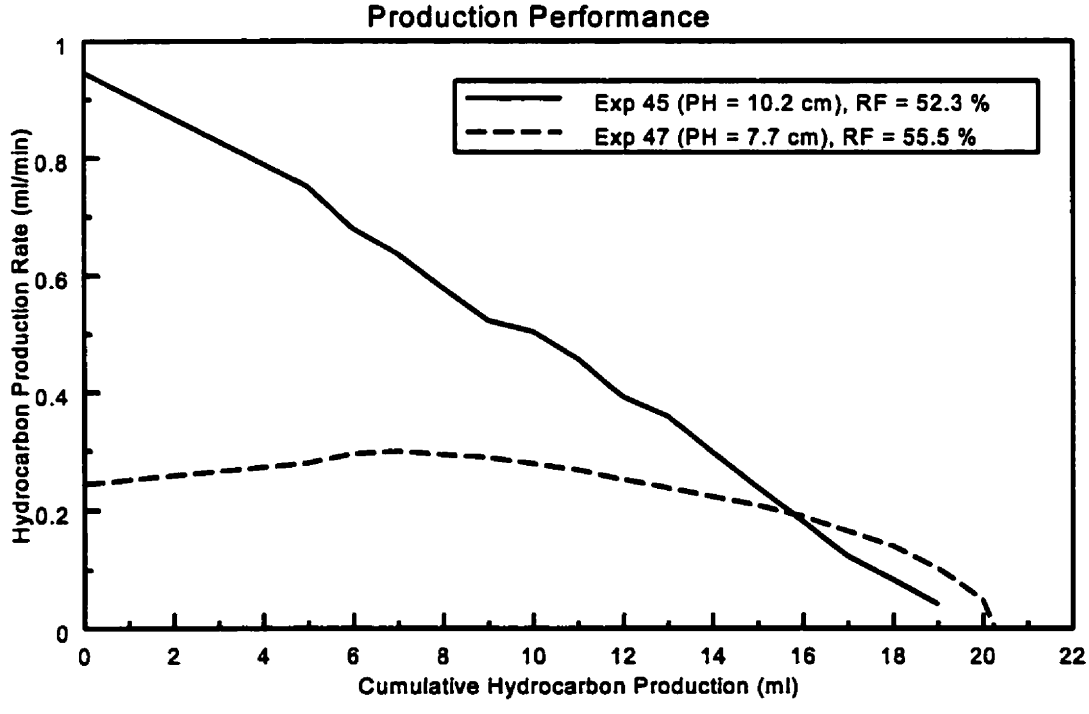

Vacuum Pressure = 1.0 inch of water

Figure 34: Effect of Production Probe Height Above the Free Water Table Set 2: Experiments 45 and 47 (Core 2)

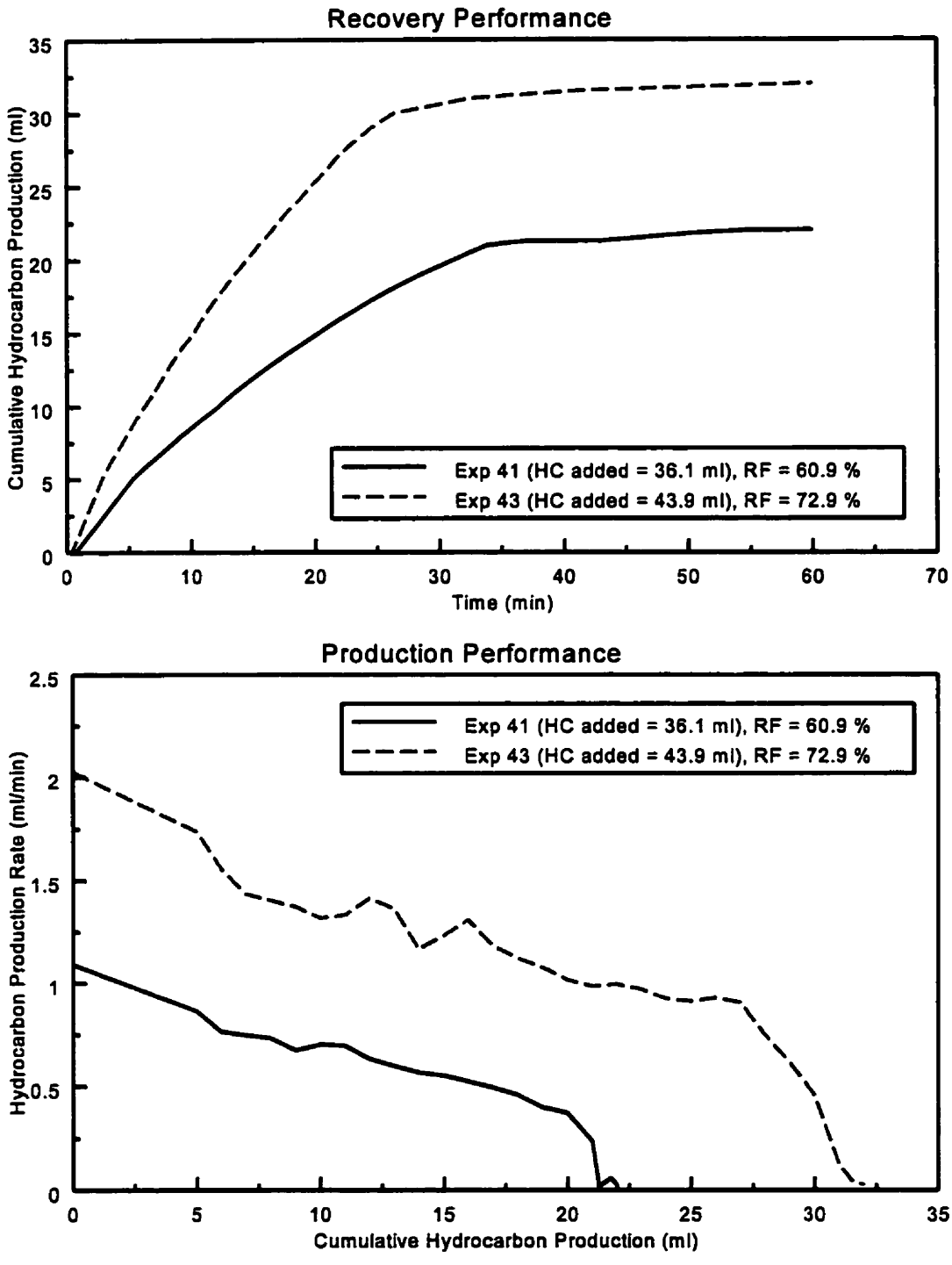

Figure 35: Effect of the Volume of Hydrocarbon Spill: Experiments 41, 42, and 43 (Core 1)

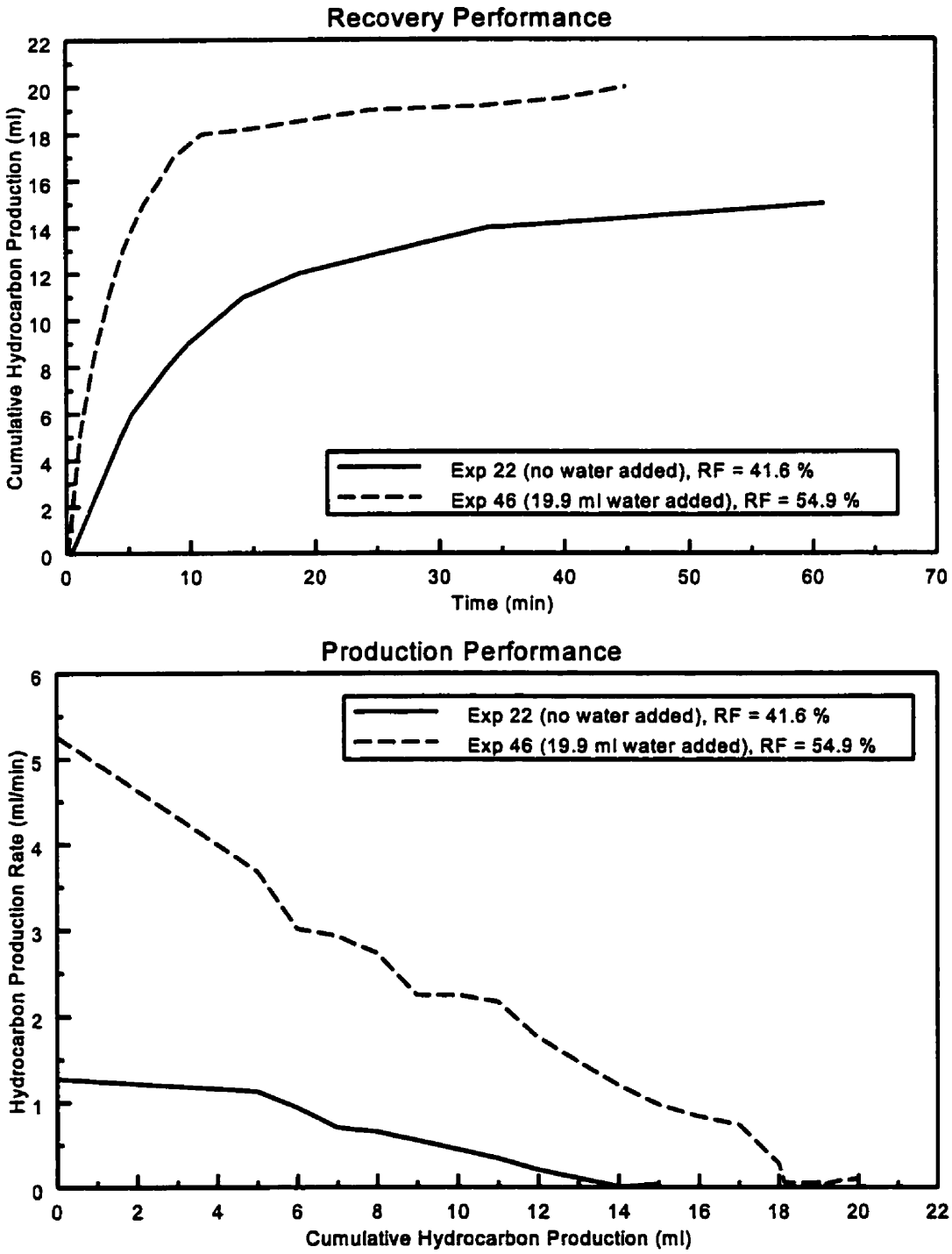

Figure 36: Effect of "Rainfall" Set 1: Experiments 22 and 46 (Core 1)

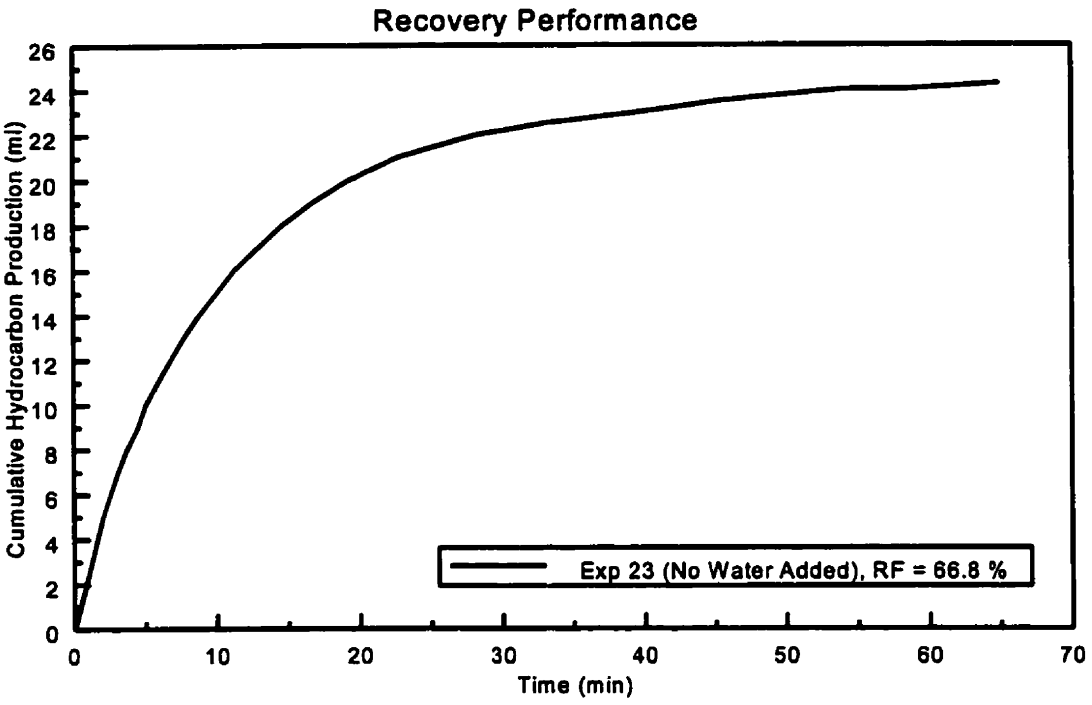

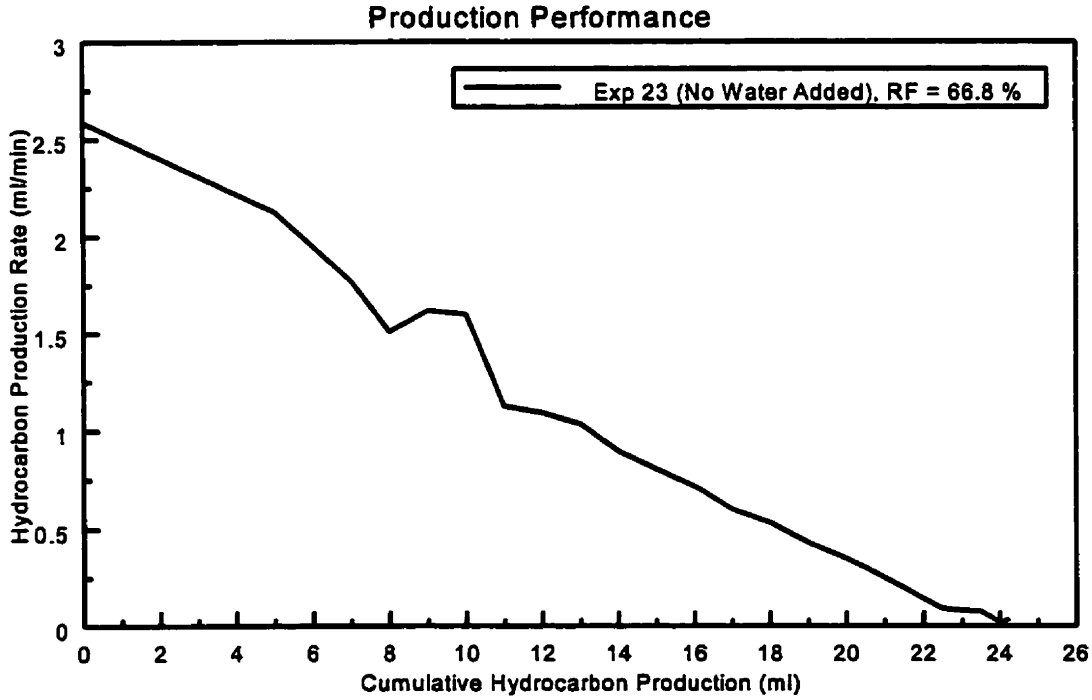

Production Height Above Free Water Table = 3.8 cm
Vacuum Pressure = 0.6 inches of water

Experiment 44 follows X axis, RF = 0.0 %

Figure 37: Effect of "Rainfall" Set 2: Experiments 23 and 44 (Core 1)

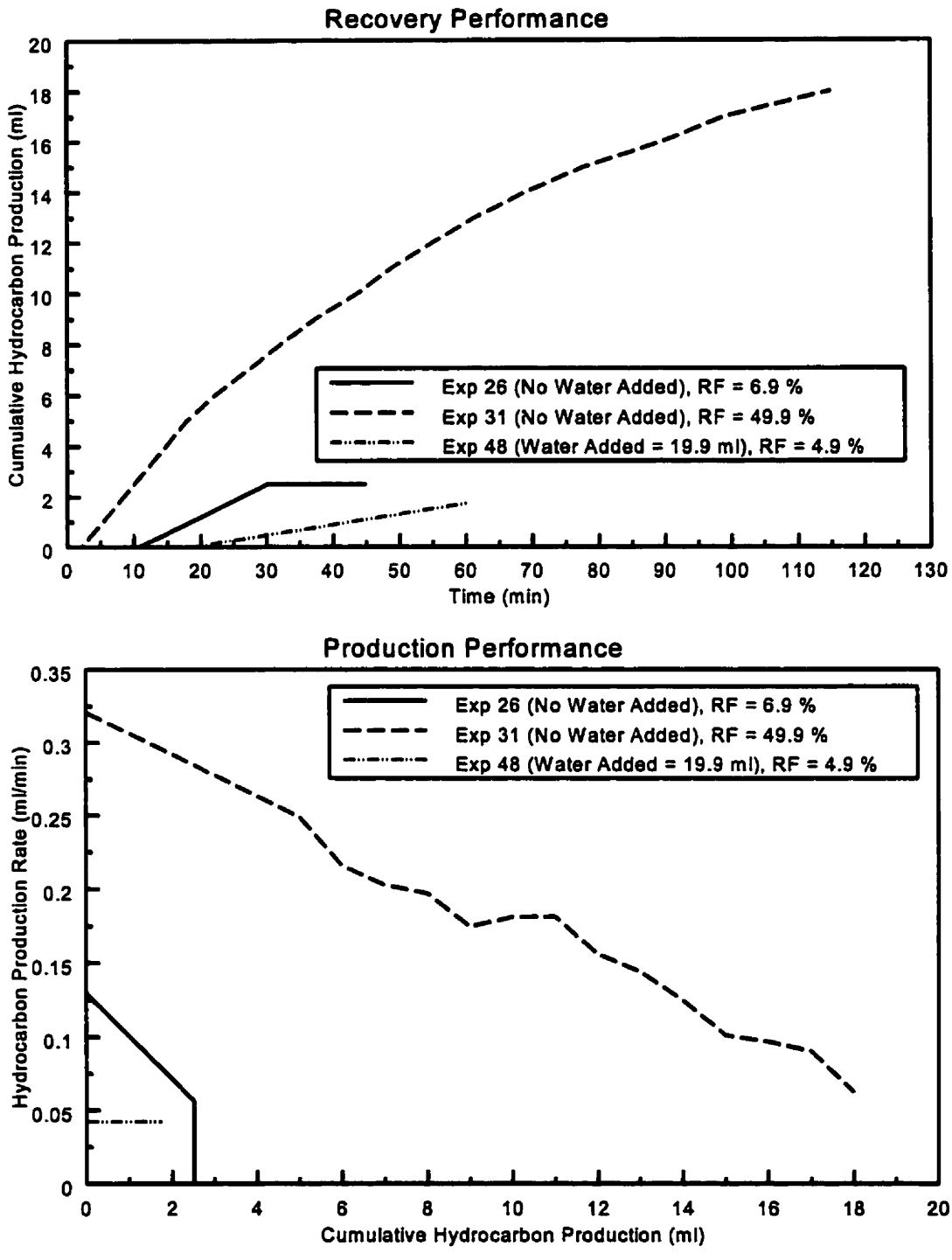

Figure 38: Effect of "Rainfall" Set 3: Experiments 26, 31, and 48 (Core 1)

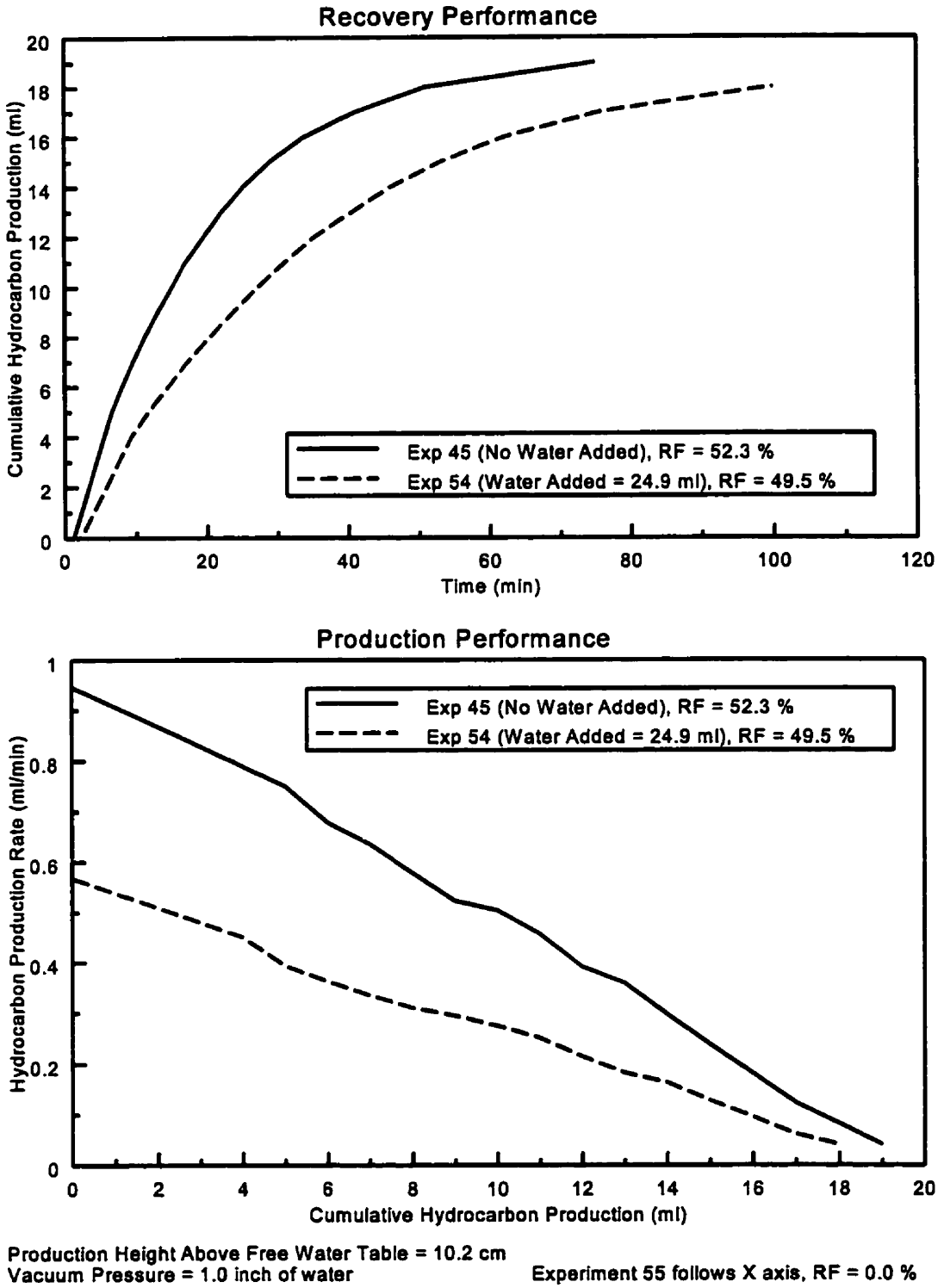

Figure 39: Effect of "Rainfall" Set 4: Experiments 45, 54, and 55 (Core 2)

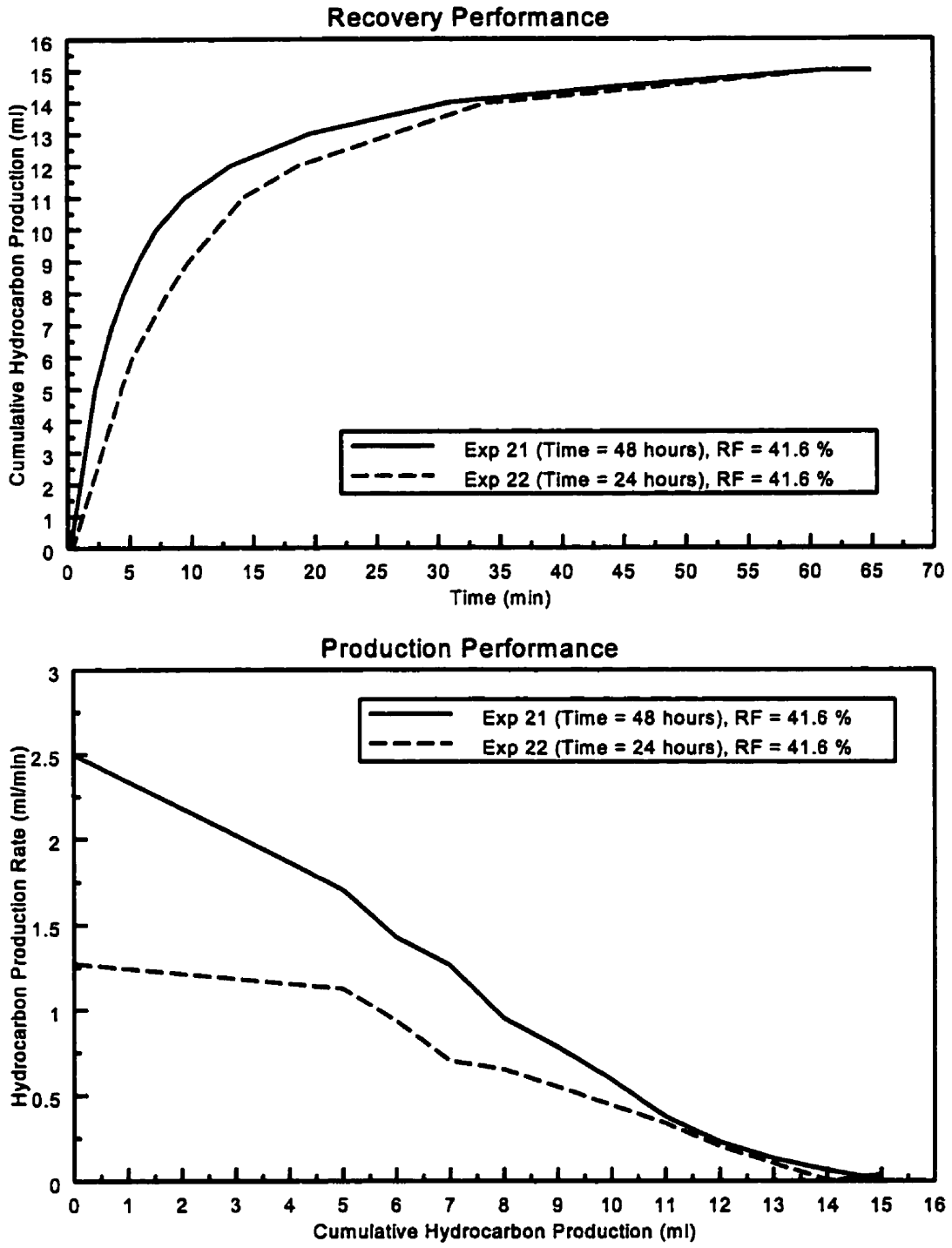

Figure 40: Effect of Time Allowed for Equilibration: Experiments 21 and 22 (Core 1)

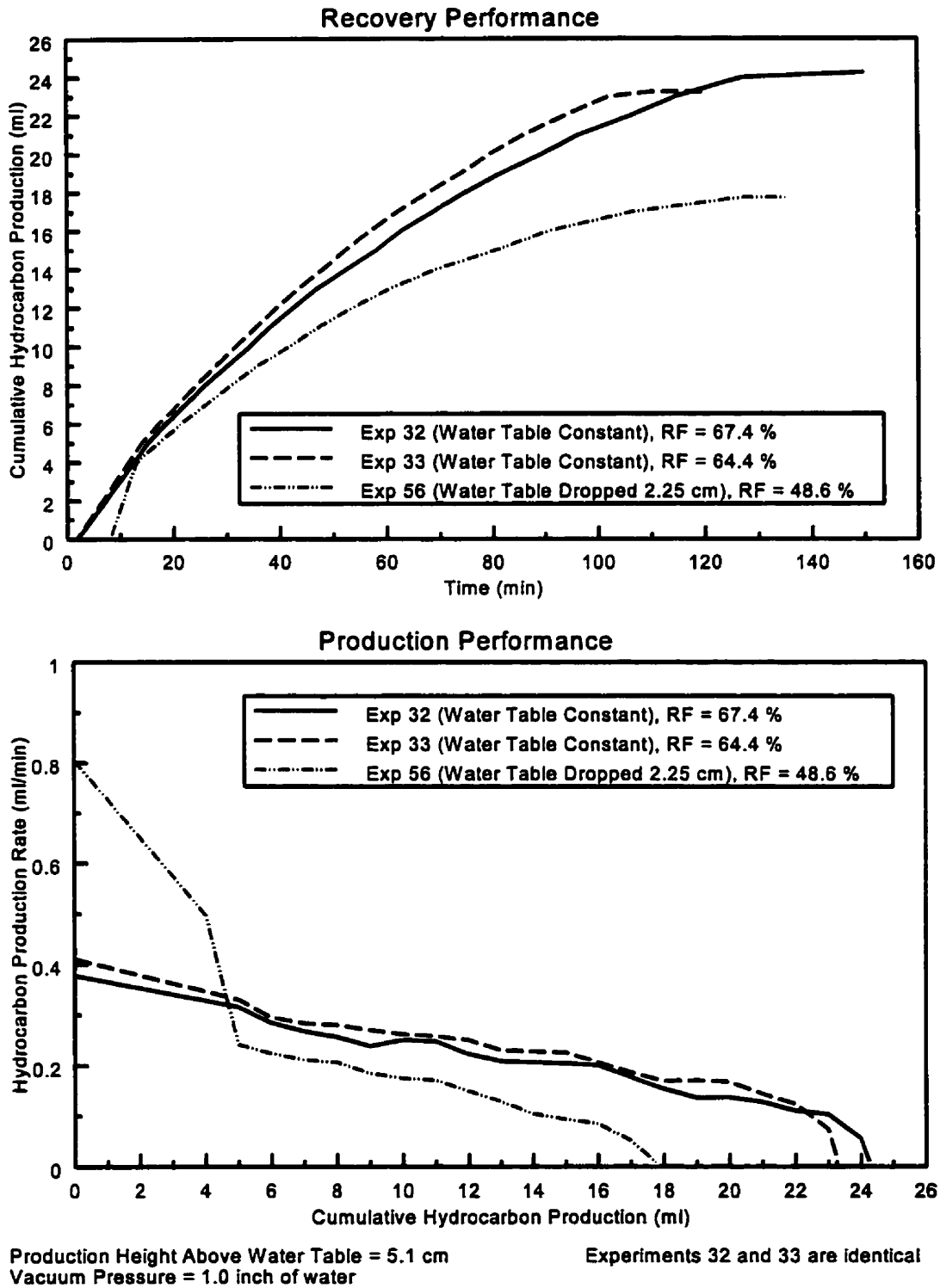

Figure 41: Effect of Dropping the Water Table: Experiments 32, 33, and 56 (Core 1)

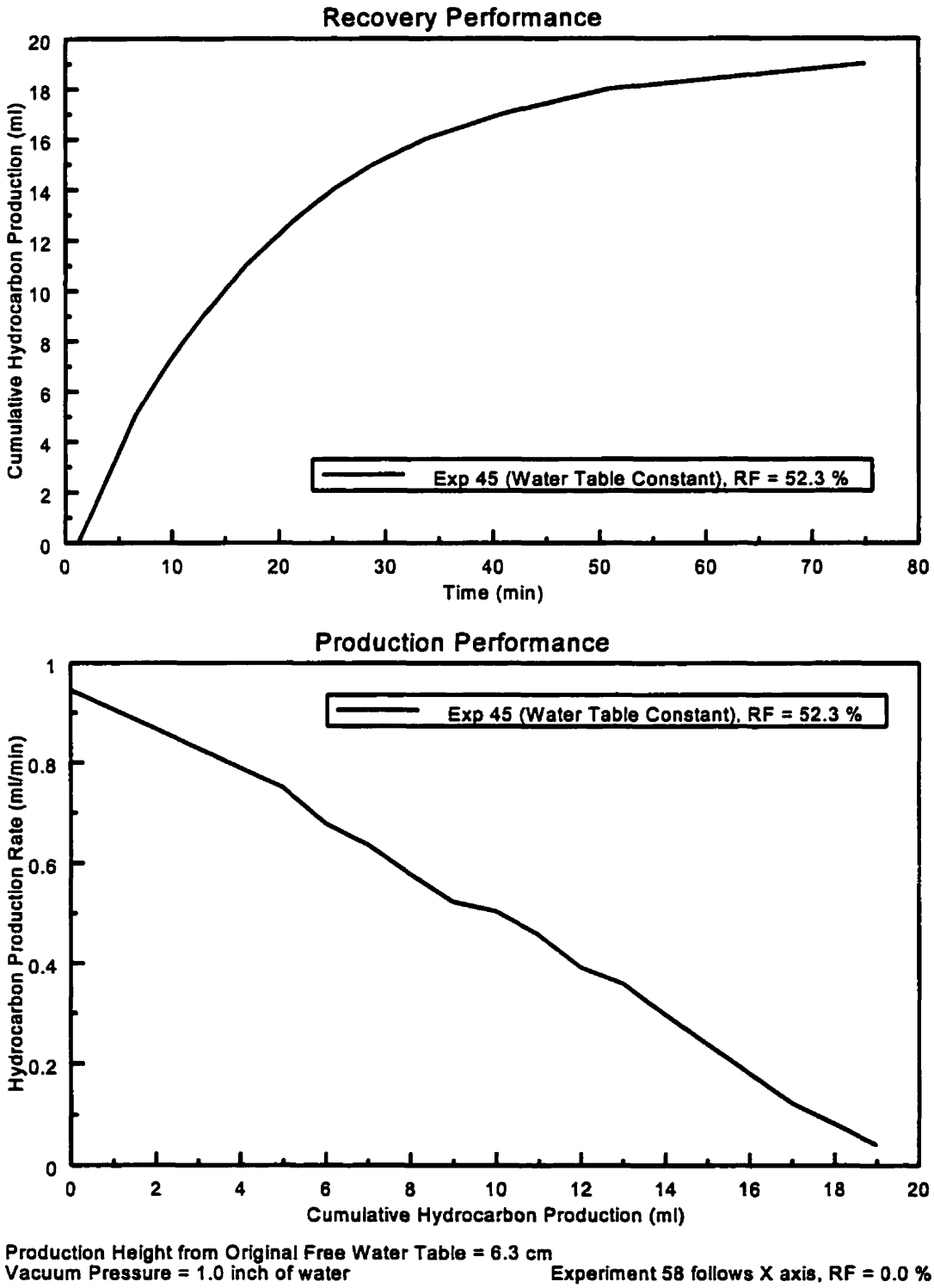

Figure 42: Effect of Raising the Water Table: Experiments 45 and 58 (Core 2)

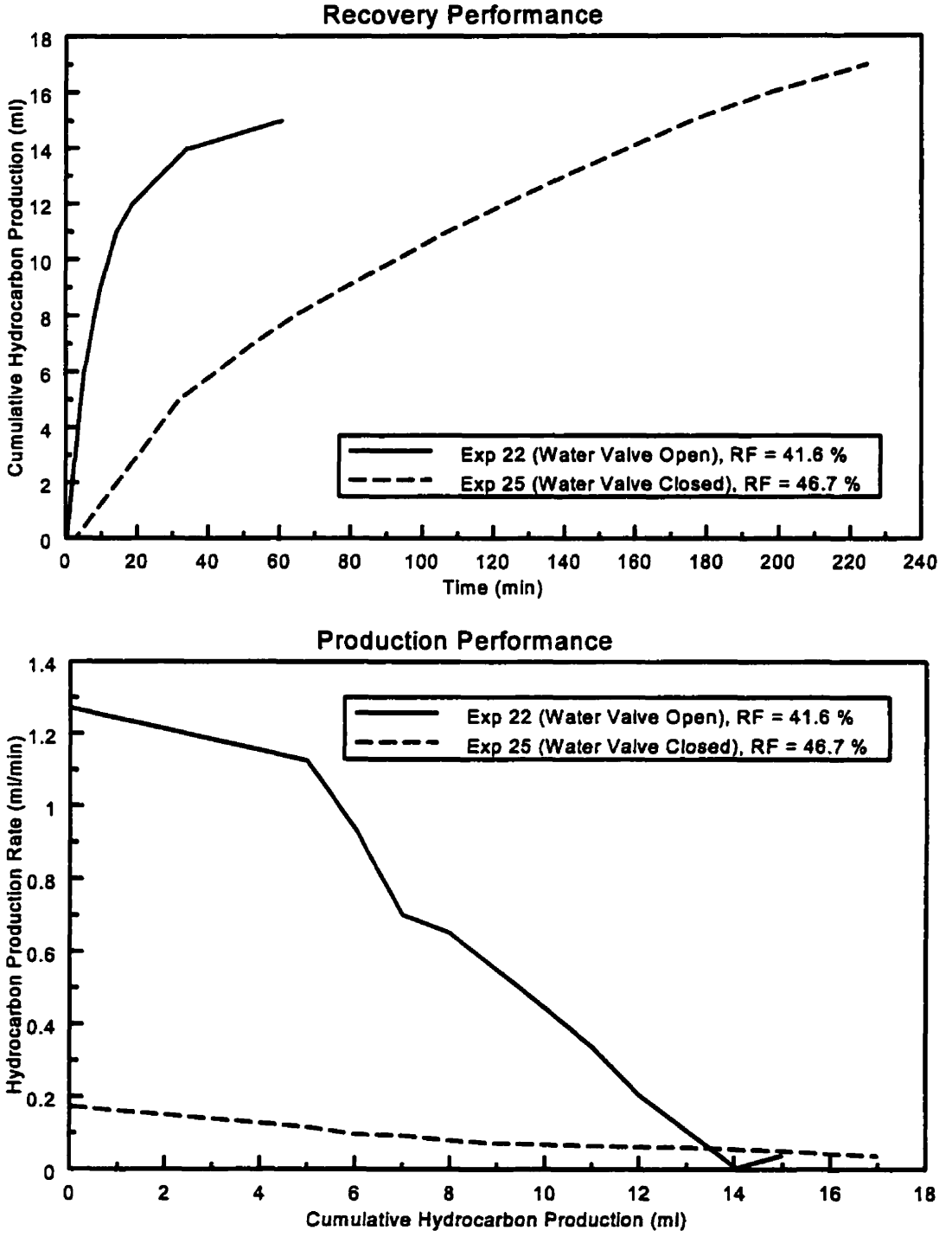

Figure 43: Effect of Method of Entering the Hydrocarbon into the Core: Experiments 22 and 25 (Core 1)

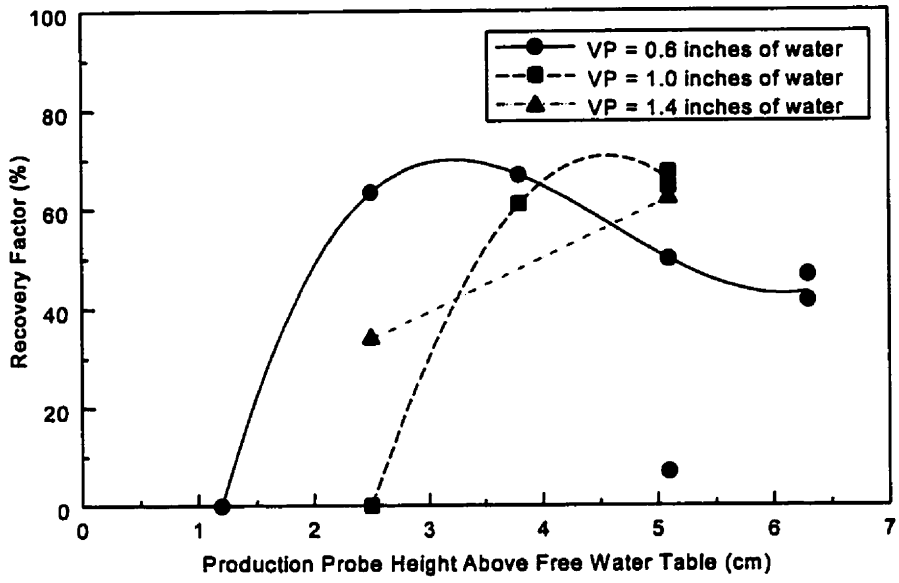

Figure 44: Effect of Production Probe Height Above the Free Water Table (Core 1)

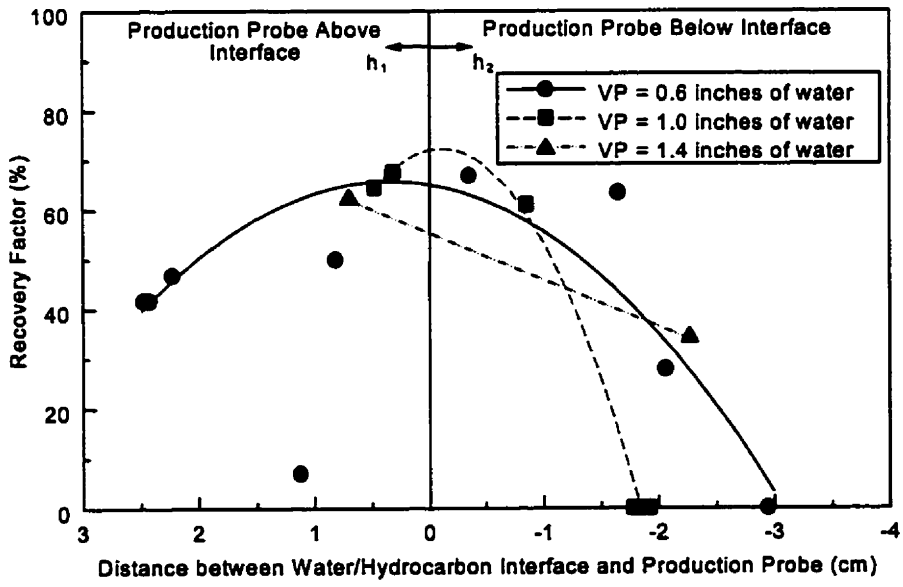

Figure 45: Effect of Distance Between Water/Hydrocarbon Interface and Production Probe (Core 1)

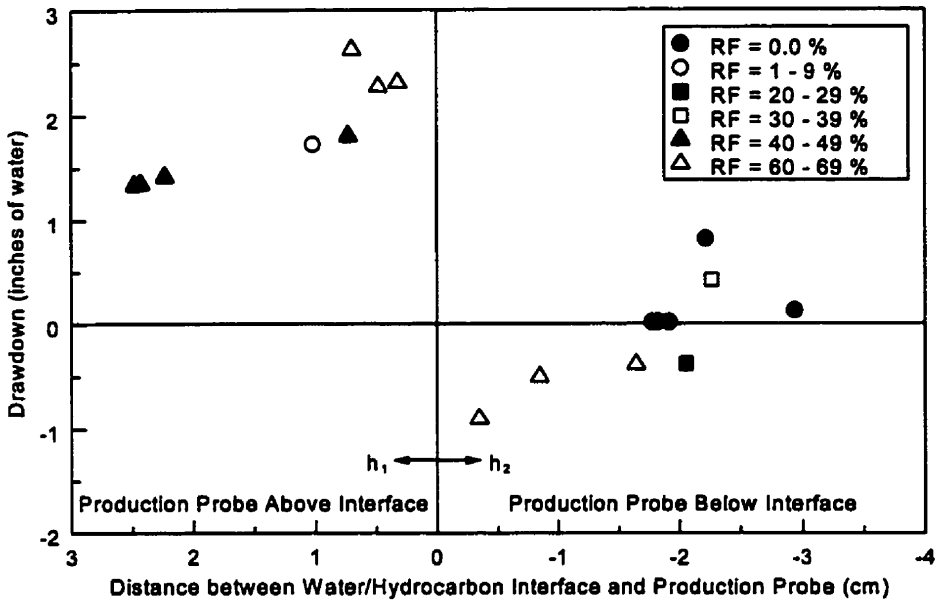

Figure 46: Recovery Factor Distribution for Core 1 (Initial Production - Water Supply Open)

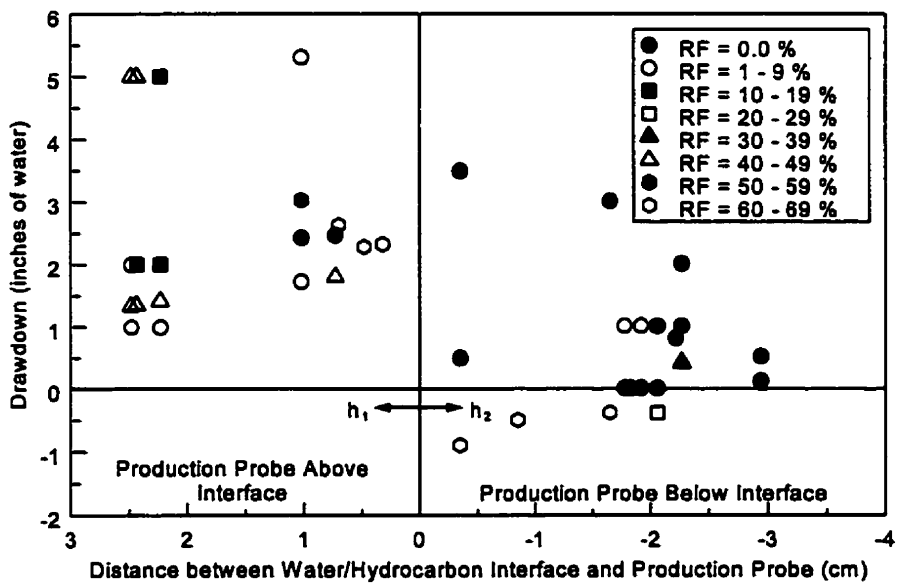

Figure 47: Recovery Factor Distribution for Core 1 (Water Supply Open)

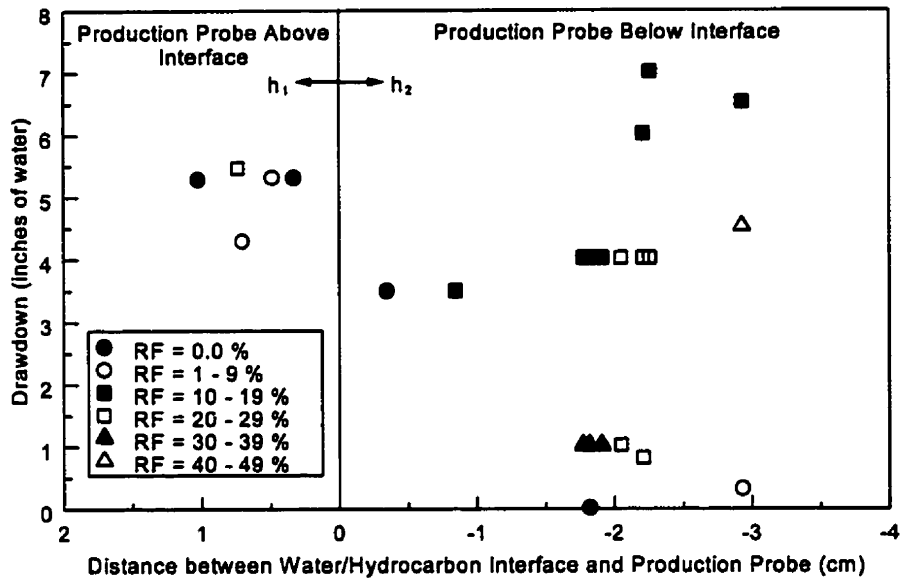

Figure 48: Recovery Factor Distribution for Core 1 (Water Supply Closed)

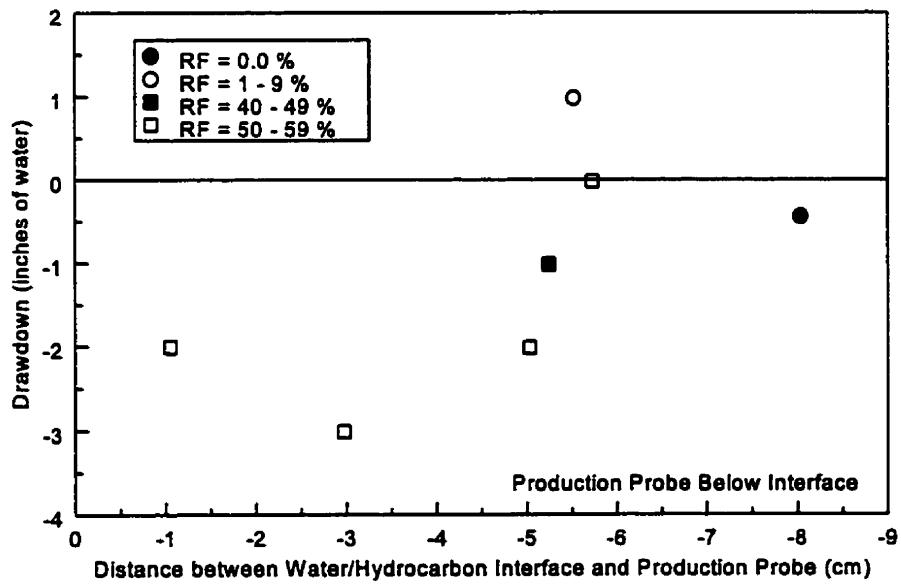

Figure 49: Recovery Factor Distribution for Core 2 (Water Supply Open)

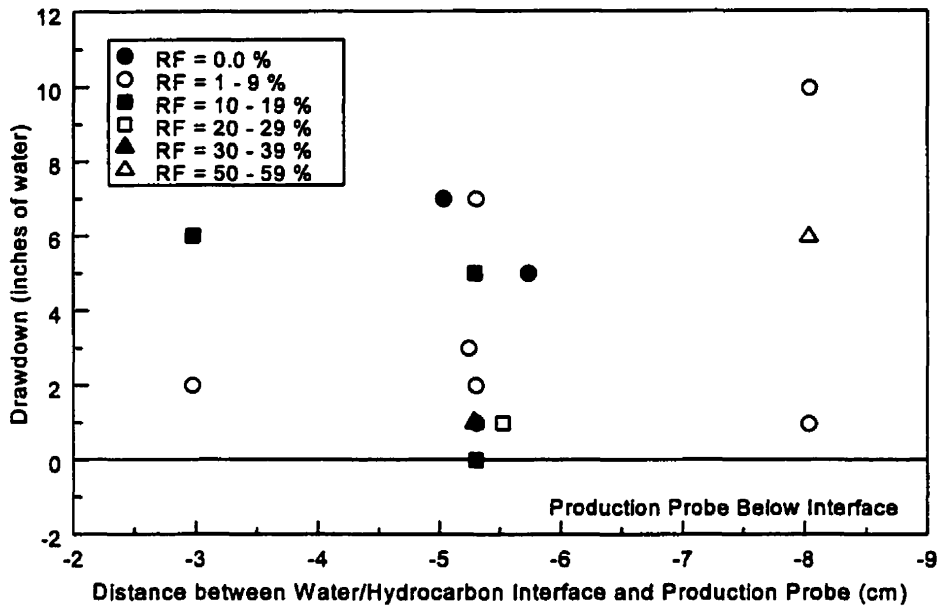

Figure 50: Recovery Factor Distribution for Core 2 (Water Supply Closed)

CHAPTER 8

CONCLUSIONS AND RECOMMENDATIONS

8.1 Conclusions

All experiments were performed manually, and all measurements were done by visual observations only. Therefore, although due diligence was used, there are inherent variances in accuracies and capillary equilibrations. These matters may affect the conclusions.

When considering the results of the performed experiments, it is clear that there are many factors affecting the outcome of these experiments. In light of the complexity of the experimental capillarity conditions, the following general conclusions can be made:

1. The recovery of hydrocarbons from the capillary fringe is affected by the location of the production probe with respect to the water/hydrocarbon interface and the vacuum suction pressure used. The optimum location for the production probe is in the vicinity of the water/hydrocarbon interface and a stronger vacuum pressure yields only a slightly better hydrocarbon recovery.
2. When the production probe is located below the water/hydrocarbon interface, and the vacuum pressure exceeds a critical value with respect to the under-pressure in the capillary fringe, then only water is sucked up into the production probe.
3. All experiments can be reproduced. However, the reproducibility is dependant on the fluid distribution in the core before the start of the experiment, and the fluid movements after the experiment has started. Fluid distribution in the core was never the same because the development of the drainage capillary fringe was never the

same for all experiments within the provided equilibration time. Also, since fluid distributions were never the same, fluid movements will not be the same for all experiments.

4. "Rainfall" may trap hydrocarbon due to capillarity. However, it may not be conducive to the more efficient recovery of hydrocarbon spills, due to phase trapping and liquid blocking.

5. The movement of the water table can affect the hydrocarbon recovery in that the rise or fall of the water table causes additional non-wetting fluid entrapment due to the spreading of the hydrocarbon over a larger porous bulk volume, thus lowering its recoverability.

6. The water/air capillary fringe interface was only visible from the outside as a jagged interface line at the inside of the core wall, with peaks and valleys. However, the distribution and the height of the peaks and valleys inside the core were unknown. Further, for each experiment, the water/air capillary fringe was never at the same height, nor was the distribution of its peaks and valleys ever the same.

7. The findings of the experiments, extended to a hydrocarbon spill in a ground water bearing strata, yield the following conclusions:

   a) In the event of a hydrocarbon spill, the application of an evacuation process using wells will stabilize the spill, reduce its areal spread (pancaking), its depth of penetration, and its volume. However, it is not a clean-up method for the scheme presented here.

   b) The capillarity of the ground water bearing strata plays a major role in the

spreading and entrapment of a hydrocarbon spill, as does the character of the ground water table in the subterranean strata (zone of intermittent saturation) and the effect of rainfall. These factors may determine whether a horizontal well or vertical well should be used for the efficient recovery of a hydrocarbon spill.

c) *In-situ* factors affecting the recovery processes are: i) the viscosity of the contaminant, ii) interfacial tension and wettability, iii) pore size distribution in the contaminated zone, iv) local heterogeneities, v) temperature with depth, vi) the volatile nature of the contaminant, and vii) in situ subsurface natural chemical processes.

8.2 Recommendations

Based on the results of the experiments performed, and given the complexity of the nature of capillarity and its effect on the recovery of hydrocarbons from the capillary region, the following recommendations are made:

1. A series of experiments should be performed to cross-correlate the minimum vacuum pressure required to produce water from the capillary fringe without the presence of a hydrocarbon column, and with respect to the probe height above the free water table for a glass bead/water/air system at equilibrium conditions.
2. A series of experiments should be performed as above but for a glass bead/water/hydrocarbon system, with the presence of a hydrocarbon column, and with the production probe below the water/hydrocarbon contact, whereby it can be

observed at what vacuum pressure and distance from the production probe to the water/hydrocarbon contact coning will take place.

3. The use of an oil with a better light refractive index difference with water, or the use of only water soluble or oil soluble dyes, to better visually observe the liquid-fluid interfaces. An alternative is to use a CAT scanner to monitor the fluid saturations inside the core and to analyse the jagged nature of the capillary fringe.

4. A shorter (e.g. 1 foot) and smaller diameter (e.g. 1 inch) core may be acceptable, assuming that the same glass bead mesh sizes are used. A longer core is more appropriate if the glass bead sizes are smaller, because it has a higher capillary fringe.

REFERENCES

Abdul, A.S. and Gillham, R.W., "Laboratory Studies of the Effects of the Capillary Fringe on Streamflow Generation", *Water Resources Research*, Volume 20, Number 6, 691-698, 1984.

Anderson, W.G., "Wettability Literature Survey, Part 4: Effects of Wettability on Capillary Pressure", *Journal of Petroleum Technology*, Volume 39, Number 10, 1283 - 1300, 1987.

Amyx, J.W., Bass, D.M. Jr., and Whiting, R.L. *Petroleum Reservoir Engineering, Physical Properties*, Mc-Graw-Hill Book Company, New York, 1960.

Bouman, J. and Westerdijk, J.B., *Algemene Natuurkunde, Section B, Mechanica* (General Physics, Section B, Mechanics); Delftsche Uitgevers Maatschappij, N.V., Delft, 1956.

Bowen, R., *Ground Water*, Applied Science Publishers Ltd., London, 1980.

Calhoun, J.C., *Fundamentals of Reservoir Engineering*, University of Oklahoma Press, 1982.

Craft, B.C. and Hawkins, M.F., *Applied Petroleum Reservoir Engineering, Second Edition*, Prentice Hall, Inc., Englewood Cliffs, New Jersey, 1991.

Craig, F.F., Jr., *The Reservoir Engineering Aspect of Waterflooding*, Monograph Volume 3 of the Henry L. Doherty Series, Society of the Petroleum Engineers of the American Institute of Mining and Metallurgical Engineers, New York, 1993.

Davis, M.L. and Cornwell, D.A., *Introduction to Environmental Engineering*, Second Edition, McGraw-Hill, Inc., New York, 1991.

Davis S.M. and DeWiest, R.J.M., *Hydrogeology*, John Wiley and Sons, New York, 1966.

Dullien, F.A.L., *Porous Media: Fluid Transport and Pore Structure*, Second Edition, Academic Pres. Inc., San Diego, 1992.

Duston, K.L., Allen, P.G., and Ward, C.H., "Influence of Hydrologic Properties on in Situ Bioremediation", in Weyer, K.U., editor, *Subsurface Contamination by Immiscible Fluids*, Proceedings of the International Conference on Subsurface Contamination by Immiscible Fluids, Calgary, Canada, April 18-20, 1990, A.A. Balkema, Rotterdam, 29-38, 1992.

EPRCo (Esso (now Exxon) Production Research Company) *Reservoir Engineering School*, Course Notes, Houston, Texas, 1968.

Fisher Scientific Company, "Lab-Crest Mark III Flowmeter Kit", Instruction Manual.

Freeze, R.A. and Cherry, J.A., *Groundwater*, Prentice-Hall, Inc., Englewood Cliffs, N.J., 1979.

Frick, T.C. and Taylor, R.W., *Petroleum Production Handbook, Volume 2, Reservior Engineering*, Society of Petroleum Engineers of AIME, Millet the Printer, Inc., Dallas, Tex., 1962.

Gillham, R.W., "The Capillary Fringe and its Effect on Water-Table Response", *Journal of Hydrology*, Volume 67, 307-324, 1984.

Hagoort, J., *Fundamentals of Gas Reservoir Engineering*, Elsevier, Amsterdam, 1988.

Hassanizadeh, S.M. and Gray, W.G., "Thermodynamic Basis of Capillary Pressure in Porous Media", *Water Resources Research*, Volume 29, Number 10, 3389-3405, 1993.

Hoag, G.E. and Cliff, B., "The Use of the Soil Venting Technique for the Remediation of Petroleum-Contaminated Soils", in Kostecki, P.T. and Calabrese, E.J., editors, *Soils Contaminated by Petroleum: Environmental and Public Health Effects*, John Wiley & Sons, Inc., New York, 1988.

Hoag, G.E., Marley, M.C., Cliff, B.L., and Nangeroni, P., "Soil Vapor Extraction Research Developments", in Kostecki, P.T. and Calabrese, E.J., editors, *Hydrocarbon Contaminated Soils and Ground water: Analysis, Fate, Environmental and Public Health Effects, Remediation*, Volume 1, Lewis Publishers, Inc., Chelsea, Michigan, 1991.

Jasper, J.J., "The Surface Tension of Pure Liquid Compounds", *Journal of Physical and Chemical Reference Data*, Volume 1, Number 4, 841-1009, 1972.

Karlsson, H., "Horizontal Systems Technology for Shallow-Site Remediation", *Journal of Petroleum Technology*, Volume 45, Number 2, 160 - 165, 1993.

Kosasih, A. and Shobirin, M., "Implementing an Environmental Management System on an Oilfield Operation in Sumatra", *Journal of Petroleum Technology*, Volume 47, Number 1, 43 - 48, 1995.

Kronig, R., editor, *Leerboek der Natuurkunde* (Textbook of Physics), Scheltema & Holkema, NV, Amsterdam, 1966.

LaGrega, M.D., Buckingham, P.L., and Evans, J.C., *Hazardous Waste Management*, McGraw-Hill, Inc., New York, 1994.

Leverett, M.C. "Capillary Behaviour in Porous Solids"; *Transactions of the American Institute of Mining and Metallurgical Engineers*, Volume 142, 152 - 169, 1940.

Lyons, W.C. editor, *Standard Handbook of Petroleum Engineering & Natural Gas Engineering*, Volume 2, Gulf Publishing Company, Houston, Texas, 1996.

Lu, T.X., Biggar, J.W., and Nielsen, D.R., "Water Movement in Glass Bead Porous Media, 1. Experiments of Capillary Rise and Hysteresis", *Water Resources Research*, Volume 30, Number 12, 3275-3281, 1994.

Lu, T.X., Nielsen, D.R., and Biggar, J.W., "Water Movement in Glass Bead Porous Media, 3. Theoretical Analysis of Capillary Rise into Initially Dry Media", *Water Resources Research*, Volume 31, Number 1, 11-18, 1995.

Mackay, D.M., Roberts, P.V., and Cherry, J.A., "Transport of Organic Contaminants in Groundwater", *Environmental Science and Technology*, Volume 19, Number 5, 384-392, 1985.

McCarthy, K.A. and Johnson, R.L., "Transport of Volatile Organic Compounds Across the Capillary Fringe", *Water Resources Research*, Volume 29, Number 6, 1675 - 1683, 1993.

Morrow, N.R. and Harris, C.C., "Capillary Equilibrium in Porous Material"; *Society of Petroleum Engineers Journal*, Volume 5, 15-24, 1965.

Mungan, N., "Enhanced Oil Recovery Using Water as a Driving Fluid, Part 3 - Interfacial Phenomena and Oil Recovery: Capillarity", *World Oil*, Volume 192, Number 5, 149 - 158, 1981.

Mungan, N., *Secondary and Tertiary Recovery*, U of C course text ENCH 629, 1993/1994 Winter Session, 1994.

Muskat, M., *Physical Principles of Oil Production*, McGraw-Hill Co., New York, 1949.

Newman, A., "Subsurface barrier trapped diverse contaminants, let water through", *Environmental Science and Technology*, Volume 29, Number 8, 354A, 1995.

Perkins, F.M., Jr., "An Investigation of the Role of Capillary Forces in Laboratory Water Floods", *Transactions of the American Institute of Mining and Metallurgical Engineers*, Volume 210, 409 - 411, 1957.

Perry, R.H., Green, D., and Maloney, J.O., *Perry's Chemical Engineers' Handbook*, 6th Edition, McGraw-Hill, Inc., New York, 1984.

Richards, L.A., "Capillary Conduction of Liquids through Porous Mediums", *Physics*, Volume 1, 318 - 333, 1931.

Rose, W. and Bruce, W.A., "Evaluation of Capillary Character in Petroleum Reservoir Rock", *Petroleum Transactions of the American Institute of Mining and Metallurgical Engineers*, Volume 186, 127 - 142, 1949.

Scaffidi, F., "Assessing Hazards: Importance of Vapour Pressure", *Dangerous Goods Newsletter*, Volume 14, Number 1, 4, 1994.

Schwille, F., *Dense Chlorinated Solvents in Porous and Fractured Media*, Translated by Pankow, J.F., Lewis Publishers, Inc., Michigan, 1988.

Strauss, S., "Iron - Filings as Pollution Scourge is no Pipe Dream", *The Globe and Mail*, August 23, 1995, A5, 1995.

Testa, S.M. and Winegardner, D.L., *Restoration of Petroleum - Contaminated Aquifers*, Lewis Publishers, Inc., Chelsea, Michigan, 1991.

Todd, D.K., *Groundwater Hydrology*, Second Edition, John Wiley & Sons, Inc., New York, 1980.

Tolman, C.F. *Ground Water*, McGraw-Hill Book Company, Inc., New York, 1937.

Trombly, J., "Engineered Enzymes for Better Bioremediation", *Environmental Science and Technology*, Volume 29, Number 12, 560A - 564A, 1995.

APPENDIX A

RAW DATA

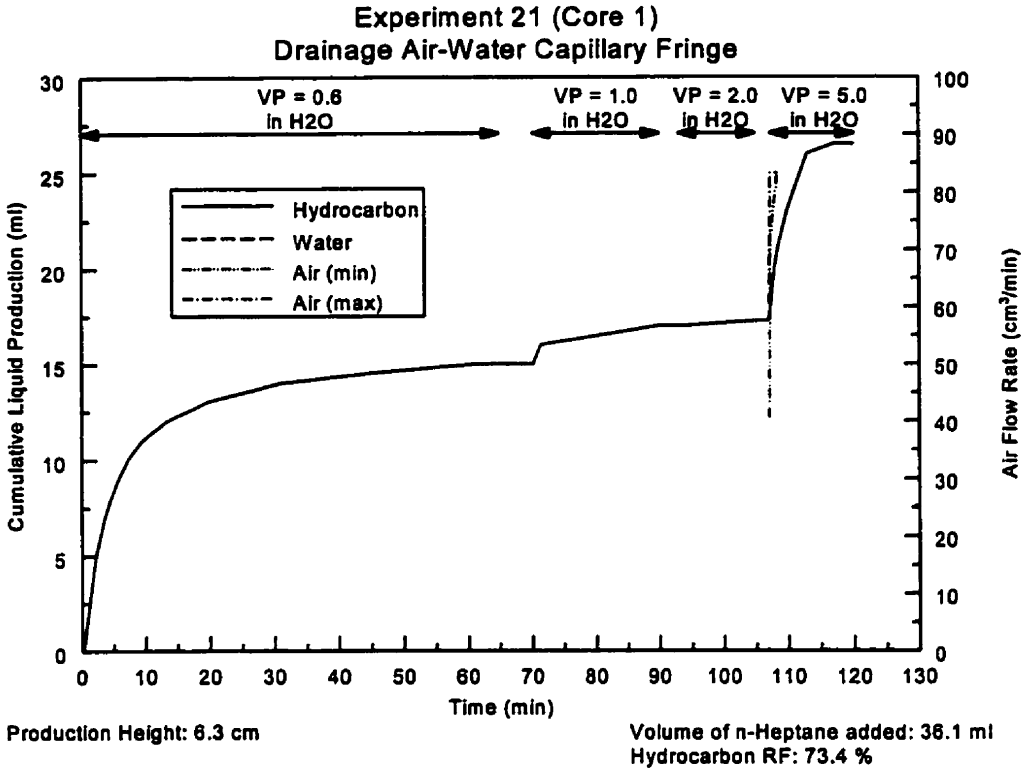
Experiment 21 (Core 1)
Drainage Air-Water Capillary Fringe
VP = 0.6 in H2O
VP = 1.0 in H2O
VP = 2.0 in H2O
VP = 5.0 in H2O
Hydrocarbon
Water
Air (min)
Air (max)
Cumulative Liquid Production (ml)
Air Flow Rate (cm³/min)
Time (min)
Production Height: 6.3 cm
Volume of n-Heptane added: 36.1 ml
Hydrocarbon RF: 73.4 %

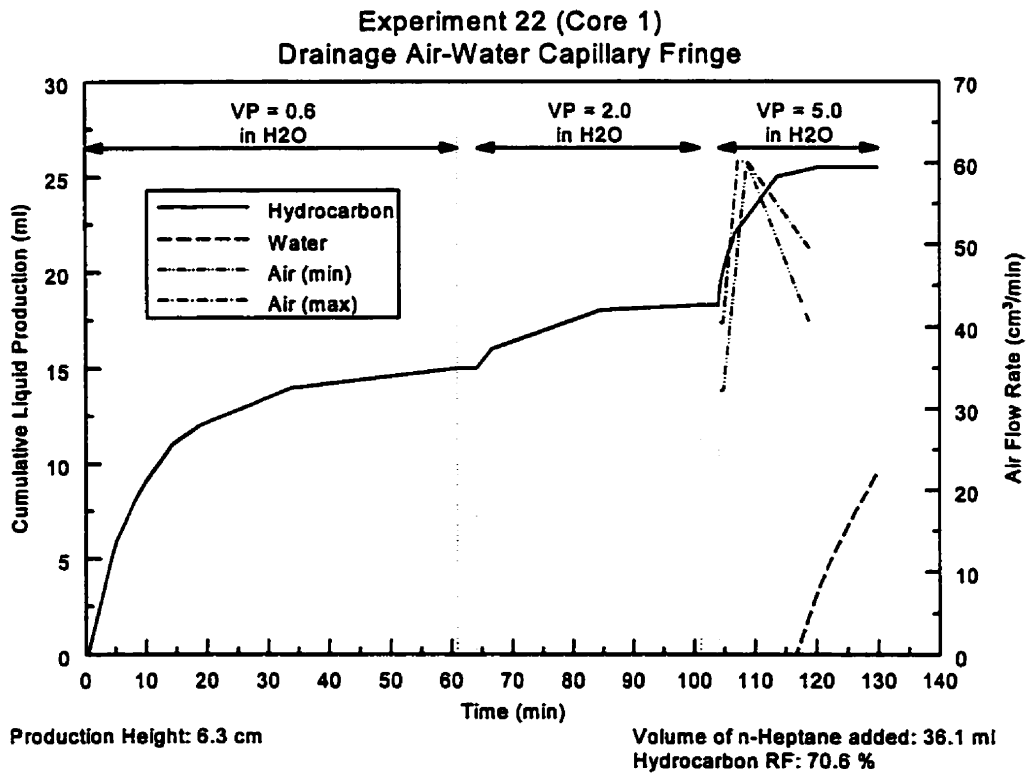
Experiment 22 (Core 1)
Drainage Air-Water Capillary Fringe
VP = 0.6 in H2O
VP = 2.0 in H2O
VP = 5.0 in H2O
Hydrocarbon
Water
Air (min)
Air (max)
Cumulative Liquid Production (ml)
Air Flow Rate (cm³/min)
Time (min)
Production Height: 6.3 cm
Volume of n-Heptane added: 36.1 ml
Hydrocarbon RF: 70.6 %

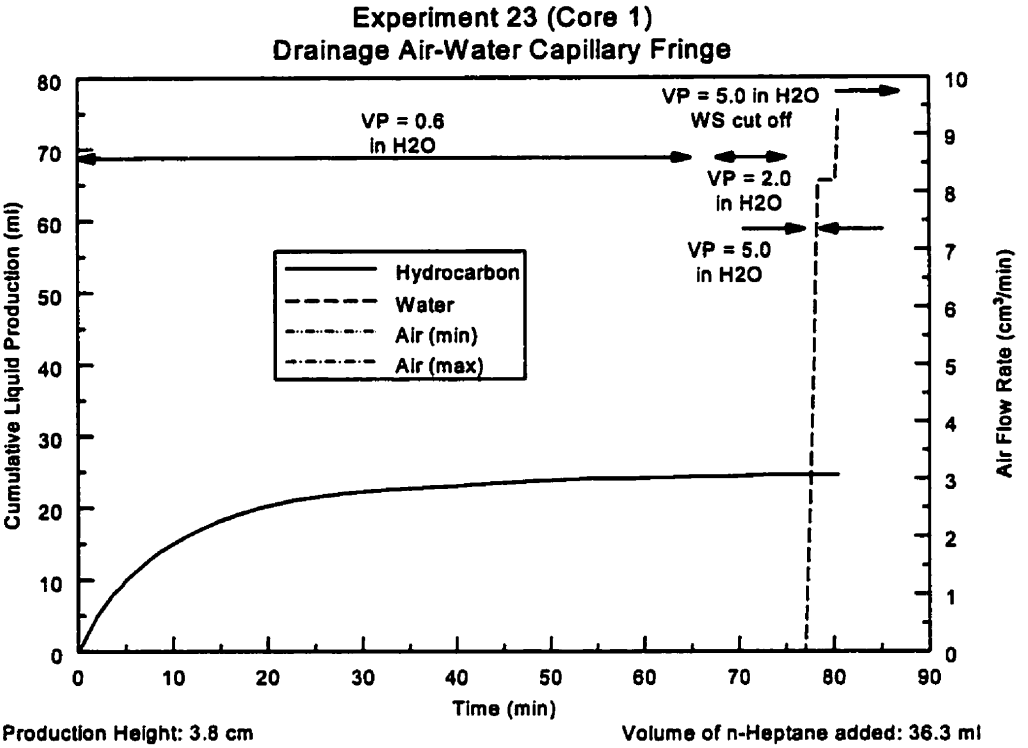
Experiment 23 (Core 1)
Drainage Air-Water Capillary Fringe
VP = 0.6
in H2O
VP = 5.0 in H2O
WS cut off
VP = 2.0
in H2O
VP = 5.0
in H2O
Hydrocarbon
Water
Air (min)
Air (max)
Cumulative Liquid Production (ml)
Air Flow Rate (cm³/min)
Time (min)
Production Height: 3.8 cm
Volume of n-Heptane added: 36.3 ml
Hydrocarbon RF: 67.5 %

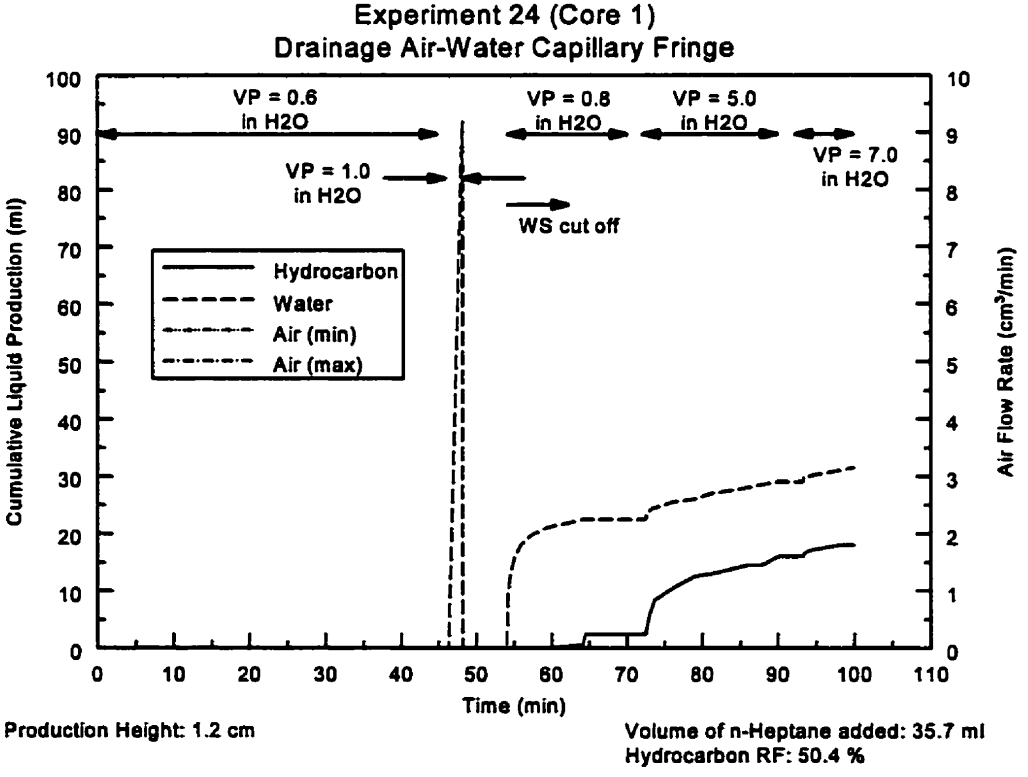
Experiment 24 (Core 1)
Drainage Air-Water Capillary Fringe
VP = 0.6
in H2O
VP = 0.8
in H2O
VP = 5.0
in H2O
VP = 7.0
in H2O
VP = 1.0
in H2O
WS cut off
Hydrocarbon
Water
Air (min)
Air (max)
Cumulative Liquid Production (ml)
Air Flow Rate (cm³/min)
Time (min)
Production Height: 1.2 cm
Volume of n-Heptane added: 35.7 ml
Hydrocarbon RF: 50.4 %

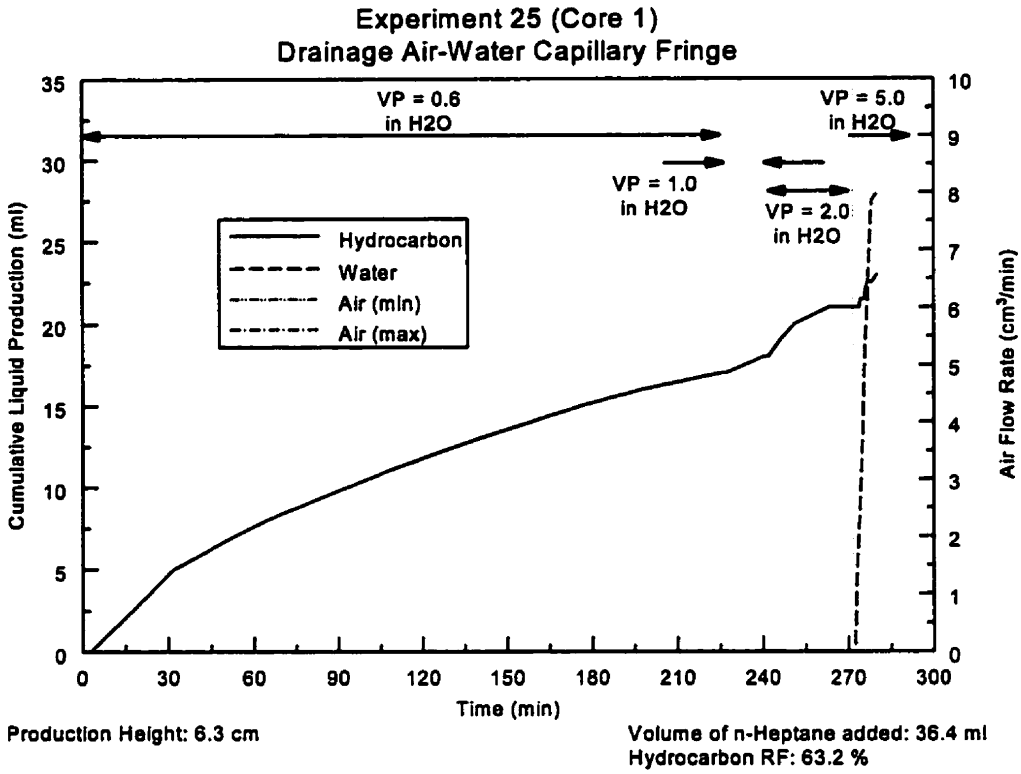

Production Height: 6.3 cm

Volume of n-Heptane added: 36.4 ml
Hydrocarbon RF: 63.2 %

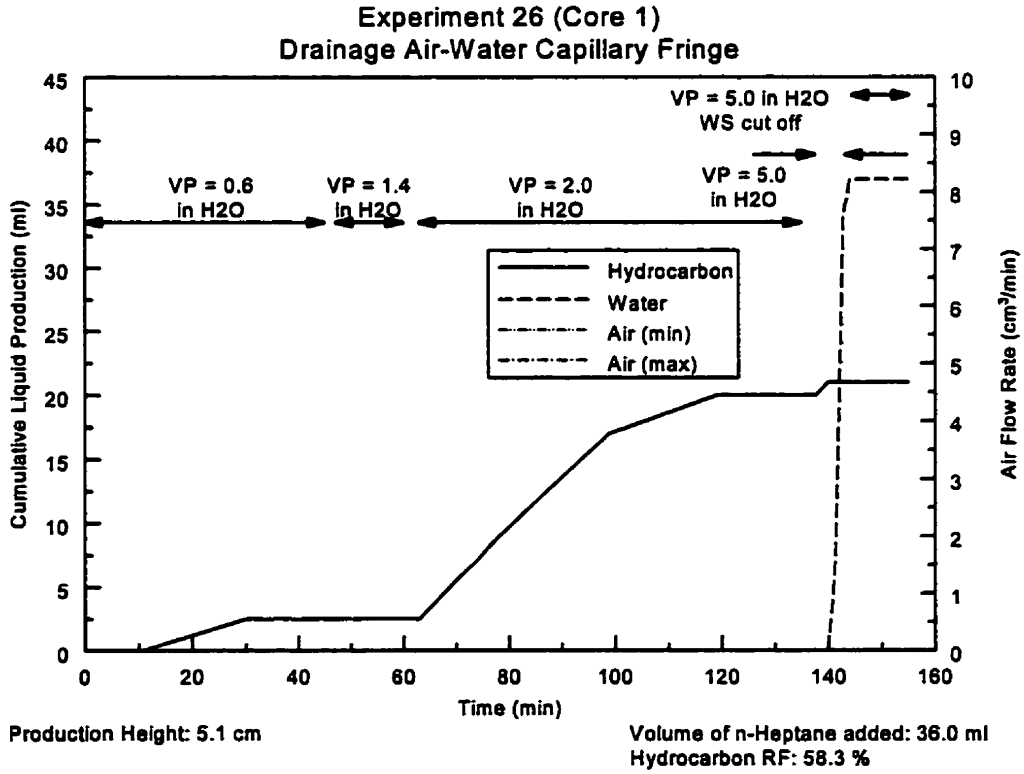

Production Height: 5.1 cm

Volume of n-Heptane added: 36.0 ml
Hydrocarbon RF: 58.3 %

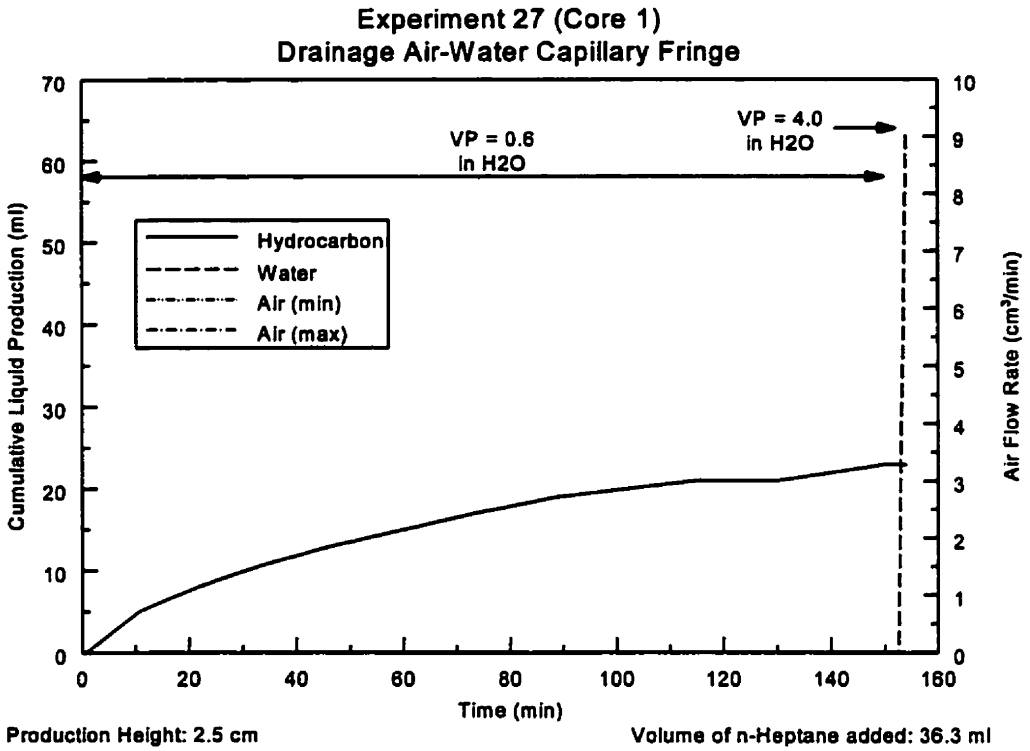

Production Height: 2.5 cm

Volume of n-Heptane added: 36.3 ml
Hydrocarbon RF: 63.4 %

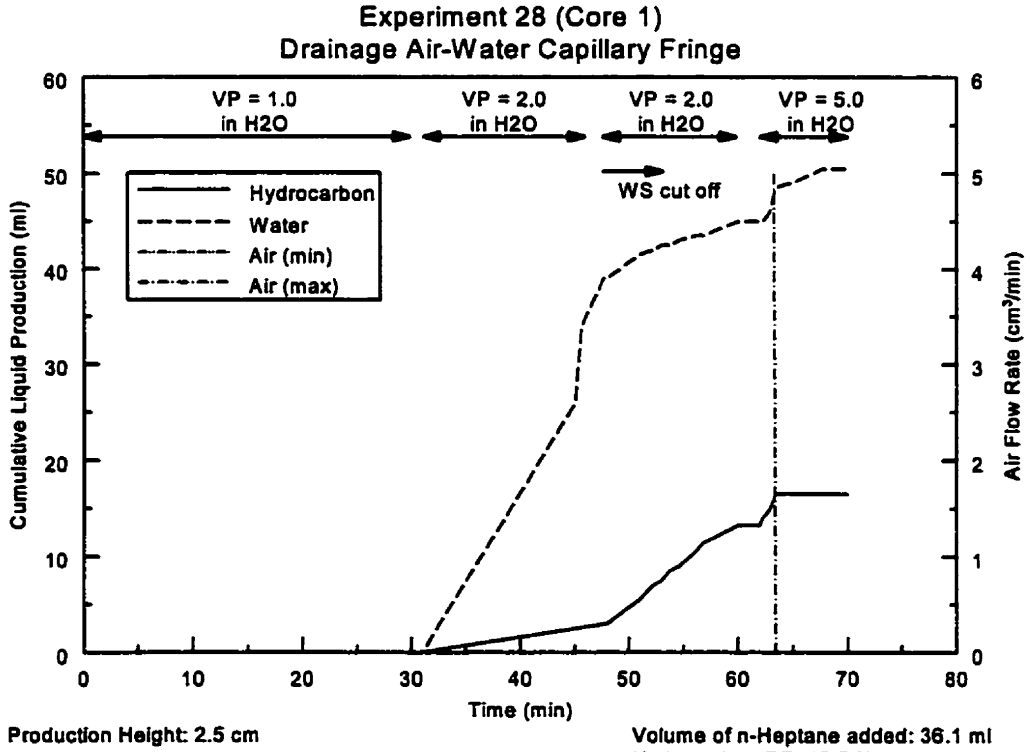

Production Height: 2.5 cm

Volume of n-Heptane added: 36.1 ml
Hydrocarbon RF: 45.7 %

Experiment 29 (Core 2)
Drainage Air-Water Capillary Fringe

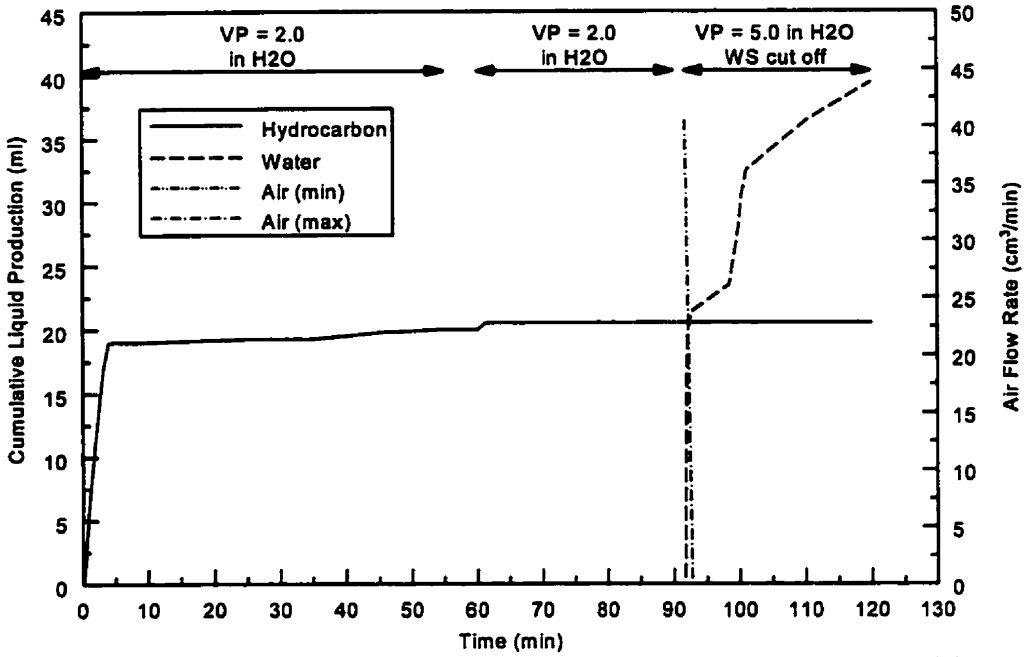

Production Height: 10.2 cm (for first 55 min)
Production Height: 5.2 cm (for last 65 min)

Volume of n-Heptane added: 36.5 ml
Hydrocarbon RF: 56.2 %

Experiment 30 (Core 1)
Drainage Air-Water Capillary Fringe

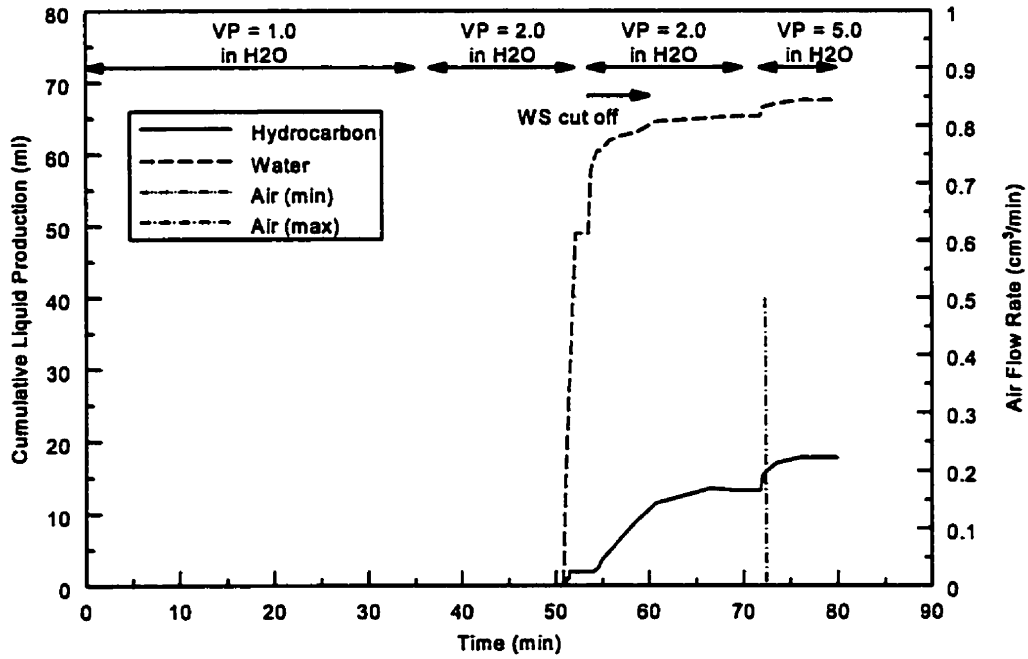

Production Height: 2.5 cm

Volume of n-Heptane added: 36.3 ml
Hydrocarbon RF: 48.9 %

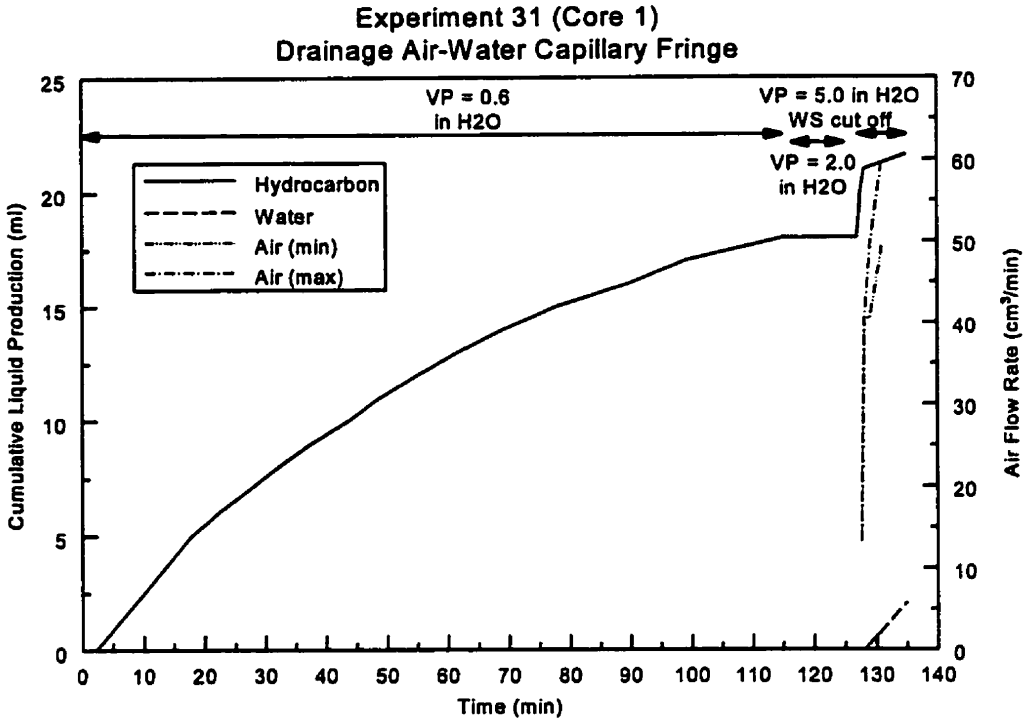

Production Height: 5.1 cm

Volume of n-Heptane added: 36.1 ml
Hydrocarbon RF: 60.0 %

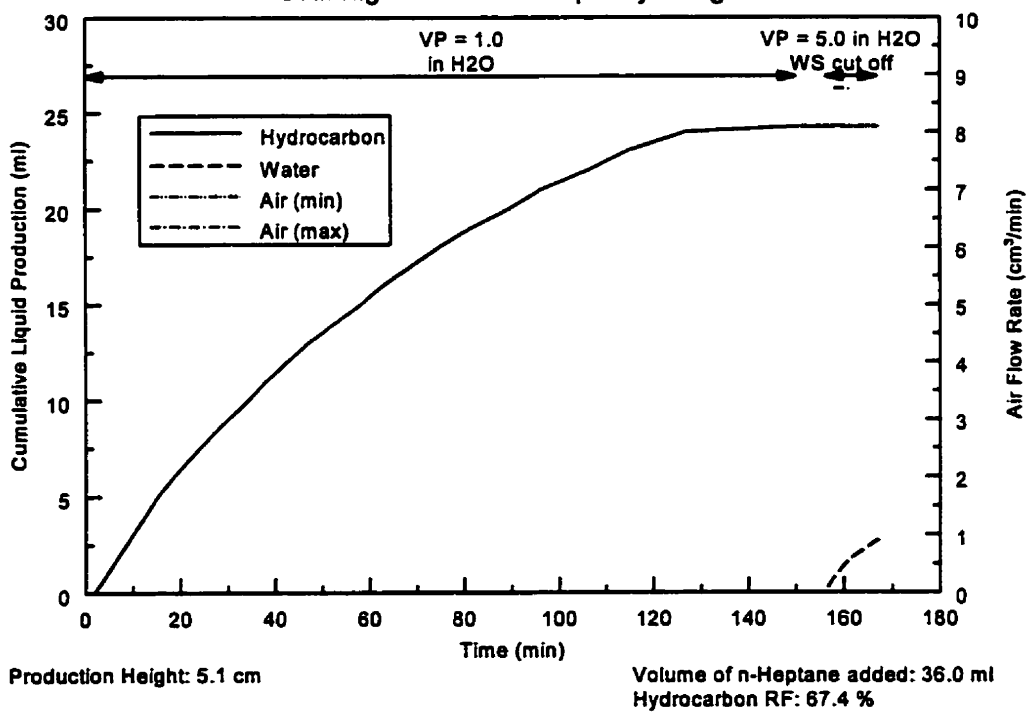

Production Height: 5.1 cm

Volume of n-Heptane added: 36.0 ml
Hydrocarbon RF: 67.4 %

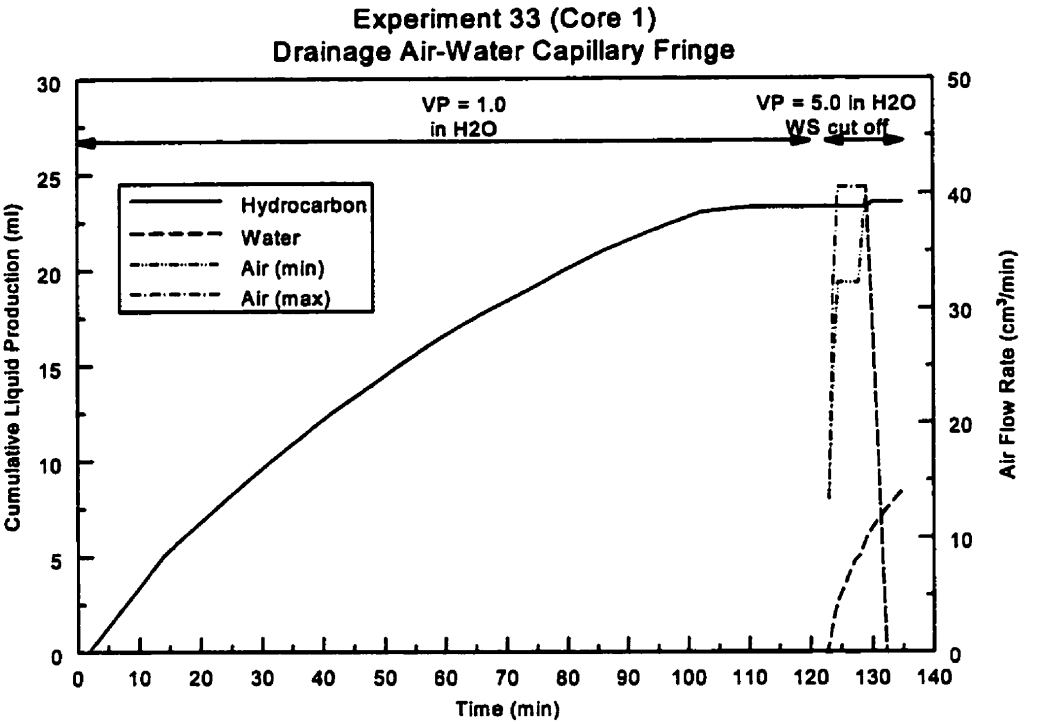

Production Height: 5.1 cm

Volume of n-Heptane added: 36.1 ml
Hydrocarbon RF: 65.1 %

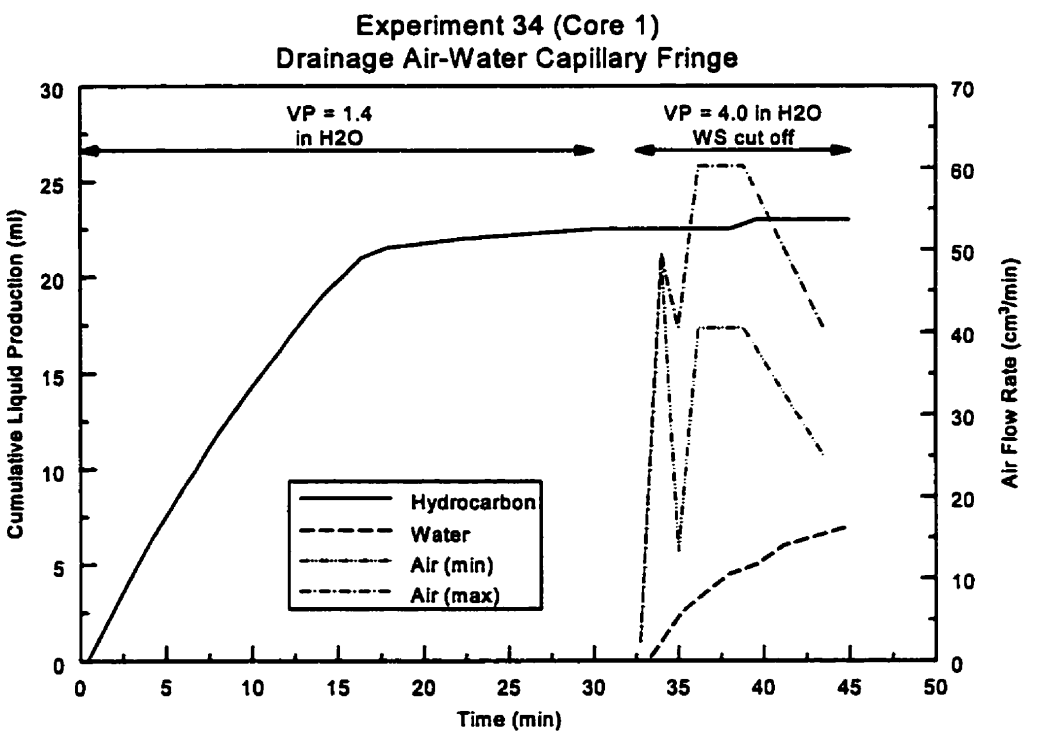

Production Height: 5.1 cm

Volume of n-Heptane added: 36.3 ml
Hydrocarbon RF: 63.4 %

Experiment 35 (Core 1)
Drainage Air-Water Capillary Fringe

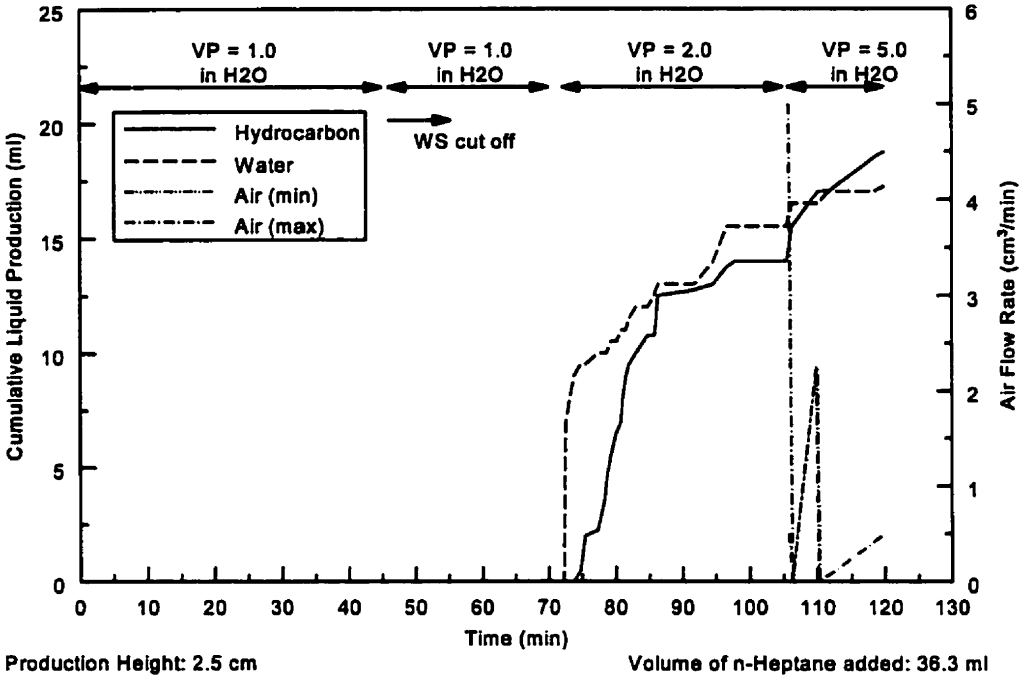

Production Height: 2.5 cm

Volume of n-Heptane added: 36.3 ml
Hydrocarbon RF: 51.7 %

Experiment 36 (Core 1)
Drainage Air-Water Capillary Fringe

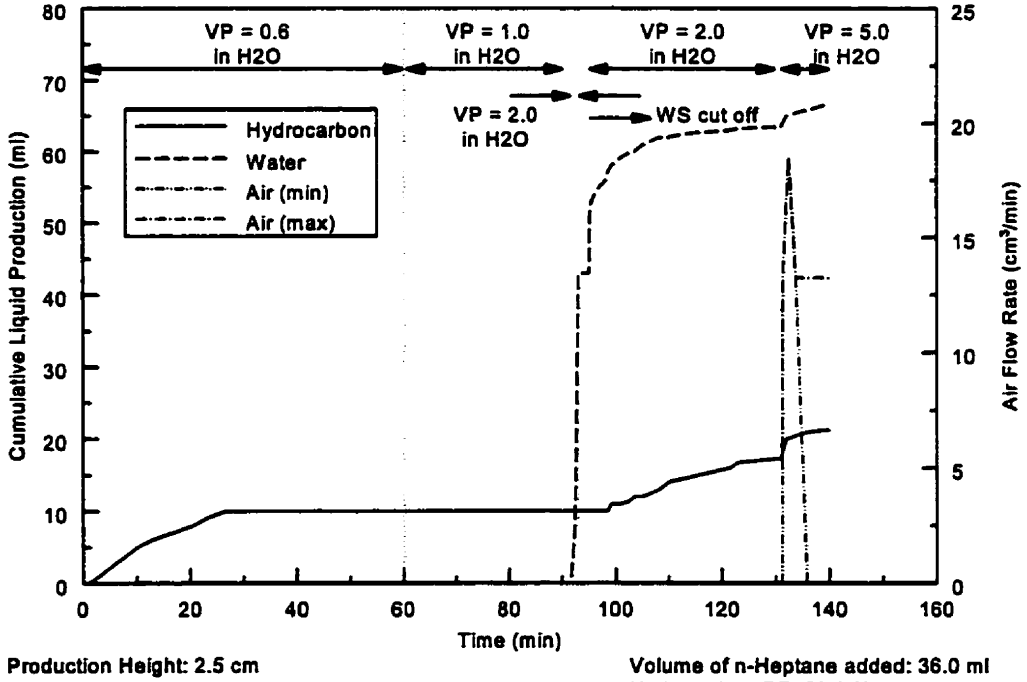

Production Height: 2.5 cm

Volume of n-Heptane added: 36.0 ml
Hydrocarbon RF: 59.0 %

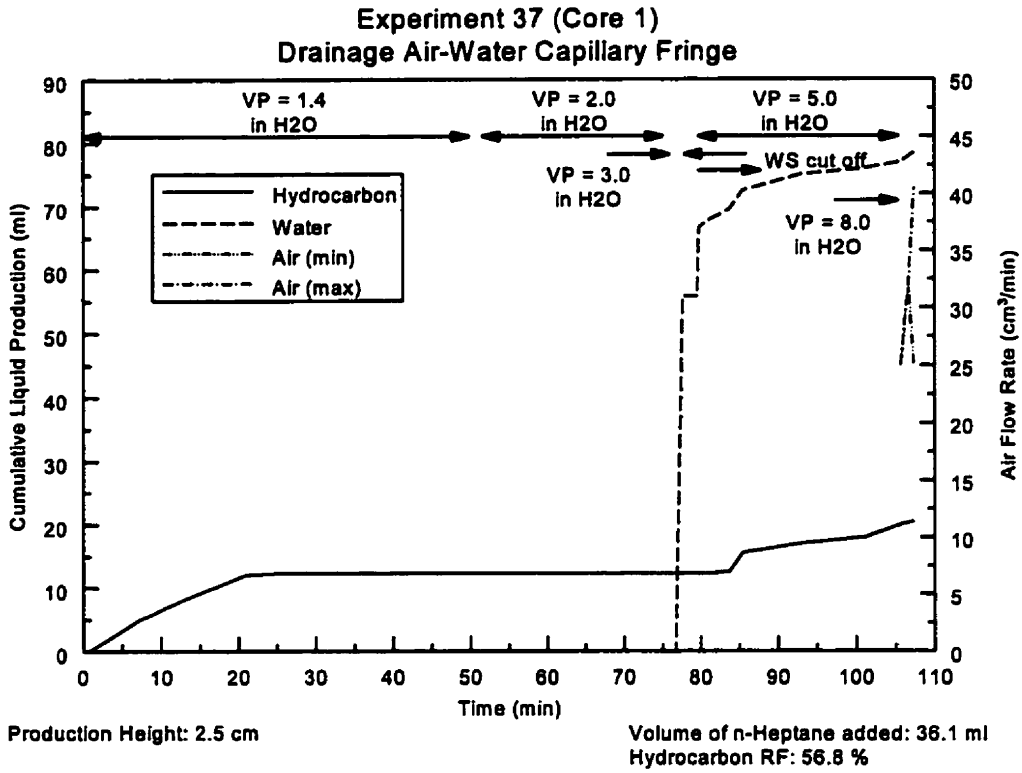
Experiment 37 (Core 1)
Drainage Air-Water Capillary Fringe
VP = 1.4 in H2O
VP = 2.0 in H2O
VP = 5.0 in H2O
WS cut off
VP = 3.0 in H2O
VP = 8.0 in H2O
Hydrocarbon
Water
Air (min)
Air (max)
Cumulative Liquid Production (ml)
Air Flow Rate (cm³/min)
Time (min)
Production Height: 2.5 cm
Volume of n-Heptane added: 36.1 ml
Hydrocarbon RF: 56.8 %

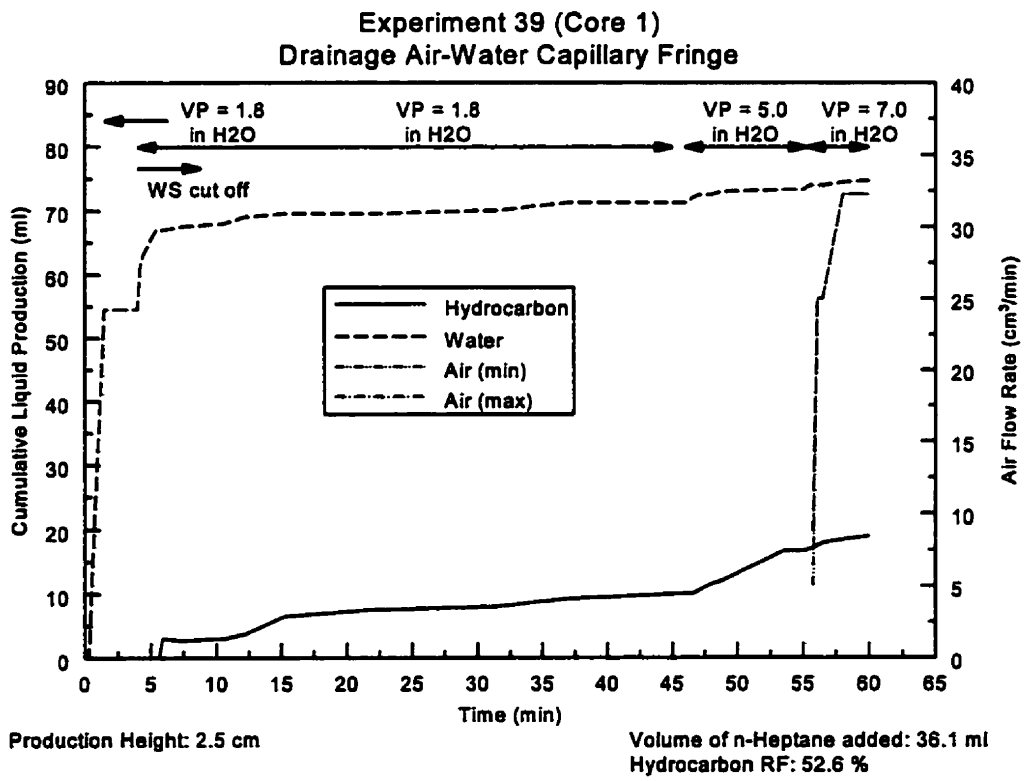
Experiment 39 (Core 1)
Drainage Air-Water Capillary Fringe
VP = 1.8 in H2O
VP = 1.8 in H2O
VP = 5.0 in H2O
VP = 7.0 in H2O
WS cut off
Hydrocarbon
Water
Air (min)
Air (max)
Cumulative Liquid Production (ml)
Air Flow Rate (cm³/min)
Time (min)
Production Height: 2.5 cm
Volume of n-Heptane added: 36.1 ml
Hydrocarbon RF: 52.6 %

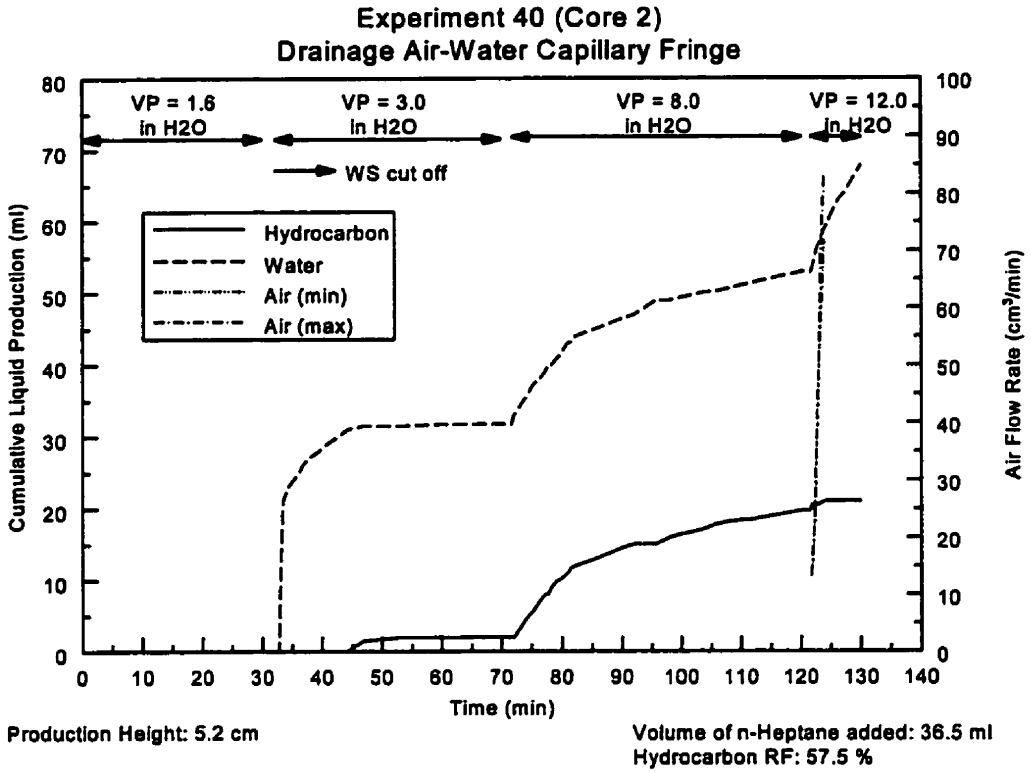
Experiment 40 (Core 2)
Drainage Air-Water Capillary Fringe
VP = 1.6 in H2O
VP = 3.0 in H2O
VP = 8.0 in H2O
VP = 12.0 in H2O
WS cut off
Hydrocarbon
Water
Air (min)
Air (max)
Cumulative Liquid Production (ml)
Air Flow Rate (cm³/min)
Time (min)
Production Height: 5.2 cm
Volume of n-Heptane added: 36.5 ml
Hydrocarbon RF: 57.5 %

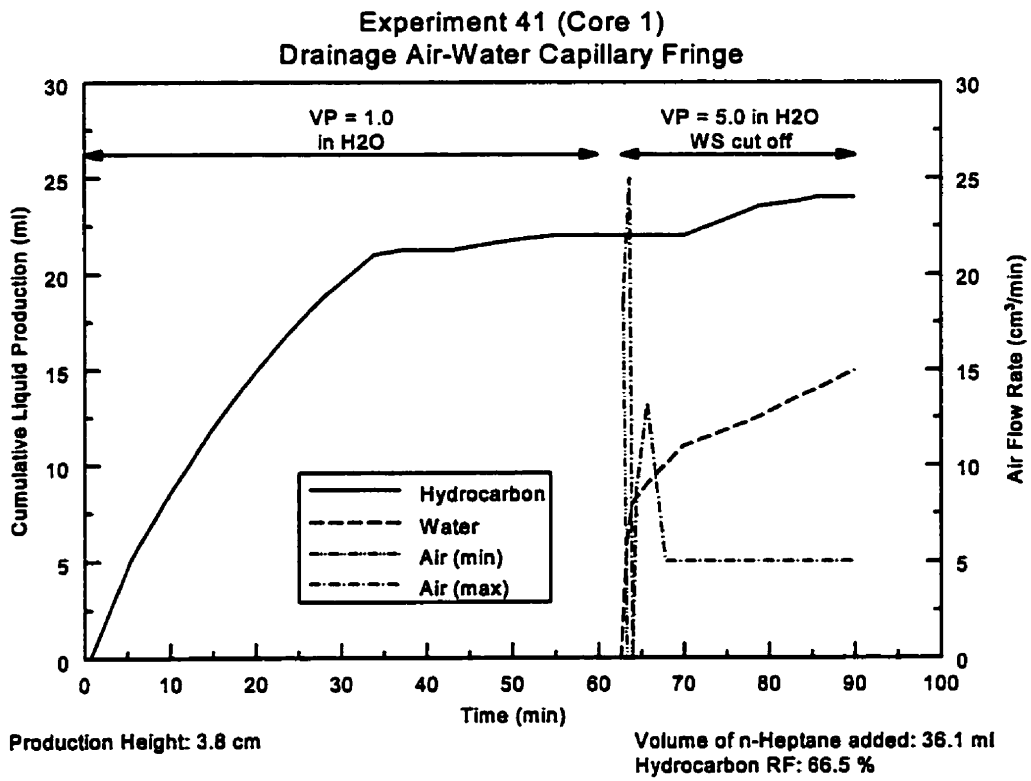
Experiment 41 (Core 1)
Drainage Air-Water Capillary Fringe
VP = 1.0 in H2O
VP = 5.0 in H2O
WS cut off
Hydrocarbon
Water
Air (min)
Air (max)
Cumulative Liquid Production (ml)
Air Flow Rate (cm³/min)
Time (min)
Production Height: 3.8 cm
Volume of n-Heptane added: 36.1 ml
Hydrocarbon RF: 66.5 %

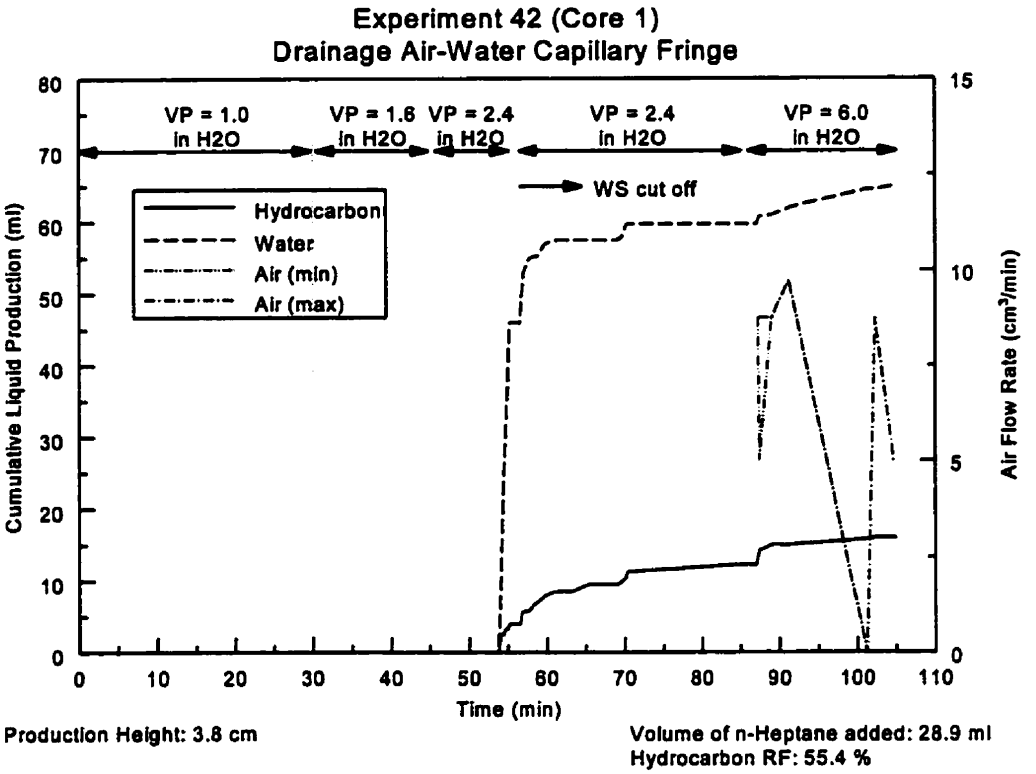

Production Height: 3.8 cm

Volume of n-Heptane added: 28.9 ml
Hydrocarbon RF: 55.4 %

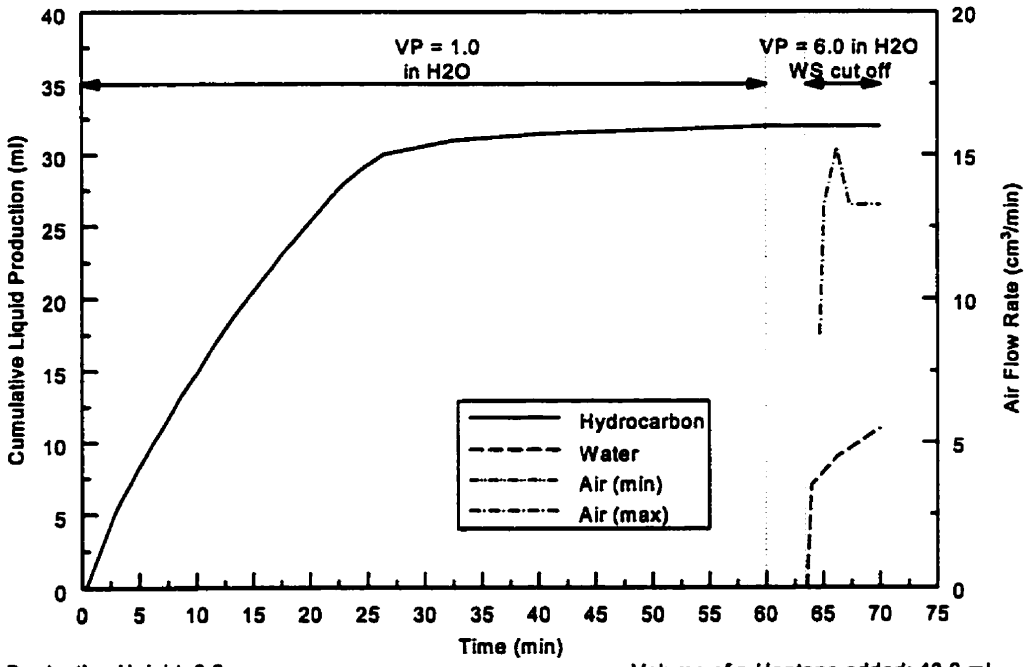

Production Height: 3.8 cm

Volume of n-Heptane added: 43.9 ml
Hydrocarbon RF: 72.9 cc

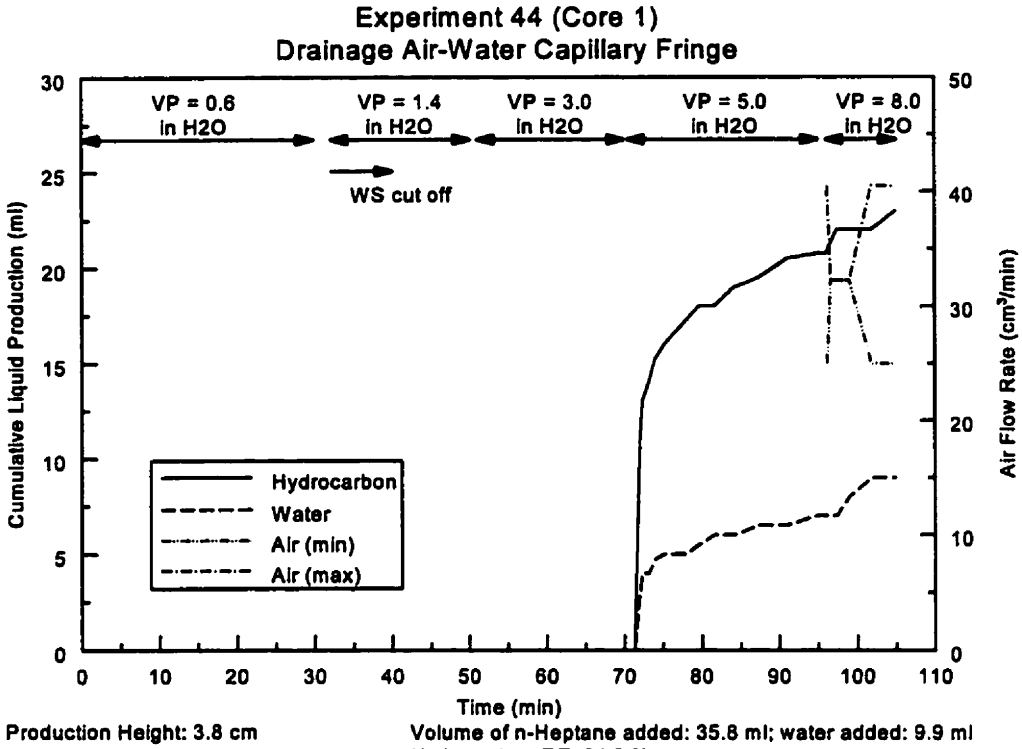

Production Height: 3.8 cm

Volume of n-Heptane added: 35.8 ml; water added: 9.9 ml
Hydrocarbon RF: 64.2 %

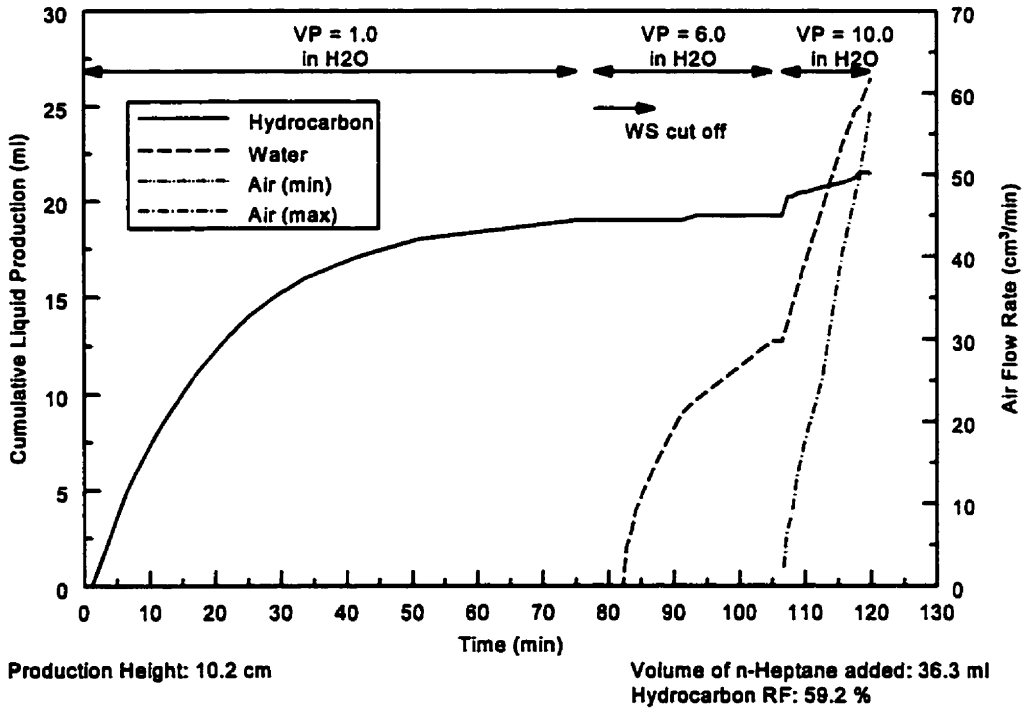

Production Height: 10.2 cm

Volume of n-Heptane added: 36.3 ml
Hydrocarbon RF: 59.2 %

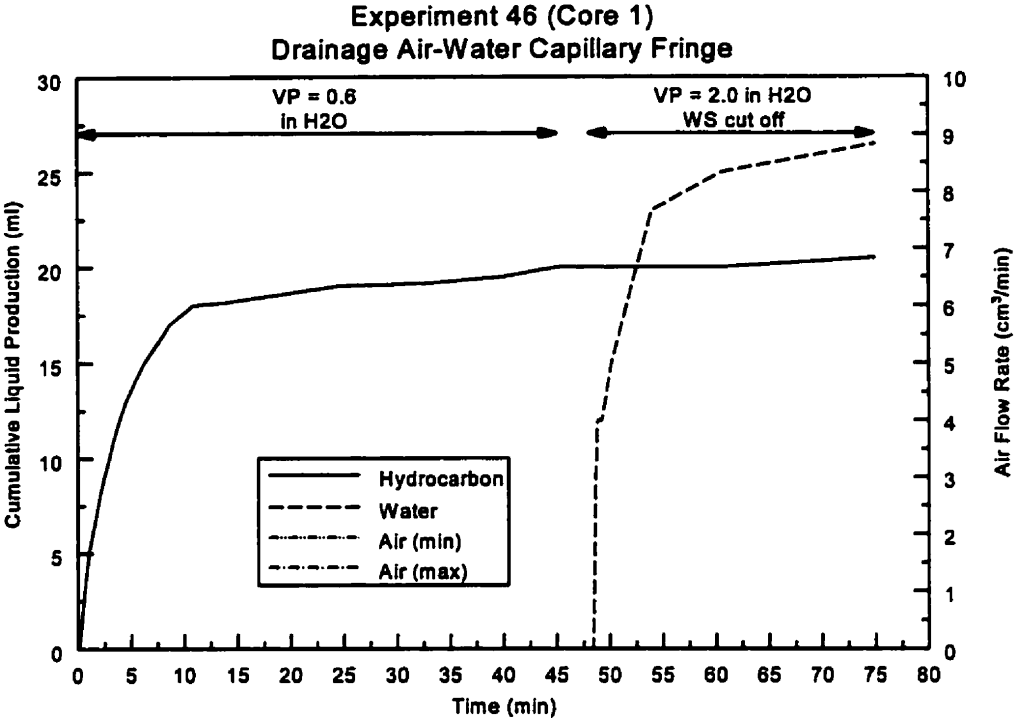

Production Height: 6.3 cm

Volume of n-Heptane added: 36.4 ml; water added: 19.9 ml
Hydrocarbon RF: 56.3 %

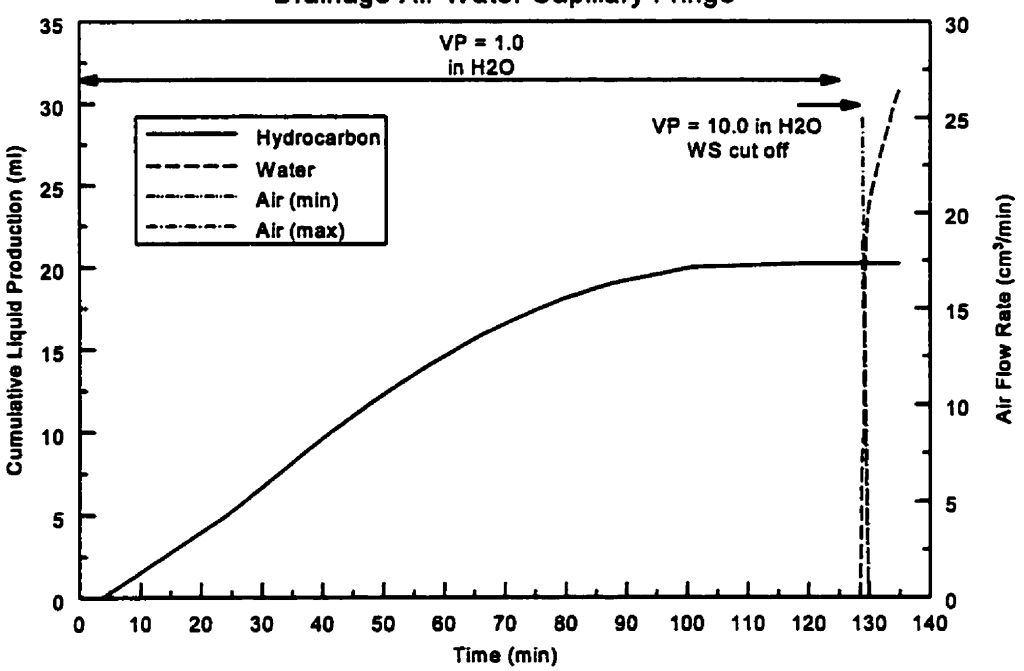

Production Height: 7.7 cm

Volume of n-Heptane added: 36.5 ml
Hydrocarbon RF: 55.5 %

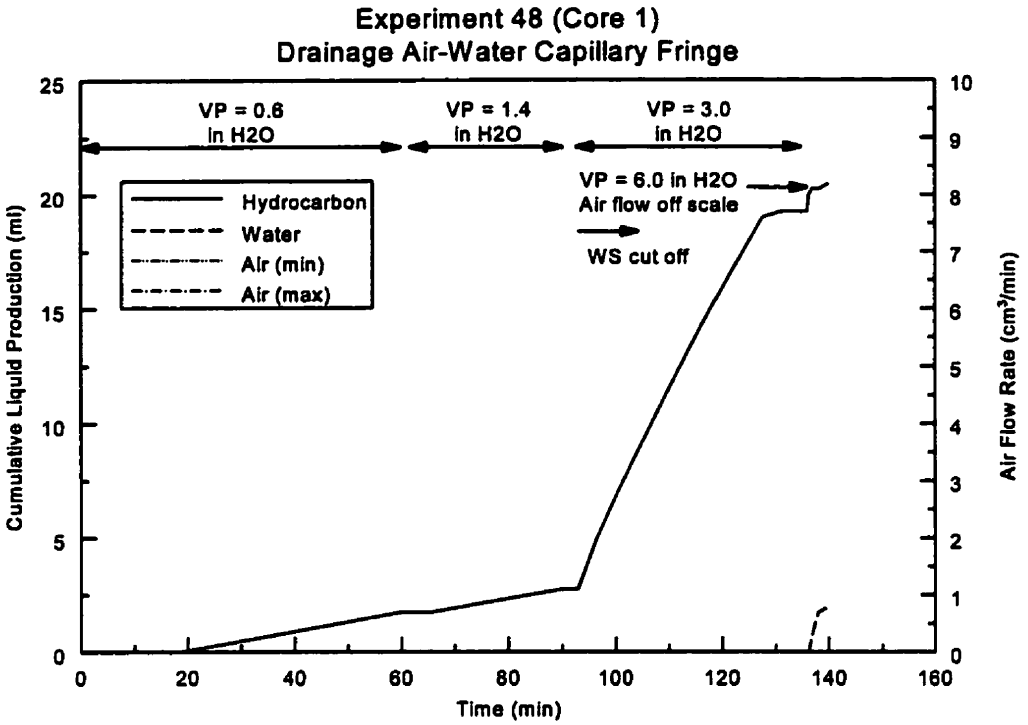

Production Height: 5.1 cm

Volume of n-Heptane added: 36.0 ml; water added: 19.9 ml
Hydrocarbon RF: 56.9 %

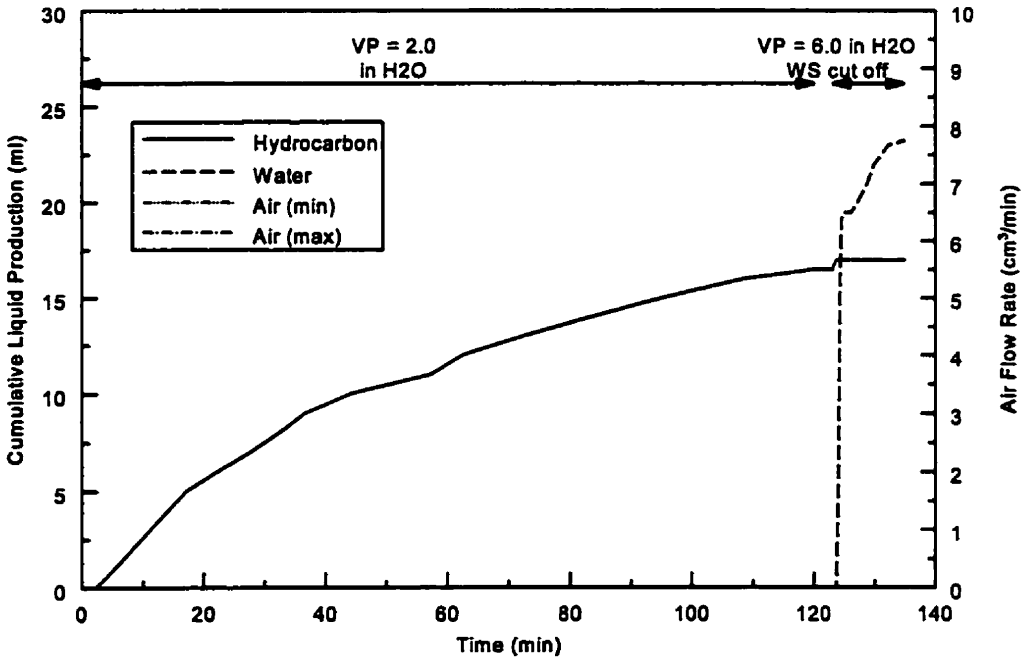

Production Height: 7.7 cm

Volume of n-Heptane added: 36.4 ml
Hydrocarbon RF: 46.7 %

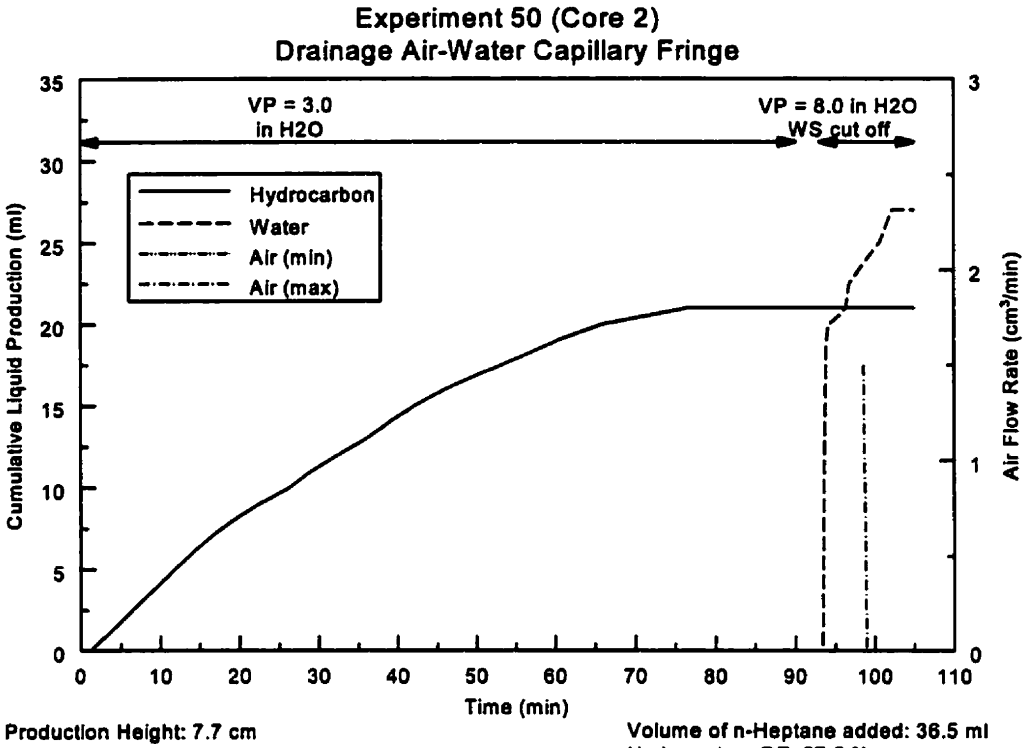

Production Height: 7.7 cm

Volume of n-Heptane added: 36.5 ml
Hydrocarbon RF: 57.5 %

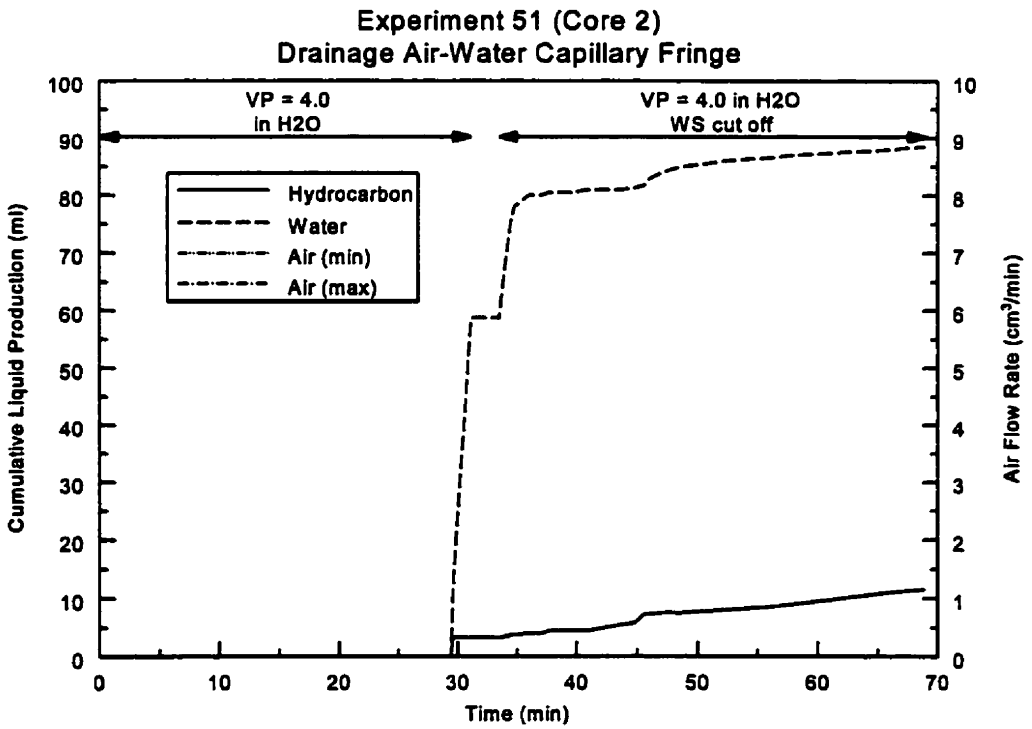

Production Height: 7.7 cm

Volume of n-Heptane added: 36.3 ml
Hydrocarbon RF: 31.7 %

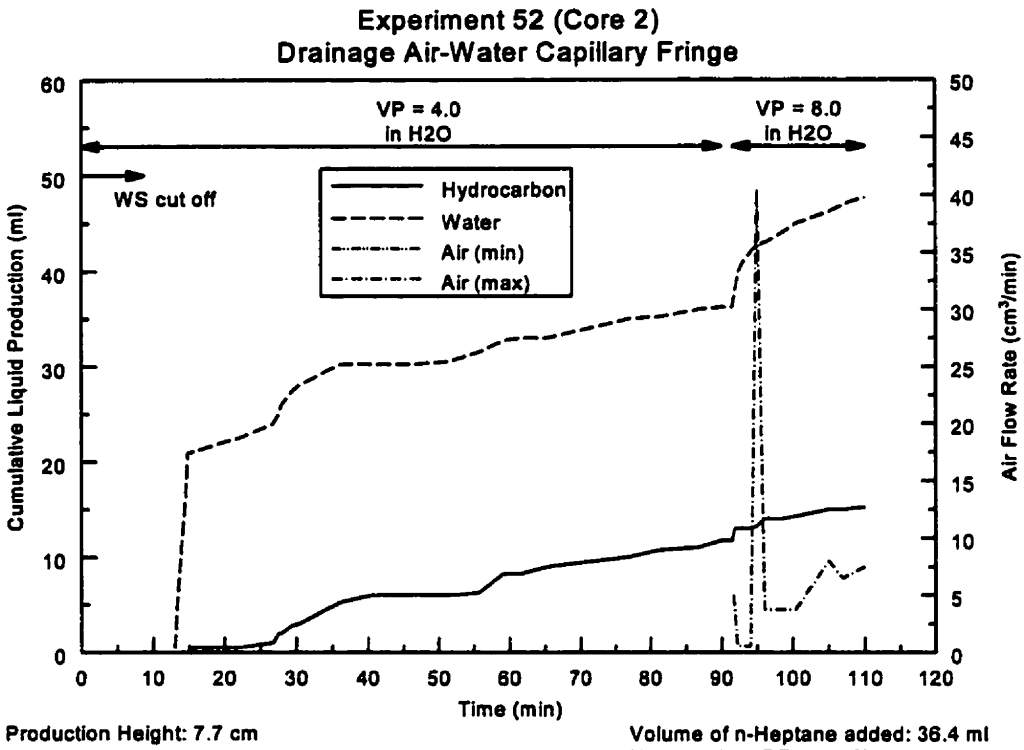

Production Height: 7.7 cm

Volume of n-Heptane added: 36.4 ml
Hydrocarbon RF: 41.9 %

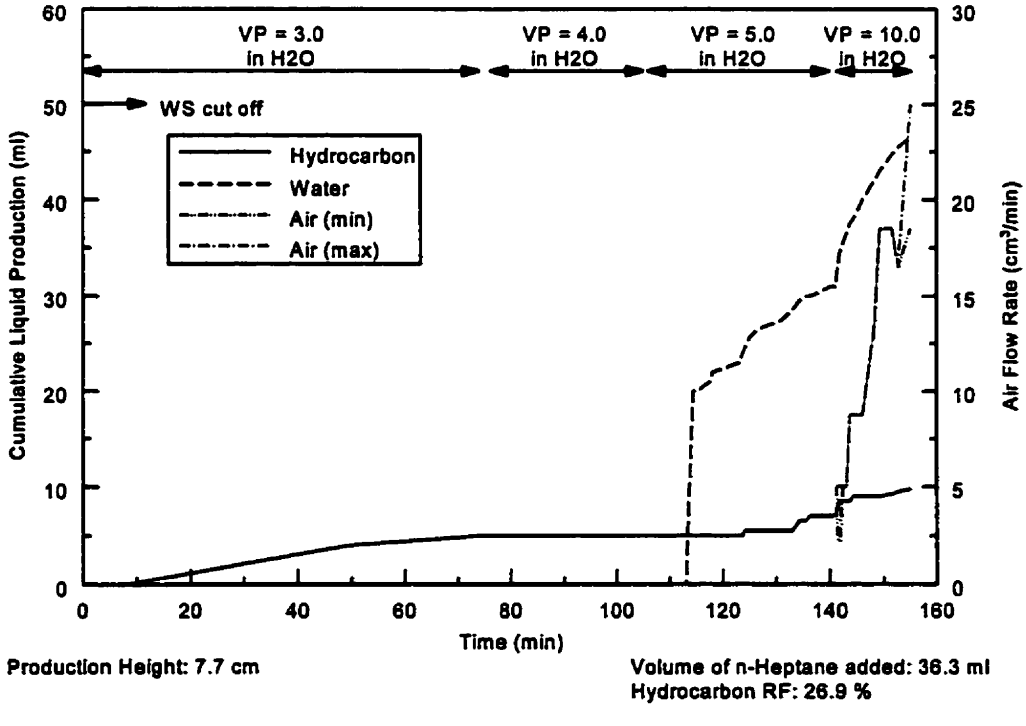

Production Height: 7.7 cm

Volume of n-Heptane added: 36.3 ml
Hydrocarbon RF: 26.9 %

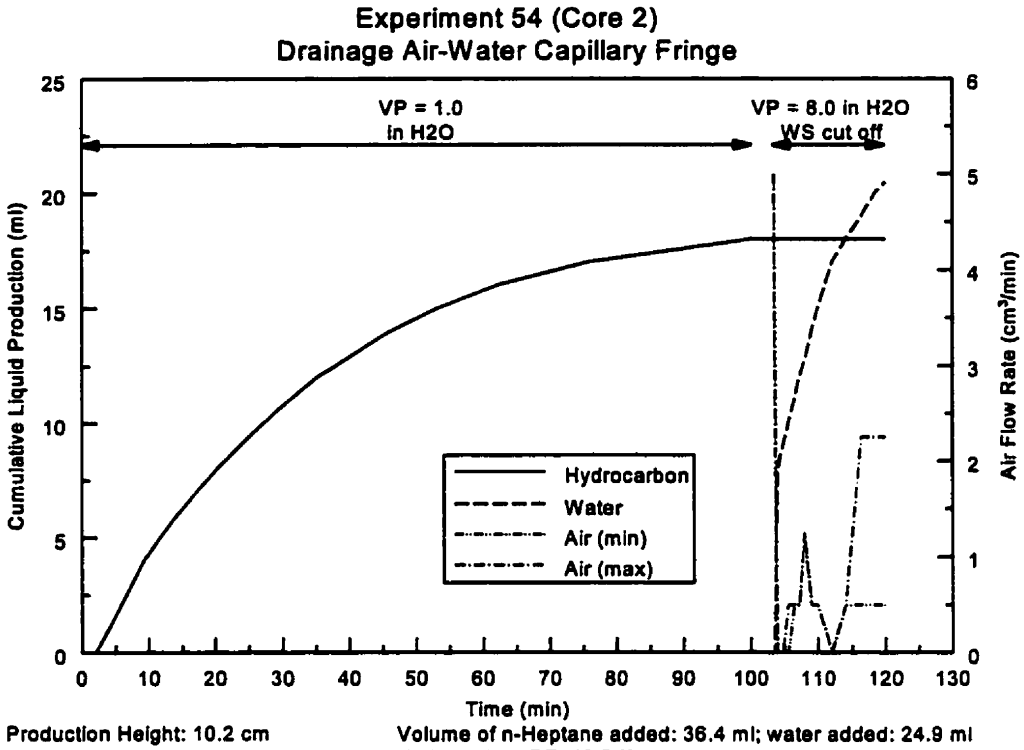

Production Height: 10.2 cm

Volume of n-Heptane added: 36.4 ml; water added: 24.9 ml
Hydrocarbon RF: 49.5 %

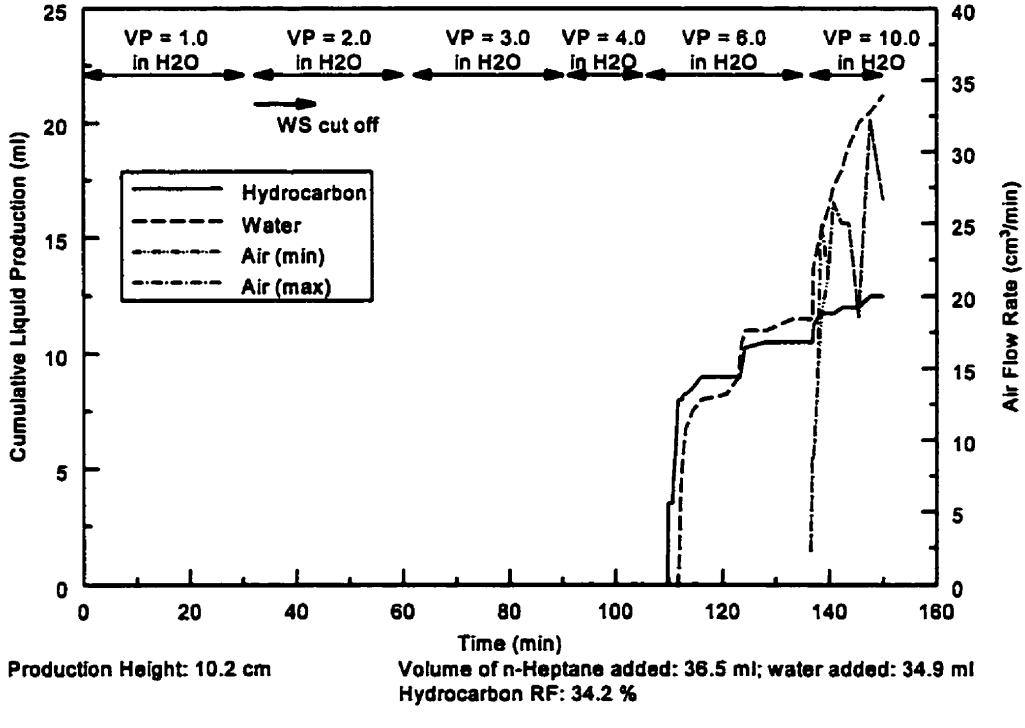

Production Height: 10.2 cm

Volume of n-Heptane added: 36.5 ml; water added: 34.9 ml
Hydrocarbon RF: 34.2 %

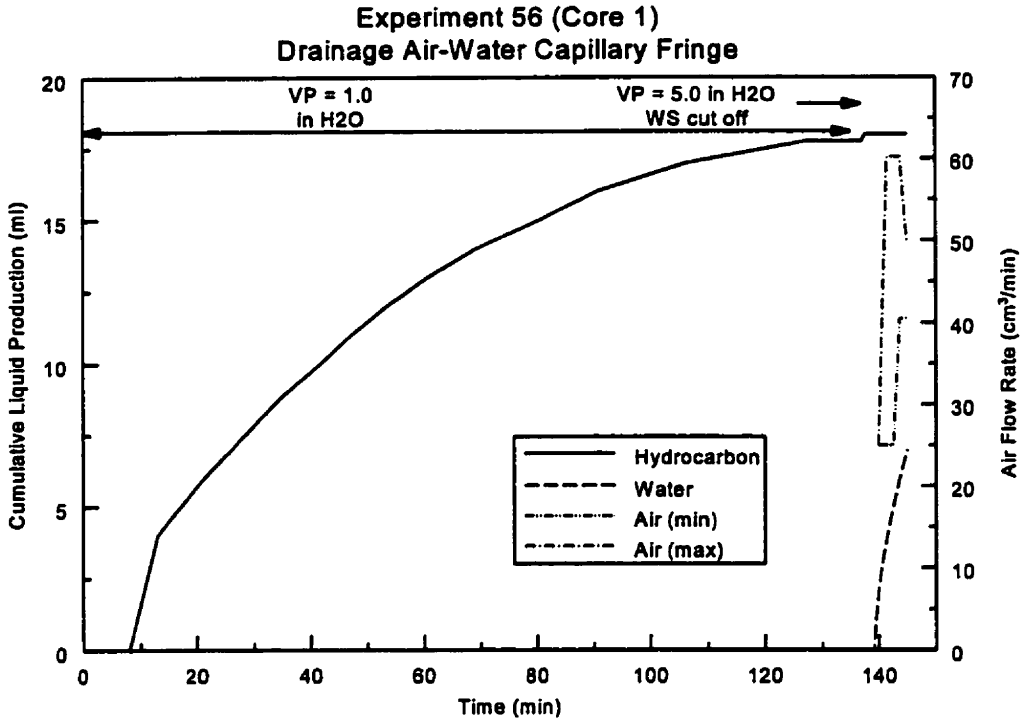

Production Height: 5.1 cm
Water Table was dropped by: 2.25 cm

Volume of n-Heptane added: 36.5 ml
Hydrocarbon RF: 49.3 %

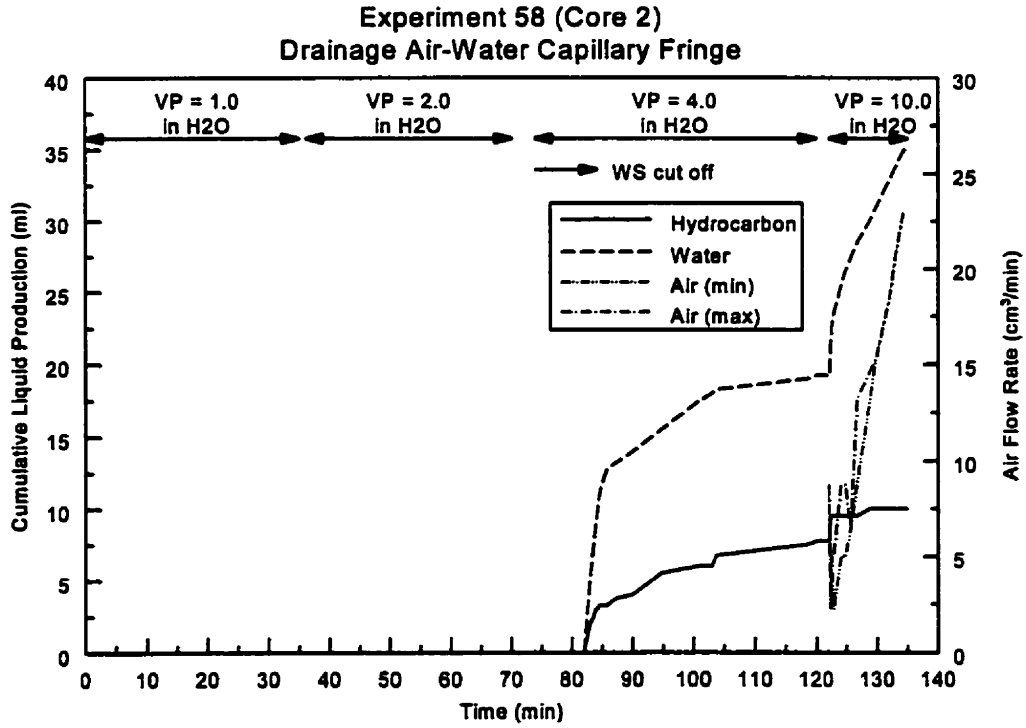

Production Height: 6.2 cm
Water Table was raised by: 4.0 cm

Volume of n-Heptane added: 36.4 ml
Hydrocarbon RF: 27.5 %

APPENDIX B

SAMPLE OF ORIGINAL DATA

Experiment 33 (Core 1: 16-20 Glass Bead Pack)

19/06/96

1. 9:10 am - Set the water table level to 28.2 cm and opened the water valve to let the water into the core.
2. 9:35 am - Capillary fringe is at 29.7 cm. Closed the water valve and dropped the water table level to 10.25 cm.
3. 9:40 am - Opened the water valve and removed water from the reservoir so that the water level remained at 10.25 cm.

20/06/96

1. 8:50 am - The capillary fringe is 18.0 to 18.9 cm above the water table.
2. Mass n-Heptane poured out: 25.0g (36.5 ml)
3. n-Heptane poured into probe 9 (22.9 cm) at 8:55 am
4. Mass n-Heptane + beaker

start	76.2 g	
end	51.5 g	
diff	24.7 g	(36.1 ml)

11/06/96

1 Vacuum/collection system hooked up to probe 6 (15.2 cm)
2 Vacuum pressure preset to 1.0 inch H2O
3 T = 20.25 °C
4 Air flow meter: 448 - 035 with Stainless Steel Float

Note: Abbreviations used:

H2O = Water
T = Ambient room temperature
TL = Total liquid volume
TW = Total water volume
THC = Total hydrocarbon volume
VP = Vacuum pressure
gas meter readings are unconverted

Time			Total	TL	TW	THC	Comments
hrs	min	secs	min	(ml)	(ml)	(ml)	
0	0	0	0	0	0	0	
0	1	45	1.75	0	0	0	
0	13	56	13.933	5	0	5	
0	17	10	17.167	6	0	6	
0	20	44	20.733	7	0	7	
0	24	13	24.217	8	0	8	
0	27	52	27.867	9	0	9	
0	31	36	31.6	10	0	10	
0	35	31	35.517	11	0	11	
0	39	21	39.35	12	0	12	
0	43	30	43.5	13	0	13	
0	48	2	48.033	14	0	14	
0	52	17	52.283	15	0	15	
0	56	53	56.883	16	0	16	
1	2	0	62	17	0	17	
1	7	39	67.65	18	0	18	
1	13	49	73.817	19	0	19	
1	19	24	79.4	20	0	20	
1	25	48	85.8	21	0	21	
1	33	30	93.5	22	0	22	
1	41	59	101.98	23	0	23	
1	50	0	110	23.25	0	23	
2	0	0	120	23.25	0	23.25	Stop
2	2	30	122.5	23.25	0	23.25	Restart, VP = +2.5 -2.4 in H2O, water supply cut off
2	2	47	122.78	23.25	0	23.25	
2	2	56	122.93				gas meter = 4, have water production
2	3	45	123.75	25	1.75	23.25	gas meter = 5 to 5.5
2	4	33	124.55	26	2.75	23.25	gas meter = 5.5 to 6
2	5	20	125.33				gas meter = 5 to 5.5
2	5	46	125.77	27	3.75	23.25	
2	7	6	127.1	28	4.75	23.25	
2	7	50	127.83	28.25	5	23.25	gas meter = 5 to 5.5
2	9	5	129.08	29.25	6	23.25	gas meter = 5.5
2	10	0	130	30	6.5	23.5	
2	12	20	132.33	31	7.5	23.5	gas meter = 0
2	15	0	135	32	8.5	23.5	Stop

5 n-Heptane recovered after experiment: 15.8 g (23.1 ml).

IMAGE EVALUATION TEST TARGET (QA-3)

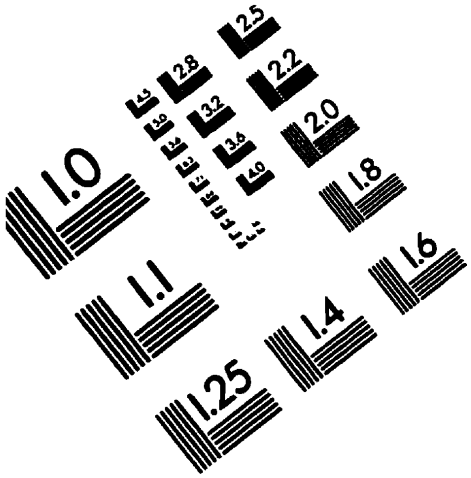

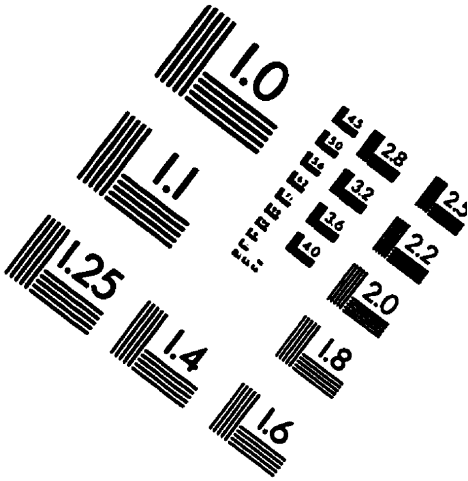

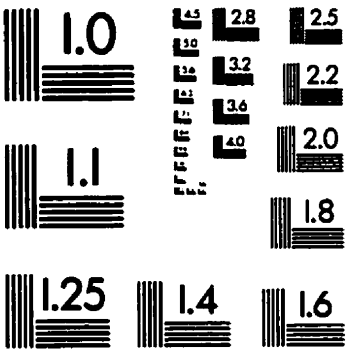

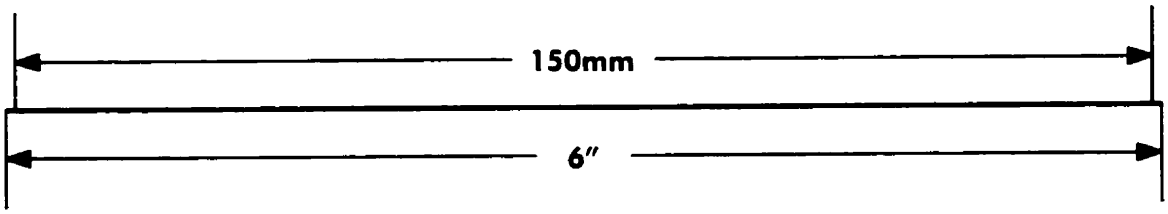

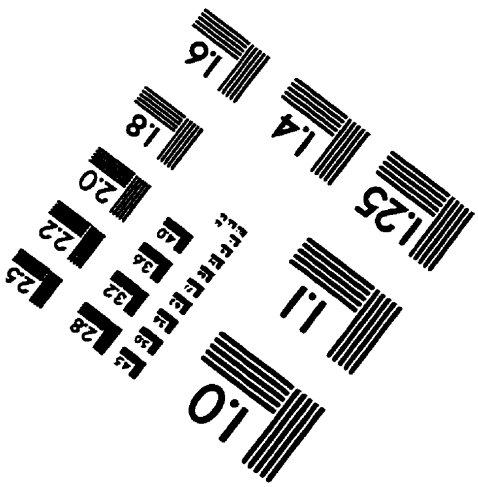

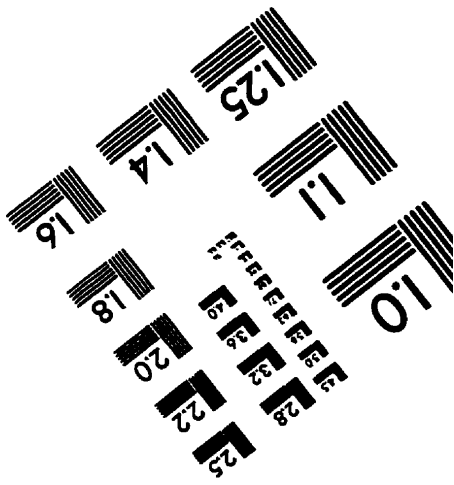

APPLIED IMAGE, Inc
1653 East Main Street
Rochester, NY 14609 USA
Phone: 716/482-0300
Fax: 716/288-5989